



ANNUAL REPORT **2022-23**



WADIA INSTITUTE OF HIMALAYAN GEOLOGY DEHRADUN

(An Autonomous Institute of Dept. of Science & Technology, Govt. of India)

Cover Photo: Durung-Drung Glacier, Doda Valley, Ladakh

(Courtesy: Vinit Kumar)

ANNUAL REPORT

2022-23



WADIA INSTITUTE OF HIMALAYAN GEOLOGY

(An Autonomous Institute of Department of Science & Technology, Government of India)

33, General Mahadeo Singh Road, Dehra Dun - 248 001

EPABX : 0135-2525100

EPABX : 0135-2525100; Fax: 0135-2625212

Email: dir.off@wihg.res.in; Web: <http://www.wihg.res.in>

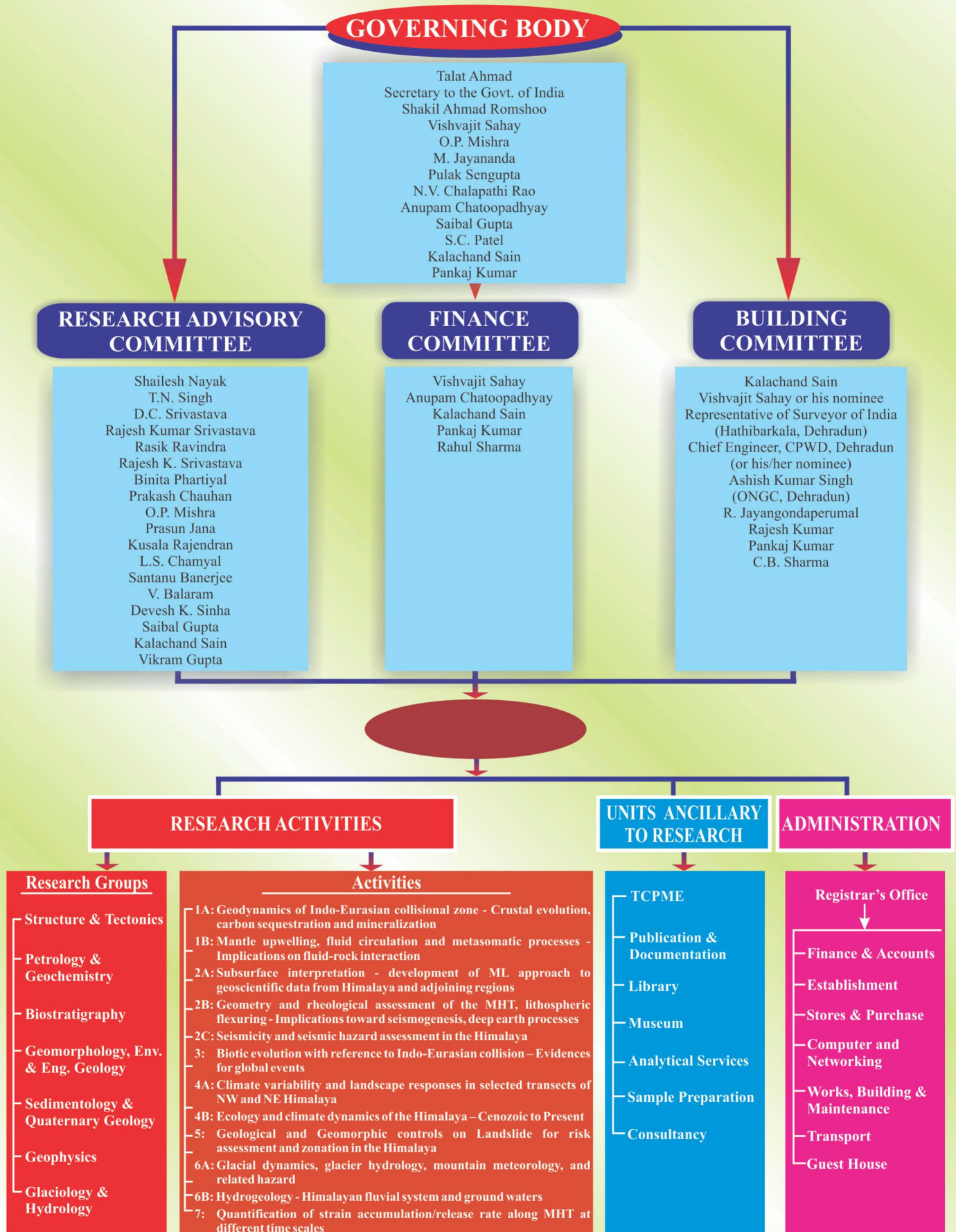
Contact :

The Director,
Wadia Institute of Himalayan Geology
33, General Mahadeo Singh Road, Dehra Dun - 248 001
Phone : 0135-2525103, Fax : 0135-2625212 / 2525200
Email : director@wihg.res.in
Web: <http://www.wihg.res.in>

CONTENTS

| | |
|--|-----|
| 1. Executive Summary | i |
| 2. Activities | 1 |
| 3. Sponsored Projects | 71 |
| 4. Research Publications | 99 |
| 5. Seminar/Symposia/Workshop organized | 110 |
| 6. Awards and Honours | 114 |
| 7. Ph.D. Theses | 115 |
| 8. Participation in Seminars/Symposia/Meetings | 117 |
| 9. Distinguished Lectures delivered in the Institute | 119 |
| 10. Distinguished Lecture series related to the celebration of “Azadi Ka Amrit Mahotsav” | 120 |
| 11. Lectures delivered/invited talk by Institute Scientists | 121 |
| 12. Membership | 125 |
| 13. Publications and Documentation | 126 |
| 14. Library | 127 |
| 15. S.P. Nautiyal Museum | 128 |
| 16. Technical Services | 129 |
| 17. Celebrations | 132 |
| 18. Distinguished visitors to the Institute | 140 |
| 19. Status of implementation of Hindi | 141 |
| 20. Miscellaneous Items | 142 |
| 21. Staff of the Institute | 143 |
| 22. Members of the Governing Body/Research Advisory Committee /Finance Committee / Building Committee | 145 |
| 23. Statement of Accounts | 149 |

WIHG ORGANISATIONAL SET-UP



EXECUTIVE SUMMARY



The Wadia Institute of Himalayan Geology (WIHG) has a mandate to study various scientific issues related to the Himalaya, including its evolution, geodynamics, glaciers, climate, and natural hazards. The institute leads in geological and geophysical

investigations of the Himalayan region, with a focus on understanding earthquake activity, glacier dynamics, climate-tectonic interactions, ores/minerals formations, biotic evolution, geohazards related to landslides, earthquakes, flash floods, and geo-resources (minerals, ore bodies, hydrocarbons, and cold/hot springs). Field observations are complemented by advanced laboratories equipped with geochemistry, isotopes, geochronology, and geophysical equipment for deep and shallow earth probing. The institute is having Research Scholars' Hostel, Food Court, Gymnasium, and state-of-the-art Analytical/Laboratory facilities open for facilitating research by students and research scholars.

The institute has advanced analytical facilities such as LA-MC-ICP-MS, Stable Isotope Mass Spectrometer, EPMA, ICP-MS, XRF, SEM, XRD, Raman Spectrometer, TL/OSL, and Magnetic Susceptibility meter. Competent scientists and technicians manage these facilities. It also houses state-of-the-art geophysical data acquisition, processing, modeling, and interpretation laboratories, along with an AI/ML Centre of Excellence for Geosciences data. These facilities serve WIHG scientists, as well as researchers from universities, institutes, and organizations. The institute has a seismological network comprising 75 Broad Band Seismographs and 15 Accelerographs across Himachal Pradesh, Uttarakhand, Punjab, Haryana, Arunachal Pradesh, Jammu & Kashmir, and Ladakh. About 20 GPS instruments are installed in Himachal Pradesh, Uttarakhand, Jammu & Kashmir, and Ladakh. The Institute is operating a 'Multi-Parametric Geophysical Observatory (MPGO)' in Ghuttu, Uttarakhand, to study earthquake precursors in the Himalayan region. The Institute offers consultancy services for engineering projects, groundwater surveys, natural hazards, and road/rail alignments in the Himalaya and neighboring areas.

The institute is a national center of excellence for Himalayan geoscience education and research. The Institute emphasizes nurturing young and dynamic talents to achieve a high level of competency through the Ph.D. program. It provides training to over 200 students annually and produces an average of 10 Ph.D. graduates. The institute publishes over 120 research papers in peer-reviewed journals each year. The institute maintains a modern Geological Museum showcasing Himalayan rocks, minerals, and fossils for educational purposes. It conducts outreach programs for science education and geo-hazards awareness and organizes prestigious award lectures and national/international seminars. The institute is carrying out collaborative research works with different universities, industries, and other institutes on Himalayan geosciences.

WIHG has achieved remarkable recognition with scientists receiving prestigious awards such as Padma Awards, National Geosciences Awards, Academy Fellowships, and Young Scientists Awards. WIHG's vision is to explore and understand Himalayan seismogenesis, geodynamics, geo-hazards, climate variability, and geo-resources to address societal needs and advance basic sciences. Ongoing research activities are centered around the major thrust area of "Characterization and Assessment of Surface and Sub-surface Processes in Himalaya (CAP-Himalaya): Implications on Geodynamics, Seismogenesis, Bio-events, Paleo-climates, Natural Hazards, and Natural Resources for Sustainable Development". The research program planned for the year 2022-2023 is accomplished through different activities as given below:

- Activity-1A :** Geodynamics of Indo-Eurasian collisional zone and crystalline thrust sheets-crustal evolution, carbon sequestration, and economic mineralization
- Activity-1B :** Mantle upwelling, fluid circulation, metasomatic processes – Implications on fluid-rock interaction
- Activity-2A :** Subsurface interpretation – Development of ML approach to geoscientific data from Himalaya and adjoining regions
- Activity-2B :** Geometry and rheological assessment

of the MHT, lithospheric flexuring - Implications toward seismogenesis, deep earth processes

Activity-2C : Seismicity and seismic hazard assessment in the Himalaya

Activity-3 : Biotic evolution with reference to Indo-Eurasian collision – Evidences for global events

Activity-4A : Climate variability and landscape responses in selected transects of NE and NW Himalaya

Activity-4B : Ecology and climate dynamics of the Himalaya – Cenozoic to Present

Activity-5 : Geological and geomorphic controls on landslide for risk assessment and zonation in the Himalaya

Activity-6A : Glacial dynamics, glacier hydrology, mountain meteorology, and related hazard

Activity-6B : Hydrogeology-Himalayan Fluvial System and Groundwaters

Activity-7 : Quantification of strain accumulation and strain release rate along the MHT at different time scales

An executive summary of significant contributions in each of the activities is highlighted below along with other activities of the Institute.

Geodynamics of Indo-Eurasian collisional zone and crystalline thrust sheets-crustal evolution, carbon sequestration and economic mineralization

- Mafic intrusives of the Abor magmatic complex (AMC), eastern Himalaya were emplaced during the late Cambrian to early Ordovician (500-473 Ma zircon U-Pb ages), whereas the evolved felsic extrusives were generated during the early Cretaceous (145-132 Ma zircon U-Pb ages). These temporally episodic magmatic events related to the eastern Gondwana assembly and the subsequent Gondwana break-up are responsible for the magmatism in the AMC of northeast India.
- Mantle peridotites of ophiolites of the Indo-Myanmar Orogenic Belt, northeast India underwent multiple episodes of partial melting, depletion, enrichment, and refertilization processes during the evolution of the Tethyan oceanic lithosphere, at a tectonic setting that changed in time from a mid-oceanic ridge to a forearc spreading setting. The undepleted lherzolite,

depleted harzburgite, and highly depleted dunites are all related to increasing degrees of depletion due to partial melting and melt-rock reactions.

- Detrital apatite and zircon Fission Track (AFT/ZFT) ages of the Siwalik Group of the Kumaun-Garhwal region, northwest Himalaya suggest that the sediments of Siwalik Group were never buried below the temperature range of 90° to 100°C and remain as unreset to retain a signal of source area exhumation. It further suggests that the Higher Himalaya Crystalline and Lesser Himalaya Sequence exhumed rapidly and slowly respectively at least since the deposition of the middle Siwalik (9-4 Ma) till the present.
- A ~15 m thick, fine-grained volcanic section, comprising frambooid aggregates has been identified from Indus Suture Zone, Western Ladakh Himalaya. Applying laser Raman spectrometry on the sediments, a combination of broad peaks spectrum is noticed at 1300-1600 cm⁻¹, attributed to amorphous carbonaceous matter.

Mantle upwelling, fluid circulation, metasomatic processes – Implications on fluid-rock interaction

- The investigations reveal that the migmatites of the North Himalayan (Leo Pargil) Domes have reached the metamorphic peak at around 30 Ma and was followed by decompression/exhumation leading to muscovite-dehydration melting as well as by water-fluxed melting reactions. The U–Pb geochronology and εHf record separate clusters of ages on the concordia plots of the migmatites are 1050–950 Ma, 850–790 Ma, and 650–500 Ma.
- A fluid inclusion study in migmatites (Leo Pargil) shows that the monophasic inclusions are pure CO₂ fluid. The fluid inclusion and thermodynamic study of migmatites suggest an initial isothermal decompression.
- The mineral and melt inclusion phases in ijolite of the Sung Valley ultramafic–alkaline–carbonatite complex (UACC) of Meghalaya suggest localized changes in oxygen fugacity due to redox reactions in the lower crust. The presence of crystallized carbonate–silicate melt as calcite, diopside, phlogopite, magnetite, apatite, and andradite suggests the presence of “nano-calciocarbonatites” in the ijolites.

- The P–T–X (Fe–Mg) phase relation of the Cumingtonite-sillimanite-cordierite-quartz-H₂O equilibrium in natural assemblages has been constructed considering the chemical system FeO–MgO–Al₂O₃–SiO₂–H₂O (FMASH system).
- Retrograde dehydration reaction of Pre-Himalayan pyroxene bearing Xenolith, Sutlej valley, NW Himalaya is demonstrated using P-T pseudosection modeling. The study shows that clinopyroxene and orthopyroxene were retrograded into hornblende and cumingtonite, respectively, during the cooling and exhumation of the terrane.
- The mineralogical, geochemical, and isotopic studies of the MMEs and Ladakh granites suggest that they were formed in an active continental margin, which was related to the collisional event between the Indian and Eurasian plates. The W–Zn–Co mineralization in MEs and host Ladakh granitoids batholith is related to the subduction via the metasomatism and fertilization of the mantle lithospheric mantle by the subduction of the Neotethyan slab.

Subsurface interpretation – Development of ML approach to geoscientific data from Himalaya and adjoining regions

- Critical analysis of 3D seismic data decoded the textural response of subsurface sediments in the Upper Assam foreland basin. The textural characteristics of the Oligocene Barail coal-shale unit are observed to be associated with deformed, wavy, chaotic, and heterogeneous texture indicating a deeper basinal condition prevailing during the deposition. Whereas, the overlying Miocene Tipam sandstone unit is associated with less chaotic and high homogeneity textures (molassic type), indicating a fluvial environment during the settlement.
- A 3D lithological model for the Lakadong-Thera (LT) formation in the Upper Assam basin has been prepared using a synergetic approach of the Walsh Transform and bed boundary demarcation technique. The analysis demonstrated that the model generated from Walsh boundaries is heterogeneous in nature. The Walsh-based approach was able to discriminate thin beds of the order of 3.2 m. This proposed bed boundary assessment technique is helpful in understanding

the position of subsurface rock layers as well as possible thick and thin beds.

Geometry and rheological assessment of the MHT, lithospheric flexuring - Implications toward seismogenesis, deep earth processes

- The shear wave velocity structure is obtained in the north-east Himalaya and Indo-Burma Ranges (IBR) regions using the surface wave earthquake data. The Bengal basin shows shear wave velocity as low as 1.7 km/s in the uppermost crust and ~4.7 km/s in the uppermost mantle beneath the Eastern Himalayan Syntaxis. The lowest group velocities in the Bengal basin suggest thick layers of sediments. Low velocities in the lower crust and uppermost mantle for the paths towards the Indo-Eurasia collision zone and northern part of IBR may indicate the presence of partial melting.
- Source parameter study using 50 local earthquakes in the Kumaon Himalaya reveals that the estimated seismic moments ($10^{12} \leq M_0 \leq 10^{16}$ N-m), source radii ($0.3 \leq r \leq 1.3$ km) and stress drops ($0.1 \leq \sigma \leq 40.6$ bar) respectively. The values are significantly lower than the overall values for the Central Seismic Gap showing incomplete dissipation of the accumulated stress in the region.
- The P-wave receiver function images show ~40-54 km thick crust beneath the Lohit Valley, whereas crustal thickness varies from ~38 km to ~50 km in the Siang Window. The MHT is identified at ~20-25 km depth beneath the Lohit Valley. However, the MHT is not visible in the Siang Window plausibly due to large-scale crustal deformation related to the formation of the Window and antiform folding.
- Magnetotelluric (MT) and Electrical resistivity tomography (ERT) Surveys have been conducted in different parts of NW Himalaya. Resistivity distribution across the MCT region along the Bijnaur-Mallari profile (Garhwal Himalaya) and the Nahan-Kourick Changu profile (Satluj Valley) is significantly different implying the role of differential tectonics.

Seismicity and seismic hazard assessment in the Himalaya

- Modeling of strong ground motion in the Uttarkashi and Chamoli regions of Uttarakhand shows simulated Peak Ground Acceleration of 231 and

347 cm/s² for the Uttarkashi and Chamoli regions respectively.

- The Spatial distribution of local earthquakes in the Siang Window of Arunachal Himalaya shows that the western part of the window is more active compared to the eastern part. The earthquakes are confined down to a depth of ~40 km.
- A probabilistic hazard assessment map of the earthquake-induced landslides corresponding to the great earthquake has been proposed for the Goriganga Valley, Kumaun Himalaya. It has been noted that ~ 25 % of the study area is susceptible to earthquake-induced landslides.
- A shear wave velocity model was obtained for the Garhwal Himalaya, which is comprised of 8 layers of the crust with a mid-crustal low-velocity layer (MC-LVL) between 10 and 20 km depth in the proximity of MCT (Main Central Thrust). The Moho depth was estimated at 46 km depth.
- Intra-crustal low velocity and thick mantle transition zones have been identified in the Garhwal-Kumaon Himalaya. The crustal thickness varies from 42 km to 54 km in the study region. The depth of the intra-crustal low-velocity layer, observed beneath the recording stations varies from 9 to 25 km.

Biotic evolution with reference to Indo-Eurasian collision – Evidences for global events

- The stable isotopes of carbon and oxygen on dental enamel of extinct herbivore mammals from Nurpur, H.P. have been studied for the first time to reconstruct their diet, habitat, and climatic change.
- A very rare madtsoiid snake has been reported for the first time from the Late Oligocene of India (the molasse deposits of Ladakh Himalaya).
- The fossil anguimorphs and snakes are documented from Haritalyangar locality, Bilaspur District (H.P.) for the first time, and helps to partially fill the gap in the knowledge of the Miocene fossil squamate record.
- New remains of sharks, ray fishes, and crocodiles have been recovered from the Middle Eocene deposits of Sylhet Limestone of Mikir Hills.
- Miocene planktonic foraminifers were recorded for the first time from the Surma Group in the foothills

of the Naga Schuppen Belt of the Indo-Myanmar Range.

- The modern pollen from Garhwal Himalaya has been identified that has established a modern pollen-vegetation relationship in the region.

Climate variability and landscape responses in selected transects of NE and NW Himalaya

- Detrital zircon and ϵNd data support for continuous sedimentation model, rule out the presence of unconformity within the Lesser Himalaya, and argues for separate evolution of the Lesser Himalayan basin on the trailing edge of the extended north Indian craton.
- Detailed rock magnetic study of Indus Molasses indicates fine-medium grained, pseudo-single domain magnetite as a dominant, and pyrrhotite and greigite as accessory magnetic minerals, suggesting their deposition over well-developed paleogeography with small-scale tectonic modulations.
- The loss of glacial area, ice volume, glacier recession, and the changes in the Equilibrium Line Altitude (ELA) was calculated by multi-year satellite images from 1990 to 2021 over Yankti Kuti valley of Kumaon Himalaya. The result showed an overall reduction of ~21 km² (~21%) of the total glacier area with an ice volume loss of ~25 km³ and ~46 ± 13m upward shifting of the Equilibrium Line Altitude (ELA) between 1990 - 2021. The average retreat rate of the glaciers shows a range between ~ 18 to 41 m per year.
- High latitude climate played a major role in the onset of Heinrich event 2, however the termination was triggered mainly by low latitude forcings such as the weakening of the South American monsoon.
- First aerosol morphological and elemental compositions from Gangotri Glacier Valley in the pristine Himalayan Glacier Valley show a range of forms, including spherical, irregular, layered, aggregated, flaky, fractal, and others. The air around Valley contains fluorine, oxygen, carbon, silica, sodium, aluminium, magnesium, sulphur, iron, zinc, potassium, calcium, barium, and phosphorus during the study period.
- Sedimentation in the Lower Assam foreland occurred in three phases in response to sea level

fluctuations. Sediment petrography combined with Sr-Nd isotopes suggests Higher Himalaya was a dominant sediment source since 8ka.

Ecology and climate dynamics of the Himalaya – Cenozoic to Present

- Tree-ring-based March-June temperature record from Dokriani glacier shows a negligible rise during 1901-1989 CE, however, captured a warming spike from 1990 CE that continued in the 21st century, which is also evident in the Northern Hemisphere temperature record. Moreover, the temperature rise is not anomalous in the past 231 years and is well within the range of the rest of the series.
- Produced the millennial to centennial-scale Indian summer monsoon (ISM) records during the Late-Pleistocene from the Baspa Valley, NW Himalaya. The study reveals the periods of strengthened ISM during ~15 to ~14 ka, ~10 to ~7 ka, ~2.4 to ~1.3 ka, and 243 yr BP and phases of weakened ISM during ~20 and ~15 ka, ~14 to ~10 ka, ~7 to ~2.4 ka, and ~1300 to ~243 yr BP, respectively.
- The Mana peat section grain-size data corroborates the lithology, and the down-depth magnetic susceptibility (χ_{lf}) fluctuation is broadly parallel to the coarse-grained (sand) fraction. The χ_{lf} values are lower at portions, where the clay fraction is higher, which reveals the energy level of the depositional condition.
- Evaluating the feasibility of biosorption technique for heavy metals removal from aquatic systems.

Geological and geomorphic controls on landslide for risk assessment and zonation in the Himalaya

- Investigation on the subsidence-induced instabilities in the Dar village reveals that the village is situated on a slope comprising soft material having ~90 % finer particles (9.8% gravel, 74.9% sand, and 15.3% silt and clay) rich in disintegrated micaceous sediments having low cohesion and plasticity index.
- The Chakrata region of Uttarakhand has been investigated based on Permanent Scatterer Interferometric (PSI) time-series analysis, and morpho-tectonic study. PS-InSAR results show a cumulative displacement up to 157 mm, with a velocity of about 100 mm/year. The slides are well

correlated with anthropogenic activities like road cuttings, lithological control, or the tectonic boundaries in which shear zones are marked.

- The sinking and subsidence in the Joshimath region have been studied. A total of 148 scenes from 10th May 2020 to 21st September 2021 have been processed to create a time series of displacement in the Joshimath region. The PS-InSAR results show well-correlated displacements in places of Ravigram, Sunil, and the Gandhinagar region with a cumulative displacement of up to 197 mm and velocity of about 83 mm/year. The maximum displacement has been observed in Sunil village, 236 mm with a velocity of about 100 mm/year.

Glacial dynamics, glacier hydrology, mountain meteorology, and related hazard

- The estimated cumulative *in-situ* average net annual mass balance of Pensilungpa Glacier (PG), Suru river basin, Zaskar Himalaya is $\sim -5.8 \times 10^6 \text{ m}^3 \text{ w.e. a}^{-1}$ with the $-0.58 \text{ m w. e. a}^{-1}$ specific balance between 2021 and 2022. The depression of equilibrium-line altitude (ELA) was ~20 m between 2016 and 2022, and the present ELA is located at 5235 m asl.
- The elevation changes and surface flow distribution for 205 ($\geq 0.1 \text{ km}^2$) glaciers in the Alaknanda, Bhagirathi, and Mandakini basins, Garhwal Himalaya have been studied. The average thinning rate of Garhwal Himalaya glaciers was $0.07 \pm 0.09 \text{ m a}^{-1}$ from 2000 to 2015, and it increased to $0.31 \pm 0.19 \text{ m a}^{-1}$ from 2015 to 2020, with pronounced differences between individual glaciers. Between 2000 and 2015, Gangotri Glacier thinned nearly twice as much as the neighboring Chorabari and Companion glaciers, which have thicker supraglacial debris that protects underlying ice from melting.
- Ambient concentration and soil flux of greenhouse gases (CH_4 , CO_2 , and H_2O) has been traced near Karnal's Kuchpura agricultural fields using a Trace Gas Analyzer (TGA) and Soil Flux Smart Chamber. It is observed that waterlogged (i.e., irrigated and rain-fed) soil contributed lower CO_2 and CH_4 flux to the atmosphere compared to the field affected by the backfilling of rice husk ash (RHA).
- The daily, monthly, and annual discharge behavior of the Pindari Glacier (PG) and Kafni Glacier (KG)

of the Kumaun Himalaya have been investigated. The mean daily discharge shows very high fluctuations in PG and KG. The mean daily discharge in PG has ranged between $6.15 \text{ m}^3 \text{ s}^{-1}$ to $83.58 \text{ m}^3 \text{ s}^{-1}$, whereas, in KG, it ranges from $2.26 \text{ m}^3 \text{ s}^{-1}$ to $49.83 \text{ m}^3 \text{ s}^{-1}$ during 2017-19.

Hydrogeology: Himalayan Fluvial System & Groundwaters

- Eastern and Western Syntaxes and the headwaters of the Gandak basin serve as hotspots of erosion in the Himalaya, determining the sedimentary budget of the IGB Rivers. Despite occupying only 0.07% of the total exoreic continental area, these hotspots contribute ~8% of sediment to the global riverine sedimentary flux. They contribute ~100 million tons of dissolved solids and 1000-2300 million tons of particulate matter. In the wake of interlinking river projects in India, such supply of sediments will be hindered, and the equilibrium of erosion-sedimentation may shift toward the erosion of bordering land mass.
- Stable water isotopes of precipitation and catchment waters were used to understand the hydraulic relationship between the water sources in the Doon Valley. The study suggests a strong hydraulic connection between surface water and groundwater, and recharge through flow-paths with higher permeability. It is evident that stream/river beds maintain a high permeability when the phreatic water table rises, enabling them to connect with nearby aquifers.
- The solute acquisition and recharge mechanism of a few major karst springs in the Kashmir Valley were determined using major ions and stable water isotopes. The study suggests that karst springs are calcite/dolomite under saturated, acquiring solute content (except NO_3^- , Cl^-) by the carbonate and silicate mineralization. The study suggests that lagged effects of $\delta^{18}\text{O}$ (or $\delta^2\text{H}$) depleted winter precipitation signal and rapid response of $\delta^{18}\text{O}$ (or $\delta^2\text{H}$) enriched spring/summer rain events could serve as indicators of hydrologic processes associated with karst aquifers in the region.

Quantification of strain accumulation/release rate along the MHT at different time scales

- The Surin Mastgarh anticline (SMA) marks the active deformation front in the northwest Sub-

Himalaya near Jammu. The southern limb of the SMA is not truncated by an emergent thrust, unlike other frontal folds along the Himalayan front. The study suggests the existence of a weak, less viscous layer beneath a brittle sedimentary detachment. The SMA was initiated as a detachment fold and sequentially deformed by passive roof thrusting. Therefore, the seismotectonic model of the Jammu Sub-Himalaya is different from that of the central and eastern Himalaya.

- New thermochronological data from Lohit Valley, Arunachal Pradesh suggests a rapid phase of exhumation as a result of the latest phase out-of-sequence thrusting along the Walong Thrust zone in this region at ~3.5 My ago. The patterns of exhumation are in good correlation with the morphometry of the region. This linkage of exhumation and morphometry results suggests that the present-day topography of the Lohit Valley was established during the Pliocene-Quaternary period. The rapid exhumation in the eastern Lohit Plutonic Complex lies in a low-precipitation zone that clearly suggests tectonic is a prime driver of exhumation in this region.
- Geodetic studies on the deformation of frontal fault systems shed light on the reasons behind the change in the course of the river Ganges towards the south-east at Haridwar in conjunction with the uplift of Siwalik Hills. GPS study shows that the crustal blocks at either side of the river Ganges are moving in opposite directions; whereas the northwestern block moves predominantly towards SE against the southeastern block. Here, the southeastern segment of the Frontal HFT, close to the Ganga Tear Fault (GTF), is undergoing significantly horizontal shear strain as compared to its Northwestern segment. It has been observed that the style of kinematic deformation of the frontal HFT in the Garhwal-Kumaun region is distinct at the mountain as well as at the non-mountain fronts.

Academic Pursuits

During 2022-2023 a total of 149 research papers have been published in peer-reviewed SCI journals of national and international repute. In addition, 12 book chapters and two books entitled (i) “Active Seismic Tomography: Theory and Applications” authored by Sain, K. & Nara, D (Publisher: Wiley) and (ii) “Meta-Attributes and Artificial Networking: A New Tool for

Seismic Interpretation”, authored by Sain, K. & Kumar, P.C. (Publisher: AGU & Wiley) were published. The scientist of the Institute prepared 3 reports and 3 excursion/field guide books. The Institute published a biannual SCI journal “Himalayan Geology”. The impact factor of the journal in 2022 is more than 1.3. The Institute also published a Hindi Magazine “Ashmika” during 2022-2023.

The Academy of Scientific and Innovative Research (AcSIR) at WIHG takes the initiative in disseminating advanced knowledge in the field of geosciences by educating Ph.D. scholars through experienced scientists of WIHG. A total of 13 research scholars were awarded Ph.D. degrees and 8 theses were submitted by scholars during 2022-2023.

In other aspects of academic pursuits, the Institute made the laboratory facilities/analytical services to researchers of the Institute as well as for researchers from national institutions and universities. The Scientist of the Institute provided training to more than 200 Summer and Winter students leading to MSc/MTech dissertations. Several national and international visitors are benefited from the museum of WIHG, that has been made virtual also.

The Institute had the privilege of organizing the 3rd Triennial Congress of the Federation of Indian Geosciences Association (FIGA) at its premises in Dehradun during November 16-18, 2022. The congress provided a common platform to eight Geosciences Associations (viz. IGU, GSI, SPG, OSI, AEG, AHI, PSI, and ISES) and seven Geosciences institutions/ministries (MoES, NCESS, AMD, CSIR-NGRI, IIG, KDMIPE-ONGC, WIHG) to discuss the role of geosciences on the societal challenges for sustainability and socio-economic development, and recommended policies for implementation at national and

international levels. The congress was preceded with a short course on Artificial Intelligence and Machine Learning (AI/ML) and followed by a post-congress field visit along the Himalayan mountain front in the Mohand-Dehradun-Mussoorie section.

The Institute also organized the 6th National Geo-Research Scholars Meet (NGRSM)-2022 jointly with the University of Ladakh at its University premises at Leh during 7-10 June 2022. WIHG has signed an MoU with Ladakh University to create WIHG-Annex within their Campus for strengthening University-Institute link on Geo-science education and area-specific research. A total of 93 geo-research scholars from 48 national Institutions, Universities, IITs, IISc, and IISER all over India with eminent resource persons attended this event of national importance. The Institute has organized 1-Day Indo-Norwegian Webinar on geo-hazards and resources on June 1, 2022 as well as convened 1-Day Indo-Russian Webinar on Seismic Forecasting on June 30, 2022.

Other highlights

The Institute participated in exhibition programs held at different places and displayed its scientific exhibits at various forums. The Institute organized several awareness programs related to earthquake hazards. The scientists have received several awards/fellowships and honors in recognition of their scientific achievements. The Institute employees participated in the 'Swacchata Abhiyan' on October 02, 2022. The Institute also celebrated the Hindi Pakhwara from 14 Sep to 28 Sep 2022. The Institute followed the Rajbhasha guidelines and issued general orders, circulars, and notices in bilingual form. All national festivals were celebrated with great enthusiasm and utmost manner.

Kalachand Sain
Director

ACTIVITIES

Activity:1A

Geodynamics of Indo-Eurasian collisional zone - Crustal evolution, carbon sequestration and mineralization

(A.K. Singh, Barun K. Mukherjee, Paramjeet Singh, Pratap Chandra Sethy, M. Rajanikanta Singh and Kunda Badhe)

Gondwana assembly and break-up magmatism in the eastern Himalaya

Studies over the last few decades have brought forth a wide range of magmatic records from different pockets of the Himalayan regions and correlated to events of the Columbia supercontinent cycle, followed by Rodinia, Gondwana, and Pangea. The advancement of the zircon U-Pb dating method and the evidence of older magmatic records flowing in the Himalayan region continue to attract enormous attention from various researchers. The Abor magmatic rocks in the Siang Window located in the southern part of the eastern syntaxis (Namche Barwa) is one such region that has remained controversial for a long for its formation age. The Abor magmatic rocks are grouped into i) mafic volcanic including basaltic flows, agglomeratic basalts, sills, and dykes with minor tuffs, volcanic breccias, lapilli, and pillow basalt; ii) felsic volcanic, such as rhyolite, dacite, and welded tuff; and iii) mafic intrusives, including gabbro and diorite. Petrogenesis and geodynamic implications of these magmatic rocks are poorly understood due to the lack of advanced geochemical and geochronological data. Previous research mainly focuses on basaltic rocks (mafic volcanic), with a few works on the associated felsic volcanic and mafic intrusive rocks. Over the last few decades, the crystallization ages of these magmatic rocks have remained controversial and far from well understood. Some researchers believed that these magmatic rocks formed during the early Eocene coeval with the initiation of the Himalayan orogeny (Acharyya, 2007). Others favored Permian ages associated with the rifting of the Cimmerian continent off the northern Gondwana margin during the late Paleozoic (Bhat & Ahmad, 1990). These ages depended solely on the limited lithostratigraphic, biostratigraphic, and paleomagnetic data. A major turn in the debate came recently with precise age reports of zircon U-Pb dating, claiming that Abor magmatic rocks were formed at 132 Ma owing to the Kerguelen mantle plume activity during the eastern

Gondwana break-up. So far, no whole-rock isotopic (Sr-Nd) ratios and zircon U-Pb geochronological data have been generated for the area except for the varying K-Ar ages from the basaltic rocks (319, 87, and 24 Ma). Moreover, the petrogenetic relationship between the different magmatic rocks is not adequately studied. With these research gaps, a comprehensive geochemical, geochronological, and isotopic dataset on the mafic intrusive and felsic volcanic rocks from the Abor magmatic rocks of Eastern Himalaya has been discussed in this present work. Since a major region of greater India was subducted during the Himalayan orogeny, these rocks will provide significant information and contribute to our understating of the geological evolution of this region before the Himalayan orogeny.

The mafic intrusives rocks are subalkaline/tholeiitic ($Nb/Y < 0.65$), with high TiO_2 (1.63–3.42 wt.%) and Ocean Island Basalt to Enriched Mid Oceanic Ridge Basalt affinities. Zircon U-Pb geochronological studies yielded late Cambrian to early Ordovician crystallization ages (500–473 Ma) for the mafic intrusive rocks (Fig. 1). A relatively narrow range of initial $^{87}Sr/^{86}Sr$ (0.703887–0.705513), $^{143}Nd/^{144}Nd$ (0.511978–0.512118), and $\epsilon Nd(t)$ (-0.323 – +2.43) of the mafic intrusives suggest fractional crystallization with negligible crustal contamination, generated by low degree (~3–13%) partial melting of an enriched mantle source (garnet and spinel lherzolite) in an extensional environment (Fig. 3).

Whereas, zircon U-Pb geochronological studies of the felsic volcanics indicate their emplacement during the early Cretaceous (145–132 Ma) and are characterized by A-type felsic affinities with high SiO_2 (66.28–73.2 wt.%) enrichment in LREE, LILE, low MgO (0.38–1.17 wt.%) and TiO_2 (0.43–0.68 wt.%) depletion in HREE, negative Eu-anomaly ($Eu/Eu^* = 0.48–0.73$), high initial $^{87}Sr/^{86}Sr$ (0.707878 to 0.717650) and negative $\epsilon Nd(t)$ (-14.35 to -9.21) (Figs. 2, 3). The felsic volcanics were formed by the interaction between high-temperature upwelling OIB-type basaltic magmas and crustal materials at shallow crustal levels.

The present study indicates that the mafic intrusives rocks of Abor magmatic rocks formed at 500–473 Ma. This age is coeval with the early Paleozoic magmatism along the Himalaya-Tibetan regions, which is regarded

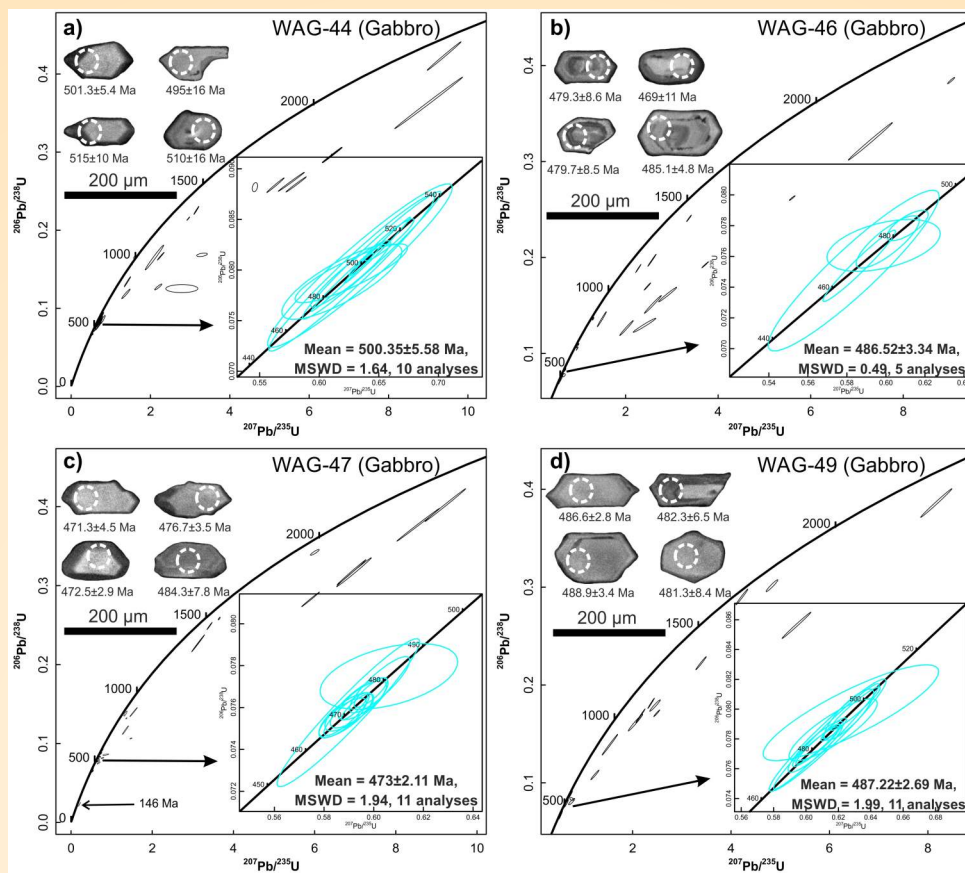


Fig. 1: Concordia curves of zircon U-Pb dating for the mafic intrusive rocks (gabbro): (a) WAG-44, (b) WAG-46, (c) WAG-47 and (d) WAG-49 of Abor Magmatic rocks, Siang Window, eastern Himalaya, northeast India; the insets show the representative cathodoluminescence (CL) images of the analyzed zircon grains. MSWD – mean square of weighted deviates.

as the final event in the amalgamation of the Gondwana supercontinent. There are two contrasting hypotheses for the evolution of this event: (1) formation of an Andean-type active continental margin at the northern Gondwana, when the proto-Tethyan oceanic crust was being subducted southward, and (2) the northern Gondwana margin which was a passive continental margin and magmatism occurred in a post-collisional extensional environment after the amalgamation of Gondwana. The data of the present study better supports the latter hypothesis as the investigated rocks are unlikely to have formed from Andean-type subduction magmatism. The theory of passive continental margin origin via intraplate rifting of our mafic samples is proposed based on geochemical evidences. The samples have strong characteristics of E-MORB to OIB, which forbids the possibility of a subduction origin. Furthermore, Nb is usually depleted in subduction zone magmas, but our mafic samples do not show such an anomaly. The mantle source modeling further suggests partial melting of the primitive-type mantle with garnet

in the source, which supports a deeper mantle melting related to a plume source. The available evidence collectively suggests that the studied mafic samples were generated in an intraplate tectonic setting at the passive continental margin of Gondwana after the termination of the southward subduction of Paleo-Tethys. The possibility of a subduction origin for the samples in an Andean-type continental margin is also disregarded by the absence of coeval intermediate rocks (andesite). Usually, Andean-type active continental margin magmatism in other places is dominated by intermediate rocks, followed by basalt, rhyolite, and granite. However, the early Paleozoic rocks along the northern Gondwana margin area are dominated by felsic rocks (granite) with a minor amount of mafic rocks. All these observations indicate that the early Paleozoic magmatic rocks of Himalaya-Tibetan regions, including the investigated mafic intrusives, formed in a post-collisional extensional environment affected by a plume upwelling at the passive margin along the northern margin of Gondwana (Fig. 4).

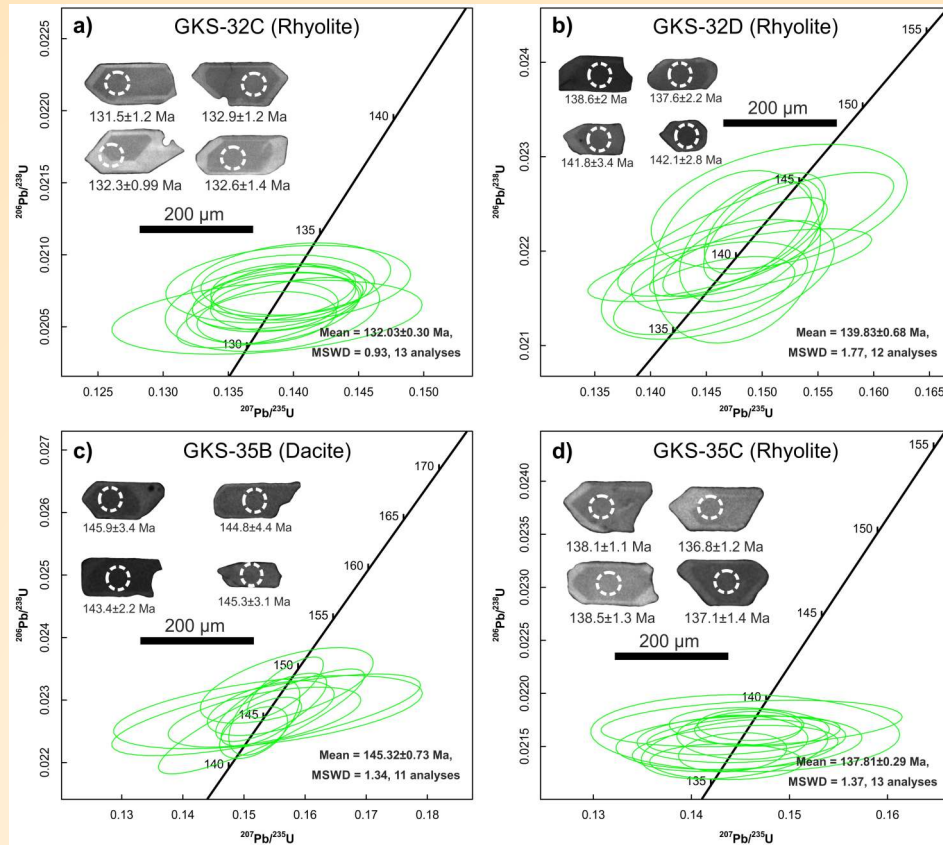


Fig. 2: Concordia curves of zircon U-Pb dating for the felsic rocks: (a) GKS-32C, (b) GKS-32D, (c) GKS-35B and (d) GKS-35C of Abor Volcanics, Siang Window, eastern Himalaya, northeast India; the insets show the representative cathodoluminescence (CL) images of the analyzed zircon grains. MSWD – mean square of weighted deviates.

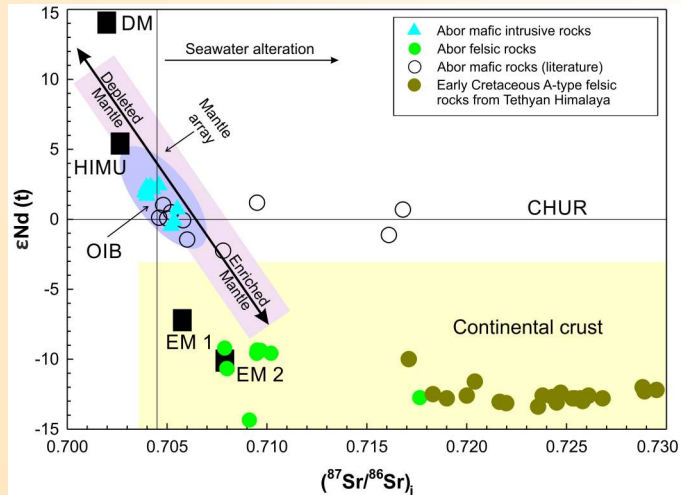


Fig. 3: $\epsilon\text{Nd}(t)$ vs. $(^{87}\text{Sr}/^{86}\text{Sr})_t$ diagram for the mafic intrusive and felsic rocks of Abor Volcanic, Siang Window, eastern Himalaya, northeast India. Mantle components such as DM (depleted mantle), HIMU (high μ or U/Pb), EM 1 (enriched mantle I), OIB (ocean island basalt), EM 2 (enriched mantle II), and mantle array and continental crust field are shown for comparison. The present values of the bulk-silicate earth (BSE) and chondritic uniform reservoir (CHUR) are also shown.

The breakup of eastern Gondwana led to the formation of the Indian Ocean (Fig. 5). The Kerguelen mantle plume has been considered the driving force behind this breakup, as witnessed by the wide distribution of early Cretaceous igneous rocks along the continental margin of SW Australia, eastern India, and Tethyan Himalayas (Fig. 5). Recently, it has been estimated the potential mantle temperature of the early Cretaceous OIB-type basalt from the Cona area of eastern Tethyan Himalayas to be 1502–1560° C, which suggested that a mantle plume did exist underneath the circum-eastern Gondwana during the early Cretaceous. Moreover, paleomagnetic data for the late Jurassic to early Cretaceous igneous rocks of the circum-eastern Gondwana suggests that the original locations of this magmatism were 48.5–55.5° S, which is also consistent with the reconstructed eruption center of the Kerguelen mantle plume (Fig. 5).

A broad mushroom-shaped Kerguelen 'plume head' formed when the plume reached the lithospheric mantle, leading to surface uplift as a consequence of the vertical

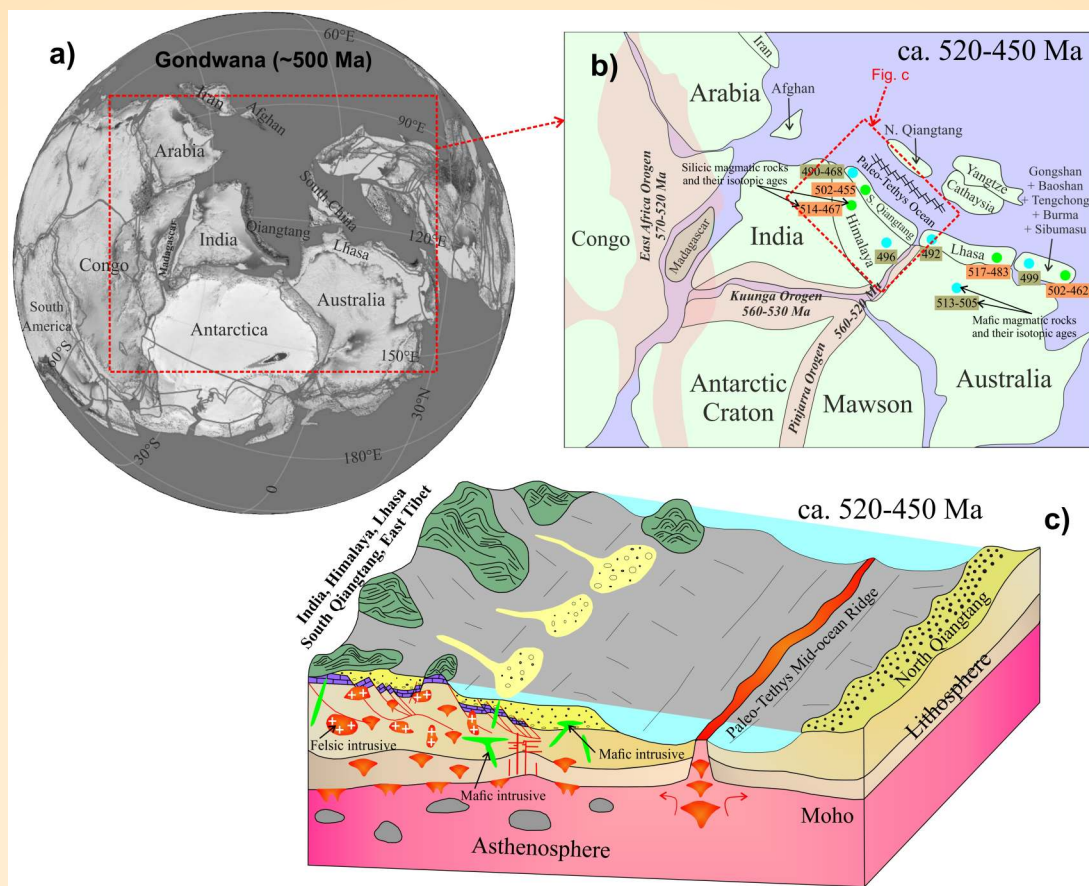


Fig. 4: (a) Paleogeography reconstruction during Gondwana assembly (~ 500 Ma) using GPlates (<https://www.gplates.org>) reconstruction framework. A combined rotation file of Müller et al., 2019, *Tectonics*, 38, 1884-1907 and Cao et al., 2022, *GR*, 102, 3-16 was used for the reconstruction. (b) Reconstruction of Gondwana at ~500 Ma showing the location of the proposed early paleozoic extensional tectonic environment and timings of major orogenic belts (modified from Cawood et al. 2007, *EPSL*, 255, 70-84 and references therein), (c) Cartoon showing the formation mechanism of the early paleozoic magmatism in the present study area.

thermal expansion of the crust due to heating and plume pressure. This plume initiated large-scale extension and development of deep normal faults leading to thinning of the overlying lithosphere (Fig. 5c), which further caused the separation of the Greater Indian Plate from the Australian Plate along with seafloor spreading and formation of OIB-type alkali basalts. This was probably the timing for the initial impact of the plume on the plate margin, thereby producing a Large Igneous Province (LIP), for which heat from the Kerguelen mantle plume aided the melting along the circum-eastern Gondwana. Due to this activity, mantle-derived mafic magmas passed through the sub-continental lithospheric mantle (SCLM), producing Light Rare Earth Elements (LREE)-enriched basalts of the Abor magmatic rocks (such as alkaline basalts). The remaining melt underwent fractional crystallization and assimilation from the crustal wall and formed the felsic rocks of this study. The continued impact of the plume led to

magmatism of the Rajmahal-Sylhet Traps, Southern Kerguelen Plateau, and Wallaby Plateau at ~120–110 Ma.

The further outpour of the plume and spreading led to the formation of the Central Kerguelen Plateau (105–100 Ma) and Broken Ridge (100–95 Ma). The Ninety-east Ridge (82–37 Ma) might represent the plume 'tail' which was followed by a gradual decline in the plume activity probably caused by the thick lithosphere in the Kerguelen Plateau (Northern Kerguelen Plateau, Kerguelen Archipelago and Heard and McDonald Island; 40–0 Ma). Therefore, it can be concluded that two episodes of pre-Himalayan orogeny are discovered from Abor magmatic rocks of Siang Window, Eastern Himalaya syntaxis, northeast India. The initial impact of magmatism at the Siang window occurred at ~500–473 Ma as a passive margin extensional environment coeval with the process of

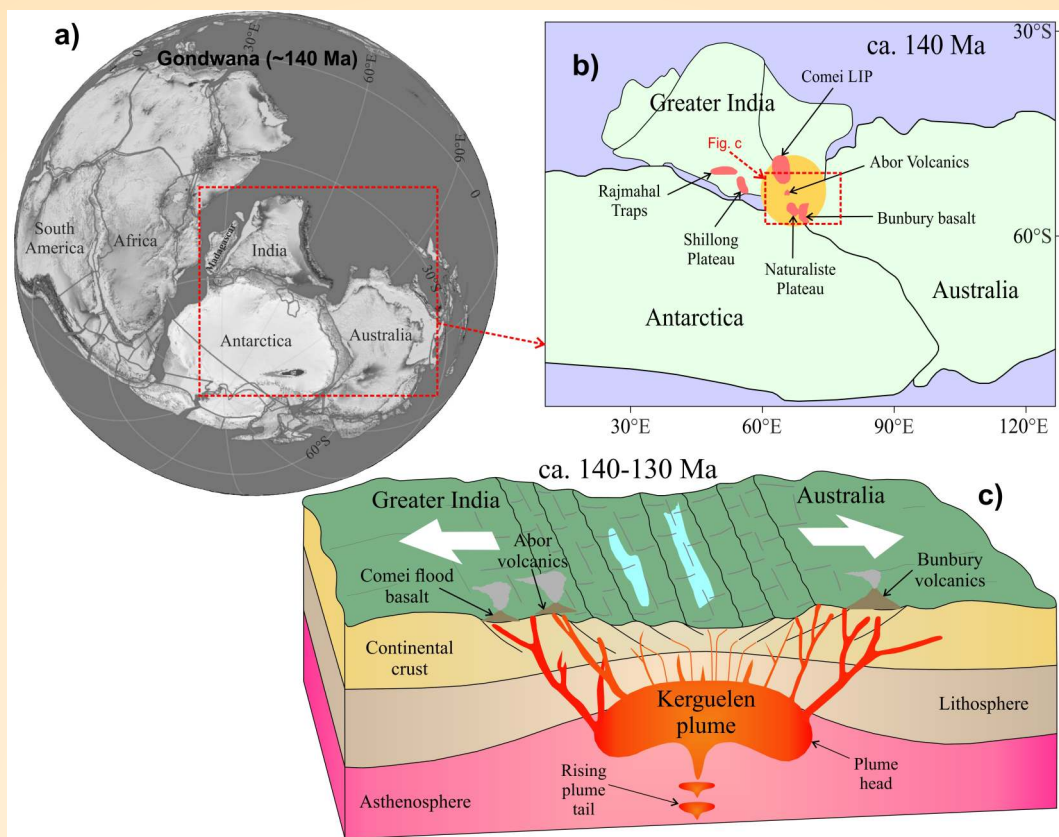


Fig. 5: (a) Paleogeography reconstruction during Gondwana breakup (~ 140 Ma) using GPlates reconstruction framework (<https://www.gplates.org>). A combined rotation file of Müller et al., 2019 and Cao et al., 2022 was used for the reconstruction. (b) Plate tectonic reconstruction of eastern Gondwana at ~140 Ma (modified after Zhu et al., 2008) and (c) Cartoon showing the break mechanism of eastern Gondwana at ~ 140 Ma; see text for explanation.

Gondwana assembly. The second phase of magmatism, probably with more aggressive volcanism, impacted the Eastern Himalaya at ~145-132 Ma due to the Kerguelen plume upwelling and the Gondwana break-up.

Exhumation and Provenance history of Siwalik Group of Kumaun region, NW-Himalaya using Detrital Fission Track Thermochronology

Fission Track (FT) Thermochronological analysis of detrital apatite and zircon derived from the lower and middle Siwalik Group of the Himalaya allows the reconstruction of the long-term exhumation history of the Higher Himalayan Crystalline (HHC) and Lesser Himalayan Sequence (LHS), and also the provenance of the Siwalik sediments. Along the entire length of the Himalayan Mountain belt, the Paleogene-Eocene sediments are exposed in the frontal part of this fold-thrust belt. The provenance and transportation of these Paleogene sediments (such as the Subathu, Dagshai and Kausali formations) and Eocene sediments exposed as the Siwalik group were transported from the different lithotectonics units. Similarly, during the Himalayan

orogeny, the sediment eroded from different source areas and traveled towards the south, accumulating in the sub-Himalayan foreland basins (Jain et al., 2009). To study the provenance and exhumation history of the Siwalik Group of the Kumaun Himalaya, A total of 14 detrital apatite and zircon Fission Track (AFT/ZFT) ages of lower and middle Siwalik subgroups have been obtained. Detrital FT ages suggest that all sandstone samples were never buried below the temperature range of 90° to 100°C and remained as unreset to retain a signal of source area exhumation. AFT age 4.4 ± 0.5 Ma, obtained from close proximity to the Main Boundary Thrust (MBT) footwall is completely reset and indicates the reactivation of MBT during the Pliocene Period. This study revealed that the provenances of Siwalik sediments are located majorly in the MBT hinterland areas and the nearest sources are Amritpur granite, the outer Lesser Himalayan meta-sedimentary (LHMS) zone, Almora klippe, Ramgarh thrust sheet, and the overlying Tethyan Himalayan Sequence (THS).

The mean exhumation rate of the source region has been estimated by dividing the estimated depth of

closure temperature of the used thermochronological system by the lag time. In our case, assuming a geothermal gradient of $\sim 35^\circ\text{C/km}$ and a mean surface temperature of 0°C , as estimated in the northwestern Himalaya, and a closure temperature for the AFT system of 110°C , a depth of closing isotherm can be estimated $\sim 3\text{ km}$. Considering the mean AFT lag time of $\sim 2.8\text{ Ma}$ and $\sim 1.6\text{ Ma}$ (mean lag time of P_1 populations) within the lower and middle Siwalik respectively, we obtain a mean exhumation rate of $\sim 1.1\text{ mm/yr}$ during 11 to 10 Ma in the lower Siwalik and $\sim 2\text{ mm/yr}$ between 9 and 4 Ma in the middle Siwalik. The AFT age of the sample BR-5a located along the transverse fault has been reset at $\sim 4\text{ Ma}$ due to thermal heating of the

transverse fault formed during the reactivation of the MBT at 5 to 4 Ma in the Kumaun region (Singh & Patel, 2022). ZFT lag time of P_1 peak within the middle Siwalik ranges between 1.1 and 3.3 Ma with a mean lag time of 1.7 Ma. Bedrock AFT and ZFT ages available from the HHC zone (Fig. 6a) in the Kumaun region (weighted mean AFT and ZFT ages of 1.6 ± 0.1 and $1.8 \pm 0.4\text{ Ma}$ respectively) are comparable with the AFT and ZFT lag ages (Average AFT and ZFT P_1 Peaks: 1.6 and 1.7 Ma respectively) which attribute to being derived from the HHC zone in the vicinity of the MCT, with the exhumation rate of $\sim 2.8\text{ mm/year}$ during 11 to 4 Ma (Fig. 6b).

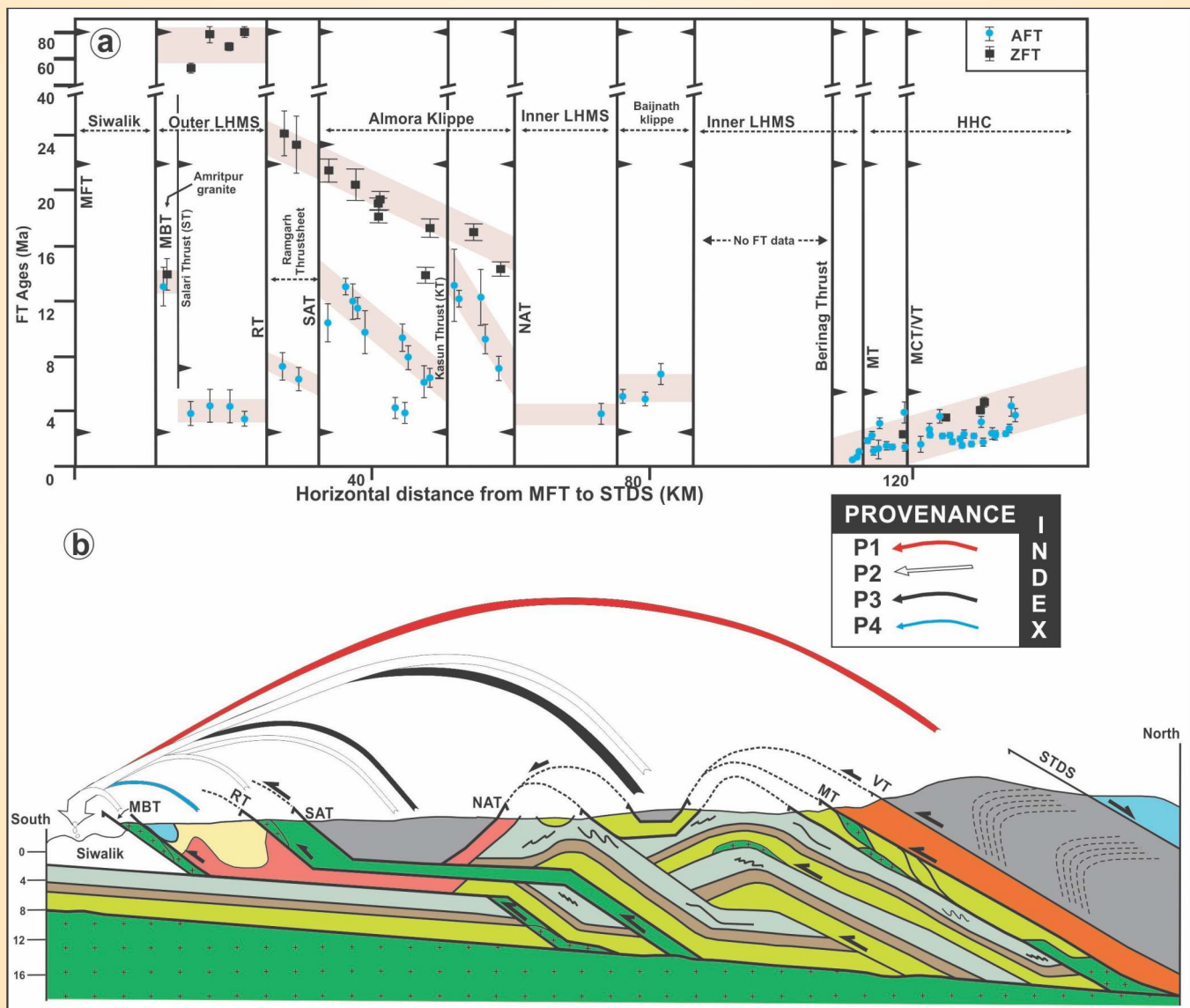


Fig. 6: (a) Plot showing the FT ages (Ma) versus horizontal distance from Main Frontal Thrust MFT to STDS (in Kms), (b) cross-section of Kumaun region of NW-Himalaya (after Singh & Patel, 2022) showing the reconstruction the Siwalik foreland basin from the Miocene to Pliocene period.

It is considered that the MCT was developed during ~24 Ma, there was a significant rise in sedimentary load in the Siwalik basin in the Kumaun-Garhwal region. Rapid erosion of the source region(s) continued during 12 to 4 Ma is supported by the short, nearly instantaneous lag time of the lower and middle Siwalik rocks. Similar rapid erosion of the source region has been described during the deposition of lower Siwalik but a progressive slowdown (~12 Ma) in the erosion rate of the source area during the deposition of the middle Siwalik. On the other hand, rapid erosion of the HHC source can be linked with the activity of the Lesser Himalayan duplex (LHD) developed over the MHT ramp below the MCT zone in the Kumaun region which resulted from the uplift of the HHC rocks. Synchronously, a major accommodation of the India-Asia convergence was occurring due to the reactivation of faults like the Ramgarh Thrust as southward thrusting, the North Almora Thrust as northward back-thrusting and the South Almora Thrust as top-to-north normal faulting (Patel et al., 2015; Singh & Patel, 2017). These source areas can be attributed to the development of the local drainage network in the Ramganga-Kosi drainage basin only draining the region during late Miocene to Pliocene (i.e. ~9 to 4 Ma). Based on detrital FT datasets, it has been envisaged that different tectonic activities in the MBT hinterland area between the Miocene to Pliocene Periods cause the tectonic upliftment and exhumation of source areas, and supply the sediment to the Siwalik foreland basin.

Biogenic imprint in Himalayan ophiolitic-melange

Identifying biosphere and biogenic sediments is ubiquitous in marine environments. And such environments are commonly observed in deep-sea carbonates, deep-sea siliceous deposits, hemipelagic silica-rich deposits, shelf carbonate deposits, lagoonal carbonate muds, etc. These interpretations show complexity when it is linked to the deep earth sediments, especially those recovered from the ophiolite-melange, this has potential importance for the reconstruction of paleo-ocean environment. Recent studies have shown the presence of bioactivity in deep marine volcanic sediments, through which substantial fluid flow occurs, providing the possible occurrences of the past massive deep biosphere. As proof of the deep biogenic realm in the volcanic sediments, an exotic volcanic section in the ophiolite melange of the Indus Suture Zone has been studied. The study involves mineralogy, mineral chemistry, and isotopic traces of fine-grained tuffaceous rock. In support of the presence of bioactivity imprint that might have been preserved in ophiolite sediments, special emphasis has been given to

the observed rare vesicular microstructure, with the aid of non-destructive techniques including Scanning Electron Microscope (SEM), Energy Dispersive Spectrometry (EDS) and Raman Spectroscopy. In the Kargil section, a ~15 m thick isolated patch of volcanic tuff, shows a dull appearance, fine-grained and prominent scaly fracture, reflecting diverse chemistry comprising silica, carbonates, TiO_2 phases, pyrite, and iron oxides. Upon microscopy, clusters of silicic vesicles have been noticed, showing spheroidal to lenticular shell structure. The vesicle walls composed of carbonaceous matter appear to be replaced by a later pyritic octahedral crystallite cluster. Applying Raman spectrometry on the vesicular wall, a mix of Raman spectra at the higher band between 1100 to 4000 cm^{-1} arises, which is attributed to amorphous organic matter and microbe, mixed with prominent D- G and defect bands. The presence of microbial elements, biominerals (pyrite), phosphorus cation signals, and the negative fractionation of organic carbon stand as evidence for life mediate transformation of FeS to FeS_2 . The Cretaceous volcanism hence favored hosting biosphere in the vanishing Neo-thetan ocean floor. Through this study, a new evidence of a biosphere hosted in volcanic tuff rocks formed in the recess of the Neo-Tethyan ocean floor will be provided, which is present as a suture zone rock in the youngest orogeny on the Earth's surface.

Activity: 1B

Mantle upwelling, fluid circulation, and metasomatic processes—Implications on fluid-rock interaction

(Koushik Sen, S.S. Thakur, Saurabh Singhal, Aditya Kharya and C. Perumalsamy)

Samples of the oldest Tethys oceanic crust (ophiolites) have been collected from the Spongtang region of the Ladakh area to study the mineralogy and geochemical aspects of ultramafic rocks. Various aspects of the metamorphism of NW Himalaya have been studied during the reporting period.

Migmatites of the North Himalayan (Leo Pargil) domes formed by partial melting of different structural levels of the Indian continental crust during a major Himalayan tectonic event. Their petrologic study helps to know the anatexis and tectono-thermal processes related to the Himalayan orogeny. The P-T conditions of migmatitization have been calculated in the $\text{MnO-Na}_2\text{O-CaO-K}_2\text{O-FeO-MgO-Al}_2\text{O}_3\text{-SiO}_2\text{-TiO}_2\text{-H}_2\text{O}$ (MnNCKFMASH) Phase equilibria system, which indicate the peak P-T conditions of 770–790 °C,

9.3–10.5 kbar for the amphibole + biotite migmatite (Fig. 7) and of 780–820°C, 9.3–9.8 kbar for the sillimanite-bearing migmatite (Fig. 8). The monophase inclusions show the eutectic temperature from -56.8 to -56.6 °C, and -56.9 to -56.6 °C for primary and secondary inclusions, respectively, suggesting pure CO₂ fluid (Goldstein and Reynolds, 1994, Kharya et al., 2020, Kharya et al., 2021). The primary CO₂ inclusions were homogenized between -5 and -23 °C, with a major

homogenization concentration between -12 and -22 °C (Fig. 9C). The secondary carbonic fluid inclusions were homogenized between 1.5 and -11 °C (Fig. 9D).

Whereas, the primary biphasic inclusions show the eutectic (Te) temperature between -56.7 and -56.6 °C, indicating that the carbonic component is pure CO₂ and advocates the presence of aqueous-carbonic (H₂O-CO₂) inclusions. The final ice melting temperature (Tm.ice) or CO₂ homogenization temperature (Th_{CO2}) in H₂O-CO₂

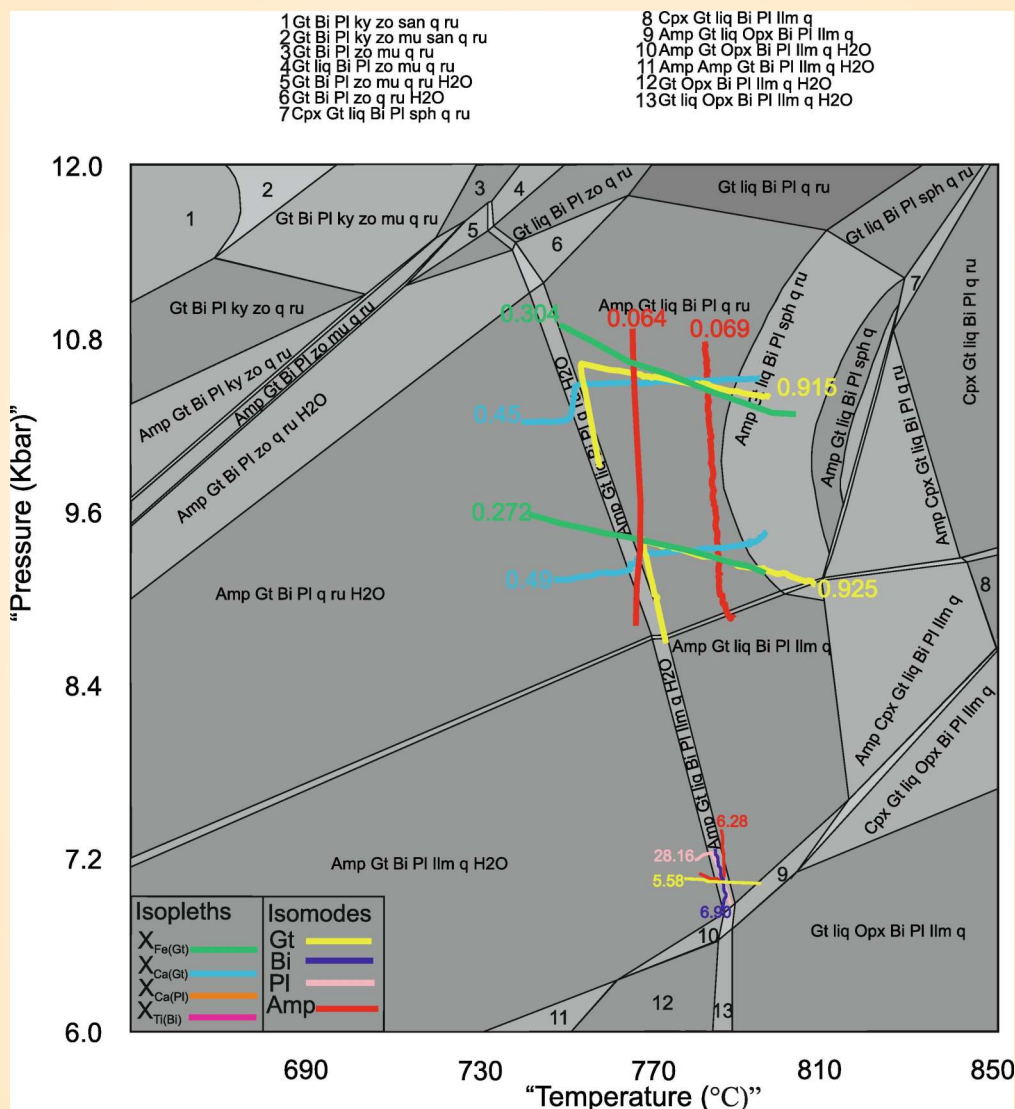


Fig. 7: P–T pseudosection modelled for sample SS6 in the MnNCKCFMASTH system. Light, medium, dark, and very dark grey fields are tri-, quadri-, penta- and esa-variant fields, respectively. The observed assemblage (melt + Grt + Pl + Bt + Amp + Qz + Ru) is modelled by a small field at 9.3–10.5 kbar, 770–790 °C. Insets show the inferred peak metamorphic assemblage field in enhanced detail. The box on left side shows the meaning of different colours for isopleths and isomodes volume amount of each phase. The modelled compositional isopleths for garnet, biotite, and plagioclase are shown. Mineral abbreviations used in the P–T pseudosections are gt – garnet; bi – biotite; mu – muscovite; sill – sillimanite; ksp – K-feldspar; Amp – amphibole; pl – plagioclase; crd – cordierite; san – K-feldspar; kf- zo – zoisite; ilm – ilmenite; ru – rutile; q – quartz; liq – silicate melt.

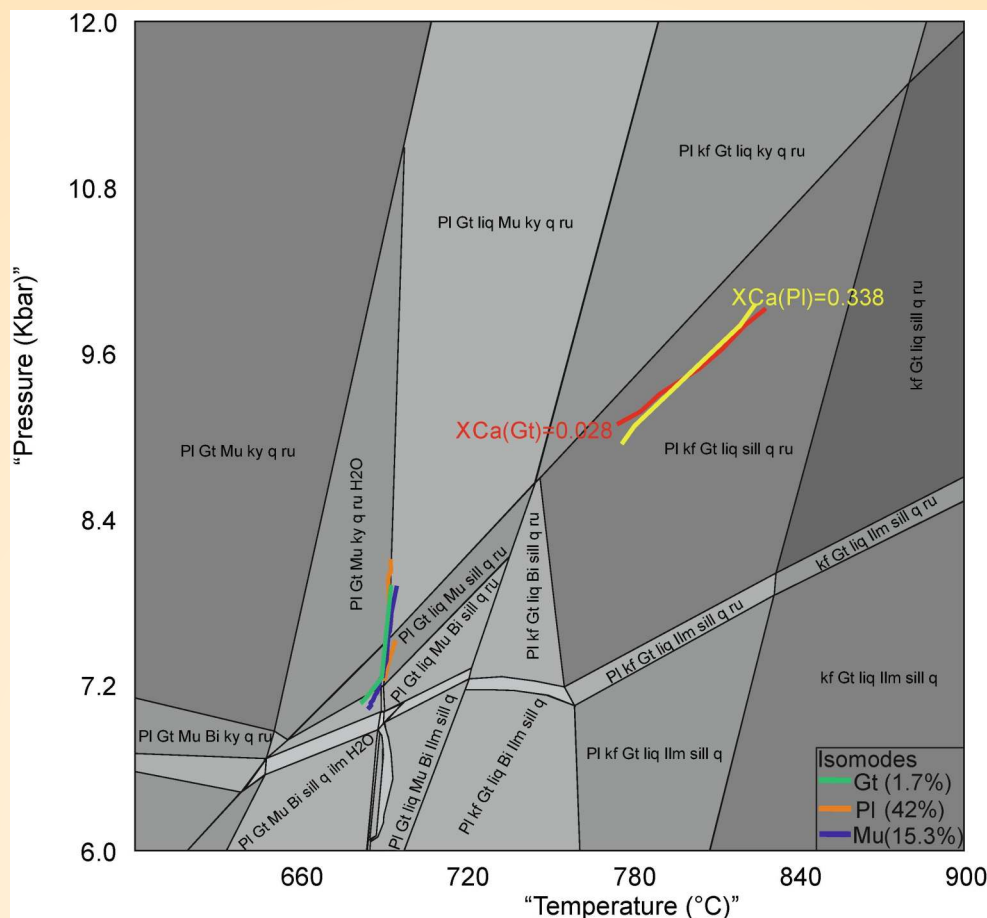


Fig. 8: P-T pseudosection modelled for sample SS15 in the MnNCKFMASH system. Light, medium, dark and very dark grey fields are tri-, quadri-, penta-, and esa-variant fields, respectively. The observed assemblage (melt + Grt + kf + Pl + Sill + Q + Ru) is modelled at and 780–820 °C, 9.3–9.8 kbar. The modeled compositional isopleths for garnet, muscovite, and plagioclase are shown. The box on the right side shows the iso modes volume amount of each phase. Mineral abbreviations as specified in figure 8.

inclusions in the migmatites range between 18 and 26 °C (Fig. 9B), and they homogenized between 170 and 210 °C (Fig. 9A). The clathrate melting temperatures of these inclusions are between 6.0 and 7.6 °C. Further, the fluid inclusion and thermodynamic study suggested that these migmatites were followed by an initial isothermal decompression (Fig. 10). The formation of these migmatites was related to water-fluxed melting (excess amount of H₂O) and muscovite dehydration melting. At peak metamorphic conditions, aqueous-carbonic (H₂O-CO₂) fluids were present in the system. Subsequently, the H₂O phase was preferentially leached out from the biphasic aqueous-carbonic inclusions, henceforth primary CO₂ inclusions remain in the system. This H₂O directly went into the anatectic melt during migmatization. The exhumation of the Leo Pargil dome (LPD) followed an early nearly isothermal

decompression path and a later isochoric cooling driven by the Kaurik-Chango normal fault.

The U–Pb geochronology and ϵ Hf record separate clusters of ages on the concordia plots of these migmatites are 1050–950 Ma, 850–790 Ma, and 650–500 Ma (Figs 11, 12). The oldest 1050–950 Ma zircon population supports a provenance from magmatic units related to the assembly of Rodinia. A minor amount of Palaeoproterozoic grains were likely derived from the Indian craton. The potential source rock of the 930–800 Ma detrital zircons (Fig. 11) may be from the granitoid present in Higher Himalayan rocks themselves and possibly from the Aravalli Range, which has 870–800 Ma granitic rocks. The arc-type basement of the Himalayan orogen recorded (900–600 Ma) igneous activity, which may depict a north-easterly extension of juvenile terranes in the Arabian–Nubian Shield. The granitoid of 800 Ma may be a potential

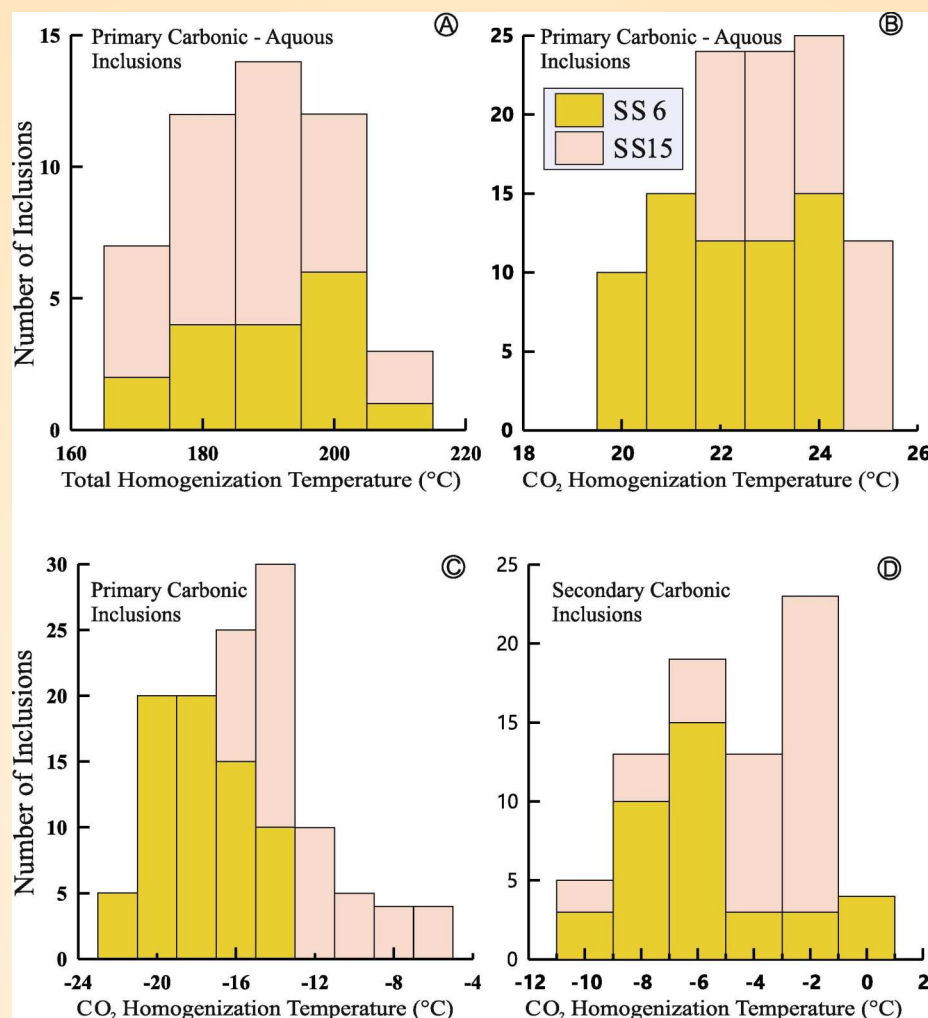


Fig. 9: (A) Histograms of total homogenization temperatures of the carbonic-aqueous inclusions in studied samples of migmatites (B) Histograms of homogenization temperatures of the carbonic phase in carbonic-aqueous inclusion. (C) Histograms of CO₂ homogenization temperatures in primary carbonic inclusion. (D) Histograms of CO₂ homogenization temperatures in secondary carbonic inclusion.

source for 790 Ma detrital zircons owing to scatter in 206/238 dates (Fig. 11). The 650–500 Ma zircon population suggests their derivation from the East African Orogen and Ross–Delamerian Orogen of Gondwana. The detrital zircon grains are not found in these migmatites; therefore, local sources could not explain. One sample yielded a discordia lower intercept age of 15.6 ± 2.2 Ma, the age of melt crystallization.

In the NW Himalaya, water-fluxed melting has been proposed as the primary mechanism of partial melting in the Higher Himalayan Crystallines (HHC), and it takes place between wet solidus and fluid-absent dehydration reactions. Kawabata et al. (2021) reported that both types of migmatites, derived from water-fluxed and dehydration melting, experienced similar Early Oligocene metamorphism and protracted

crystallization up to ca. 38–25 Ma; monazites ages of 38–24 Ma supporting this evolution are also reported by Catlos et al. (2007) from the middle HHC. Lederer et al. (2013) reported monazite U-Pb-Th ages from 30 to 18 Ma for the partial melting event and suggested that this event lasted until 18 Ma. It is also suggested that the partial melting event extended up to 15 Ma.

The metamorphic peak occurred in the Leo Pargil dome at around 30 Ma and was followed by decompression/exhumation leading to muscovite-dehydration melting as well as by water-fluxed melting reactions. To support this evolution, Štípská et al. (2020) observed two distinct phases of exhumation at c. 38 Ma and at c. 27 Ma respectively, from the nearby Garhwal Himalaya. This decompression stage is also very well constrained by the re-equilibration textures of fluid

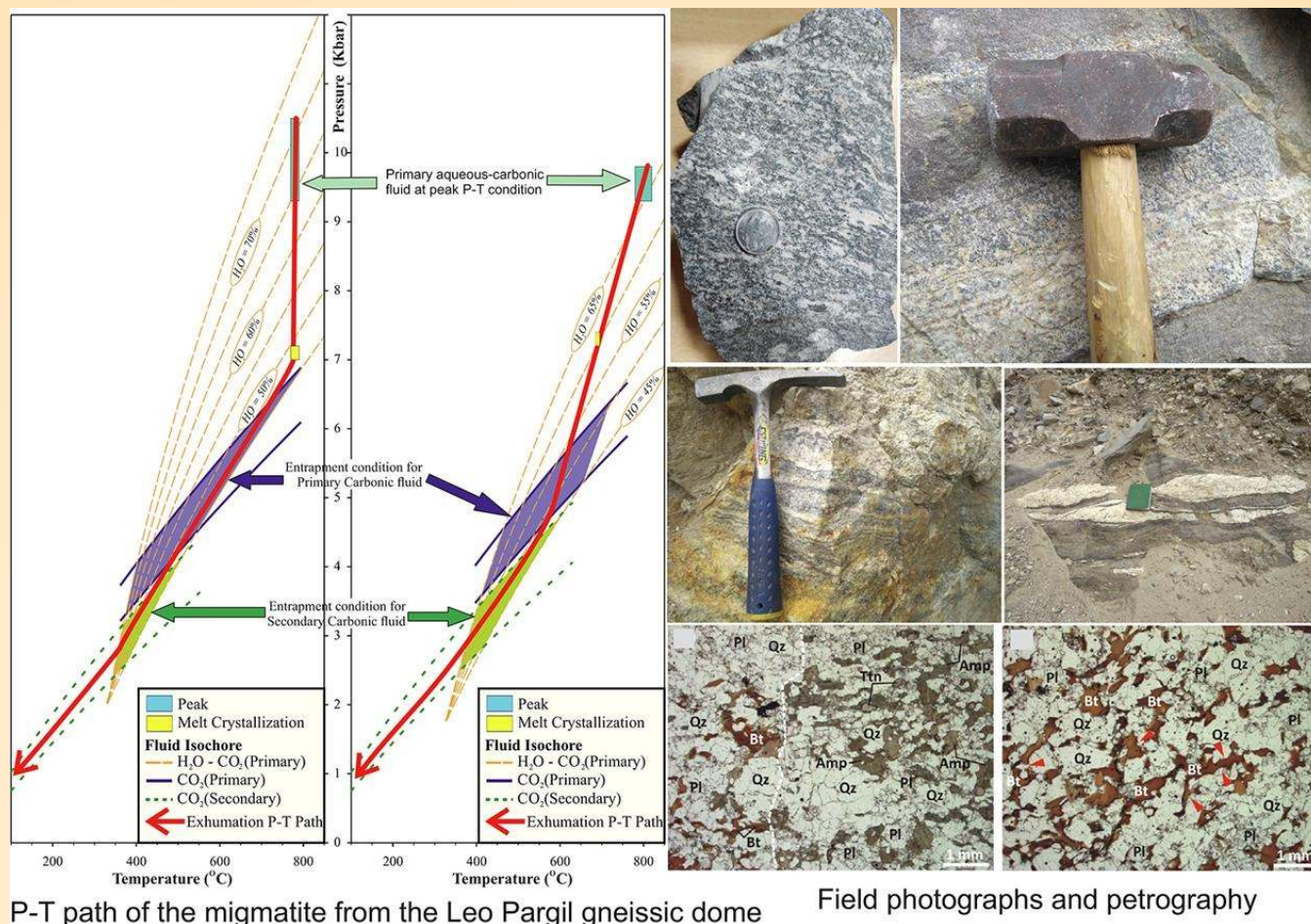


Fig. 10: P-T path of the migmatite from the Leo Pargil gneissic dome constrained from thermodynamic modeling and fluid inclusions study. P-T conditions inferred from phase equilibria modeling (near-peak and melt crystallization stages) are shown by yellow and blue boxes, respectively. Representative isochores of CO_2 inclusions (primary and secondary) and CO_2 - H_2O primary inclusions obtained from fluid inclusions micro thermometry are shown. Field photographs showing the occurrences of migmatites in the south-western flank of the LPD, upper Sutlej Valley. Photomicrographs show Contact between a biotite-rich mesosome domain and an amphibole-rich leucosome domain. Amphibole in the leucosome is slightly oriented parallel to the poorly developed foliation defined by biotite in the mesosome. The leucosome domain shows a diffuse boundary against the mesosome. Detail of the mesosome domain, with a poorly developed foliation defined by biotite. The red arrows highlight the corroded morphologies of biotite.

inclusions. The timing and evolution of partial melting in Leo Pargil are nicely comparable with those of migmatites from Eastern Nepal and Sikkim and support the possibility that the melting stage has faded around 15 Ma all over the Himalayan belt.

The weakening of mid-crust and strain localization during exhumation led to the development of a shear zone at around 23 Ma, known as the Leo Pargil shear zone. It is proposed that the development of the Leo Pargil shear zone may have flushed the excess water in the system leading to water-flux melting and the formation of migmatites and leucogranites, which ended around 15 Ma. Anatexis was confined to the shear

zone, where melting of a sedimentary protolith (e.g., calcareous pelite and/or marl) generated leucosomes with peritectic hornblende while melting of neighboring metasedimentary didn't produce any anhydrous peritectic phases. Similar melting behaviours have also been observed in Ladakh, India, and Nanga Parbat, Pakistan. It can be further suggested that the H_2O phase present in the primary carbonic-aqueous inclusions was selectively leaked and went directly into the melt, while CO_2 remained leftover at the last stage of melt crystallization in the fluid inclusions. The monophasic CO_2 inclusions were further re-equilibrated. Consequently, their isochores plot below the P of

retrogression due to density reversal; therefore, the pure CO_2 inclusions were entrapped at P–T conditions later than those of water flux melting (Fig. 10). The P–T exhumation paths of the LPD show an initial isothermal decompression (ITD) followed by an isochoric cooling (ICC) up to the surface (Fig. 10), which took place through the Kaurik-Chango normal fault from 10 Ma to 2 Ma.

The $\epsilon\text{Hf}(t)$ values (-16.6 to $+3.5$; see Fig. 11) for the 650–500 Ma zircons (Fig. 12) of these migmatites (LPD) are similar to western Australia (part of Gondwana) and Tethyan Himalayan rocks, suggesting that these zircons were reworked mainly from the old continental crust. Our interpretations are consistent with these blocks having been close to Gondwana (Fig. 13). The plentiful late Mesoproterozoic–early Neoproterozoic and middle Cambrian zircons are consistent with a Gondwanan origin. The late Neoproterozoic collision of East Gondwana (India, East

Antarctica, Australia) with Eastern Africa wedged the Indian craton amid the East Antarctic and African cratons (Fig. 13). The northern margin of the Indian continent was consequently in a palaeogeographic position to receive zircons from, even though distant, mountain belts established during and proximately after the Gondwana assembly, which may be the East African Orogen, comprising the juvenile Arabian–Nubian Shield, Kuunga–Pinjarra orogen and the outer part of the Ross–Delamerian orogeny as the East African Orogeny was active from c. 680 to 500 Ma. The Ross magmatic-arc activity had been initiated by 580 Ma. The penecontemporaneous igneous activity was observed in the HHC and within the Lhasa terrane, Qiangtang terrane, and Amdo basement during the early Palaeozoic time. These Palaeozoic arc-type igneous rocks along the northern margin of Gondwana can be inferred to be evidence of convergent-margin magmatism and tectonism.

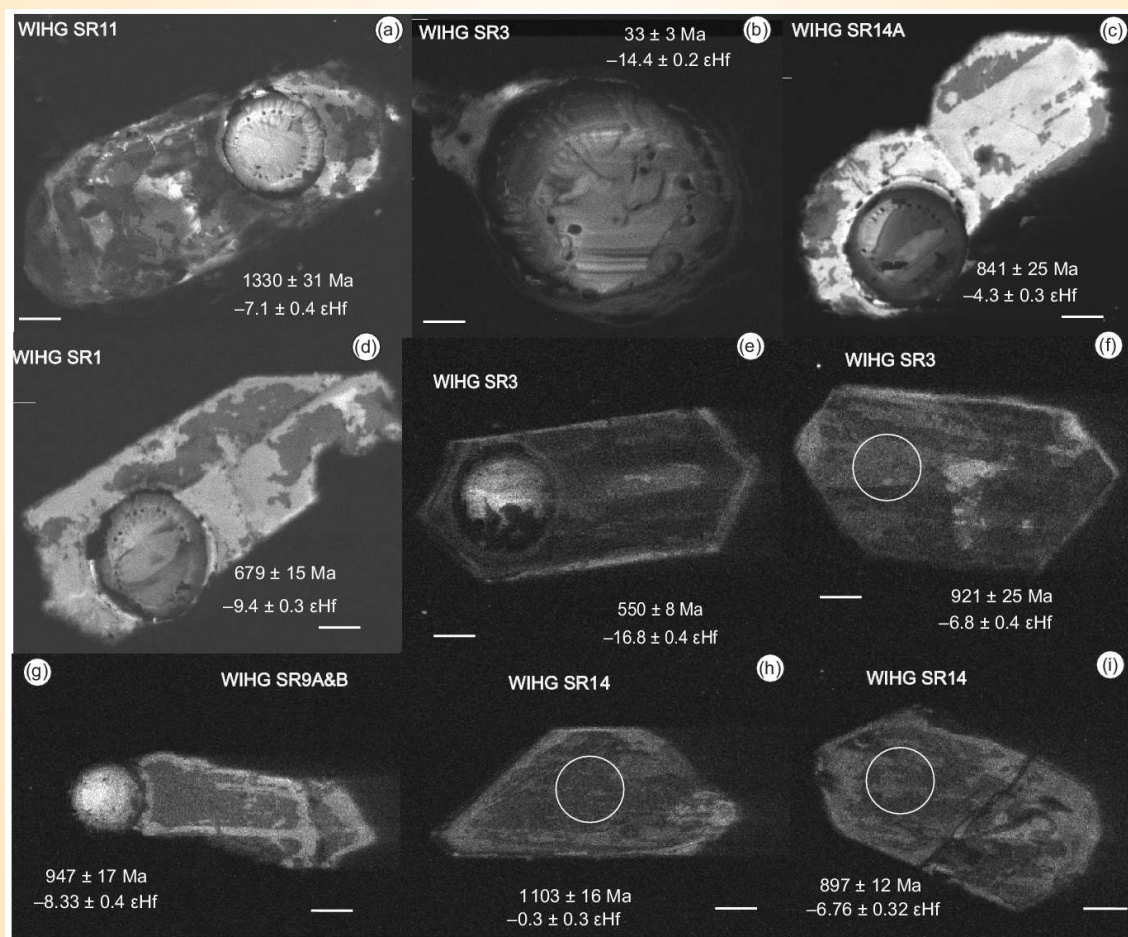


Fig. 11: Cathodoluminescence images of analyzed zircon grains of representative samples of migmatite from the upper Sutlej valley (Leo Pargil region), India. (a) WIHG-SR1; (b) WIHG-SR3; (c) WIHG-SR9; (d) WIHG-SR11; and (e) WIHG-SR14A with analyzed spots, their ages, and ϵHf value.

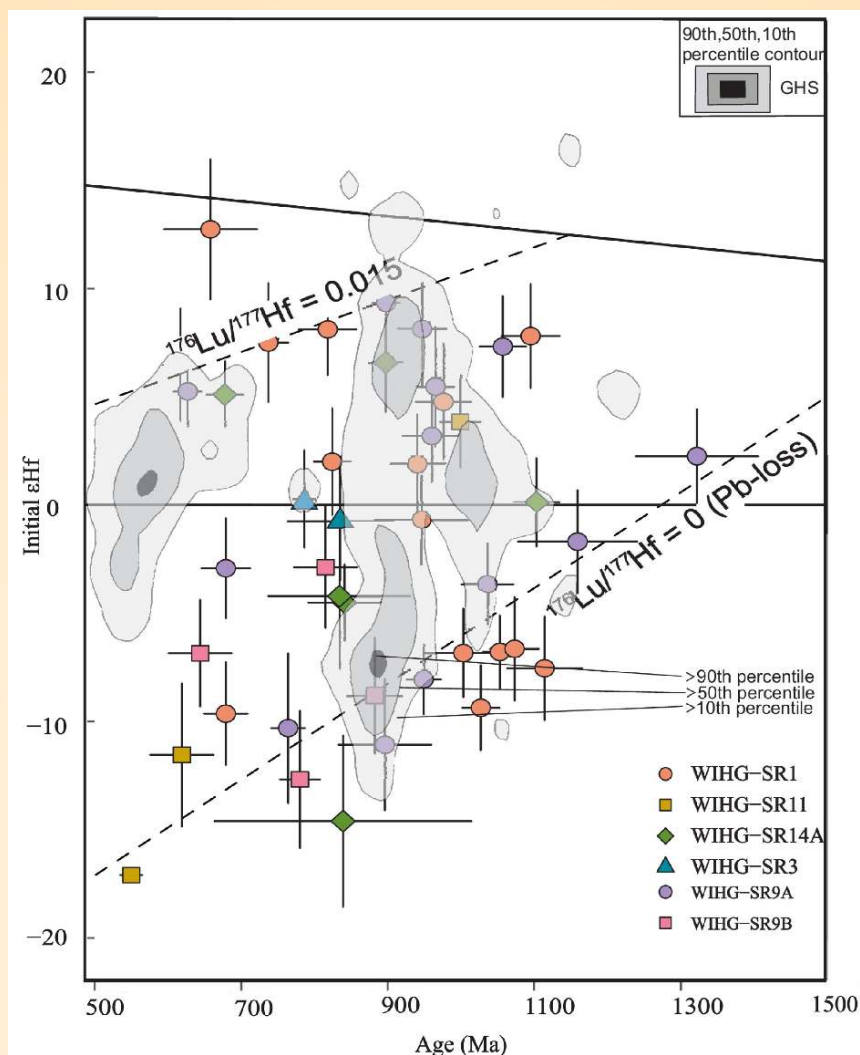


Fig. 12: 2dKDE of the GHS (Spencer et al. 2019), compared with this study. A plot of ϵ_{Hf} and U–Pb crystallization ages for zircon and probable source regions. DM – depleted mantle; CHUR – chondritic uniform reservoir. Note the widespread values for most samples indicating potential crustal mixing. ϵ_{Hf} data were calculated using the decay constant of $1.867 \times 10^{-11} \text{ year}^{-1}$ (Söderlund et al. 2004) and the CHUR parameters of Bouvier et al. (2008). DM evolution curve was defined by $(^{176}\text{Hf}/^{177}\text{Hf})_{\text{DM}} = 0.28325$ and $(^{176}\text{Lu}/^{177}\text{Hf})_{\text{DM}} = 0.0388$.

Evidence for the Cambro-Ordovician Bhimphedian Orogeny related to Gondwana effects can be found from Pakistan to the eastern part of the Himalaya. The basaltic and andesitic volcanism is related to the magmatic arc, active from 530 to 490 Ma. The activity of the magmatic arc was imbricated by regional deformation, anatexis processes, and emplacement of a granite pluton (S-type) that was protracted before 470 Ma. It may be possible that the zircon grains with an age of ~500 Ma were mostly sourced from the prevalent granite occurrences all over the Himalaya and in numerous sections around Gondwana.

The Sung Valley ultramafic–alkaline–carbonatite complex (UACC) of Meghalaya, NE, India, is a result of

magmatic activity related to the Kerguelen mantle plume spanning from 101 to 115 Ma. Integrated crystal size distribution (CSD), mineral chemistry, and melt inclusion analysis were carried out on the ijolites present within this UACC. The CSD analysis shows that these ijolites were formed in multiple stages through changes in the crystallization environment, such as cooling and nucleation rates. Raman spectroscopy of mineral inclusions of rutile, apophthalite, apatite, carbonate–silicate melt inclusions, and disordered graphite within clinopyroxene and titanite, respectively, indicates a heterogeneous composition of the parental magma. These minerals and melt inclusion phases further suggest localized changes in oxygen fugacity

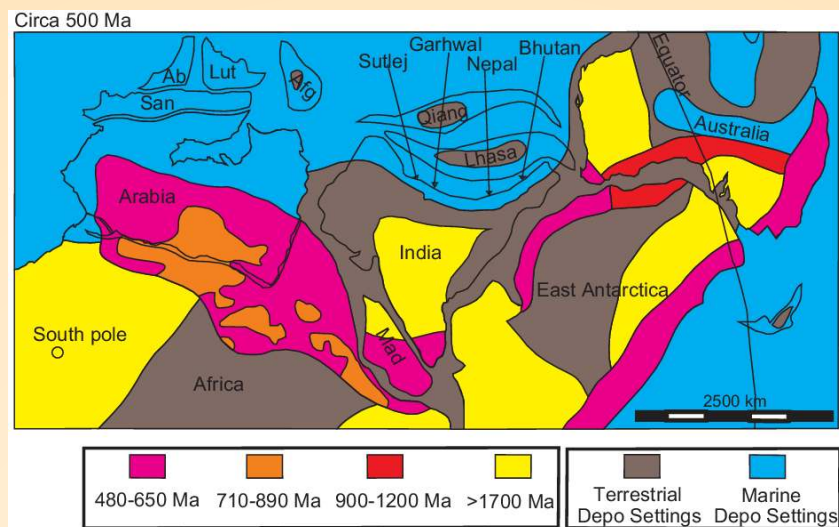


Fig. 13: Palaeogeographic reconstruction of eastern Gondwana c. 500 Ma (after Torsvik & Cocks, 2009; Myrow et al. 2010) and age of various terranes. Ab – Alborz terrane; Afg – Afghan terranes; San – Sanand terrane; Mad – Madagascar.

(fO₂) due to redox reactions in the lower crust. Scanning electron microscopy-energy dispersive X-ray (SEM-EDX) analysis of the exposed melt inclusions reveals the presence of alkali-bearing diopside, phlogopite, and andradite, along with an unidentified carbonated silicate daughter phase. The studied melt inclusions are dominated by carbonate, whereas silicates are subordinate. The presence of this fully crystallized carbonate–silicate melt as calcite, diopside, phlogopite, magnetite, apatite, and andradite suggests the presence of “nano-calciocarbonates” in these ijolites. This study provides insights into different mechanisms of the loss of alkalis from initially entrapped alkaline carbonate melt in clinopyroxenes.

New Mineral equilibrium: Cumingtonite-sillimanite-cordierite-quartz-H₂O equilibrium

The P–T–X (Fe–Mg) phase relation of the Cumingtonite-sillimanite-cordierite-quartz-H₂O equilibrium in natural assemblages has been constructed considering the chemical system FeO–MgO–Al₂O₃–SiO₂–H₂O (FMASH system). The equilibrium is a divariant continuous reaction: cum + sil + qz = crd + H₂O. The slope of end-member reactions of this divariant reaction is calculated using the available experimental and thermodynamic data. The isothermal P–X (Fe–Mg) loop and isobaric T–X (Fe–Mg) loop have been constructed using the Fe- and Mg-end member reactions as boundary conditions (Figs. 14 - 16). It is predicted that, at constant pressure, the three phases cum–sil–crd assemblage in the AFM diagram displaces towards Fe-end with increasing metamorphic

temperature whereas, at a constant temperature, this assemblage displaces towards Mg-end member in the AFM diagram with increasing pressure. The end member reactions have a positive slope in the P–T space. The study of the P–T–X relationship of cumingtonite-sillimanite-cordierite-quartz-H₂O equilibria is compared with the natural mineral assemblages reported from various parts of the earth's crust. The study suggests that the cum–sil–crd bearing metamorphic assemblages were developed at low-P and medium/high-T metamorphic conditions.

Retrograde dehydration reaction of Pre-Himalayan pyroxene bearing Xenolith, Sutlej valley, NW Himalaya

P–T and P–MH₂O pseudo sections have been constructed considering the NCFMASH system to understand the retrograde hydration reactions in pre-Himalayan pyroxene-bearing mafic xenoliths of Sutlej Valley, NW Himalaya. The pseudo-section modeling demonstrates the destabilization of orthopyroxene and clinopyroxene in mafic granulites after decompression to 0.3 GPa pressure resulted in the formation of cumingtonite and hornblende-bearing mafic xenoliths (Fig. 17). The study shows that the secondary mineral assemblage is controlled not only by P and T but also by the amount of water available for hydration. The study shows that the Higher Himalayan Crystalline Sequence (HHCS), from which the xenoliths have been derived, must have been subjected to pre-Himalayan high-grade metamorphism, although it is not evident because of pervasive overprinting by Himalayan

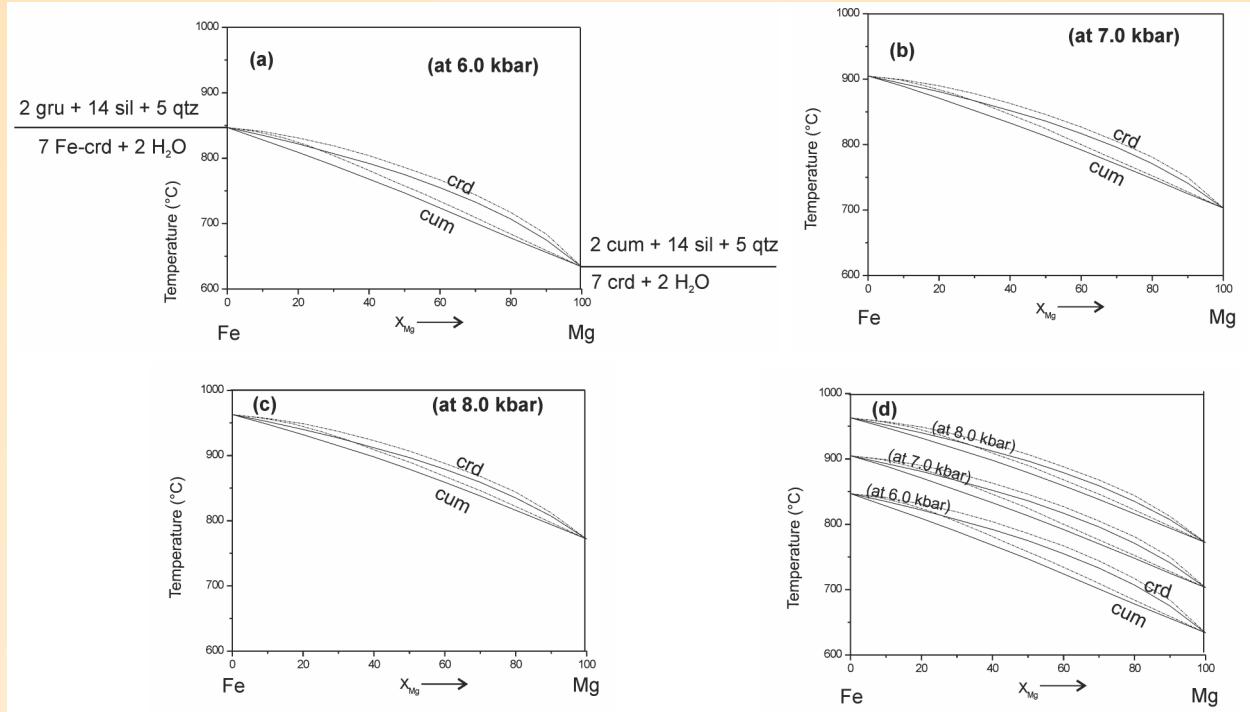


Fig. 14: (a-c) Isobaric T-X (Fe-Mg) loops for Fe- and Mg-end member reactions of continuous reaction: $\text{cum} + \text{sil} + \text{qtz} = \text{crd} + \text{H}_2\text{O}$, considering ideal and non-ideal mixing models at a constant pressure of 6.0, 7.0 and 8.0 kbar. T-X (Fe-Mg) loops of the ideal solution model are shown in solid line whereas T-X (Fe-Mg) loops of the non-ideal mixing model are shown in dash line;

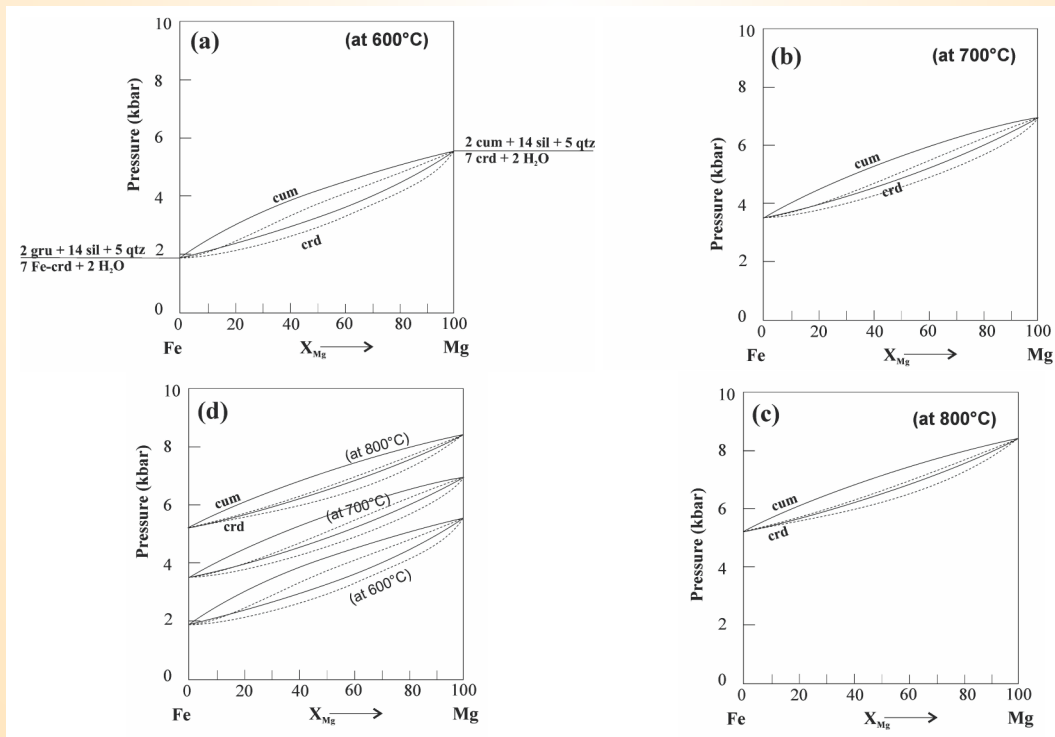


Fig. 15: (a-c) Isothermal P-X (Fe-Mg) loops for Fe- and Mg-end member reactions of continuous reaction: $\text{cum} + \text{sil} + \text{qtz} = \text{crd} + \text{H}_2\text{O}$, considering ideal and non-ideal mixing models at a constant temperature of 600, 700 and 800°C. P-X (Fe-Mg) loops of the ideal solution model are shown in solid line whereas P-X (Fe-Mg) loops of the non-ideal mixing model are shown in dash line; (d) comparison of P-X (Fe-Mg) loops of ideal and non-ideal mixing models.

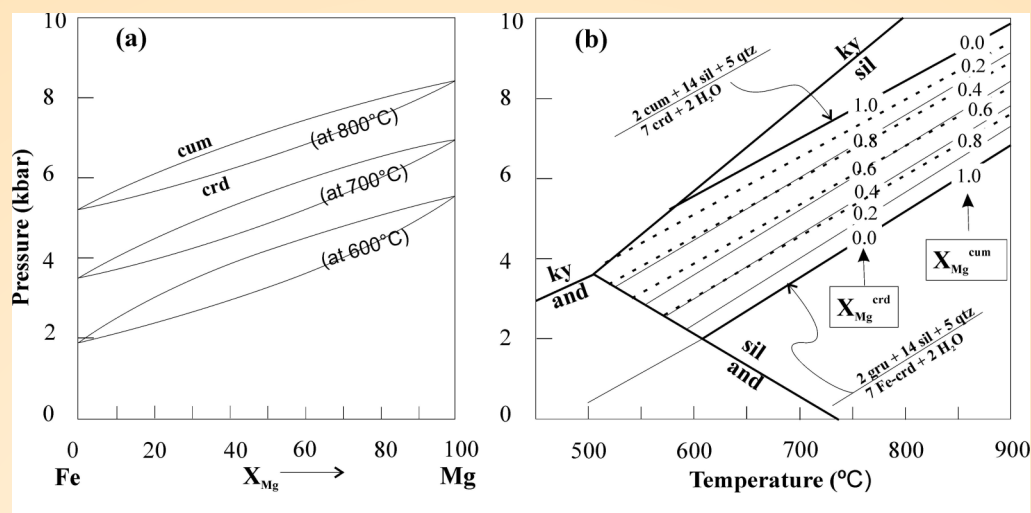


Fig. 16: (a) isothermal P-X (Fe-Mg) loops of the Fe- and Mg-end member reactions of continuous reaction: $cum + sil + qtz = crd + H_2O$ using ideal mixing model; (b) P-T stability diagram of Fe- and Mg-end member reactions. The isopleths of X_{Mg}^{Crd} and X_{Mg}^{Cum} are constructed from the isothermal P-X (Fe-Mg) loops of the Fe- and Mg-end member reactions.

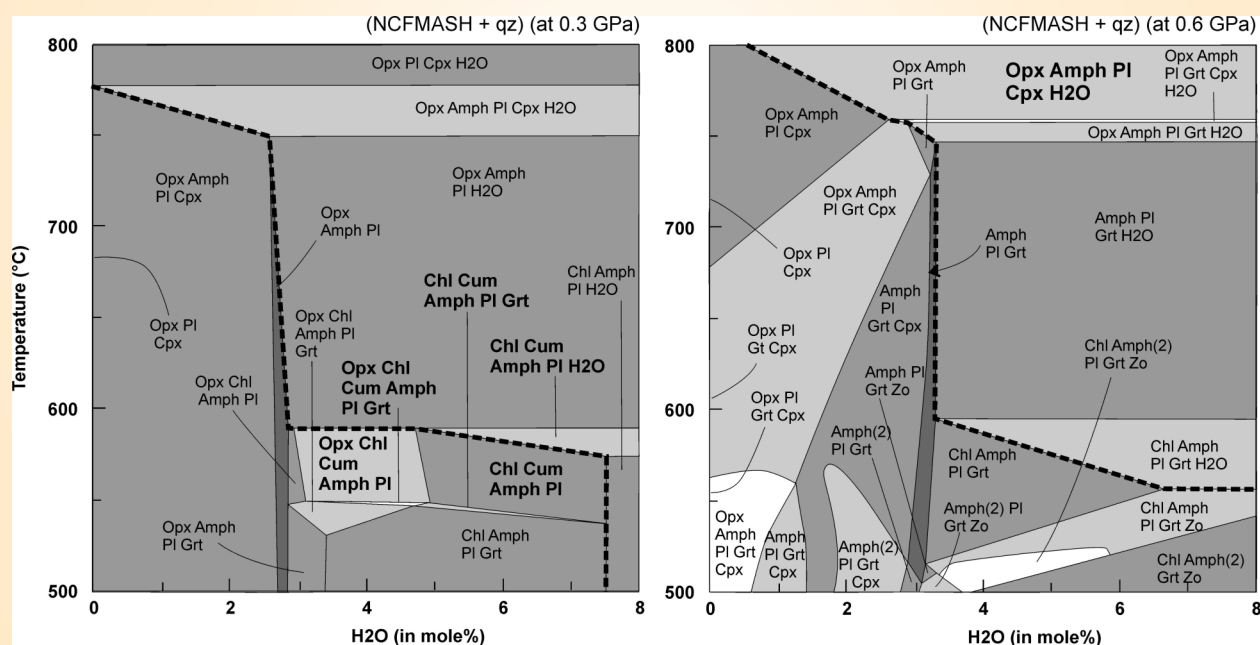


Fig. 17: T-MH₂O pseudo section, at pressures of 0.3 GPa (a) and 0.6 GPa (b) for sample XN10 in the model system NCFMASH system (+ qz) using oxide modal proportions of $SiO_2 = 53.98$, $Al_2O_3 = 7.98$, $FeO = 10.98$; $MgO = 9.65$, $CaO = 11.50$, $Na_2O = 0.78$, H_2O (range) = 0–8. The thick dashed line represents H₂O saturation. Cum-bearing fields are labeled in bold letters in (a); peak assemblage is labeled in bold letters in (b).

metamorphism. The present-day metamorphic pattern of the HHCS is expectedly the result of both pre-Himalayan and Himalayan metamorphism and careful petrological investigation is required to distinguish their signatures so that a better understanding of the tectono-thermal evolution of the Himalayas can come into the

picture. The present study provides new insights into pre-Himalayan metamorphism and constrained the P-T conditions of hydration.

The new geochemical, mineral chemical, and Sr, Nd isotopic data constrain the petrogenesis and geodynamic evolution of mafic micro-granular

enclaves (MMEs) and Ladakh granites in the southern active margin of the Eurasian plate. The Neotethyan oceanic slab-sediment-melts favour the depleted lithospheric mantle into the metasomatized lithospheric mantle-wedge before the collision between India and Eurasia plate. The more mafic, high K calc-alkaline, isotopically depleted monzo-diorite MMEs produced the partial melting of the metasomatized lithospheric mantle-wedge and evolved through the fractional crystallization process. The lower crustal signature with enriched large-ion lithophile elements (LILE: Rb, Th, U, and Pb) and depleted in high-field-strength elements (HFSE: Nb, Ta, Zr, Hf, Ti) and Sr, Nd isotope composition (initial $^{87}\text{Sr}/^{86}\text{Sr} = 0.7047\text{-}0.7056$, $\varepsilon \text{Nd}_{t=0} = 3.32\text{-}1.40$) lead to juvenile two-stage Nd model age of 718-1010 Ma. The mineral chemistry (plagioclase, amphibole, biotite compositions) in monzo-diorite supports the mantle-derived primitive basaltic magmas. The more mafic, shoshonitic, isotopically evolved monzo-gabbro MMEs formed from the mixing of granitic magma from the partial melting of northern Indian upper crustal metasedimentary basement and underplated mafic magma that was derived from metasomatized mantle wedge. The upper crustal signature with enriched large-ion lithophile elements (LILE: Rb, Ba, Th, U, and Pb) and Sr, Nd isotope composition (initial $^{87}\text{Sr}/^{86}\text{Sr} = 0.7073\text{-}0.7166$, $\varepsilon \text{Nd}_{t=0} = -3.45$ to -8.93) and depleted in high-field-strength elements (HFSE: Nb, Ta, Zr, Hf, Ti) lead to the two-stage Nd model age of 1050 to 1547 Ma reflects the mantle-derived mafic magma mixing with evolved granitic host magma. The mineral amphibole and biotite compositions in Monzo-diorite represent their mantle-derivation. The high K calc-alkaline to shoshonitic Ladakh granites may be generated by AFC processes with interactions between underplated mafic magma of sediment melts modified mantle-wedge derived with granitic magma of northern Indian deep lower crustal metasedimentary basement-derived. The variable tracer elemental patterns with enriched LILEs and evolved Sr, Nd isotopic compositions (initial $^{87}\text{Sr}/^{86}\text{Sr} = 0.6967\text{-}0.7192$; $\varepsilon \text{Nd}_{t=0} = -12.3$ to -4.2), ancient the two-stage Nd model age of 1160 Ma to 1858 Ma and depletion in HFSE, Y, HFSE (Nb, Ta, Zr, Hf, Ti, P), K indicates the partial melting of northern Indian metasedimentary lower crustal basement derived. The plagioclase composition reflects their evolved magma source. The mineralogical, geochemical, and isotopic evidence of MMEs and Ladakh granites formed in an active continental margin, which related to the collisional event between the Indian and Eurasian plates.

Activity: 2A

Subsurface interpretation – Development of ML approach to geoscientific data from Himalaya and adjoining regions

(Kalachand Sain, Priyadarshi Chinmoy Kumar and Bappa Mukherjee)

Decoding depositional environment of subsurface sediments in Dibrugarh field of Upper Assam basin

The Upper Assam basin in NE India is surrounded by the Himalayan mountain belt in the north, Naga Hills in the south, and Mishmi Hills in the east. Most of the sediments belong to the Tertiary period (66 - 2.5 million years ago) and recent alluvium cover. Seismic data can play an important role in unraveling the depositional environment of these sediments in the basin. The study shows that the textural characteristics of the Oligocene Barail coal-shale unit (deposited between 33.9 to 20.4 million years ago) are associated with the deformed, wavy, chaotic, and heterogeneous texture indicating a deeper basinal condition prevailing during its deposition (as shown in Fig. 18). Whereas the overlying Miocene Tipam sandstone unit (deposited between 20.4 to 11.6 million years ago) is associated with less chaotic and high homogeneity textures (molassic type), indicating fluvial environment during its deposition (as shown in the maps). Such study is useful not only for the exploration of hydrocarbons in the thrust-fold belt but can also provide insightful implications to the geo- or seismo-tectonics of an area on a finer scale.

Finer 3D litho-model of the Lakadong Therria formation of the Bhogpara oil field, Upper Assam foreland basin

In the oil industry, interpreters have carried out such analysis through expensive software with their own experience, and geological knowledge of the study area. However, identifying bed boundaries using traditional interpretation is a tedious staff. Therefore, a synergetic approach of Walsh transform and a bed boundary demarcation technique is adopted to discriminate the lithological boundaries. This bed boundary detection technique was tested over self-potential (SP), gamma ray (GR), and laterolog deep resistivity (LLD) logs. Initially, the possible lithological boundaries were detected from GR log variations and hence proposed a lithological model as per the knowledge of traditional log interpretation techniques. Subsequently, the Walsh low pass filter was applied to the SP, GR, and LLD logs to obtain their step function. Afterward, those step functions of logs were processed through the boundary detection algorithm to find out the possible thick and thin beds. Further, bed correlation was made among the

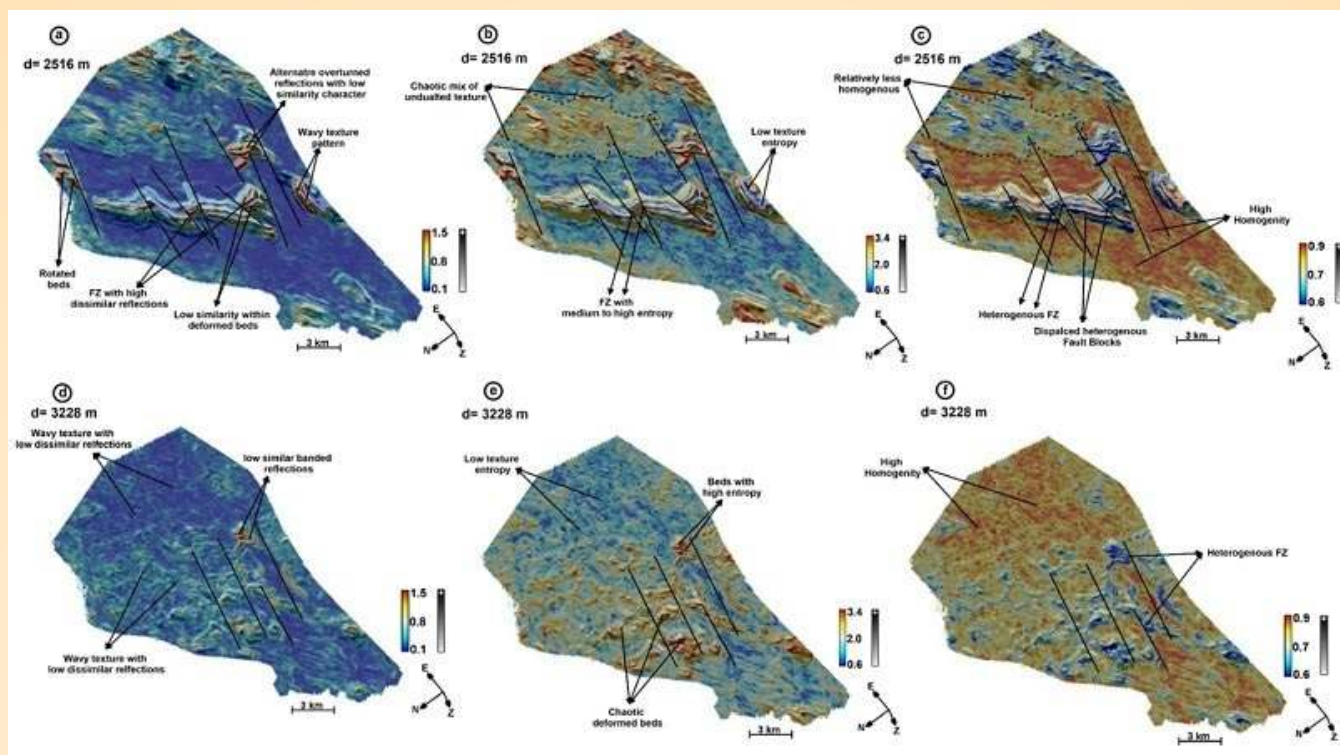


Fig. 18: Depth slices at 2516 m (a-c) and 3228 m (d-f), displayed with different attributes: Texture-Dissimilarity (a & d); Texture-Entropy (b & e), Texture-Homogeneity (c & f), co-rendered with relief attribute reveal varied textural characteristics such as wavy, chaotic, dissimilar and homogeneity prevailing within the Oligocene-Miocene intervals. Thick black lines mark the faults. Note that a pastel colour scale is used to represent the Texture attributes, whereas a grey colour scale is used to represent the relief attribute.

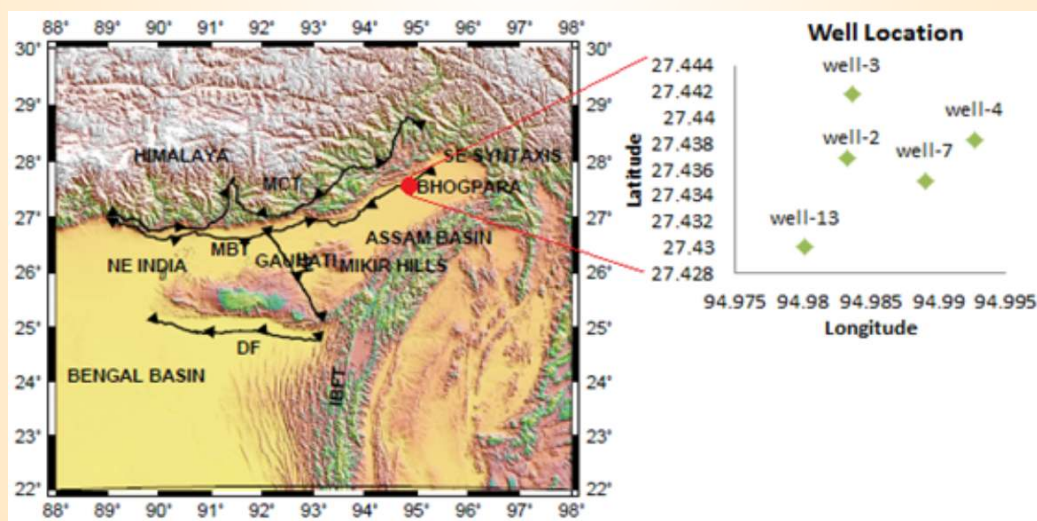


Fig. 19: Geographical location of the study area and studied wells are specified by their latitude and longitude (after Mukherjee et al., 2016).

Walsh-detected boundaries for the studied wells of the Bhogpara oil field (Fig. 19). Finally, a bed boundary model was generated using the boundaries picked from the Walsh-based approach. Our analysis exhibits that, the model generated from Walsh boundaries more explicitly envisaged the possible heterogeneity.

Traditionally the minimum bed thickness of the order of 5.15 m, was discriminated whereas, the thin bed of the order of 3.2 m was obtained from the Walsh-based approach. This proposed bed boundary assessment technique (Fig. 20) is also helpful in understanding the position of the subsurface rock layers as well as possible

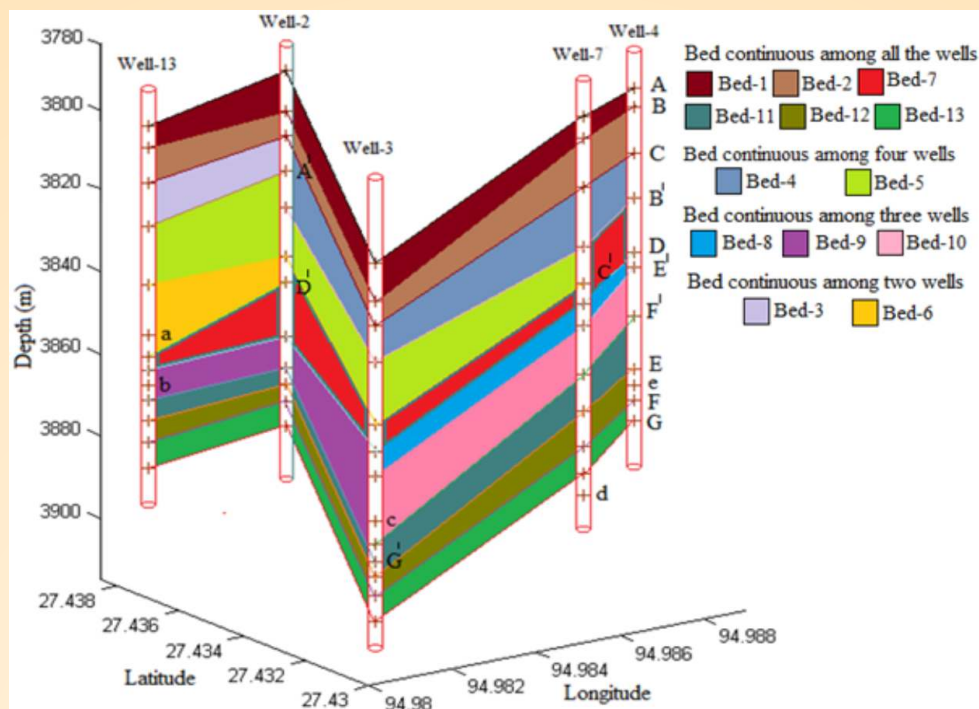


Fig. 20: 3D litho-model, generated based on the Walsh picking boundaries.

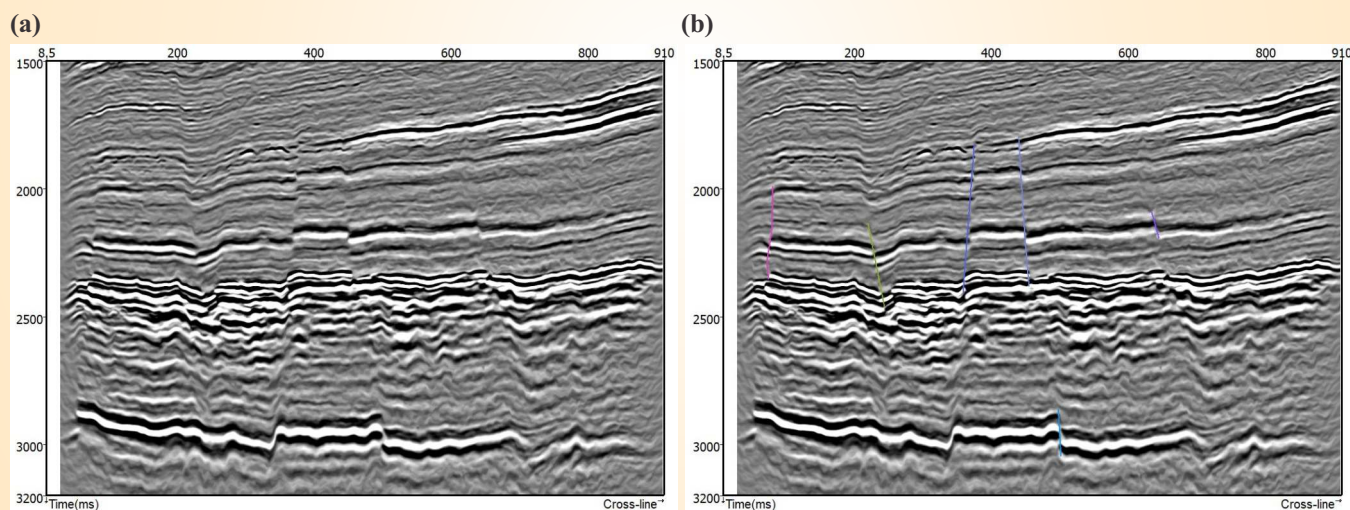


Fig. 21: (a) Depicted seismic section at inline 266 and (b) manually interpreted faults on the seismic section in line 266.

thick and thin beds when any pre-received core information is not available.

CNN derived fault network in the Amguri-3D block of Upper Assam foreland basin

Interpretation of fault networks from seismic data has paramount importance in hydrocarbon exploration, reservoir characterization, and field development strategies. Indeed, elucidation fault represents the plausible path for fluid migration, reservoir compartmentalization, model establishment and to prevent hazards in drilling activity. However, in

Exploration and Production (E&P) industry faults are interpreted manually from seismic sections, and it's a tedious and time-consuming task. Sometimes, interpreters may come out with dissimilar results as it depends on the interpreter's experience and geological knowledge about the study area. Therefore, to circumvent the tedious human intervention our study utilizes convolutional neural networks to predict faults on a time-migrated, 3-D seismic reflection dataset situated in the Amguri area of the Assam-Arakan basin, NE India. A convolutional neural network (CNN), employs a base dataset trained for a specific task. Then

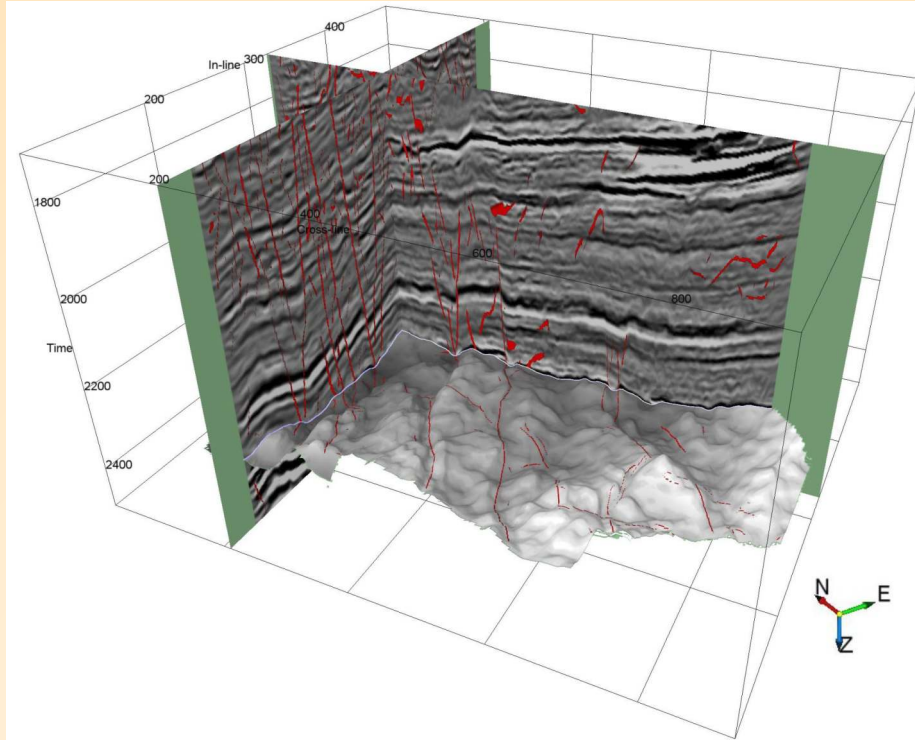


Fig. 22: CNN-derived faults on the seismic section inline 296 and BCS horizon.

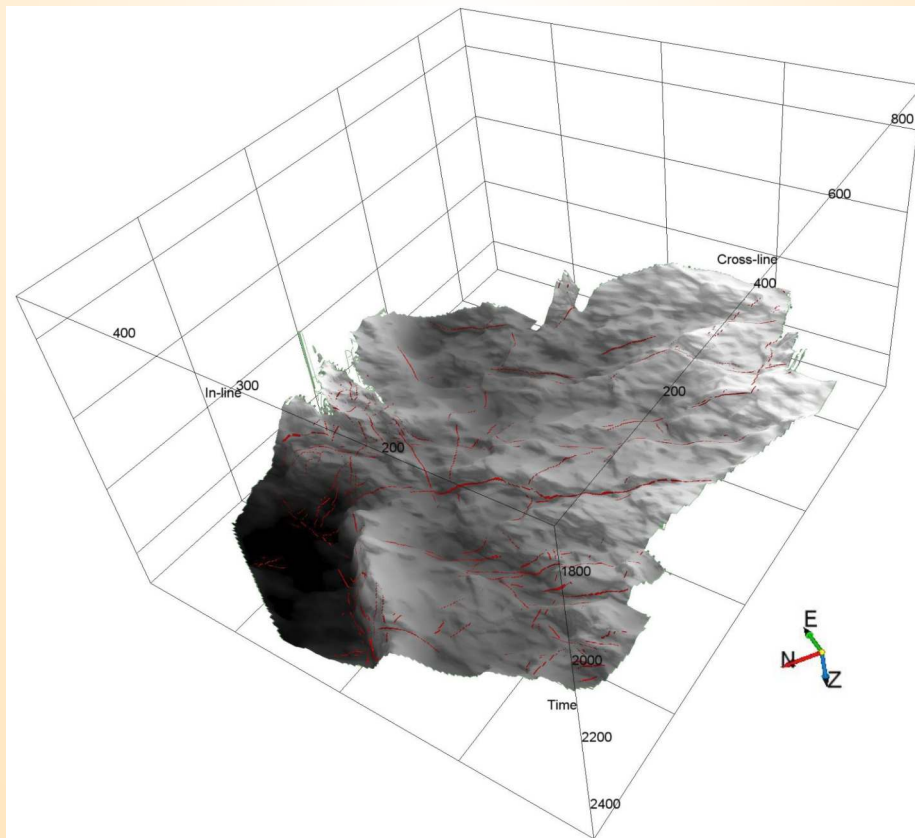


Fig. 23: CNN-derived faults on the seismic section inline 296 and BCS horizon.

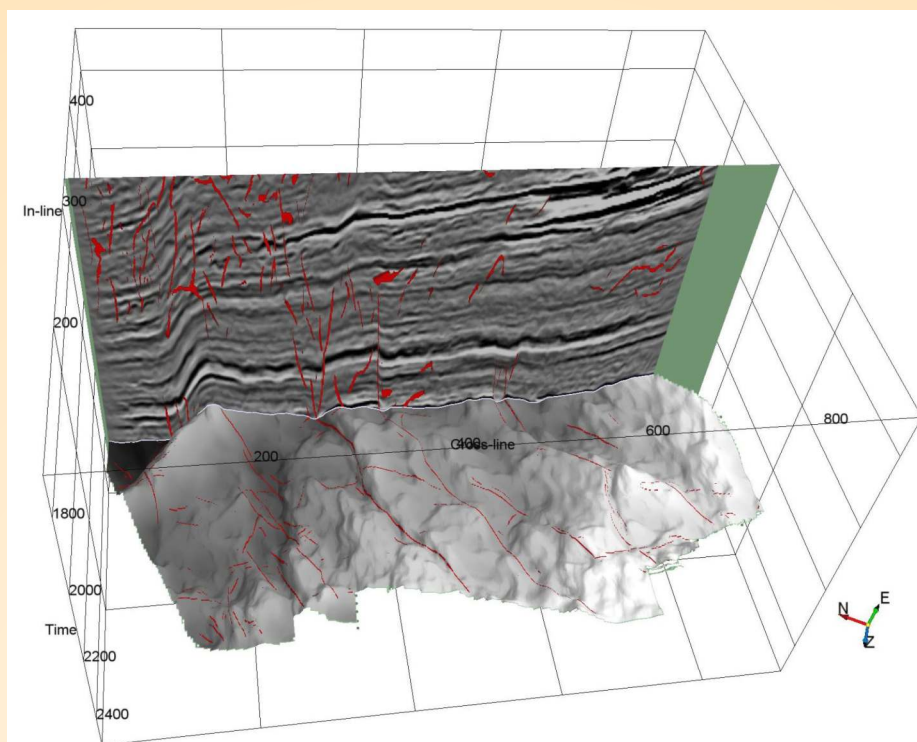


Fig. 24: Depicted CNN-derived faults on the seismic section inline 366, X-line 211 and BCS horizon.

the generated model parameters, or learned features (i.e., kernels at successive steps), are transferred to a second CNN target to be trained on a different task. CNN application falls in the dominion of supervised machine learning because it uses a small training set to find patterns for the data classification. In summary, CNN is used as a feature extractor to classify image data and, in our case study, predict faults. The data used for training and CNN-derived faults are located on the seismic sections and horizons are shown in figures 21-24.

Activity: 2B

Geometry and rheological assessment of the MHT, lithospheric flexuring - Implications toward seismogenesis, deep earth processes

(Naresh Kumar, Devajit Hazarika and Gautam Rawat)

Along-strike variation in the shear wave crustal structure of the northeast Himalaya and Indo-Burmese Arc

The shear wave velocity structure variation is obtained in the north-east Himalaya and Indo-Burma Ranges (IBR) regions using the surface wave earthquake data. A total of 25 earthquakes (M: 5.0–6.7, epicentral distance range: 368–800 km, and focal depth < 50 km) were used. Ray paths from the earthquake epicenter to the seismic station are transversely passing different

geotectonic units of the Himalaya, NE India, Bengal basin (BB), and IBR. The weighted average dispersion curve and its non-linear inverted shear wave velocity model are computed for groups at different azimuths around Shillong seismic station. Non-linear least-square inversion is performed to obtain the shear wave velocity and anisotropy of the crust and uppermost mantle using Rayleigh and Love waves group velocities. A high variation of dispersion curves and the shear wave velocity from one group to another indicates that the region is geotectonically very complex. An approximately 80 km-thick zone beneath the study region has shear wave velocity as low as 1.7 km/s in the uppermost crust in the southern part beneath BB and ~4.7 km in the uppermost mantle beneath the Eastern Himalayan Syntaxis (EHS) (Fig. 25). Inferred radial anisotropy varies even within the northern part from the Indo-Eurasian collision zone to EHS and northern to southern IBR. Anisotropy is comparatively stronger in the deeper part below ~40 km for the three paths, except for the EHS, where the result is contrary.

The lowest group velocities of Group 4 (Fig. 25) indicate thick layers of sediments in the BB and IBR. Shear velocity is quite different from the PREM and AK135 models suggesting the presence of lower velocity thicker crust in the Indo-Eurasia and IBR. Low velocities in the lower crust and uppermost mantle for

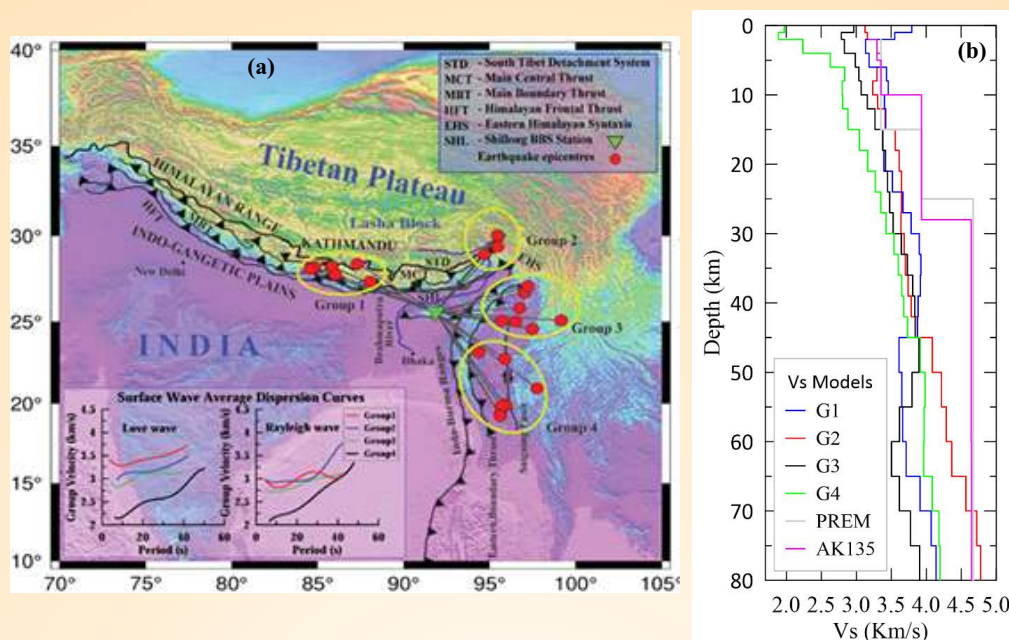


Fig. 25: (a) Surface wave ray paths from the earthquake location (red-filled circles) to the Shillong seismic station (green inverted triangle) are transversely passing different geotectonic units of the Himalaya, Indo-Gangetic plains, and Indo-Burma Ranges. The weighted average dispersion curve (line plots in inset) and the path averaged shear wave velocity models are computed for the four groups located at different azimuths around Shillong. (b) Shear wave 1D velocity models obtained after joint inversion of Rayleigh and Love waves for four Groups 1, 2, 3, and 4.

the paths towards the Indo-Eurasia collision zone and the northern part of IBR may indicate the presence of partial melting. Radial anisotropy has almost opposite trends for the Indo-Eurasia collision zone and IBR regions.

Precursory seismic tremors during the Rishingga rockfall event of 7th February 2021

The present work investigates the prior distribution of acoustic energy in terms of seismic signals/tremors generated from the source of a detached wedge of rock-ice avalanche event of 7th February 2021. The detection criteria and selection of tremors are based on the high signal-to-noise ratio (SNR) with threshold maintained ($\text{SNR} > 10$), amplitude variation, correlation coefficient, and frequency time analysis (Fig. 26). A long trend of continuous harmonic tremors was observed for hours with high-frequency signals (10–35 Hz) before the main detachment. Also, the clusters of precursory signals (4-hour duration) were detected at the Tapovan (TPN) station. The cumulative number of selected tremors increases abruptly after ~3:10 h which indicates the advancement of gliding harmonic tremors with a frequency that varied between 1 and 35 Hz and these events reflect the fracture propagation and subsequent flow of water in the cracks or fractures. The spatiotemporal distribution and continuous propagation

of seismic tremors are observed only in the nearest station, ~12 km from the source. It is detected that the high-frequency tremors get quickly decayed/attenuated with distance than the low-frequency signals depending on the attenuation characteristics of seismic energy. It is also noticed that the high-frequency seismic tremors got saturated and restricted only to the seismic station in proximity to the source zone. Whereas, a portion of precursory seismic tremors was weakly recorded in the Garurganga (GRGA) seismic station. The quantification of tremors at the TPN station follows the given threshold condition of the correlation coefficient trace. The precursory tremors of frequency > 32 Hz indicate an average increase in tremor amplitude with time. The spacing between two subsequent seismic tremors decreased with time which probably indicates the static to dynamic changes in surficial activity within the source.

In the recent wedge failure mechanism, three phases of time-dependent creep were observed i.e. an initial accelerating period of strain advancement termed as transient creep, followed by static to dynamic changes within multiple weak zones, and resulting in material failure by the localization of significant deformation termed as the accelerating creep. The recorded precursors of high-frequency continuous

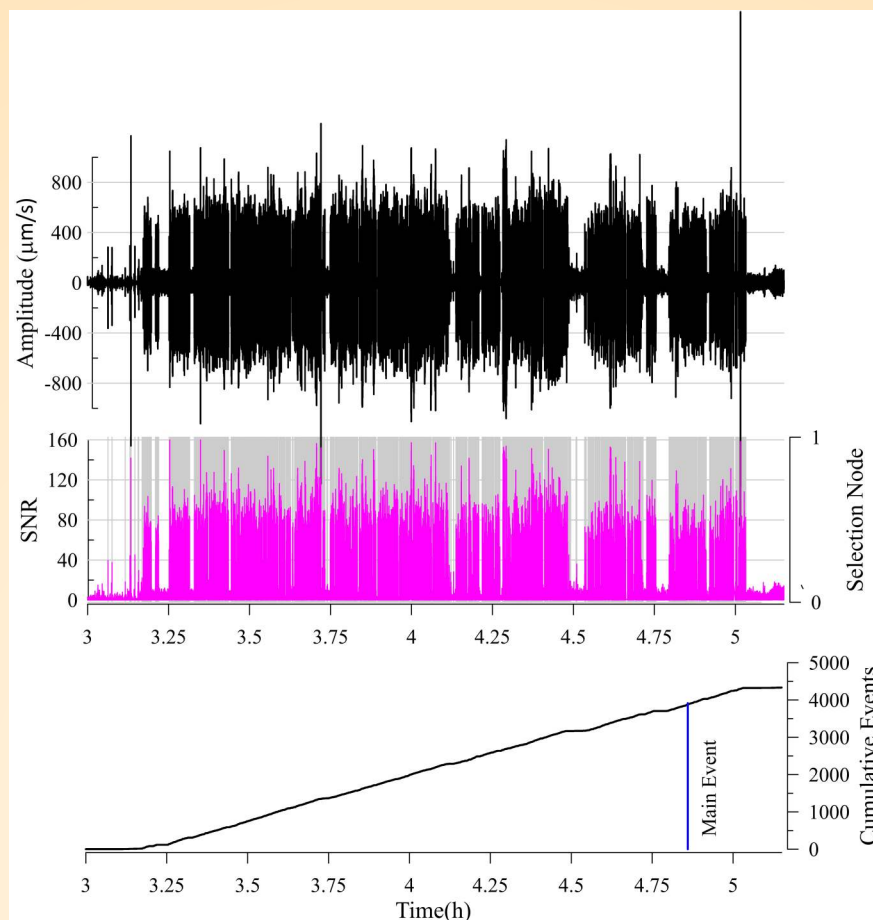


Fig. 26: A cumulative number of detected precursory events showing the huge number of detected tremors with high SNR before the main failure of the Rishiganga rock-ice avalanche. The selection criteria are based on the SNR threshold and amplitude variation.

seismic tremors imply the active source dynamics, fracture propagation, and subsequent flow of water in the cracks due to internally driven force in the weak section of the rock/material. This suggests that the surroundings of a weak wedge in which an enormous volume of material is progressively added for the avalanche before reaching its threshold of material failure and simultaneously increase in tremors amplitude and signal duration. Alternatively, it infers that a significant amount of added material exerts a strong force within the weak zone and generates a strong SNR for a longer time. The seismic records of the main detachment and associated rock slide in the peak time of material failure can be seen in 1–5 Hz. This is recorded at most of the seismic stations of NW Himalaya. But other associated precursory seismic signatures were recorded in the high-frequency range (10 – 35 Hz) which are captured by the nearest seismic stations only. The dynamicity of tremors continued after the rock-ice avalanche for some time. The seismic tremors after the main event are suggested as a relaxation time to recover

the stability of the material within the source zone. Here, the observations highlighted the importance of background noise characterization and high-frequency seismic tremors which got sharply saturated and recorded only in the nearby seismic observatory.

Stress dissipation and seismic potential in and around the Kumaon Himalaya

The distributions of earthquakes are not uniform throughout the Himalayan Arc. The region between the 1905 Kangra and the 1934 Bihar-Nepal earthquakes has not yet experienced an earthquake of $M \geq 8.0$ in the last more than 500 years and is recognized as the Central Seismic Gap (CSG). The Garhwal-Kumaon region is one of the most seismically active regions that has experienced several moderate earthquakes, such as the 1991 (M_w 6.8) Uttarkashi and the 1999 (M 6.5) Chamoli earthquakes, and the more recent Rudraprayag (M_w 5.5) and Dharchula (M_w 5.1) earthquakes. The region is also thought to have experienced three $M \geq 7$ earthquakes in the past namely, 1720 ($M \sim 7.5$), 1803 (M

~ 7.7), and 1916 ($M \sim 7.3$). However, there is no instrumental record of these historical earthquakes to confirm their magnitude and precise locations. It is still uncertain whether these earthquakes were adequate to dissipate the accumulated stress in this segment of the Himalaya. One of the significant ways to address this issue is the determination of the earthquake source parameters, particularly the stress drop (i.e. the difference in stress before and after an earthquake event) of local earthquakes. Since the occurrence of earthquakes is directly related to the accumulation of stress, the estimation of stress drop is an important parameter to explain the seismogenesis and the state of stress in a given area and their variation in time.

In this study, source parameters of 50 local earthquakes ($2.9 \leq M_w \leq 5.5$) of the Kumaon Himalaya recorded by the local seismological network of Wadia Institute of Himalayan Geology, Dehradun and Kumaun University, Nainital have been analyzed using *P*-wave spectral analysis method. The dataset was selected based on a high signal-to-noise ratio ($SNR \geq 3$) and epicentral distance ≤ 100 . The displacement spectra have been computed from time-domain waveform data

with the help of Fourier transformation. Two parameters i.e. low-frequency spectral level (Ω_0) and the corner frequency (f_c) were obtained from a body wave displacement spectrum. From these two quantities, source parameters such as seismic moment (M_0), source radius (r), and the stress drop ($\Delta\sigma$) have been computed. Brune's circular model (Brune, 1970, Journal of Geophysical Research, 75, pp. 4997–5009) was considered to compute the source parameters. The estimated seismic moments ($10^{12} \leq M_0 \leq 10^{16}$ N-m), source radii ($0.3 \leq r \leq 1.3$ km) and stress drops ($0.1 \leq \sigma \leq 40.6$ bar) for Kumaon Himalaya are observed to be significantly lower than the overall values for the CSG showing incomplete dissipation of the accumulated stress. The low-stress drop (σ : 0.1–40.6 bar) is interpreted by the crustal duplex structure that transfers stress into the brittle upper crust. Based on the variation of corner frequency, f_c with the seismic moment, M_0 , a scaling relation $M_0 \cdot f_c^{3.677} = 6E + 15$ N-m/s³ has been obtained. In addition to this dataset, the results of stress drop for 326 earthquakes from previous studies have been compiled to portray regional variation of source parameters. The regional variations of stress drop

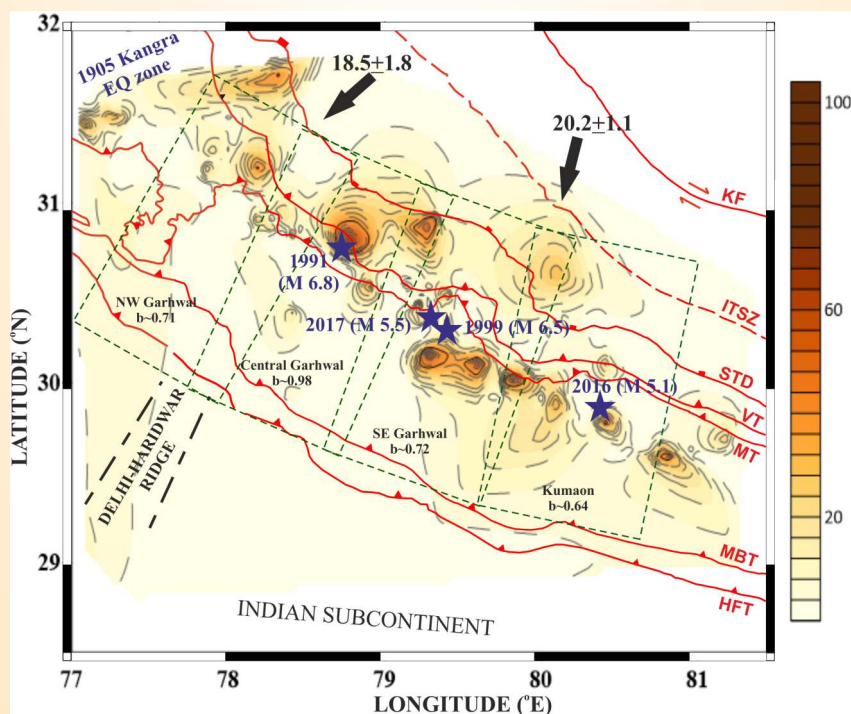


Fig. 27: Contour showing the variation of stress drop estimated in the present study as well as from published literature available in and around the study region. The earthquakes of $M \geq 5.0$ recorded during the period have been marked by blue stars. The legend (right) shows the stress drop value in bars. The green broken boxes represent the b-values zones for different segments of Garhwal and Kumaon Himalaya. The black arrows at the top represent the zonal convergence rates in mm/year for the NW Himalaya. The simplified tectonic features e.g. Himalayan Frontal Thrust (HFT), Main Boundary Thrust (MBT), Munsiri Thrust (MT), Vaikitra Thrust (VT), South Tibetan Detachment (STD), Indus Tsangpo Suture Zone (ITSZ) and Karakoram Fault (RF) are shown by red lines.

values are depicted in figure 27. The majority of the earthquakes are traced along the Main Himalayan Thrust (MHT) zone at 10–20 km depth, with barely any high-stress drop events. The b -value has been estimated for the Kumaon Himalaya using the local earthquake catalog, which is observed to be low (0.64 ± 0.08) compared to the Garhwal and the rest of the NW Himalaya (Hajra et al., 2022, JAES, 239, 105432).

Imaging the crustal structure in the Lohit Valley and Siang Window

Crustal imaging was done in the Lohit Valley and Siang Window (Fig. 28) based on Common Conversion Point (CCP) stacking of receiver functions (RF) and inversion based on the Neighborhood Algorithm. Both low as well as high-frequency RFs could image the Main Himalayan Thrust (MHT) beneath the Lohit Valley at ~20–25 km depth, however, MHT is not visible in the Siang Window plausibly due to large-scale crustal deformation related to the formation of the Window and antiform folding (Fig. 29). Unlike NW Himalaya, the MHT does not play a major role in seismogenesis in the region where seismicity is active up to the crustal depth of ~40 km. The CCP image shows ~40–54 km crust beneath Lohit Valley whereas crustal thickness varies from ~38 km to ~50 km in the Siang Window (Fig. 29). The thinner crust beneath the Tidding-Tuting suture compared to the Indus Tsangpo Suture Zone of northwest Himalaya is caused due to the differences in convergence rate, higher exhumation rate, and mechanism to accommodate collision and rotational tectonics.

Spatial variations of crustal thickness and Poisson's ratio in the northeastern region

Crustal configuration beneath the northeastern region of India has been investigated with the help of receiver function (RF) analysis of teleseismic earthquakes recorded by 19 broadband seismological stations. The H-k stacking method was adopted to estimate crustal thickness and Poisson's ratio beneath each recording station. The study reveals a large variation in crustal thickness and Poisson's ratio which are correlated with the complex geology and tectonics of the region. The crust is observed to be thinner (36.5–41.6 km) beneath Bengal Basin, Shillong Plateau, and the Brahmaputra Valley compared to the Indo-Burma Ranges (IBR) (~40–54 km) and Arunachal Higher Himalaya (TAWA station, ~45 km) and Sikkim Himalaya (GTK station, ~46.5 km). A large variation of Poisson's ratio is observed in the region (~0.230–0.306). Poisson's ratio is generally low-to-intermediate in the Shillong-Mikir Plateau, Bengal Basin, and the Brahmaputra Valley, while it is intermediate-to-high in the Tripura Fold Belt

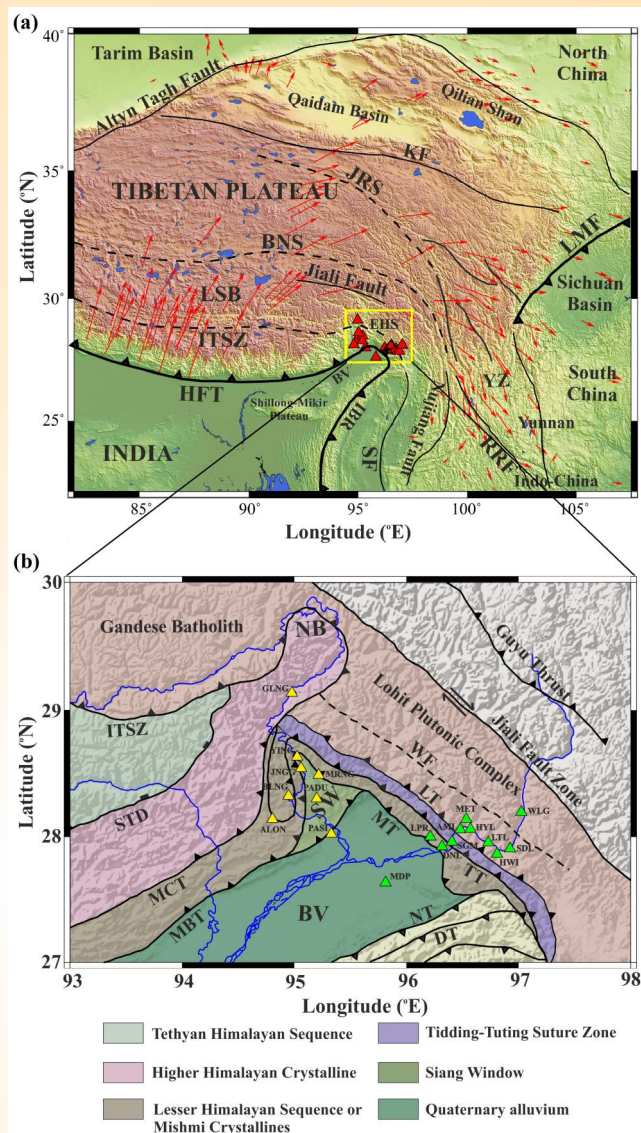


Fig. 28: (a) Topographic map of the Eastern Himalayan Syntaxis (EHS) and surrounding regions with major tectonic features: Himalayan Frontal Thrust (HFT), Indo-Burma Ranges (IBR), Indus-Tsangpo Suture Zone (ITSZ), Lhasa Block (LSB), Bangong Suture (BNS), Jinsha River Suture (JRS), Longmen Shan Fault (LMF), Sagaing Fault (SF), Kunlun Fault (KF), Yangtze platform (YZ), Brahmaputra Valley (BV). The red arrows show the movement of crustal materials obtained from the GPS observations. Figure (b) shows a simplified geological map of the study area marked by a yellow box in (a). Yellow and Green triangles mark the locations of BBS stations used in this study along the Siang Window and Lohit Valley, respectively. The major tectonic features marked on the map are as follows: Main Boundary Thrust (MBT), Main Central Thrust (MCT), Southern Tibetan Detachment (STD), Mishmi Thrust (MT), Tidding Thrust (TT), Lohit Thrust (LT), Walong Fault (WF), Naga Thrust (NT), Disang Thrust (DT), Namche Barwa (NB).

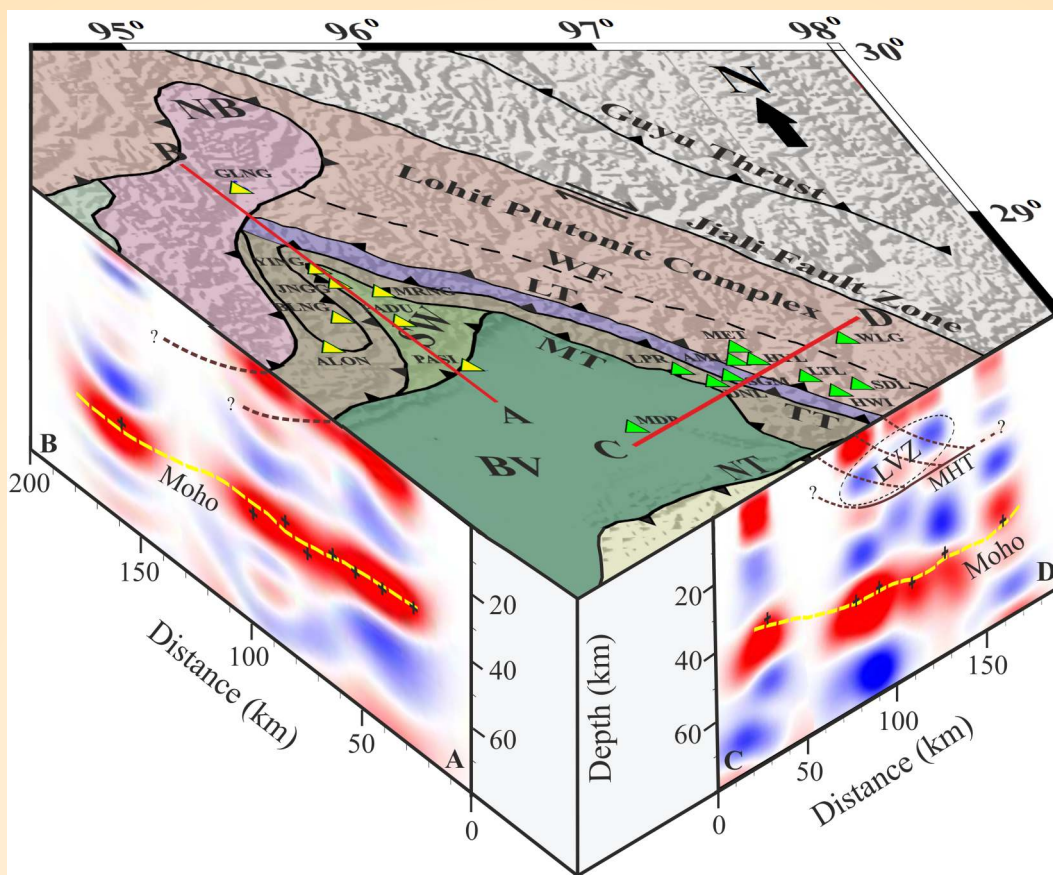


Fig. 29: 3-D view of crustal configuration interpreted from the CCP image along the two profiles AB and CD. The tectonic map and the stations (triangles) belonging to AB and CD profile are shown at the top. The Moho interpreted from the CCP image, and NA inversions are marked by dashed yellow lines. '+' signs indicate the Moho depth obtained from the NA inversions. The MHT is visible in the inverted models at a few stations of Lohit Valley (CD profile) marked by a black line at a depth of ~20-26 km, whereas MHT is not clearly visible in the CCP image of Siang Window (AB profile).

and the northern part of the IBR (Shukla et al., 2022).

Long Period Magnetotelluric and Electrical resistivity tomography Survey in NW Himalaya

Long Period Magnetotelluric (LMT) a time series data along the Yamunotri-Gangotri-Saharanpur profile is processed for apparent resistivity curves. This profile is parallel to the MT profile in the Sutlaj Valley and the Garhwal and Kumaun Himalaya. The subsurface resistivity variations in these profiles help in understanding along-strike variations in the MHT. Resistivity distribution across the MCT region along the Bijnaur-Mallari profile of Garhwal Himalayan and the Nahan-Kourick Changu profile in Satluj Valley is significantly different in resistivity variations and structure. This implies the prevailing role of differential tectonics in different segments of the Himalaya.

Further Pillibhit-Malpa profile is completed for dimensionality and directionality analysis. Two dimensionality of the subsurface resistivity model is

valid for 2-D modeling. Few observations suggest higher-order complex resistive subsurface structure along the profile. Two-dimensional modeling for estimating subsurface resistivity variations along the profile is in process.

Time series processing of MT sites along the NCR-MT 2nd profile (Sohna-Delhi) is in process for MT transfer function estimation using “Resistics”, an open-source Python code. It incorporates standard robust regression methods and adopts a modular approach for processing MT time series.

Electrical resistivity tomography (ERT) data around the Pangong Lake region was collected at three places. The idea is to identify sedimentological features in the subsurface in the resistivity variations. Three-dimensional ERT data at Mirak is modeled for 3D resistivity variation (Fig. 30). In the volume of resistivity alignment of resistive features along a particular direction is an important observation that indicates the presence of some track/channel.

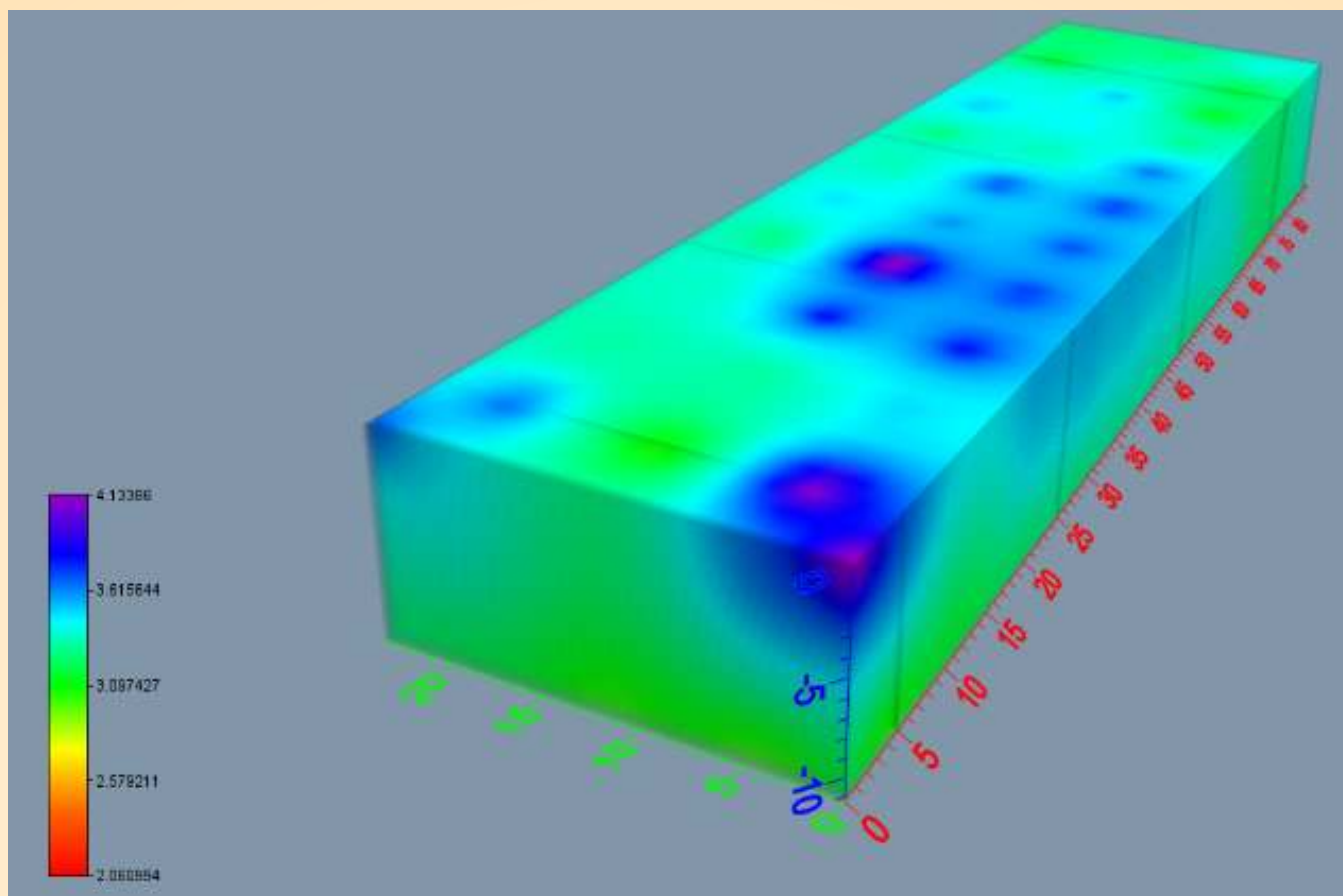


Fig. 30: 3D resistivity variation in Mirak.

Activity: 2C

Seismicity and seismic hazard assessment in the Himalaya

(Ajay Paul, Dilip Kumar Yadav, Narendra Kumar, Praveen Kumar and Chinmay Haldar)

Simulation of strong ground motion for hazard estimation and mitigation

Earthquake waveforms of the Uttarkashi earthquake (1991) and Chamoli earthquake (1999) have been simulated using a hybrid technique which is the combination of two existing techniques i.e. envelope technique and composite source model technique. The simulated waveforms and their corresponding response and Fourier spectra for seismic recording sites have been generated. Simulation has been done at 11 and 9 recorded stations of the Uttarkashi and Chamoli earthquakes respectively. Important frequency and time domain parameters i.e. Fourier spectra, response spectra, peak ground acceleration (PGA), and duration at stations have been estimated and compared with the observed accelerograms. It has been observed that the

simulated pga (231 cm/s^2) at the closest distance Bhatwari (22 km) matched with the observed one (248 cm/s^2) for the Uttarkashi earthquake. The same has been observed at the nearestmost station, Gopeshwar (19 km) of the Chamoli earthquake. The highest recorded pga of 352 cm/s^2 is well-matched with the simulated value i.e. 347 cm/s^2 . Similar matching has been observed for other stations also. The present technique is independent of velocity- Q and aftershock data of small earthquakes, this study brings light to the site effect and high-frequency decay parameter. This study can be very helpful in the estimation of seismic Hazards in a specific region and for designing an earthquake-resistant building.

Source characterization of the local earthquakes in Siang Valley, Arunachal Pradesh

The Earthquake data recorded from December 2020 to December 2021 by 8 BBS seismic stations of the Siang Valley network of Arunachal Pradesh, NE India are extracted and processed for the estimation of hypocentral parameters. The Spatial distribution of

local earthquake seismicity in Siang Valley shows that the western part of Siang Antiform is more active compared to the eastern part. The cross-section along the SW-NE direction shows deeper events in the Namche Barwa region (Fig. 31). Comparatively fewer earthquakes are observed in the core of the Siang window. The seismicity is broadly correlated with the Himalayan Seismic Belt, within the MBT and MCT zone. Depth sections of the microseismic events show that the earthquakes are more or less uniform and

confined to a depth ≤ 40 km. Thus, it is essential to assess the status of seismicity in the northeastern region and also to evaluate the seismic performance of existing buildings.

Focal Mechanism Solutions (FMS) of the earthquake of $M \geq 3.5$ are determined using the waveform inversion technique implemented on ISOLA software (Fig. 32). This method is based on the iterative deconvolution technique. The results are stated in the expression of the double-couple component of the deviatoric solution,

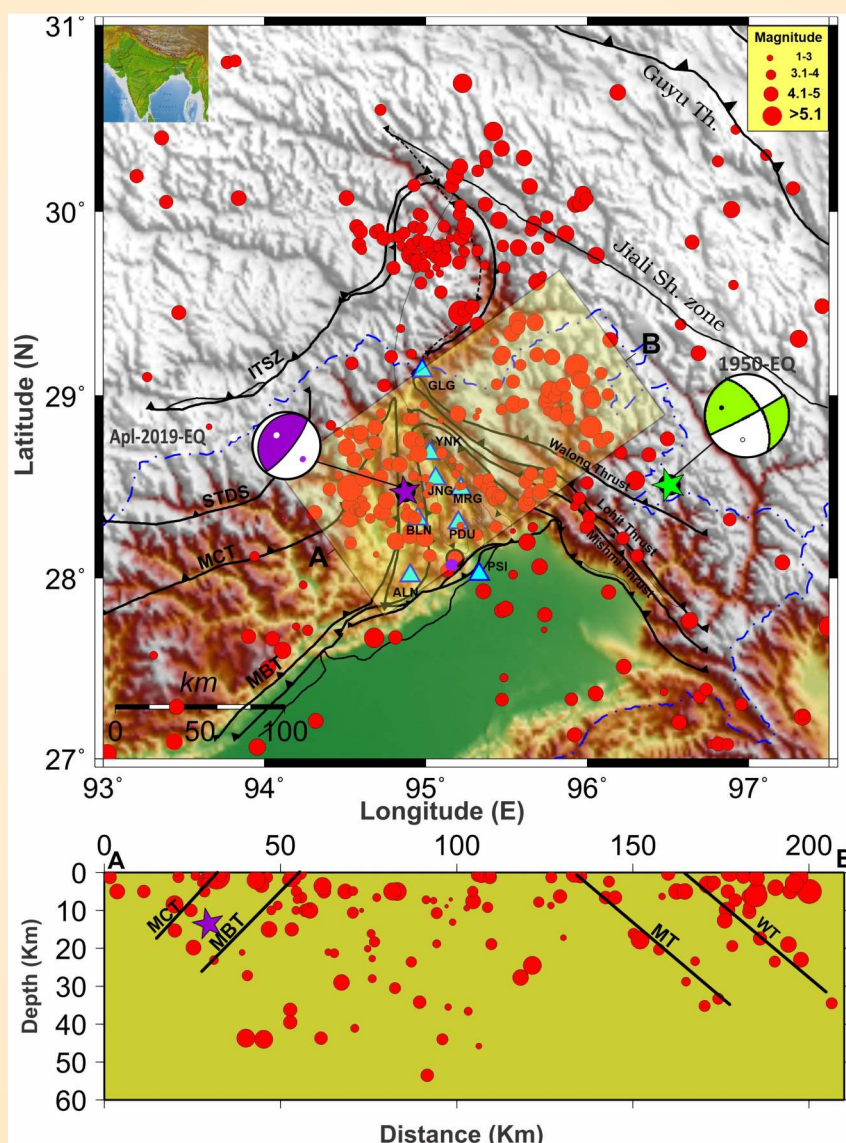


Fig. 31: Seismicity distribution in Siang Valley of Arunachal Pradesh, NE India for the period December 2020-2021. The earthquakes with different magnitudes are shown by filled circles of different sizes as indicated in the Legend (top right corner). The depth distribution of the earthquakes along the A-B section is shown in the lower panel. The tectonic features Main Central Thrust (MCT), Main Boundary Thrust (MBT), Mishmi Thrust (MT), and Walong Thrust (WT) are shown on the map.

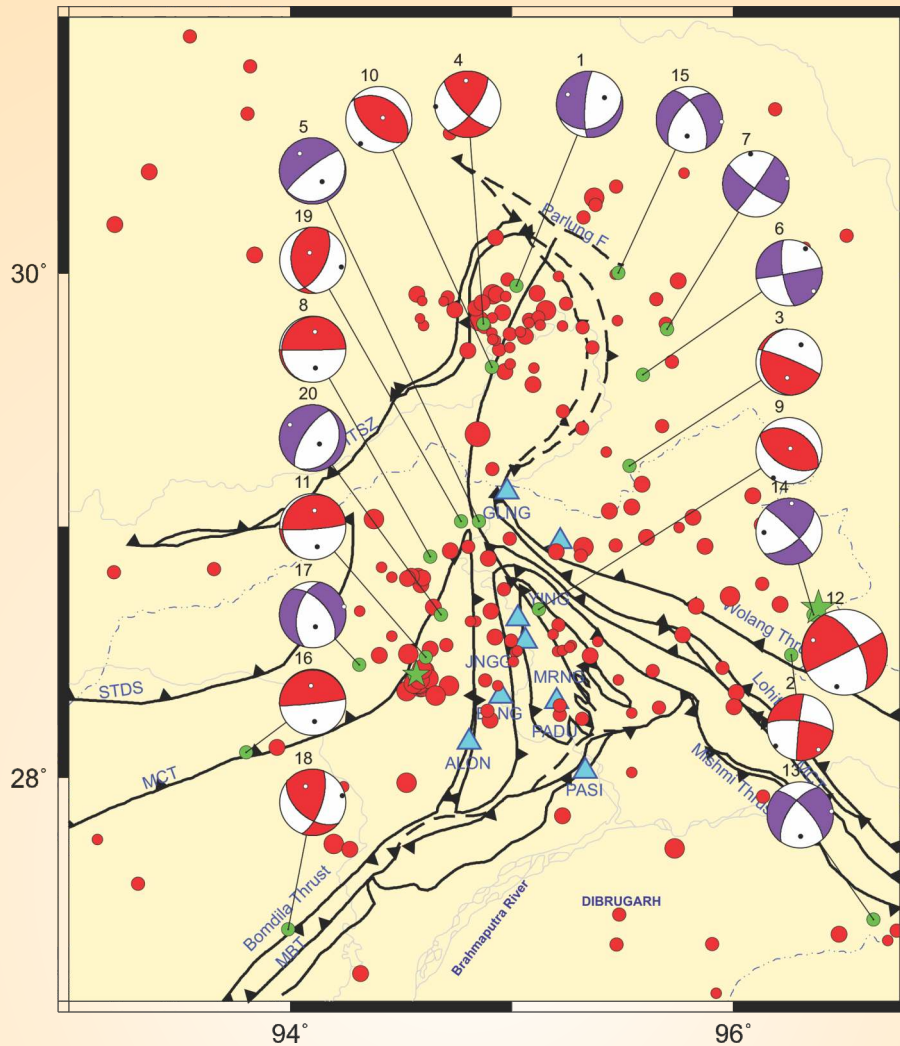


Fig. 32: Plots of the Focal mechanism solutions of the past earthquakes and present seismicity (December 2020–December 2021) of the Siang Window, NE Himalaya (modified after Yadav et al., 2021). The red circles with variable sizes represents the earthquake with different magnitudes. The cyan triangles show the locations of BBS stations. The green circles are the epicentral locations of FPS (beachballs), the shaded area in the beach ball is compressional, and the open area dilatational quadrant. The red beachballs are thrust type FPS with a few strike slip components and purple beachballs are the Normal type of FPS. The small black dots inside the beachballs are the P (black dots) and the T axes (white dots). The tectonic faults/lineaments are ITSZ: Indus Tsanpo Suture zone, MCT: Main Central Thrust, MBT: Main Boundary Thrust, and STD: South Tibet Detachment.

represented by the scalar moment, strike, dip, and rake. The selection of local earthquake for FMS solution has been made based on a high signal-to-noise ratio (SNR), a clear and impulsive record of P and S phase arrivals. The variation of the pressure axis (P-axes) orientations was obtained from the FMS. The P-axis orientation of the events to the west of the Siang Window shows WNW-ESE orientation, whereas the Namche Barwa (NB) region and core of the Siang Window show mostly northeast orientation (Fig. 33). In contrast, the P-axis is observed to be predominantly NE-SW in the east of the Siang window and Walong fault zone.

Inclusion of arias intensity for the evaluation of earthquake-induced landslides

Earthquake-induced landslide hazard is the most serious threat in seismo-tectonically active mountains like the Himalaya. It has been frequently noted that the damage caused by earthquake-induced landslides is significantly greater than the earthquake itself. Therefore, assessing the susceptible zones of earthquake-induced landslides in seismically active areas is essential. In this study, the probabilistic hazard assessment of the earthquake-induced landslides has

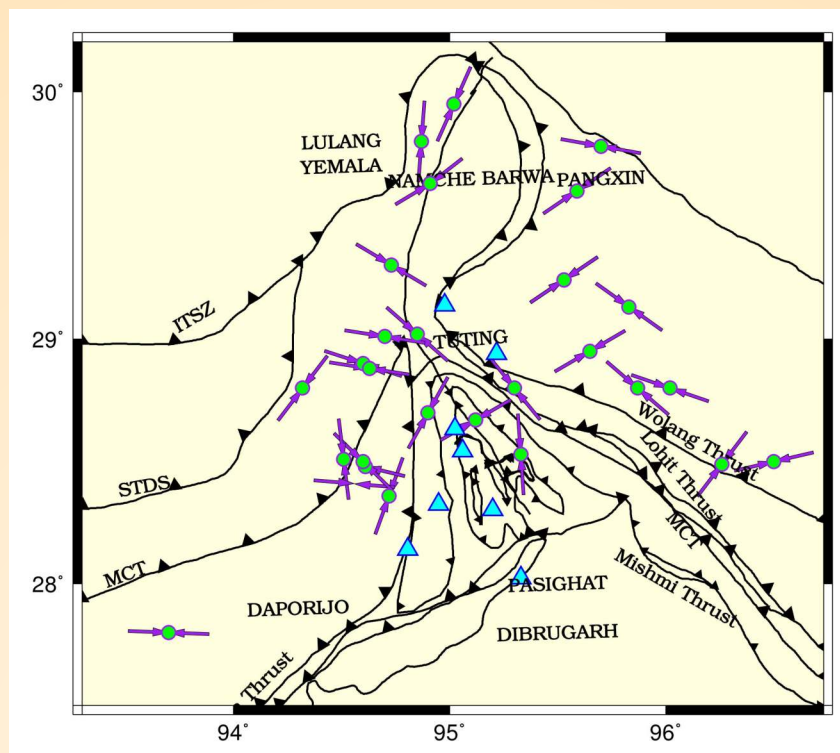


Fig. 33: P-axis orientation of Siang Valley, NE India which shows preferably NE-SW trending compressional axis. The purple bar with green dots shows the direction of P-axes over the epicentres and the cyan triangles are the Broadband Seismic (BBS) stations of Siang Valley Network in Arunachal Pradesh.

been conducted for the Goriganga valley, Kumaun Himalaya. Numerous studies indicate that a great earthquake of magnitude $8 M_w$ or higher could strike this area at any time. Hence, mapping earthquake-induced landslides using an improved Newmark's model has been conducted for earthquakes of magnitude $8 M_w$ (Fig. 34). The inclusion of arias intensity to estimate the permanent displacement of the slope for future scenario earthquakes make this work unique from others. Arias intensity has weightage over Peak ground acceleration (PGA) for slope failure studies as it comprises both amplitude and duration information, so the present work gives upgraded results for better assessment of hazard. It has been noted that $\sim 25\%$ of the study area is susceptible to earthquake-induced landslides when subjected to direct shaking of an earthquake of magnitude $8 M_w$. The results of this work provide great insight to planners and civil engineers for hazard mitigation and assessment of the study region.

Seismological evidence for intra-crustal low velocity and thick mantle transition zones in the North-West Himalaya

High-quality three-component teleseismic waveform data are used to investigate the detailed subsurface

structure of the crust, the intra-crustal low-velocity layer (LVL), and the upper mantle discontinuities beneath the Kumaun-Garhwal, North-West Himalaya. The results, derived from the inversion of the stacked P-receiver functions (PRFs) of individual stations using the neighborhood algorithm approach, show that the crustal thickness varies from 42 km to 54 km beneath the study region. The depth of LVL observed beneath six stations from individual and stacked PRFs, varies from 9 to 25 km. The LVL zone with a high V_p/V_s ratio may be due to fluid or partial melt, thereby leading to shallow seismic activity within the study region. The presence of fluid or partial melts in the LVL may be due to the shear heating, cooling, and decompression. The 2D PRF migration image depicts a thick mantle transition zone due to the elevated 410 km discontinuity with respect to the global average values predicted by the IASP91 velocity model (Fig. 35). The present research suggests that this might be due to the colder transition zone in this region, indicating the cool underthrust Indian plate with respect to the ambient mantle has reached down to the upper mantle transition zone.

Shear wave velocity model for Garhwal Himalaya

In the past decade, the seismic activity in the Garhwal Himalaya has been monitored by 10 three-component

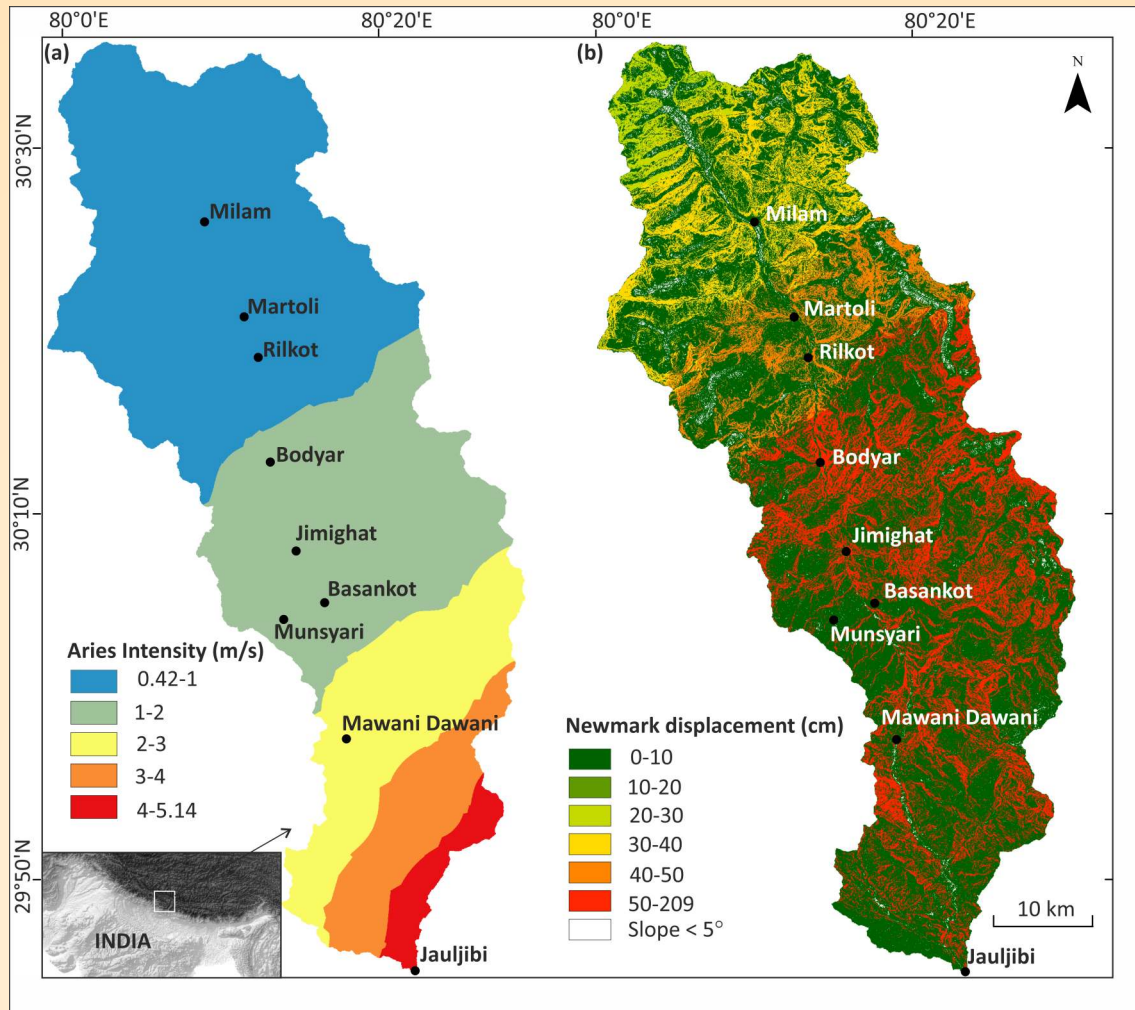


Fig. 34: (a) Arais Intensity and (b) Newmark's permanent displacements for the ground shaking of an earthquake magnitude of 8.0 (M_w).

broadband seismographs deployed all along the Garhwal Himalayan Seismic Belt (GHSB). In this study, seismological data during 2016–2017 have been used, and seven 3-component broadband seismographs have been selected for our present study. Digital waveform data of 80 regional earthquakes (M_w : 5.0–6.8) recorded by the seven stations have been used to estimate fundamental mode group-velocity dispersion (FMGVD) characteristics of surface waves (Rayleigh and Love waves) and the final average 1-D regional shear wave velocity (V_s) structure below the Garhwal Himalayan region. First, FMGVD curves have been computed for Rayleigh waves (5.8–81.9 s) and Love waves (at 6–82 s) period, and then, these dispersion curves have been inverted to compute the final average 1-D regional shear wave velocity (V_s) structure of crustal and upper mantle beneath the study region. The

best-fit model in the Garhwal Himalayan region, India, reveals the 8-layered crust with a mid-crustal low-velocity layer (MC-LVL) between 10 and 20 km depth in the proximity of MCT. The models show a variation of V_s within the range of 3.40 – 3.65 km/s in the upper crust (0–20 km depth) and 3.65 – 4.65 km/s in the lower crust (20–46 km depth). The Moho-depth is calculated to be 46 km deep below the Garhwal Himalaya, and the shear-velocity (V_s) in the sub-crustal sector is 4.65 km/s (Fig. 36). Our estimated mid-crustal low-velocity layer (MC-LVL) could be linked to the presence of metamorphic fluids in the fractured MHT, resulting from the weakening of the crustal material at the interface between the overriding Eurasian plate and upper-part of the underthrusting Indian plate.

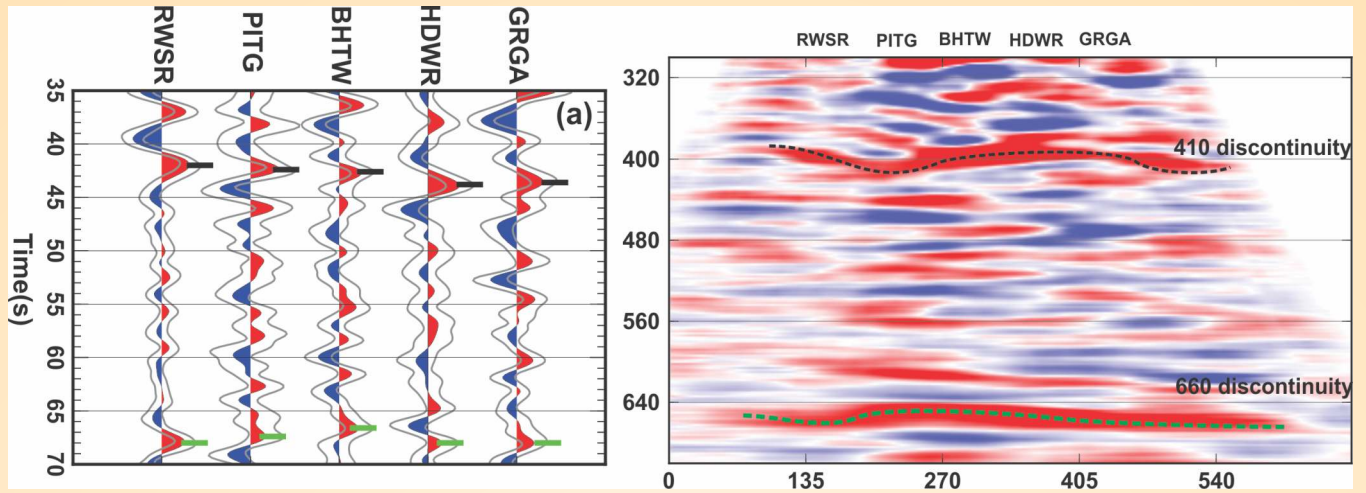


Fig. 35: (a) Observed stacked receiver functions. Red and blue colors represent the positive and negative conversion. The Black dash line shows the P_s conversion time from 410 km and 660 km discontinuities. (b) 2D migrated receiver function image. The 410 and 660 km discontinuity are clearly visible and marked by the black dotted line. Red and blue colors represent positive and negative conversions.

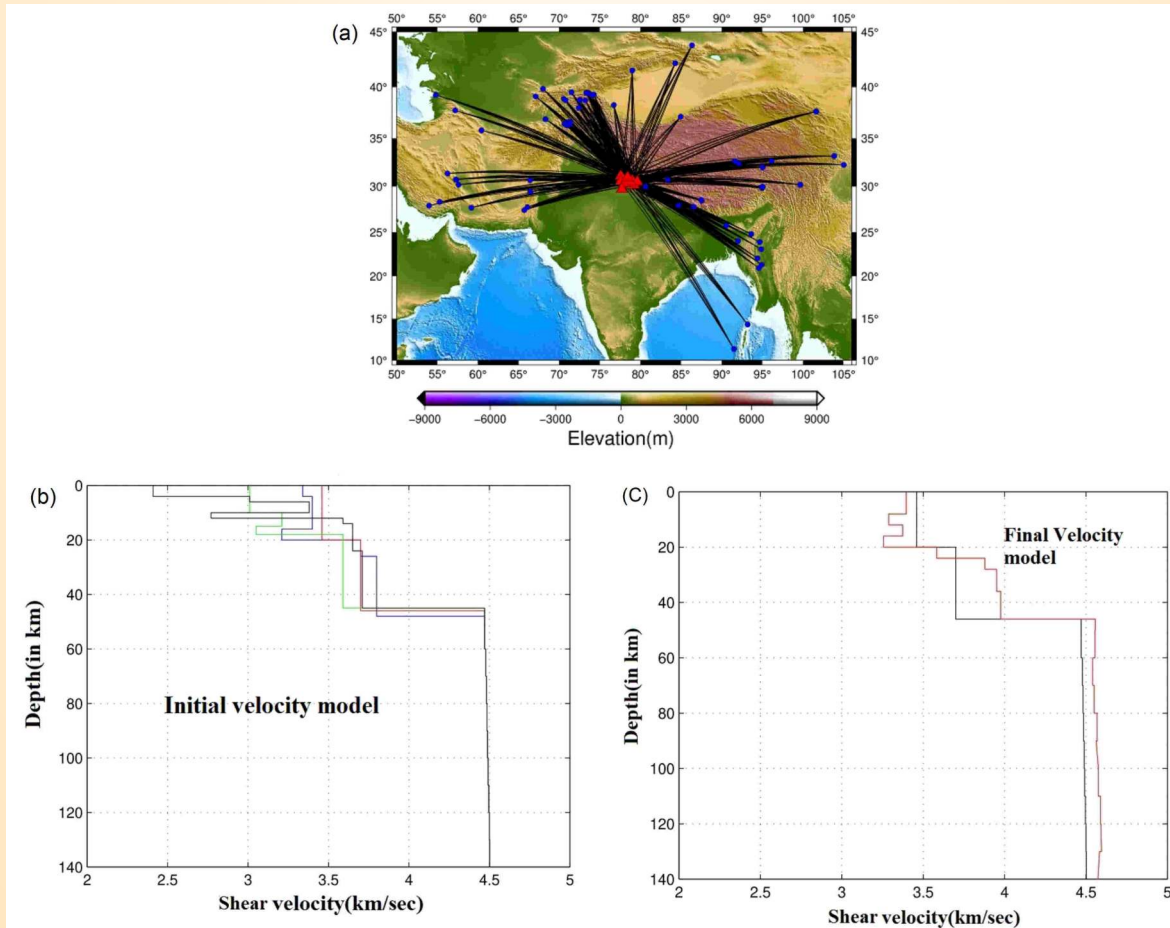


Fig. 36: (a) Ray sampling of the surface wave dispersion study. Locations of different regional events of the Garhwal Himalayan region are marked by large filled blue circles while the broadband stations are shown by filled red triangles. (b) The initial velocity models are shown by a thick blue line (Mandal et al., 2022), a thick green line (Kumar et al. 2009), a black line (Kanaujia et al. 2015), and a red line (Negi et al. 2008), (c) Final velocity model is shown by the thick red line.

Activity: 3**Biotic evolution with reference to Indo-Eurasian collision – Evidences for global events**

(R.K. Sehgal, Kapesa Lokho, Suman Lata Srivastava and Ningthoujam Premjit Singh)

Stable carbon ($\delta^{13}\text{C}$) and oxygen ($\delta^{18}\text{O}$) isotopic composition of 75 serial samples (tooth enamels) from five mammalian fossil groups, which include giraffids, equids, bovids, tragulids, and suids have been carried out to reconstruct their diet and habitat. These mammalian faunas were recovered from a late Miocene Middle Siwalik succession exposed in Nurpur, Himachal Pradesh, India (8.14–5.26 Ma). The average $\delta^{13}\text{C}$ data of the studied mammals, that is, -13.30 ± 0.71 (giraffids), -11.29 ± 0.63 (equids), $-12.68 \pm 0.49\%$ (bovids), -12.97 ± 1.11 (tragulids), and -12.01 ± 0.47 (suids) indicates a mainly C3 diet with a minor component of C4 grass (up to 17%) and a habitat dominant by forest/woodland. The average $\delta^{18}\text{O}$ value of giraffids (-5.83 ± 0.85) is slightly enriched as compared to other herbivore mammals, such as equids (-8.85 ± 1.71), bovids ($-7.86 \pm 0.62\%$), tragulids (-8.26 ± 1.92), and suids (-10.65 ± 0.23). It suggests that the browsing giraffids could likely intake water from enriched ^{18}O sources, whereas the other browsing mammals consume water from depleted ^{18}O sources in the local ecosystem. However, the $\delta^{18}\text{O}$ values indicate

the existence of a warm, humid climate and more precipitation in the Siwalik during the late Miocene (Fig. 37).

A very rare madtsoiid snake has been reported for the first time from the Late Oligocene of India (the molasse deposits of Ladakh Himalaya). Madtsoiidae is an extinct group of medium-sized to gigantic snakes, that first appeared during the late Cretaceous and mostly distributed in the Gondwanan landmasses. Although, their Cenozoic record is extremely scarce. From the fossil record, the whole group disappeared in the mid-Paleogene across most Gondwanan continents (except for Australia, the group survived here with its last known taxon *Wonambi* till the late Pleistocene). The occurrence of madtsoiid from the Oligocene of Ladakh indicates their continuity at least to the end of the Paleogene and shows that the members of this group were successful in this subcontinent for a much longer time than previously thought. The global climatic shifts and the prominent biotic reorganization across the Eocene-Oligocene boundary (which correlates to the European Grande Coupure), did not cause the extinction of this important group of snakes in India (Fig. 38).

Further, remains of fossil lizards and snakes have been discovered from a locality (dated 9.1 Million Years) in Haritalyangar, Himachal Pradesh, India (Figs.

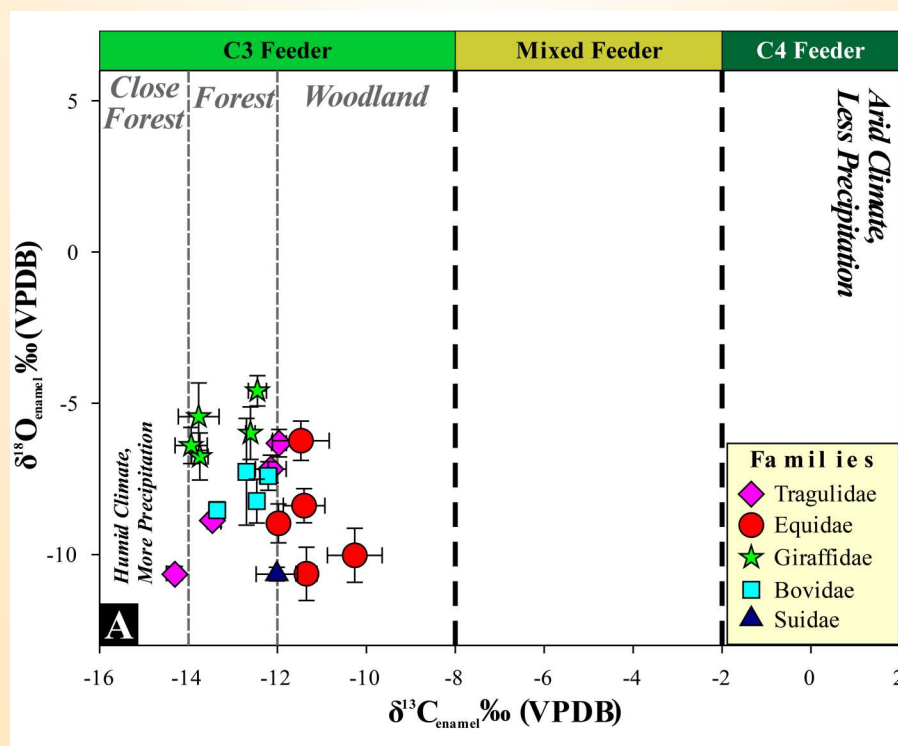


Fig. 37: $\delta^{13}\text{C}$ and $\delta^{18}\text{O}$ isotope bivariate plot of Nurpur mammals.

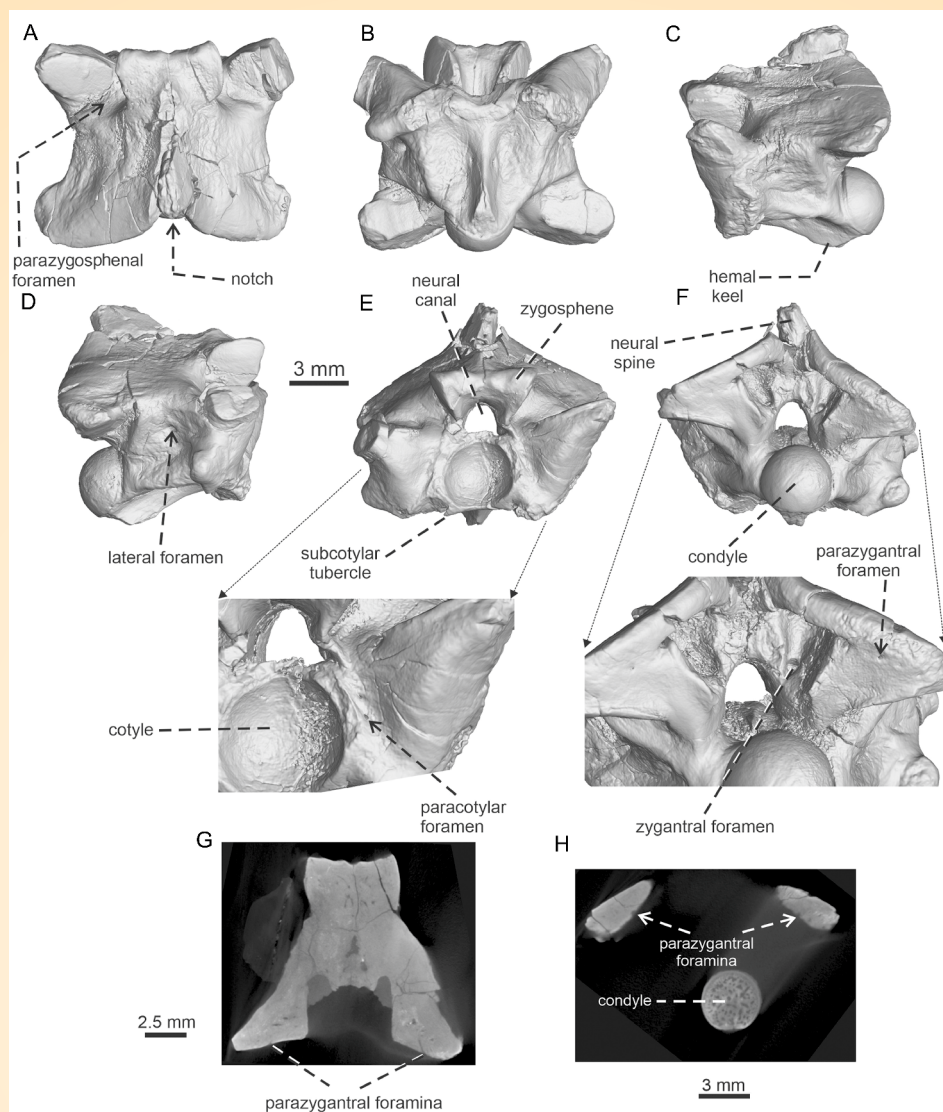


Fig. 38: Madtsoiidae indet. from Ladakh Himalaya. The specimen WIMF/A 4816 in A, dorsal; B, ventral; C, D, lateral; E, anterior (with detail of subcotylar foramen); F, posterior (with detail of parazygantral foramina) views. Virtual slices of the vertebra with a special emphasis on the parazygantral foramina: G, horizontal; H, coronal.

39 and 40). The material consists of the following taxa: *Varanus*, *Python*, a colubrid, and a natricid. These squamates are documented from this region for the first time. The occurrence of *Varanus* in Haritalyangar is important concerning its past biodiversity because varanids have a limited fossil record in Asia. Also, the fossil *Python* from South Asia remains poor except for the earliest record from Pakistan (dated ca. 18 Ma) and Kutch, Gujarat (dated ca. 14-10 Ma). A co-existence of *Varanus* and *Python*, two iconic squamates, revealed a wider distribution of the clade in this southern Asian territory. As ectothermic animals, the distribution, richness and diversity of squamates are highly dependent on temperature and climatic conditions. For this reason, squamates are widely regarded as excellent

indicators of past climates, particularly ambient temperatures. The overall Haritalyangar squamate fauna, which is dominated by both large and small semi-aquatic and terrestrial taxa, indicates seasonally wet sub-humid to semi-arid climate in the area during the Late Miocene, 9.1 Ma. Moreover, the mean annual temperature must have been high in the region at that time (not less than 15–18.6°C, similar to the mean annual temperature in this area today), indicated by the occurrence of important thermophilic elements such as *Varanus* and *Python*.

A new assemblage of both invertebrate and vertebrate faunas have been described from the middle Eocene deposits of the Sylhet Limestone of Mikir Hills.

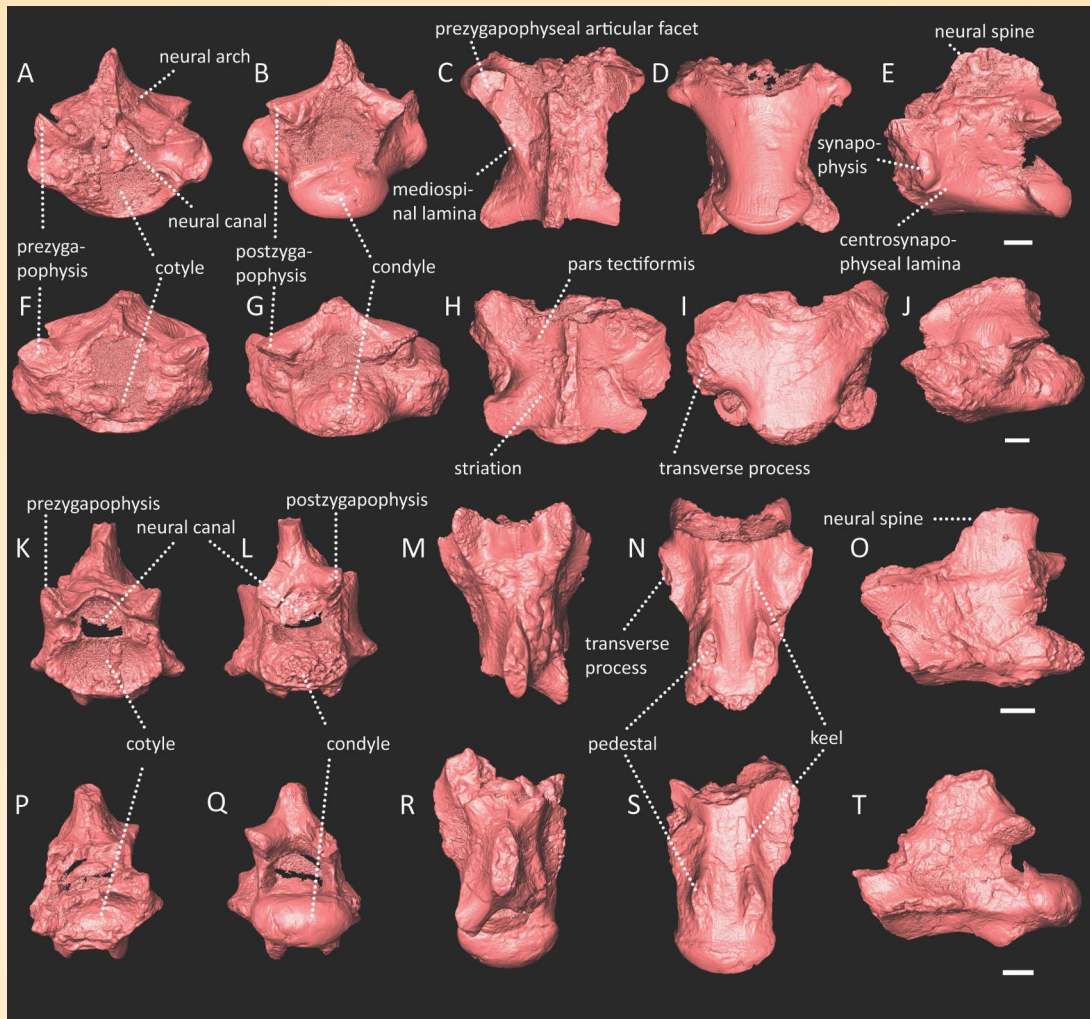


Fig. 39: *Varanus* sp. Vertebrae in anterior (A, F, K, P), posterior (B, G, L, Q), dorsal (C, H, M, R), ventral (D, I, N, S), and lateral (E, J, O, T) views. Scale bars: 1 mm.

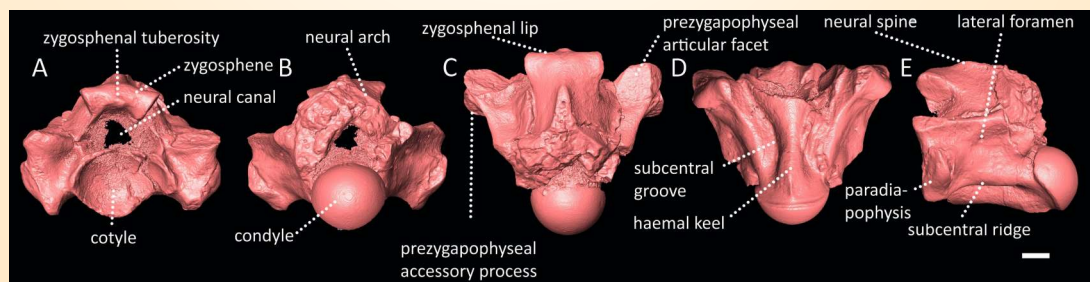


Fig. 40: *Python* sp. Trunk vertebra in anterior (A), posterior (B), dorsal (C), ventral (D) and lateral (E) views. Scale bar: 1 mm.

The new assemblages consist of shark, ray, crocodile, and echinoderm spines (Figs. 41 and 42) and were recovered from Shallow Benthic Zone (SBZ) 16-18 in the upper part of the Sylhet Limestone succession corresponding to late middle Eocene age. All these fossils were recovered from the muddy limestone horizon of the succession full of Nummulites forming packstones. The presence of muddy limestone at 29 m

level forming packstones which have yielded an extensive population of Nummulites and other faunas testifies to the high stand sea levels attaining maximum flooding surface (MF). The collected invertebrate and vertebrate fossils and sedimentological observations imply a typical shallow marine environment for the Sylhet Limestone Formation of Mikir Hills. Also, as indicated by the remains of sharks and rays in the

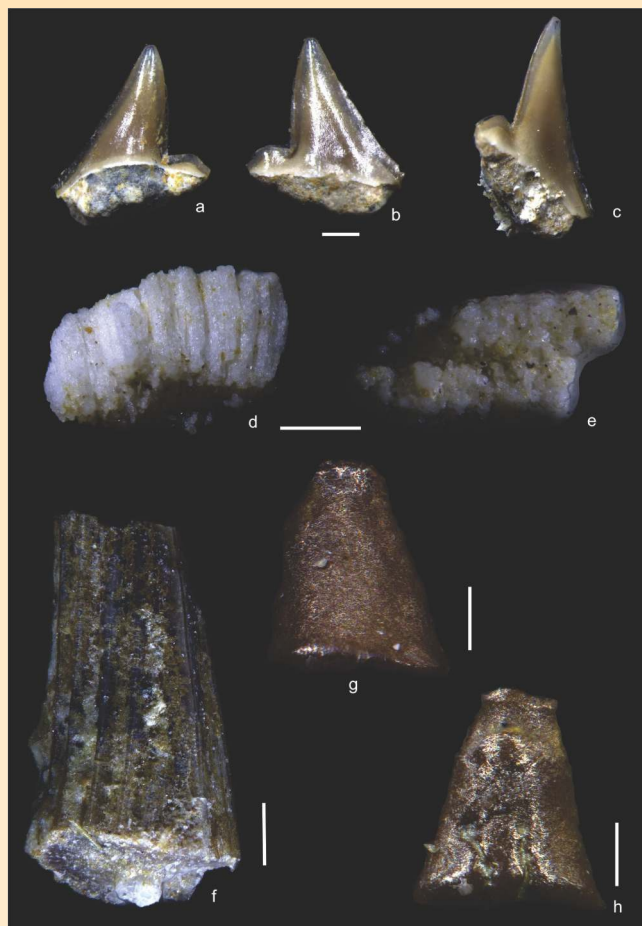


Fig. 41: Shark and Ray tooth from the Mikir Hills. (a) Lingual views of Shark tooth; (b) & (c) labial views of shark tooth; (d), (e) ray tooth (median tooth fragment); (f) crocodile broken tooth; (g), (h) conical tooth. The scale for all is 200 μm except for (a)-(c) 500 μm .

present study, which mostly prefer shallow marine water of tropical to temperate climates and they feed on invertebrates and small fishes. This faunal-yielding horizon of Mikir Hills is of considerable use in understanding the paleoenvironment, paleobiogeography, and paleo biodiversity. The recovery of sharks, rayfish, and crocodiles in this study have a common feature with many marine middle Eocene formations of the world, in particular middle Eocene of Kutch, Subathu, Rajasthan (India), New Hampshire, Libya, Iraq, Iran, North Western Sahara (Algeria), Tanzania (East Africa), Italy, Germany, and Southern North Sea basin (Europe). The present discovery of middle Eocene shark and ray in this region with other published data from other parts of India and elsewhere signifies an open connection of the Tethys Sea during the middle Eocene age.



Fig. 42: (a)-(i) Spines of echinoderms; (j)-(k) broken fragments; (l) broken tooth fragment. Scale for all is 500 μm except for (c), (j) & (l) 200 μm and 1 mm for (e), (f), (g) & (k).

The first Miocene planktonic foraminifers were recorded from the Surma Group in the foothills of the Naga Schuppen Belt of the Indo-Myanmar Range. The present fossil assemblage has a significant bearing on biostratigraphy, paleoenvironment, and paleogeography.

The modern pollen from the surface sample of Garhwal Himalaya was identified and quantified and established a modern pollen-vegetation relationship in the Garhwal Himalaya.

Fieldwork in Lahaul-Spiti, Himachal Pradesh is carried out for the collection of soil/paleolake/peat samples. A total of ~80 surface samples and 50 modern plant specimens were collected. In addition to this, 4 cores from Parashar, Ghepan, Chicham, and Tashigang were retrieved and 2 soil profiles from Chicham and Aliyas were sampled at one cm intervals in the field for the biotic and abiotic proxies, and AMS ^{14}C dating. Samples were also collected for the OSL dating. Three cores are sliced in the laboratory at 0.5 to 1 cm intervals

for multi-proxy analysis. A total of 200 samples are analyzed for Total organic (TOC) content and 20 samples for grain size measurements. Chemical treatment of ~120 samples for stable carbon isotopes ($\delta^{13}\text{C}$) and 16 samples for black carbon (BC) measurements is also performed. The AMS ^{14}C dating of the cores and sedimentary profiles will be performed in the IUAC, New Delhi.

In the sedimentary profile of Chamoli Garhwal, a multi-proxy analysis was carried out. Analyzed samples for pollen (54 nos.), $\delta^{13}\text{C}$ (50 nos.), and major and trace elements (50 nos.). Development of ~11000 years of climate history is in process.

Activity: 4A

Climate variability and landscape responses in selected transects of NE and NW Himalaya

(Khayingshing Luirei, Som Dutt, Anil Kumar, Chhavi Pandey, Pinkey Bisht, Subhojit Saha, Mahesh Kapawar)

Sedimentation, extreme events, landscape and cave deposits responses to the climate variability

A speleothem study from the Bhiar Dhar cave, western Himalaya suggests a coherence in oxygen isotopes and microfabrics interpreted climate variability on a millennial time scale. Depleted oxygen isotopes showing increased precipitation are associated with the prograded nature of the stacking pattern and columnar fabrics whereas enriched oxygen shows dark micritic layers developed during arid conditions. Another study from the same cave examines the geo-tourism potential of the cave. The Bhiar Dhar cave is one of the very few caves in the Himalaya, showing a variety of speleothem features and forms. The cave encompasses stalagmites, stalactites, flowstones, straw, columns, cave curtains, diapirs, etc., and has immense potential to be developed as a geo-tourism site and demands immediate actions for its conservation for education and scientific studies.

The study from the western Assam lowland areas, based on geomorphic mapping, lithofacies analysis, and geochemical (Sr-Nd analysis) provenance characterization, as well as optically stimulated luminescence (OSL) ages, provides sedimentation framework. The findings suggest that the alluvial fan is composed of three distinct lithofacies associations during 27 to 3 ka. The bottom-most gravelly-sandy facies indicates the progradation of the fan during the last glacial maximum (LGM). The middle facies is a sheet flow deposit that formed during the early

Holocene period. During the Mid-Late Holocene, the uppermost facies have been deposited as rivers lost their gradient. In the present study, it is found that the fan accretion in the Brahmaputra foreland is controlled by sea level (Fig. 43). The Sr-Nd isotope fingerprints have been used to identify fan sediment sources from the Himalayas' southern front (i.e., Lesser and Higher Himalaya).

Lower Ganga plains (LGP) along the Ajay River in the Rarh region were focused to document sedimentation patterns and the timing of deposition. The fluvial packages in the study area correspond to two significant channel phases: Period-I (2.4 ka to 1.3 ka) and Period-II (800 years to 200 years ago). Period-I is characterized by the episodes of floodplain development and lateral migration of the trunk river during ~2.4 ka due to ISM intensification. Conversely, Period II is characterized by flooding phenomena and the aggradation of channel bodies across much of the present valley area during the last 800 years.

A study from the Mawmluh cave in northeastern India suggests significant regional variability of the Indian summer monsoon during the Meghalayan age. A significant wet phase was witnessed in northeastern India between ~3.5 and 2.9 kyr BP which was also observed in other parts of the country (Fig. 43). Northeastern India observed an abrupt and pronounced weakening of summer monsoon rainfall at around 4.2 kyr BP that lasted for around 200 years (Fig. 44) whereas the same events lasted longer in the western and northwestern part of the Indian subcontinent.

Debris flow susceptibility analysis of Leh Valley by detailed investigation of sediment availability, topographic conditions, and their relation with known events was quantified by the index of connectivity (IC) model, the Flow-R model, and the Weights of evidence (WOE) method. The study suggests that if the sediment-stuffed hill slopes have high connectivity with the downstream area then there is a large likelihood that even a small debris flow event initiated in the headwater region can turn into a disastrous event downstream. The results of this study can be used as preliminary data though they recommend further development of the susceptibility model. In addition, the preparation of a detailed inventory map of past debris flows is highly recommended for much more improved prediction accuracy.

Depositional age and provenance of Lesser Himalaya

U-Pb detrital zircon geochronology and radiogenic isotopic ($^{87}\text{Sr}/^{86}\text{Sr}$, ϵNd) study from the Proterozoic

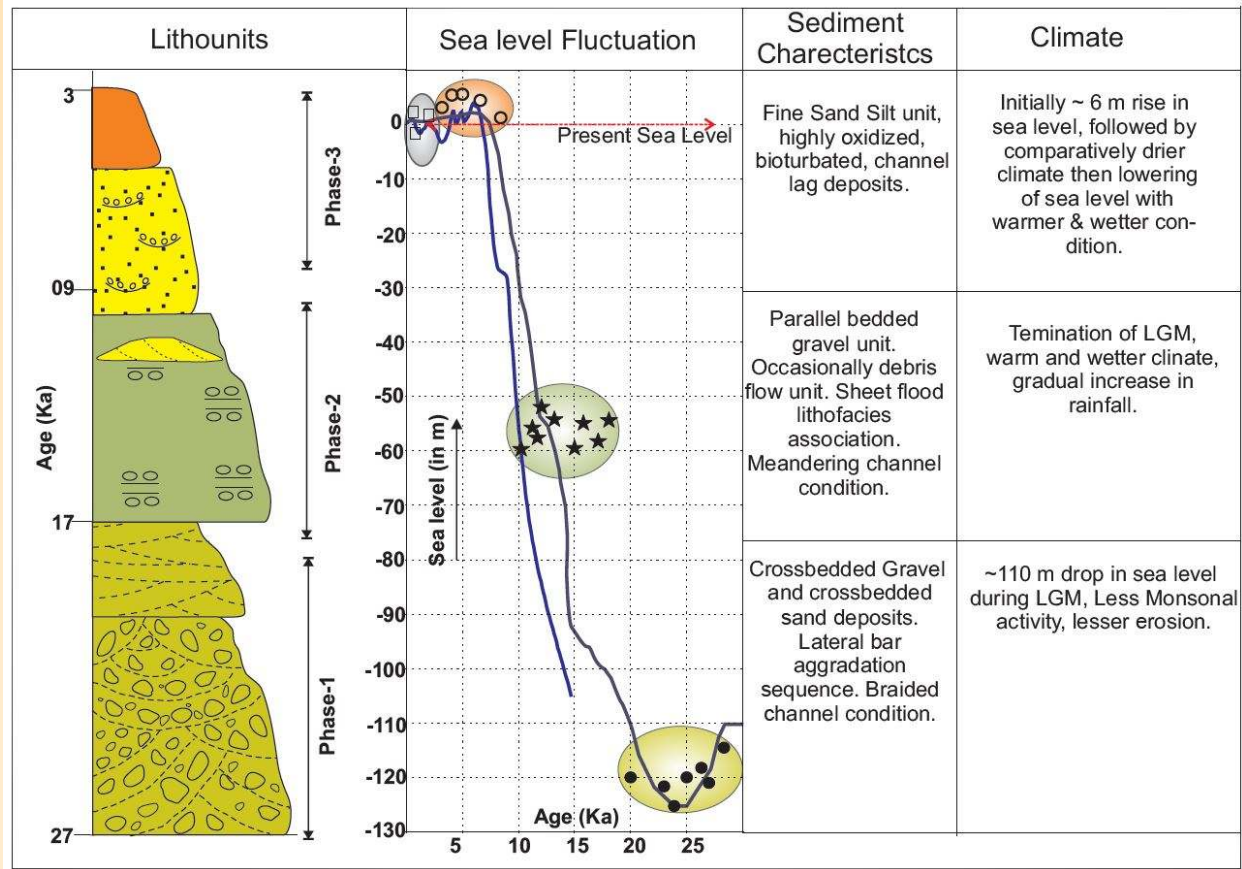


Fig. 43: Development of different phases plotted against Sea level fluctuation. (●) marked are the ages obtained from phase-1 while (★) marked are ages from phase-2, (○) marked are the ages obtained from Phase-3 and (□) are the ages obtained from meander scrolls.

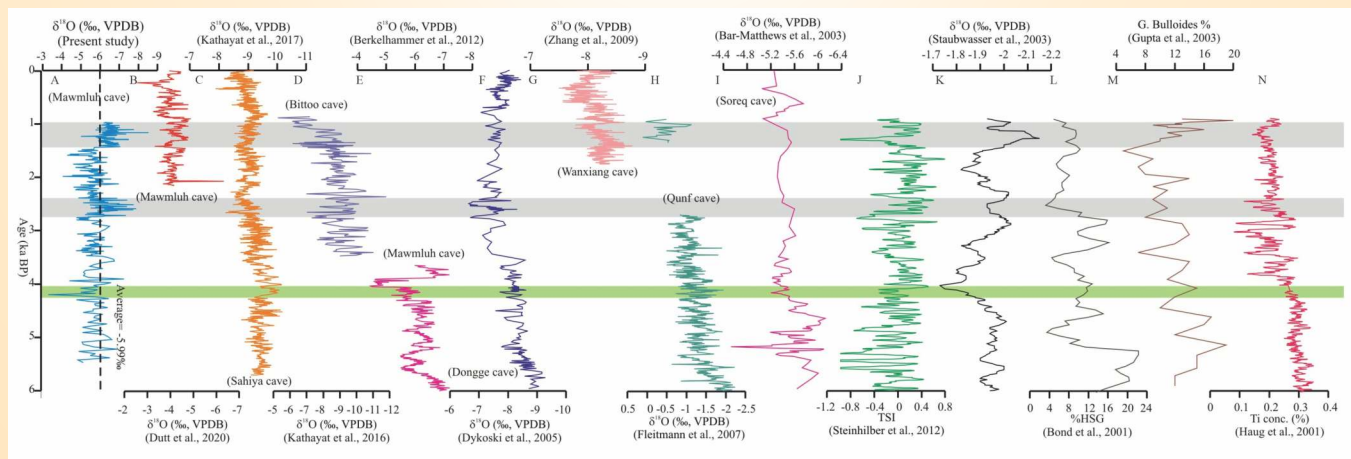


Fig. 44: Comparison of ISM proxy record from Mawmluh cave with other proxies. A) Present study B) ISM proxy record from Mawmluh Cave C) ISM proxy record from Sahiya Cave D) ISM proxy record from Bittoo Cave E) ISM proxy record from Mawmluh Cave F) ISM proxy record from Dongge Cave G) ISM proxy record from Wanxiang cave H) ISM proxy record from Qunf cave I) ISM proxy record from Soreq cave J) Total Solar Irradiance (TSI in W/m²) record K) ISM proxy record from Arabian Sea core (G. Ruber oxygen isotope) L) Bond event proxy record from Haematite Stained Grains (HSG) M) ISM proxy record from G. bulloides % from Arabian Sea N) Ti% as a proxy record of Intertropical Convergence Zone (ITCZ) movement from Cariaco Basin.

clastic successions of the Garhwal-Kumaon Lesser Himalaya supports a mixed source as reflected by the wide range of Mesoproterozoic to Neoproterozoic age probability peaks. Only the ILH (Inner Lesser Himalaya) and OLH (Outer Lesser Himalaya) vary in the relative proportion of the Neoproterozoic ages. The present age data identified that the sedimentation within the Rautgara Formation of the ILH continued till Neoproterozoic. Tracking the detrital Zircon U-Pb ages in the near adjacent cratonic parts points towards the Aravalli orogenic belt as the major source region. Whole rock $\epsilon\text{Nd}(0)$ values for the ILH rocks range from -37.6 to -14.6. Whereas for OLH $\epsilon\text{Nd}(0)$ values range from -19.6 to -6.7. More negative ϵNd values of ILH indicate supply from more evolved protolith or older continental crustal rocks or recycled sources and less negative ϵNd values of OLH support less evolved protolith. The change from more negative ϵNd to less negative ϵNd values progressively upward the stratigraphy can be due to shift in source with time. Both detrital zircon and ϵNd data support for the continuous sedimentation model, rule out the presence of unconformity within the Lesser Himalaya, and argues for separate evolution of the Lesser Himalayan basin on the trailing edge of the extended north Indian craton.

Mineral magnetic characteristics of Indus Molasse

The easternmost successions of the Indus molasses (syn-collisional Indus molasse sedimentary rocks) along the Nyoma-Rhongo transect were sampled to perform the first-ever detailed rock magnetic and magnetostratigraphy study with orientations. Standard paleomagnetic specimen sizes ($L=22$ mm and $D=25$ mm) were prepared and the initial magnetic susceptibility measurements were performed which averaged $\sim 3.758 \times 10^{-3}$ SI, suggesting they sufficiently carry magnetic remanence. The detailed rock magnetic study on the Indus Molasse sedimentary rocks involves measurements of isothermal remanent magnetization (IRM), Coercivity, Hysteresis loops, and thermomagnetic (Susceptibility vs. Temperature) curves. Combined rock magnetic results indicate fine-medium-grained, pseudo-single domain magnetite as a dominant, and pyrrhotite and greigite are other accessory magnetic minerals present in Indus molasses. These results indicate that the sedimentary rocks of the Indus molasses could have lithified over well-developed paleogeography with signs of post-lithification and small-scale cyclic variations. It is finally remarked that the ambient environment that existed during the formation of Indus molasses was likely stable with small-scale tectonic modulations

(localized, i.e., in the easternmost part of Indus molasse in ISZ) within the large-scale deformation regime (regional, i.e., Himalayan Orogeny). Early syn-collisional Indus molasse sediments were feasibly deposited directly upon an uplifted and eroded surface that developed over the Ladakh Batholith (south of the Eurasian Plate), these sediments were entirely derived from the north, with the Ladakh arc being the most likely source.

Glacial response to climate change

This study provides the first comprehensive account of the glaciation of the Yankti Kuti valley of the upper Kali Ganga catchment of the Kumaon Himalaya, Uttarakhand. Employing multi-year satellite images from 1990 to 2021, the loss of glacial area, ice volume, snout recession, and the changes in the Equilibrium Line Altitude (ELA) in the Yankti Kuti valley were investigated. The results showed an overall reduction of ~ 21 km² ($\sim 21\%$) of the total glacier area of the basin. The basin witnesses an ice volume loss of $\sim 46\%$ and ~ 46 m upward shifting of the Equilibrium Line Altitude (ELA) between 1990 - 2021 (Fig. 45). The retreat rate of the four studied glaciers show ranges from ~ 18 to 41 m per year. The glaciers in the valley are melting at a significant rate due to global warming, giving rise to the increasing number of pro-glacial lakes in the studied region from 04 numbers in 1990 to 10 numbers in 2021 and making them vulnerable to glacial lake outburst floods (GLOFs) in the near future.

Optical and physicochemical characterization of atmospheric aerosols from central Himalayan Glaciers valleys

To investigate the optical and physicochemical properties of ambient aerosols, random mobile monitoring campaign was conducted at various locations along the Vyas and Darma Himalayan glacier valleys in the Kumaun region of the central Indian Himalaya, close to the Indo-Nepal-Tibetan border figure 46(a). The investigations were carried out at a variety of locations, with elevations ranging from around 900 masl (at Dharchula) to 5000 masl (at Jolingkong), as shown in figure 46(a). As shown in figure 46(b), an optical characterization was employed in conjunction with a handheld mobile monitor (microAeth AE51) to estimate the number of black carbon aerosols. In addition, rainwater samples were collected from the area and analyzed based on the events that took place there. The results of the ICPMS analysis are depicted in figure 46(c), which shows the average content of the elements. In addition, the ionic content was investigated, and the results are displayed in figure 46(d).

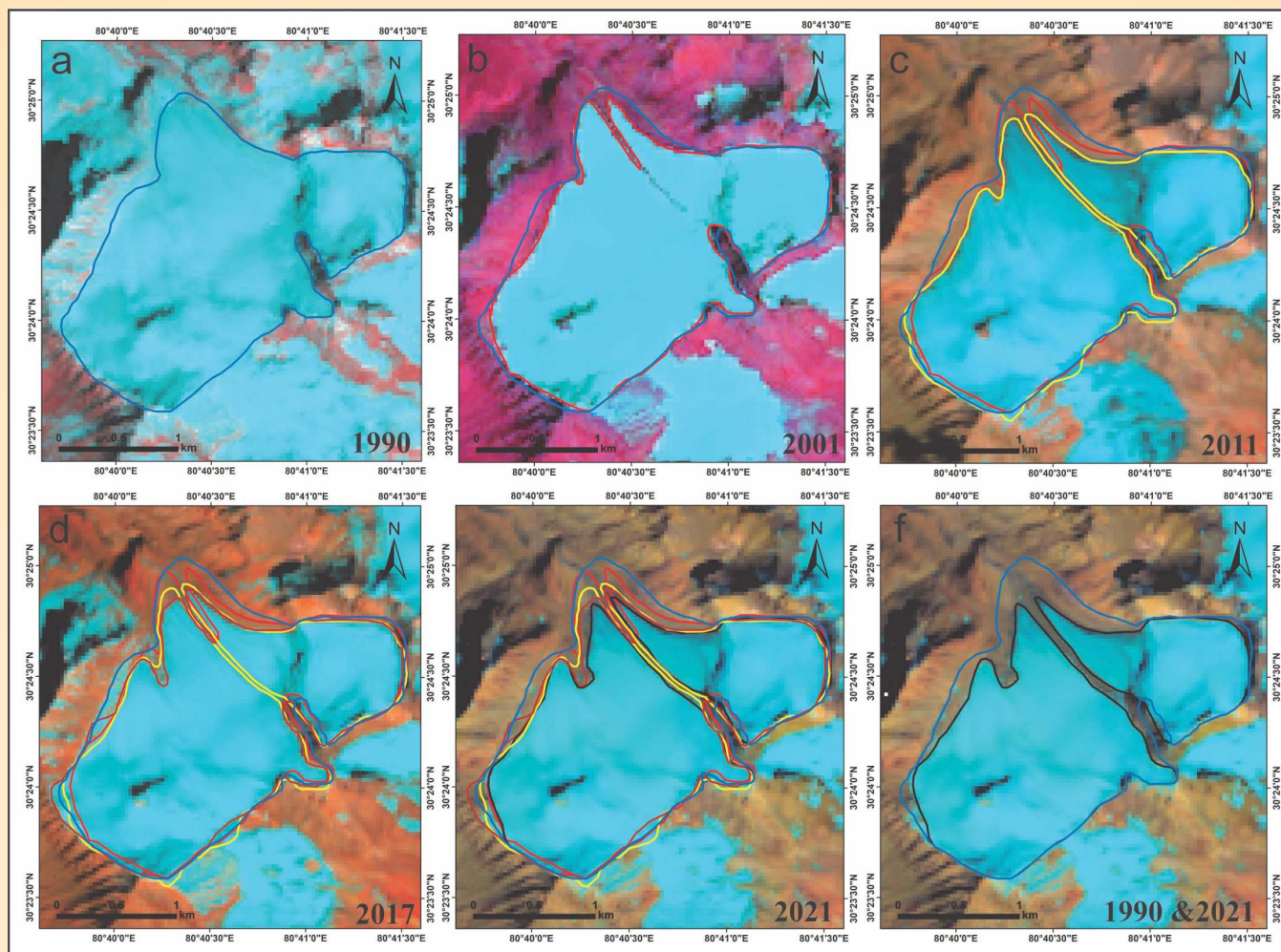


Fig. 45: Landsat Image showing the glacier area changes from 1990 to 2021.

Reactivation of the old landslides caused by extreme rainfall in the Main Central Thrust zone of the Bhagirathi Valley, Garhwal Himalaya, India

Barsu village and adjoining settlements are nestled over old landslide debris. Barsu village is a small hamlet of about 1 sq km with a population of 469 and households of 98. It is bounded by multiple landslide scarps, the SE dipping scarp measures about 2.1 km in length while the two NW dipping scarps measure 1.65 km and 0.72 km in length, respectively (Fig. 47). The type of landslide is debris slide and is retrogressive as it is propagating in the upslope direction towards the crown of the landslide. For settlement and cultivation purposes the villagers have leveled the midsection which is gentler in slope, while in the head and toe portion, the slope is undulating and steeper. Landslides cracks and fissures both along and transverse are observed towards the main scarp (Fig. 47b,c,d,e). The old main scarp portion has been thickly vegetated; just below it, minor scarp

has developed as the result of recent landslide activity. The minor scarp measures about 1.5 m in height, and below is the number of cracks and tilted and uprooted trees. The landslide has also resulted in the formation of paleochannels due to stream piracy and small ponds. The slope is gently sloping and the average slope percentage drawn across is 28%. Slope movements have affected many houses and infrastructures such as footpaths, roads, retaining walls, and drainage (Fig. 48). Infiltration of the waters along the cracks and fissures is observed at different portions of the slid mass, the infiltrated water oozes at the toe of the landslide at Swari Gad. Another implication of the landslide is that the water in the water tank constructed at the heart of the village is infiltrating along the cracks and fissures. Across the spur, Pala village is also nestled on the top of landslide debris. From the slope morphology, this portion of the slope is also affected by phases of landslides which at present are not active as evident from thinly vegetated old scarps. The affected slope

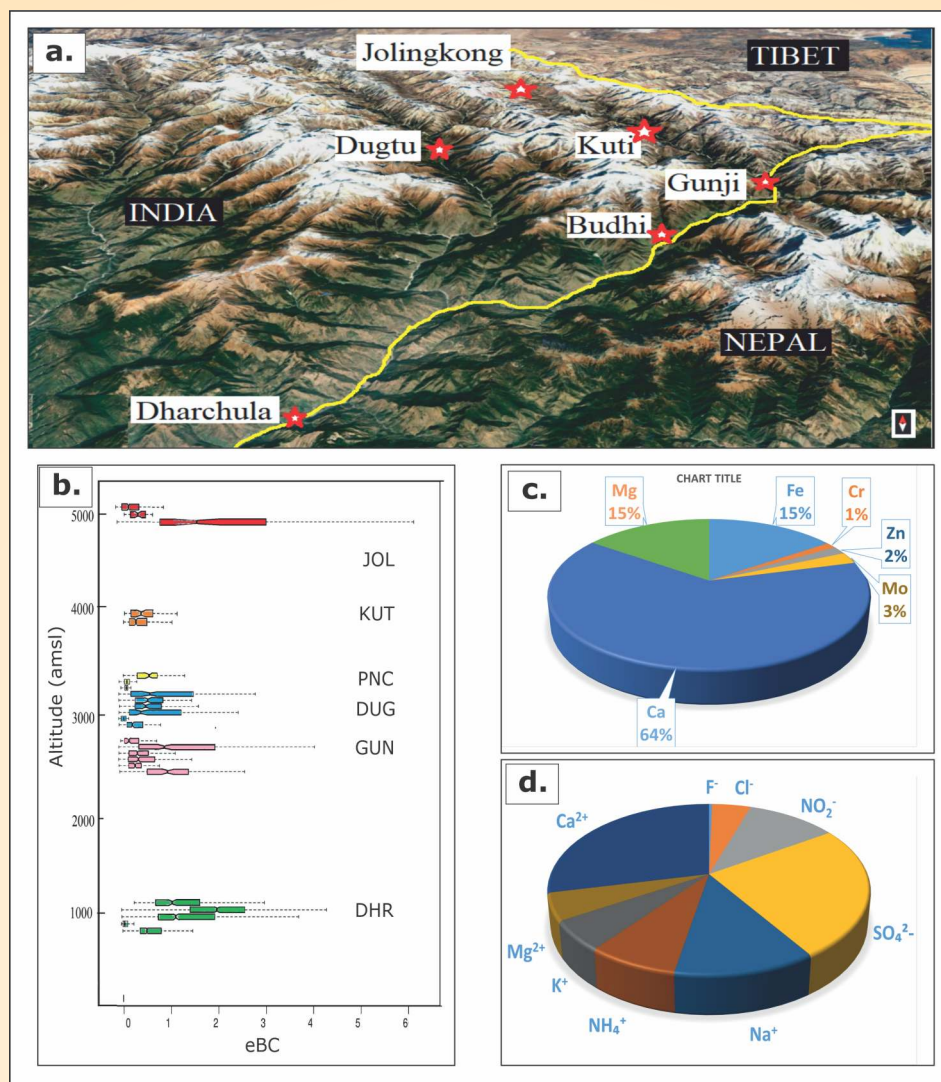


Fig. 46: (a) Vyas and Darma glacier valley along Central Himalaya, India; (b) eBC mass concentration at different altitudes (Dharchula, Gunji, Dugtu, Kuti, Jolingkong); (c) elemental concentration in rainwater samples analyse using ICPMS; (d) anion-cations present in rainwater samples acquired from these valleys based on events during the expedition along these valleys.

measures 485 m in width and 915 m in length. The average slope percentage is 44.1%, and the upslope is more gentle than the downslope, which has an average slope percentage of 66%. South of Pala 0.40 km old landslide section is observed and the exposed section is comprised of highly fractured and weathered migmatites. A stretch of road section is constructed across this landslide debris is subsiding and may affect the downslope in case the slope fails. In the adjoining areas of Bhatwari and Raithal, various workers have documented the landslides and its rate of movement. Four main types of rocks were observed at the exposed sections; the head scarp towards SE of Barsu is made up of phyllite and chlorite schist bedrocks. The western and northern part of Barsu is made up of gneissic rocks, east

of Barsu along the Swari Gad, it is made up of migmatites. The southeastern part of Barsu is made up of gneiss and migmatites. The phyllite and chlorite schist are highly weathered and the schistosity planes dip steeply to almost vertical. The rocks are traversed by steeply dipping joints that intersect. The gneissic rocks are highly fractured forming intersecting joint sets. The migmatite rocks exposed along the Swari Gad are highly fractured and weathered.

The following are the causative factors for the landslide. The settlement of village Barsu is on the debris of old landslides. This paleo landslide must have taken place in a thin patch of country rocks made up of sericite-chlorite schist and brownish-purple biotite

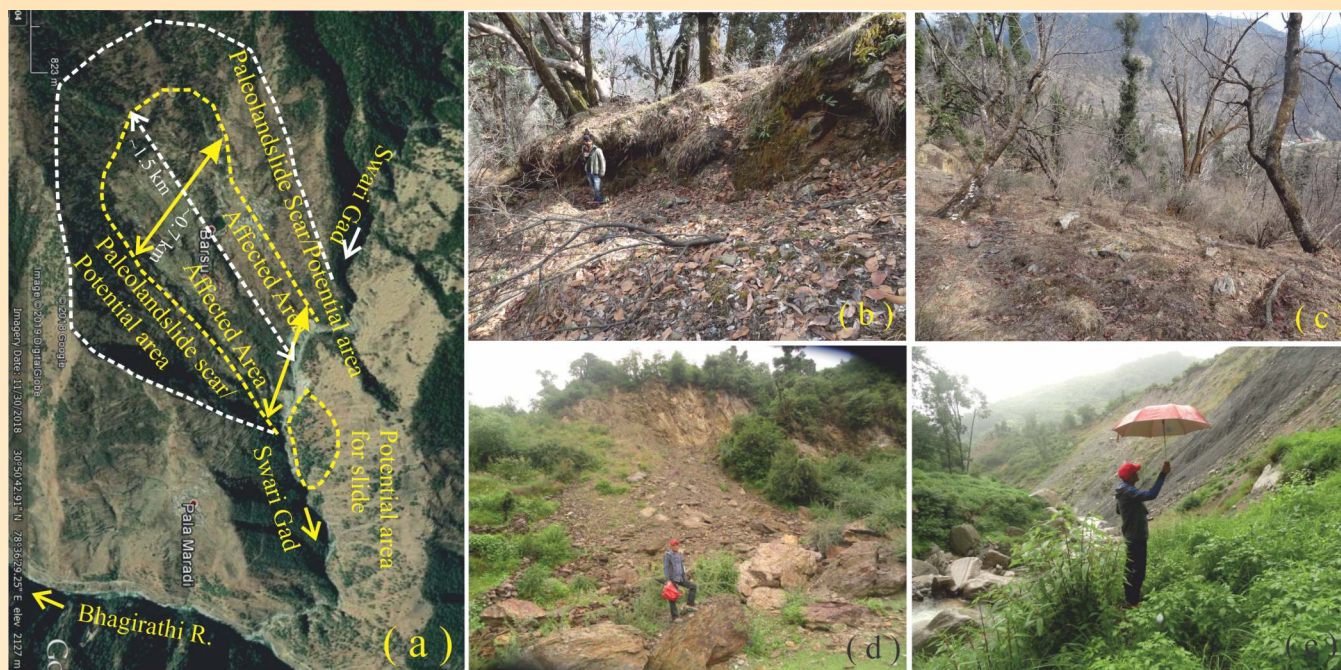


Fig. 47: Google Earth image and field photographs showing the slope affected by a landslide at Barsu in the upper catchment of Bhagirathi Valley in Garhwal Himalaya.



Fig. 48: Footpaths and houses affected by landslides at Barsu which result from toe cutting by Swari Gad a tributary of Bhagirathi River.

schist intervening between mylonitized augen gneiss on either side. The topography of landforms developed also suggests that some portion of the hill slope has been scooped out from the less competent friable sheared rocks. The schistose rocks are highly weathered. Toe erosion is one of the main factors that have destabilized the hill slope. The overburden is made up of old landslide debris as such continual removal of the base support through toe erosion by Swari Gad has made the slope unstable. Infiltration/seepage of water from small streams and domestic water is also one of the causative factors. This process has made the over-saturated slopes by the seepage water, which has subsequently triggered the landslides. Water from perennial streams and domestic water also infiltrates through cracks and fissures into the slope-forming material and has facilitated the reduction in the shear strength of the slope and the slope instability. This water percolates through the slip circle along which the mass movement is taking place periodically. This village falls in an orographic area and thus receives a good amount of rainfall during the monsoon. As already stated the landslide debris is the slope-forming material and as such the infiltrating water results in further reducing the cohesive strength of the material.

Activity: 4B**Ecology and climate dynamics of the Himalaya – Cenozoic to Present**

(Narendra K. Meena, Jayendra Singh, Sudipta Sarkar and Prakasam M.)

Dendrochronology

Tree-ring-based March-June temperature reconstruction back to 1785 CE developed from Din Gad valley, Dokriani glacier region, Uttarakhand, NW Himalaya captured strong coherence with tree-ring-based temperature reconstructions from the Garhwal Himalaya. There was also a broad agreement with other tree-ring-derived temperature records from the Western Himalaya, Central Himalaya, and the Tibetan plateau, indicating the relevance of the reconstructed temperature in understanding climate variability at a regional scale. March-June temperature record also showed an association at low-frequency levels with global temperature records (Asia and Northern Hemisphere). A negligible rise was observed in March-June temperature during 1901-1989 CE with respect to Asia 2k and Northern hemisphere records, however, a surge in the rise was observed from 1990 CE that continued in the 21st century, which is also evident in the Northern hemisphere temperature record.

A 330-year-long tree-ring chronology of *Abies pindrow* has been prepared from the Joshimath region, Uttarakhand. Tree growth climate analysis of the chronology shows a positive relationship of precipitation and a negative relationship of temperature over tree growth.

Peat /lake records in Central Garhwal Himalaya (Mana village)

To understand the late Holocene climatic and environmental variations in the Central Garhwal Himalayan region, a multi-proxy (sedimentological, geochemical, etc.) approach was adopted. The samples, collected from a 1.25 m deep peat section, located in the Mana Village, Chamoli district, Central Garhwal Himalaya were analyzed for grain-size, using the Laser Particle Size Analyzer (LPSA), magnetic susceptibility, MS-2B Bartington Magnetometer; and, total organic carbon (TOC), and TOC-Analyzer. The study area is pristine, naturally preserved, and, undisturbed due to the absence of human interference, and the section appears to be ideal for the reconstruction of the past climate and environment of the Central Garhwal Himalayan region. While the grain-size data corroborates the lithology of the peat section, the down-depth magnetic susceptibility (χ_{lf}) fluctuation is broadly parallel to the

coarse-grained (sand) fraction. The χ_{lf} values are lower at portions, where the clay fraction is higher. The χ_{lf} increased down the depth of the section, and thus, it corroborates the fact that with a higher energy level of the depositional condition, the coarser fraction (sand) was carried and deposited in the basin, with a simultaneous increase in magnetic susceptibility values. Around 07 samples from this peat section were analyzed for AMS-C¹⁴ age-dating at IUAC, New Delhi, and, the age-dates were received as 1353±23 years BP, and 8701±36 years BP at the depths of 5 cm, and 79 cm, respectively.

The samples from ~200 cm high river cliff section from the upstream region of Saraswati River near Mana Village have been analyzed for grain size, magnetic susceptibility, and OSL age dating, while the samples from ~350 cm high river cliff section from the downstream region of Saraswati River near Mana Village have been analyzed for grain-size, magnetic susceptibility, and AMS-C¹⁴ & OSL age dating. The near-bottom of the downstream section represents an age of ~17490±78 Yrs BP, while the near-top of the section represents an age of ~3748±27 Yrs BP.

Peat/lake records in Chopta Bugyal

During the reporting period, the samples were analyzed for grain size, Magnetic susceptibility in samples collected from the Chopta area. The Multi-proxy data has been generated from a Peat Section from the Chopta area, Rudrapryag, Central Garhwal Himalaya, and, preliminary interpretation has been made towards the Bugyal ecosystem. To establish an efficient chronology of the Garhwal Himalaya peat, 15 more samples have been proposed at IUAC, New Delhi.

Peat /lake records in Baspa Valley (Kinnaur region, Himachal Pradesh) and Lahaul-Spiti

Produced the millennial to centennial-scale Indian summer monsoon records (ISM) during the Late-Pleistocene to Holocene using multi-proxy (magnetism, carbon isotope, and TOC) approach in the Baspa Valley, NW Himalaya. The following periods of strengthened ISM ~15 to ~14 ka, ~10 to ~7 ka, ~2.4 to ~1.3 ka, and 243 yr BP to present, and phases of weakened ISM ~20 and ~15 ka, ~14 to ~10 ka, ~7 to ~2.4 ka, and ~1300 to ~243 yr BP. These phases are attributed to global cooling events, i.e., the Last Glacial Maximum, Younger Drays, and the Little Ice Age.

Ocean Core studies

To understand the paleoclimatic variability and Himalayan weathering, two ocean cores from two

different locations, one in the Arabian Sea, and the other in the Andaman Sea are being studied. The cores from the Arabian Sea and the Andaman Sea are expected to provide around 140 Kyr and 40 Kyr records, respectively.

Evaluating the feasibility of the biosorption technique for heavy metals removal was completed. Heavy metals are well-known environmental pollutants for terrestrial and aquatic ecosystems that have serious consequences for public health. Evaluating the feasibility of biosorption technique for heavy metals removal. The potential of various biosorbents has been comprehensively examined. After reviewing the test conditions, mechanisms, and removal capacity, it is observed that the use of biosorbent has been mainly restricted to the laboratory scale, and shifting to the ground level requires more emphasis on adsorbent availability, durability, and reusability.

Activity: 5

Geological and geomorphic controls on landslide for risk assessment and zonation in the Himalaya

(Vikram Gupta, Swapnamita C. Vaideswaran, Tariq Anwar and Naveen Chandra)

During the reporting year, subsidence-induced instabilities in the Dar village, which is situated over deposits of palaeo-landslide in the Kumaun Himalaya were studied. A detailed field investigation has been carried out in and around the study area to identify the indications of subsidence and understand the factors responsible for activating the same. Subsequently, the geotechnical characterizations of overburden slope material and numerical slope stability assessment have been performed to substantiate the field observations. It has been found that the village is situated on a slope comprising soft material having ~ 90 % finer particles (sand, silt, and clay) rich in disintegrated micaceous sediments having low cohesion and plasticity index. The granulometry analysis exhibits that soil contains 9.8% gravel, 74.9% sand, and 15.3% silt and clay. Besides this, the physiographical characteristics of the slope make it vulnerable to mass movement.

The slope stability assessment also indicated the critical state of the slope with a safety factor of 1.05, posing vulnerability to sliding failure. However, it is evident that modification of slope geometry with the construction of the road from Sobla to Tidang, that is passing through the base of the village, and consequently modification of the hydrological characteristics in the area are the most important contributing factor for the ongoing subsidence in Dar.

Since the village is at the stake of a possible disaster, preliminary mitigation measures are also proposed, which will be helpful to minimize the risk to life and property in the region.

Numerous subsidence-induced cracks were observed in the ground as well as in almost all the buildings of the village. As reported by the locals, the rate of subsidence has increased substantially since the construction of the Sobla - Sela-Tidang road in 2017, which pass through the lower section of the slope at an elevation of ~1920 masl. The study area experienced 3300 mm of rainfall in 2021 with the highest number of rainfall days (i.e., 106 days) during the monsoon in the last five years, and subsequently, almost all the houses in the village have developed either new cracks or the older cracks got widened. This has forced ~35 families in the village to leave their homes. The ongoing subsidence also led to the complete collapse of a primary school and several houses in the village just after the 2021 monsoons (Fig. 49).

Landslide study in Chakrata

The region within the Chakrata Block in the Uttarakhand state is undergoing a boom in developmental activities. Tourism in this region is mushrooming with the rapid growth of small and big hotels and resorts. This growth renders villages and small towns to develop into bigger towns. In the mountains, it is imperative to understand the stability of such small towns in advance so that planning to avoid future disasters can be done. Therefore, the region around the Chakrata Block and its adjoining areas were taken up for Permanent Scatterer Interferometric (PSI) time-series analysis, and morpho-tectonic study. The results were correlated with the seismo-tectonic regime of the region. A total of 62 scenes from the Sentinel 1 radar satellite with a good baseline were used over a period starting from 4 March 2020 to 30 March 2022. PS-InSAR results show a cumulative displacement of up to 157 mm, with a velocity of about 100 mm/year. Further, the slides are well correlated with anthropogenic activities like road cuttings, lithological control, or the tectonic boundaries in which shear zones are marked. This study forms the basis of a Landslide Early-warning System, which is designed to work in real-time to monitor the shallow slip on the slope of Kunain, Chakrata. The project has been sponsored by CRG, Department of Science and Technology (DST).

Landslide subsidence study in Joshimath

Joshimath has been witnessing sinking and subsidence for several years. Since the Rishi Ganga disaster, followed by three days of incessant rains in October



Fig. 49: Photographs showing subsidence-induced indications as observed at various places in Dar village (a) cracks in the ground, (b) displaced stairs, (c) leaning wall of a house, (d) cracks in the walls of a house, (e) collapsed building of a primary school and (f) a collapsed house.

2021, reports of cracks on the ground and houses started pouring in. Fieldwork conducted in August 2021 showed extensive damage to houses, especially in Ravigram wards, Gandhinagar and Sunil. A total of 148 scenes from 10 May 2020 to 21 September 2021 have been processed to create a time series of displacement in the Joshimath region. The PS-InSAR results show well-correlated displacements in places of Ravigram, Sunil, and the Gandhinagar region. PS-InSAR results show a cumulative displacement of up to 197 mm in the study time frame, with a velocity of about 83 mm/year. The clusters of displacement around Ravigram show the topographical control of Ravigram Nala, which is seen to be obstructed by construction in the area. Gandhinagar and Upper Bazar area show a cumulative displacement of up to 195 mm in the study time frame, with a velocity of about 82 mm/year. This area is adjacent to the Nauganga Nala. This Nala is also showing active tow erosion from the Alaknanda River, ahead of the Vishnuprayag confluence. The maximum

displacement has been observed in Sunil village, 236 mm in the study time frame, with a velocity of about 100 mm/year. This is well-correlated with observations on the ground during a field visit in August 2022.

At the beginning of January 2023, there was a sudden increase in the pace of subsidence which is accompanied by the frequent occurrence of cracks on the ground and in houses. Many houses were severely damaged and had to be evacuated. A whole zone of subsidence in an arcuate flow direction was initiated from the Manohar Bagh ward down towards Singdhar, Marwari, and up to the river Alaknanda below. Houses in Manohar Bagh were the worst hit, and two big hotels had to be eventually demolished. There were close to 800 damaged houses. To understand the subsidence in the area, pits were excavated to collect the undisturbed soil samples along the eastern as well as the western sections of the identified subsidence zone, particularly in localities where some damage was detected. Further,

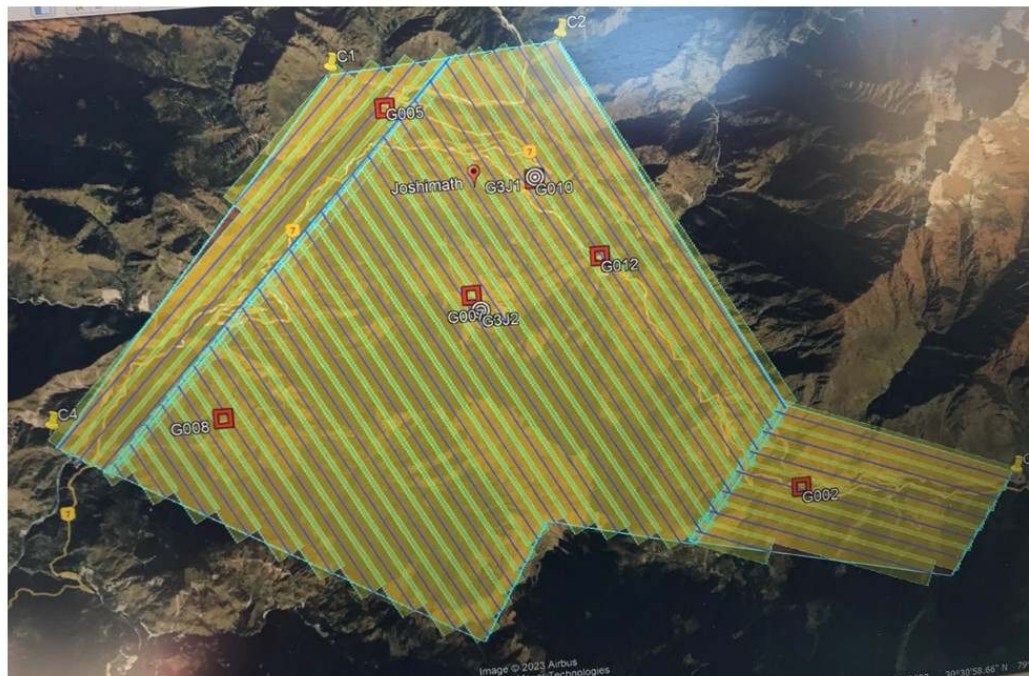
the geotechnical properties of these samples are being determined by various experiments and slope failure analysis is required to understand the hazard and risk assessment.

Joshimath was declared a 'disaster-prone area' in the first week of January 2023. A complete topographical map of the region was required in very high-resolution for mapping, planning, and rehabilitation. WIHG initiated an airborne LiDAR survey to generate high resolution data to generate the Digital Elevation Model (DEM), classified data of bare-ground, vegetation, and built-up area in Joshimath and around through a project awarded by Uttarakhand State Disaster Management Authority (USDMA) in February 2023. Data was collected for a 100 sq. km area surrounding Joshimath, from Alaknanda River in the north, Tapovan in the east, and Helang in the south, to generate the required topographical maps, and Global Positioning System (GPS) measurements were done on six ground control points (GCPs) and two Base Stations (Figs. 50-52). The Survey of India (SoI) leveling on these GCPs and base stations were also done. The Survey of India benchmarks data for Pipalkoti, Pandukeshwar and Badrinath were collected for the construction of the Joshimath geoid, and hence the creation of the DEM and

contours. This data will be used to understand the cause of the slope subsidence at Joshimath, and it will also be a powerful tool for the generation of rehabilitation maps and town planning for the drainage systems and sewer plans of the Joshimath area.

Slope stability analysis in Rudraprayag and Karnaprayag area, Uttarakhand

The Himalayan region is quite common for landslides due to the collision of the Indian plate with the Eurasian plate subjected to severe seismic activity. Also, in the rainy season, these mountainous regions receive high precipitation that accelerates various landslides. Further, the construction of roads, dams, and other development activities has increased the fragility to enhance the landslides in the entire Himalayan region. Slope stability analysis of individual slopes between Rudraprayag and Karnaprayag area along road corridor NH-7 is not well explored for stability analysis using different numerical methods. NH-7 holds immense religious importance as it connects to the holy shrines of Kedarnath and Badrinath and many holistic places in the remotely inaccessible part of the Himalayan terrain. It is also a strategic and single route for public transport as well as for military possessions in the hilly terrain of the Indian Himalaya. The fieldwork has been carried out



Flight Tracks for LiDAR survey and GCP Locations and Base Stations



GCP: GPS Monitoring



Base Station: Permanently Running

Fig. 50: An area of 100 sq. km covering the region around the Joshimath area was surveyed, and data were collected by Airborne LiDAR systems. Six GCPs were monitored by GPS and two Base Stations located at NTPC Helipad and Auli were continuously running during the survey.

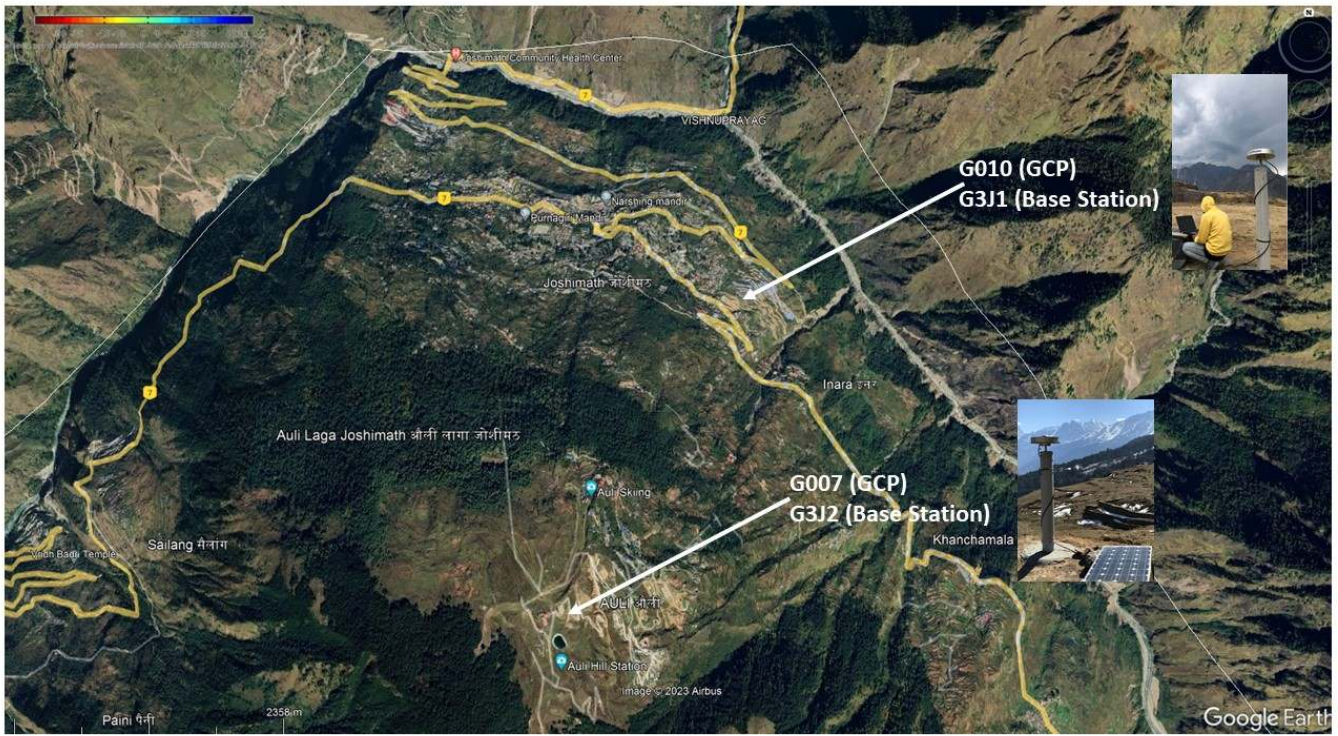


Fig. 51: Two continuously operating base stations for GPS measurements.



Fig. 52: Collection of LiDAR data using a helicopter. Intermittent bad weather, with snowfall, rain clouds, and winds inhibited the survey, and the acquisition was done in weather gaps in three sorties, on 26th February forenoon, afternoon, and on 27th February 2023.

and data are collected from six different rock slope and four debris slopes sections for further analysis.

From the field visit, different slope parameters (Slope height, Slope angle variation, and slope orientation), material properties, various discontinuity parameters, and representative samples are collected from different locations. The area is highly fractured with phyllitic and quartzitic rocks as from field examination, where two and three sets of joints are commonly identified and their characteristics are noted carefully. The number of joint sets, spacing of discontinuities, and condition of discontinuities for each slope are observed carefully for each joint set. The physical condition of the slope surface is also examined carefully to know the weathering and loosening due to excavation and blasting or cyclic erosion effect due to water conditions or ice wedging. Major discontinuity with their physical condition and infilling materials like clay and quartz is noted carefully in the field. In the individual slope more critical location or weak zone for low strength area is localized for strength and stress ratio for the weakest zone in the slope.

Further, the experimental works have been accomplished to attain the specific gravity, moisture content; dry density, grain size distribution, compressive strength, liquid limit, and plastic limit, and shear strength of different soil samples of three different locations. The different soil samples collected from Rudraprayag and Karnaprayag have a dry density in the range between 2.02-2.32 g/cc, optimum moisture

content 7.1-8.2%, porosity 35-38%, compressive strength 8-10.52 n/m^2 , less cohesion value with 43-44 friction angle, liquid limit 26-34%, and Plastic limit 22-25%. Additionally, collected rock samples are being tested for mechanical strength characterization under different conditions. Further, these data will be utilized in the slope stability analysis using different modeling methods.

Deep Learning Approaches for Landslide Information Recognition

A study titled “Deep Learning Approaches for Landslide Information Recognition: Current Scenario and Opportunities”. In the current era, remote sensing is a powerful platform for detecting and predicting landslides. Moreover, the advancement in computing technologies has proven significant in artificial intelligence studies. Researchers have made significant attempts in the existing literature by introducing landslide detection procedures from remote sensing images through deep learning algorithms. The quantitative results are based on the following parameters: (1) contributing nations, (2) key study locations, (3) data set distribution, and (4) model utilization.

Further, an Efficient U-Net Model for Improved Landslide Detection from Satellite Images is developed and suggested (Fig. 53). Detecting landslides from satellite images can be significant for various governing authorities. Here, an enhanced U-Net model is

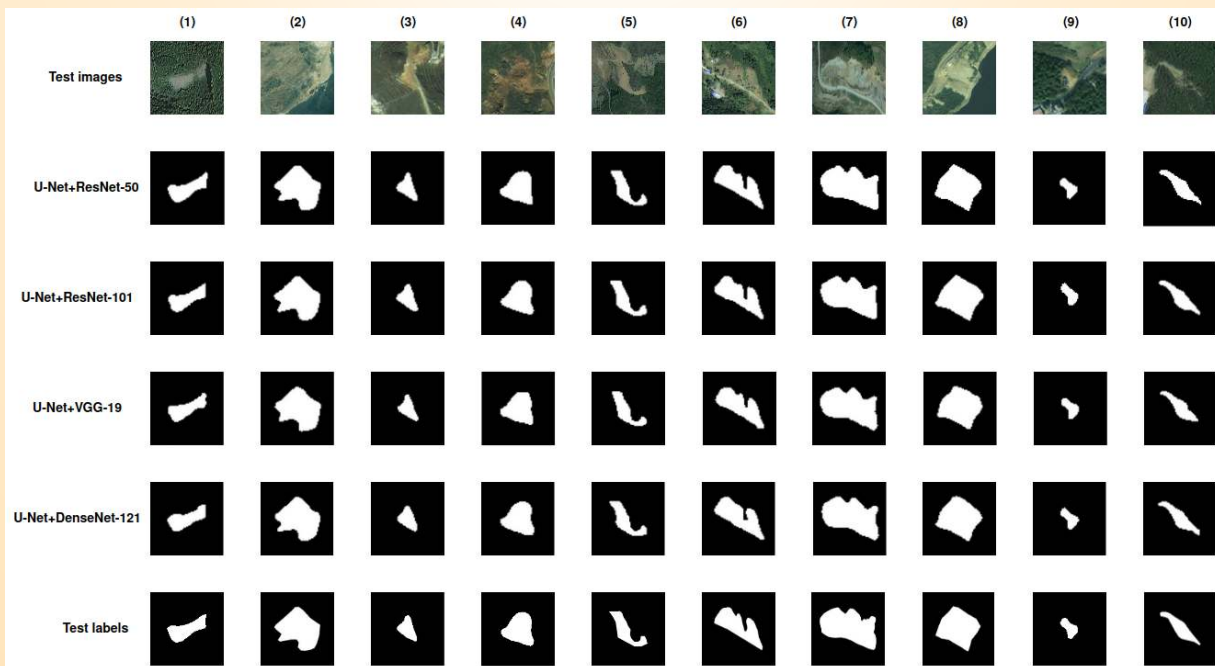


Fig. 53: Results of the detected landslides by different deep-learning models.

suggested for detecting the landslides from the newly introduced open-source landslide data set. The proposed study uses the ResNet-50, ResNet-101, VGG-19, and DenseNet-121 as backbone models. The performance of U-Net+ResNet-50 is found to be the best in terms of precision (0.98), f1-score (0.98), and overall accuracy (1.0).

Moreover, the single-staged algorithm, particularly YOLOv5, YOLOv6, YOLOv7, and YOLOv8, is proposed for predicting landslide events from remote sensing data. The other variants of YOLO models are also investigated for landslide information extraction, specifically “YOLOv6, and YOLOv7: Recent Object Detection Models for Automated Identification of Landslides from Distinct Data Sources”. In addition, YOLOv8 (a recent deep learning algorithm) is proposed for predicting landslide events from remote sensing data. Furthermore, a study on predicting landslide scars from satellite imagery in Nepal based on YOLO models is proposed.

Activity: 6A

Glacial dynamics, glacier hydrology, mountain meteorology, and related hazard

(Kalachand Sain, Manish Mehta, Vinit Kumar, Sameer Tiwari, Amit Kumar, Rakesh Bhambri, Pankaj Chauhan and Jairam Singh Yadav)

Status of Glacier Surface Changes in Doda and Suru River basins; Past and current status, priorities and prospects

The estimated cumulative *in-situ* average net annual mass balance of Pensilungpa Glacier (PG) is $\sim -5.8 \times 10^6 \text{ m}^3 \text{ w.e. a}^{-1}$ with the $-0.58 \text{ m w.e. a}^{-1}$ specific balance between 2021 and 2022. The average specific balance is -0.55 m a^{-1} . Whereas the depression of equilibrium-line altitude (ELA) was $\sim 20 \text{ m}$ between 2016 and 2022, and the present ELA is located at 5235 m asl. The field base study between 2015 and 2022 shows that the PG retreat $\sim 45 \pm 18 \text{ m}$ with an average rate of $\sim 6.4 \pm 3 \text{ m a}^{-1}$ and DDG retreat $\sim 95.5 \pm 53 \text{ m}$ with an average rate of $\sim 13.6 \pm 7.5 \text{ m a}^{-1}$. The broad snout of the DDG creates wide discrepancies for the frontal retreat. The field base study between 2015 and 2022 shows that the Parkachik Glacier retreated by $210.5 \pm 80 \text{ m}$ with an average rate of $4.21 \pm 1.6 \text{ m a}^{-1}$ between 1971 and 2021 (Fig. 54). Whereas, the field studies from 2015 to 2022 suggested that the glacier accelerated retreat, i.e., $123 \pm 72 \text{ m}$ at an average rate of $20.5 \pm 14.4 \text{ m a}^{-1}$. The surface elevation loss is spatially variable in both of the glaciers, with a maximum value of 13 m by Durung-Drung Glacier

(DDG) at 4233 m asl, while the maximum ablation of PG is 6 m near 4815 m asl between 2016 and 2022. The rate of surface melting by DDG was 5.53 m a^{-1} , whereas the PG lost 1.46 m a^{-1} . In addition, a resistivity survey was conducted over the surface of DDG to assess the volume of the lower ablation area between 4100 and 4600 m asl.

In the present study, the morphological and dynamic changes of Parkachik Glacier (PKG), Suru River valley, Ladakh Himalaya, India has been investigated. Medium to high-resolution satellite images were used from CORONA KH-4, Landsat, and Sentinel from 1971-2021 field surveys (2015-2021). In addition, the laminar flow-based Himalayan Glacier Thickness Mapper (HIGTHIM) tool was used, and comprehensive results for recent changes (snout fluctuations and surface morphology), surface ice velocity (SIV), and ice thickness have been provided. The glacier-bed over-deepening (for potential lake sites) has also been identified. The results revealed that overall the glacier retreated by $-210.5 \pm 80 \text{ m}$ with an average rate of $4.21 \pm 1.6 \text{ m a}^{-1}$ between 1971 and 2021. Whereas a field study from 2015 to 2021 suggested that the glacier retreat, i.e., $-123 \pm 72 \text{ m}$ at an average rate of $-20.5 \pm 14.4 \text{ m a}^{-1}$ (Fig. 55). SIV was estimated using a feature tracking algorithm in COSI-Corr on the Landsat time-series data. SIV of PKG in the lower ablation zone (3600 to 4300 m asl) was estimated to be $23.49 \pm 0.72 \text{ m a}^{-1}$ in 1999-2000 and $17.08 \pm 0.21 \text{ m a}^{-1}$ in 2020-2021, which is 27.28% lower than the earlier. Further, the maximum modeled thickness of the glacier is estimated to be $\sim 441 \text{ m}$ in the accumulation zone, while the thickness of the snout of the glacier is $\sim 44 \text{ m}$ (Fig. 56). The simulation results suggest that if the glacier retreats and shrinks at a similar rate, three lakes of different dimensions may form on the glacier surface at different elevations.

Monitoring of the Himalayan Glaciers and associated hazards

The elevation changes and surface flow distribution for 205 ($\geq 0.1 \text{ km}^2$) glaciers in the Alaknanda, Bhagirathi, and Mandakini basins, located in the Garhwal Himalaya, have been studied. This study also investigates a detailed integrated analysis of elevation changes and surface flow velocities for 23 glaciers with varying characteristics to understand the impact of ice thickness loss on overall glacier dynamics. Significant heterogeneity in glacier thinning and surface flow velocity patterns is observed using temporal DEMs and optical satellite images with ground-based verification (Fig. 57). The average thinning rate was $0.07 \pm 0.09 \text{ m a}^{-1}$

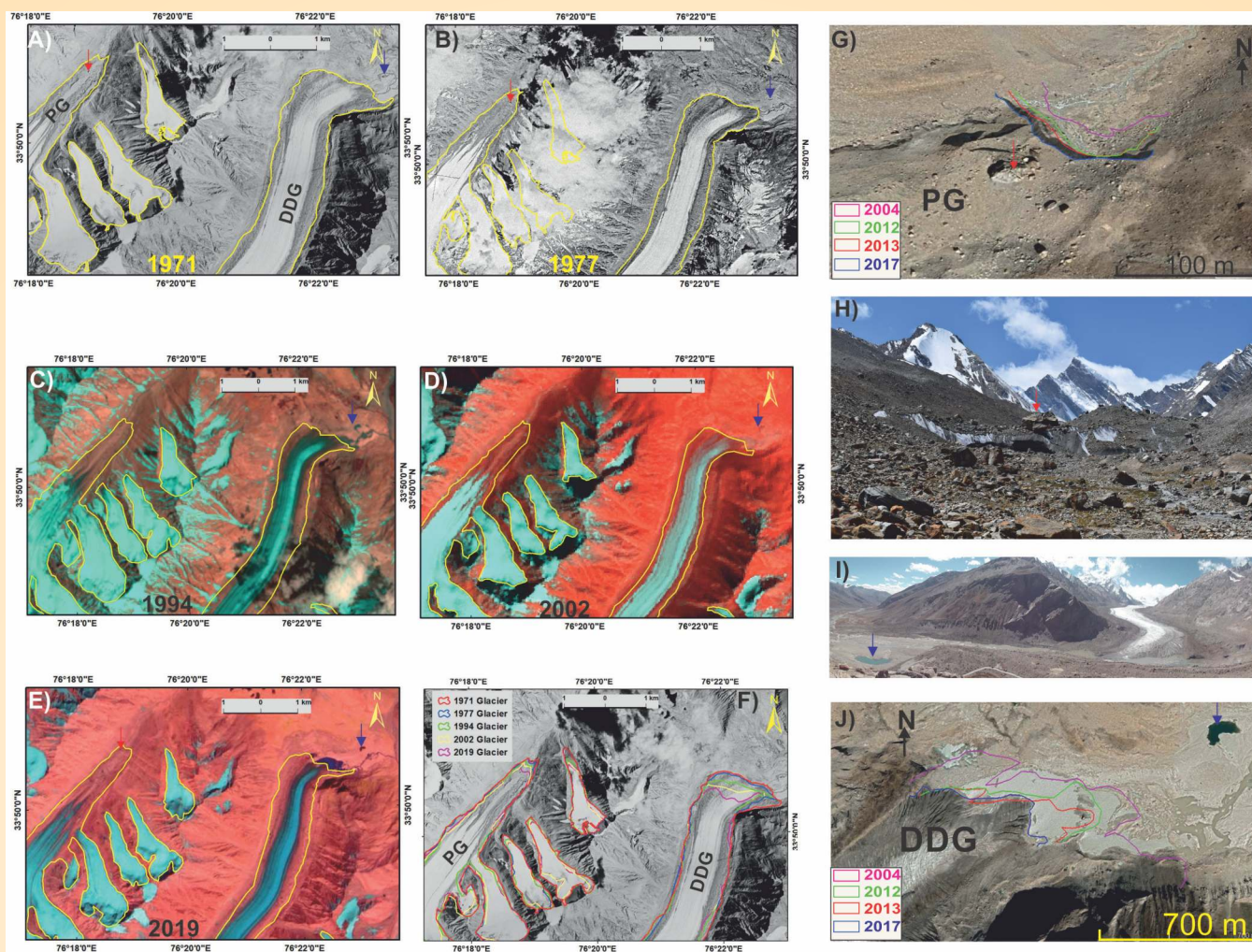


Fig. 54: Temporal changes in the snout position of the PG and DDG during the period between 1971 and 2019. (A)- The respective glacier boundaries for 28, September 1971 (Corona KH-4B), (B) 6, October 1977 (Hexagon KH-9), (C) 27 August 1994 (Landsat TM), (D) 4 September 2002 (Landsat ETM⁺), (E) 15 September 2019 (Sentinel Multispectral Imagery). (F) The glacier boundaries are dropped on the Corona KH-4B showing the glacier recession between 1971 and 2019. (G) Snout retreat of PG measured using Google Earth Image during the periods between 2004 and 2017, (H) field photograph showing the snout of the PG and red arrow indicating reference point (big boulder). (I) Snout and proglacial kidney-shaped lake (blue arrow) of DDG, and (J) Snout retreat of DDG during the periods between 2004 and 2017.

from 2000 to 2015, and it increased to $0.31 \pm 0.19 \text{ m a}^{-1}$ from 2015 to 2020, with pronounced differences between individual glaciers. Between 2000 and 2015, Gangotri Glacier thinned nearly twice as much as the neighbouring Chorabari and Companion glaciers, which have thicker supraglacial debris that protects the beneath ice from melting (Fig. 57).

The transitional zone between debris-covered and clean ice glaciers showed substantial flow during the observation period. However, the lower reaches of their debris-covered terminus areas are almost stagnant. These glaciers experienced a significant

slow-down ($\sim 25\%$) between 1993–1994 and 2020–2021, and only the Gangotri Glacier was active even in its terminus region during most observational periods. The decreasing surface gradient reduces the driving stress and causes slow-down surface flow velocities and an increase in stagnant ice. Surface lowering of these glaciers may have substantial long-term impacts on downstream communities and lowland populations, including more frequent cryospheric hazards, which may threaten future water and livelihood security.

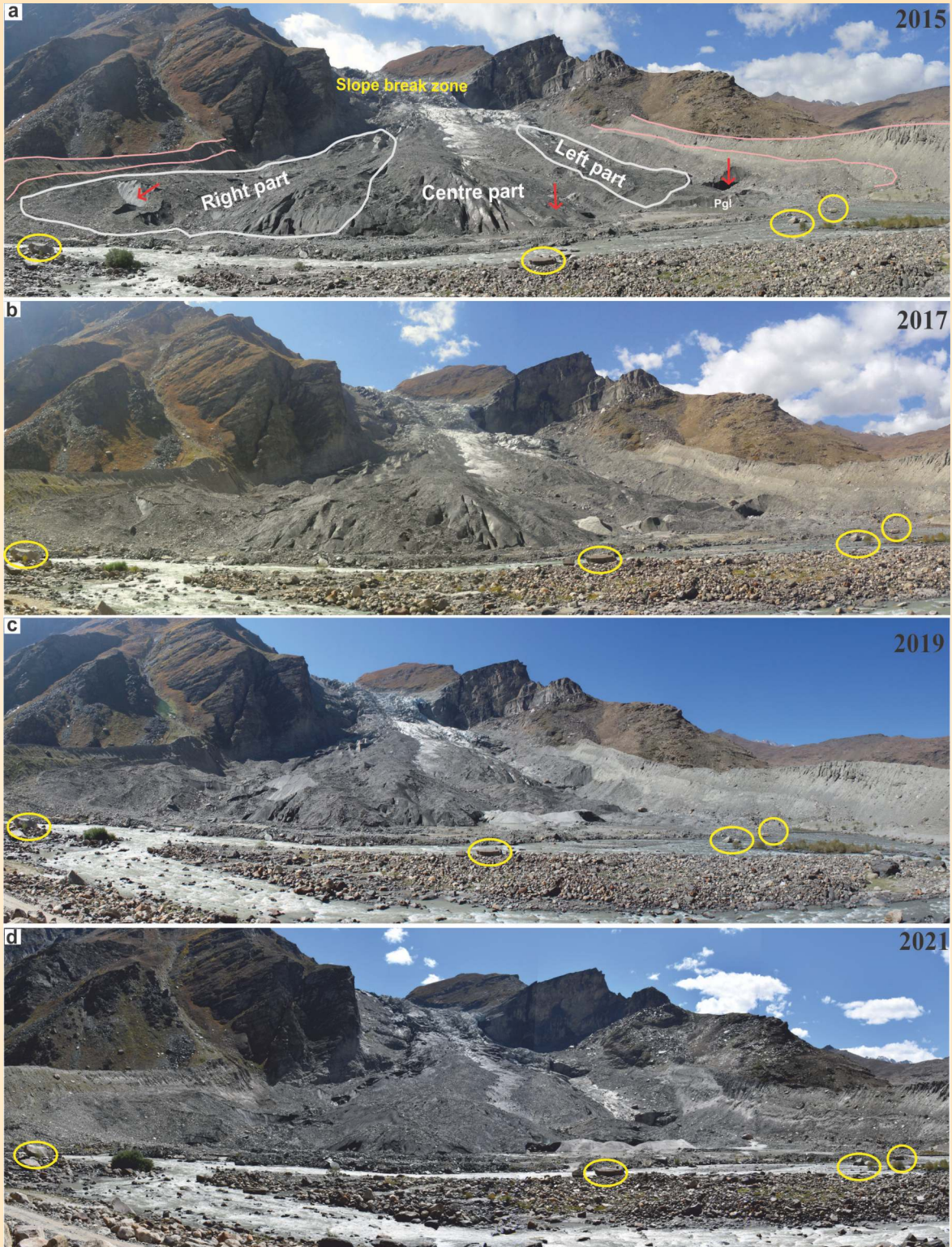


Fig. 55: Field photographs (A to D) from 2015, 2017, 2019 and 2021 (two years interval), showing the panoramic view of the glacier front and lower ablation zone of the glacier which is divided into three parts i.e., left, middle, and right shown in photo A. (A) is also showing slope break zone, lateral moraines (light pink colour lines), arrows are indicating the changes observed (2015 to 2021), and yellow circles are highlighting the ground control points (stable boulders) taken as reference points for frontal (retreat) monitoring.

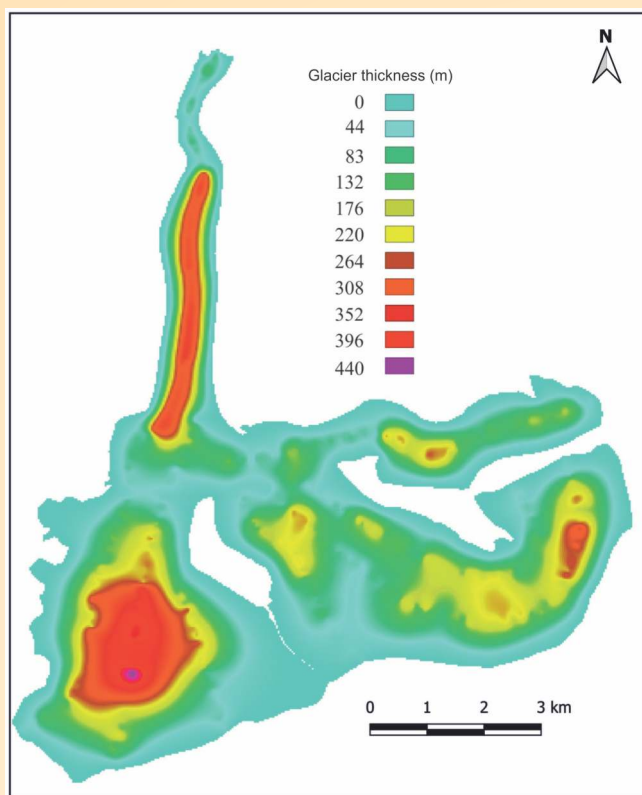


Fig. 56: (A) Ice thickness of the glacier varying from ~44 to 83 m at the terminus, between 200 and 350 m in the upper ablation zone, and reaches >400 m in the accumulation zone. Maximum thickness is modeled as 440 m.

Emission of Greenhouse Gases due to Anthropogenic Activities: an Environmental Assessment from Paddy Rice Fields

Paddy rice fields (PRFs) are a potent source of global atmospheric greenhouse gases (GHGs), particularly CH_4 and CO_2 . Despite socio-environmental importance, the emission of GHGs has rarely been measured from Haryana agricultural fields. New technology has been used to track ambient concentration and soil flux of GHGs (CH_4 , CO_2 , and H_2O) near Karnal's Kuchpura agricultural fields. The observations were conducted using a Trace Gas Analyzer (TGA) and Soil Flux Smart Chamber over various parts, i.e., disturbed and undisturbed zone of PRFs. The undisturbed zone usually accounts for a maximum ambient concentration of ~ 2434.95 ppb and 492.46 ppm of CH_4 and CO_2 , respectively, higher than the average global concentration. Soil flux of CH_4 and CO_2 was highly varied, ranging from 0.18 to 11.73 $\text{nmol m}^{-2}\text{s}^{-1}$ and 0.13-4.98 $\mu\text{mol m}^{-2}\text{s}^{-1}$, respectively. An insignificant correlation was observed between ambient

concentration and soil flux of GHGs from PRFs. Waterlogged (i.e., irrigated and rain-fed) soil contributed slightly lower CH_4 flux to the atmosphere. Interestingly, such an agricultural field shows low CO_2 and CH_4 fluxes compared to the field affected by the backfilling of rice husk ash (RHA). This study suggests farmers not to mix RHA to increase soil fertility because of their adverse environmental effects. Also, this study is relevant in understanding the GHGs' emissions from paddy rice fields to the atmosphere, their impacts, and mitigating measures for a healthy ecosystem figure 58.

Isotopic and geochemical studies in the Upper Ganga Basin, Uttarakhand, India: Implications on Dissolved Inorganic Carbon systematics

In the recent scenario of global warming, the release of organic and inorganic carbon from the melting glaciers has been a subject of scientific research since it can have a pronounced effect on the riverine carbon cycle and primary productivity. Apart from being one of the largest Himalayan glaciers, the Gangotri glacier provides water to the Bhagirathi River (Ganga River) which is the most important perennial river in India in terms of economy and livelihood. In the last decade, the melting and recession of the Gangotri glaciers have increased significantly leading to the formation of glacial lakes and debris-covered areas. As a result, primary productivity and microbial activity have increased in the subglacial areas which release a great amount of soil CO_2 that has not been documented previously in the literature. In the present study, the Bhagirathi River, which is the proglacial melt-stream of the Gangotri glacier has been sampled during the Post-monsoon period. A total of 27 samples including river, groundwater, geothermal spring, and reservoir were collected and have been analyzed for pH, surface temperature, Electrical conductivity (EC), major ions, and stable isotopes of carbon. From the study of major ion abundance patterns and mixing ratios, it has been inferred that carbonate weathering is predominant in the basin, though the major rock type of the area are silicates. The ($\text{HCO}_3^- \approx$ Dissolved Inorganic Carbon, DIC) values of river water show no correlation with altitude (mean = 42.8 mg/L), while $\delta^{13}\text{C}$ values show a decreasing trend with a decrease in altitude, with an overall range between -10 and -5‰. As altitude decreases, organic matter activity increases, and thus more CO_2 is washed out from the Soil Organic Matter (SOM), which makes the $\delta^{13}\text{C}$ values of the river depleted. The $\delta^{13}\text{C}$ of groundwater (mean = -11.8‰) and reservoir water (mean = -9.4‰) are more depleted than

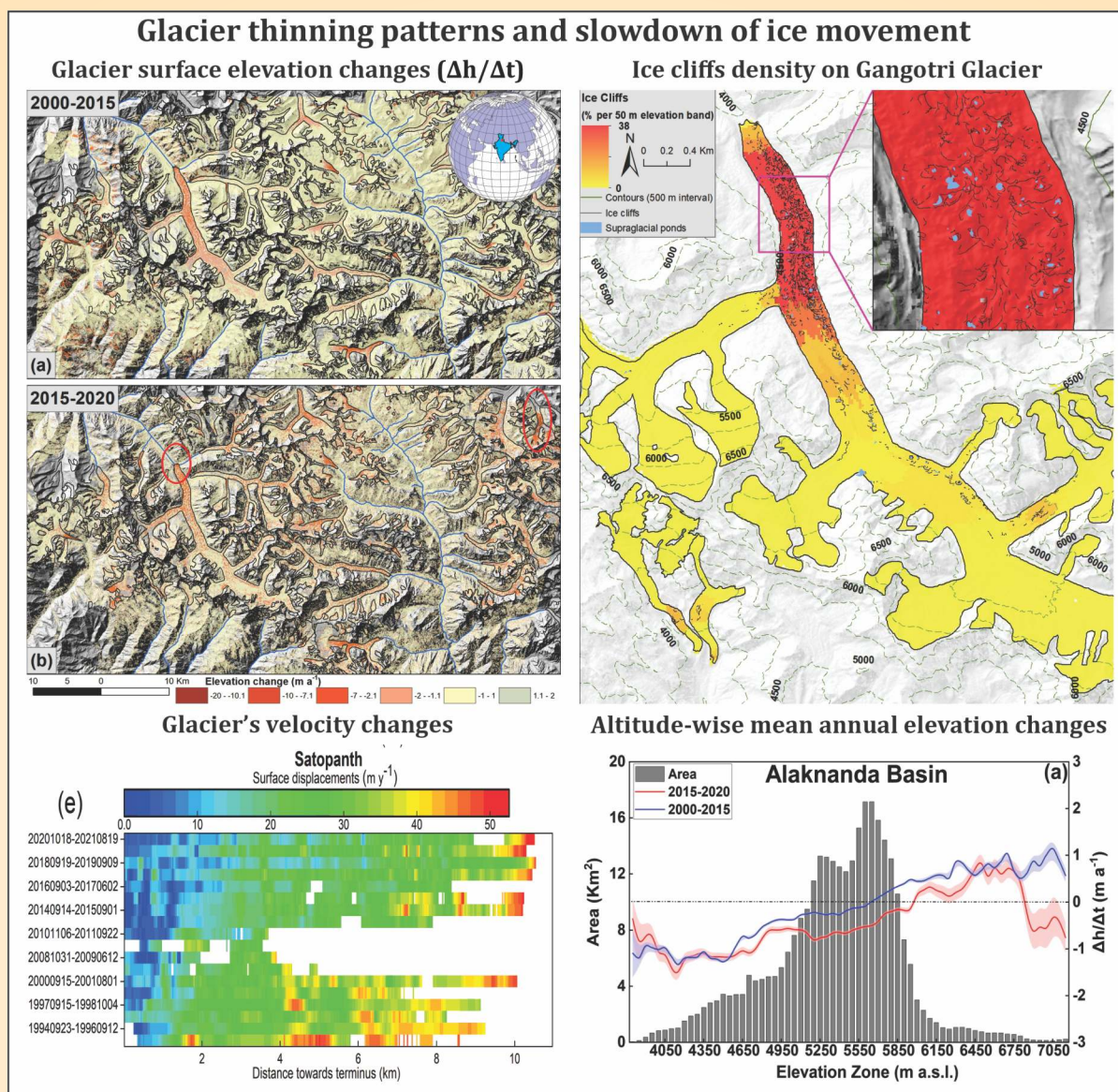


Fig. 57: Overview of glacier thinning patterns and ice movement slow-down in the Garhwal Himalaya. The upper left panel shows the glacier surface elevation changes between 2000-2015 and 2015-2020. The lower left panel presents surface flow velocity changes of Satopanth Glacier from 1994 to 2020. The upper right panel presents the distribution of ice cliffs on the surface of Gangotri, Chorabari, and Companion glaciers. The lower right panel presents altitude-wise mean annual elevation changes over 50 m elevation bands of the Alaknanda basin's glaciers.

river water due to the mixing of soil carbon in them, and $\delta^{13}\text{C}$ of geothermal spring water (mean = -3.6‰), shows enriched values since these are places of active CO_2 degassing. The source of DIC in the river water is mainly carbonate weathering in the upstream part and soil CO_2 in the downstream part of the study area. Quantifying pCO_2 values of the river water and calculating carbon flux from the river would provide important information on whether the Bhagirathi River is acting as a carbon source or sinking into the atmosphere.

Comparative Discharge and Sediment Flux Behaviour from two Adjacent Glacierized Basins in the Central Himalayas

The Pindari glacier (PGS) and Kafni glacier (KGS) lie in the Pindari valley, Alaknanda basin, Kumaun Himalaya in the central Himalaya and are located in the Bageshwar district of Uttarakhand state. The daily, monthly, and annual discharge behaviour of the PGS and KGS during 2017-19 has been shown in figure 59. The mean daily discharge has shown very high

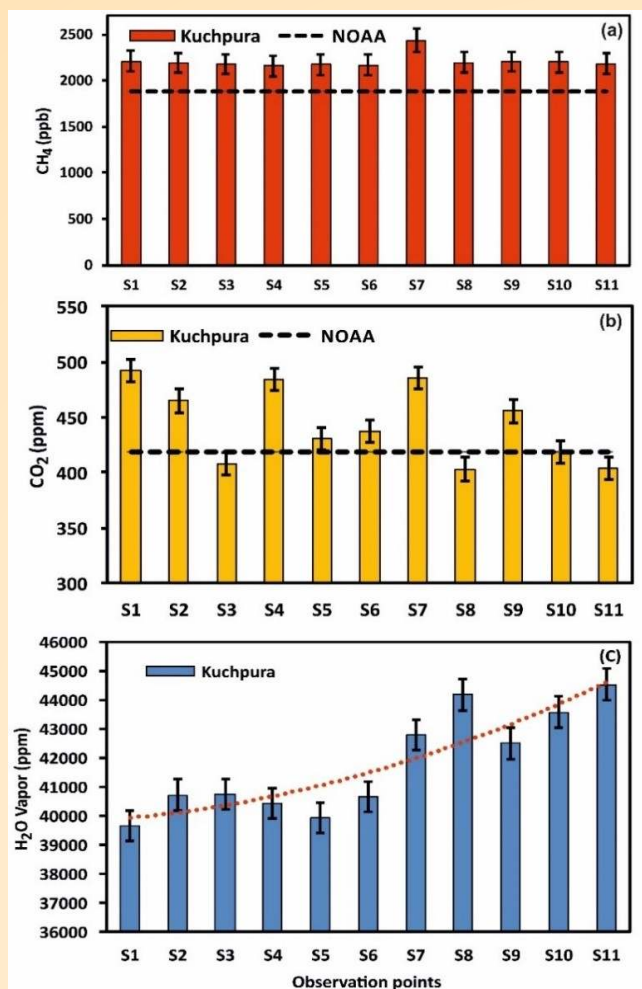


Fig. 58: Ambient concentration of the GHGs (CH₄, CO₂, and H₂O) from the Kuchpura experimental site (S1 to S11). The concentration of CH₄ and CO₂ are compared with the global values of GHGs provided by NOAA (2021), indicated with a black dashed line. The red dotted line showed the trend line of water vapour for observation points. Sites (S1-S8) were affected by human activity (soil backfilled with RHA), and the remaining sites (S9-S11) were undisturbed.

fluctuations in PGS and KGS. The mean daily discharge in PGS has ranged between $6.15 \text{ m}^3 \text{ s}^{-1}$ to $83.58 \text{ m}^3 \text{ s}^{-1}$, whereas, in KGS, it ranges from $2.26 \text{ m}^3 \text{ s}^{-1}$ to $49.83 \text{ m}^3 \text{ s}^{-1}$ during 2017-19 (Fig. 59). The PGS has recorded maximum discharge ($108.96 \text{ m}^3 \text{ s}^{-1}$) on July 25, 2018, whereas in KGS, it has been reported on August 18, 2018 ($55.76 \text{ m}^3 \text{ s}^{-1}$). The mean monthly discharge in PGS has varied from $8.59 \text{ m}^3 \text{ s}^{-1}$ (October) to $71.55 \text{ m}^3 \text{ s}^{-1}$ (August), while in KGS, it fluctuates between $4.40 \text{ m}^3 \text{ s}^{-1}$ (October) to $43.68 \text{ m}^3 \text{ s}^{-1}$ (August). The maximum ($88.80 \text{ m}^3 \text{ s}^{-1}$) and minimum ($7.95 \text{ m}^3 \text{ s}^{-1}$) discharge in PGS have been recorded in July (2018) and October

(2017), respectively. Likewise, KGS experienced a maximum discharge of about $48.09 \text{ m}^3 \text{ s}^{-1}$ in August 2018 and the lowest $3.46 \text{ m}^3 \text{ s}^{-1}$ in October 2019. The PGS has exceptionally reported maximum discharge in July 2018 due to very high rainfall over the basin in this month. Otherwise, both the glaciated streams have experienced their peak discharges in August and minimum in October, which is almost correspondence with rainfall occurrence. Approximately, two-thirds of the annual discharge of PGS and KGS has been recorded in July and August, detail behaviour of the discharge can be seen in figure 59. The annual average discharge in PGS and KGS during 2017-19 have been found about $35.06 \text{ m}^3 \text{ s}^{-1}$ and $20.47 \text{ m}^3 \text{ s}^{-1}$, respectively. It has been found approximately 1.71 times higher in PGS than in KGS. Both glaciated streams PGS and KGS have observed comparatively higher annual discharge in the year 2018 ($42.72 \text{ m}^3 \text{ s}^{-1}$ and $24.49 \text{ m}^3 \text{ s}^{-1}$), as compared to 2017 ($31.84 \text{ m}^3 \text{ s}^{-1}$ and $18.79 \text{ m}^3 \text{ s}^{-1}$) and 2019 ($30.30 \text{ m}^3 \text{ s}^{-1}$ and $18.01 \text{ m}^3 \text{ s}^{-1}$), respectively, which may be attributed to the occurrence of high rainfall over this region. The annual discharge in PGS and KGS is directly proportional to the rainfall amount. More than 80 percent of the total annual discharge and rainfall in both glaciated streams have been reported in monsoon months. An earlier study also found that about 81 percent of discharge of the Kafni river basin is rainfall dominated (Kayastha et al., 2014); however, snow and ice melt can increase under the future climate scenario. Apart from this, a high variability has been detected in annual streamflow in both PGS (0.76) and KGS (0.78) during 2017-19. However, PGS has witnessed a continuous decline in annual variability since 2017, i.e., 0.81 (2017), 0.79 (2018), and 0.75 (2019); but in KGS, the minimum variability (0.73) has been detected in 2018, followed by 2019 (0.85), and highest (0.86) in 2017. Considering the months, the lowest variability has been reported in August and the highest in September in both glaciated valleys (exceptionally in October 2018 in KGS).

In general, sediment concentration largely depends on the amount of stream flow. The higher the stream flow, the greater will be the sediment concentration. The mean daily, monthly, and annual SSC in PGS and KGS have been presented in figure 59. The mean daily SSC in PGS varies between 91.03 mg/l to 967.83 mg/l, whereas in KGS, it varies from 61.97 mg/l to 900.17 mg/l. The PGS has observed a maximum SSC (1200 mg/l) on July 16, 2018, and a minimum (70.1 mg/l) on October 31, 2019. Similarly, maximum (1022.20 mg/l) and minimum (60 mg/l) SSC in KGS have been witnessed on July 22, 2018, and October 26, 2018, respectively.

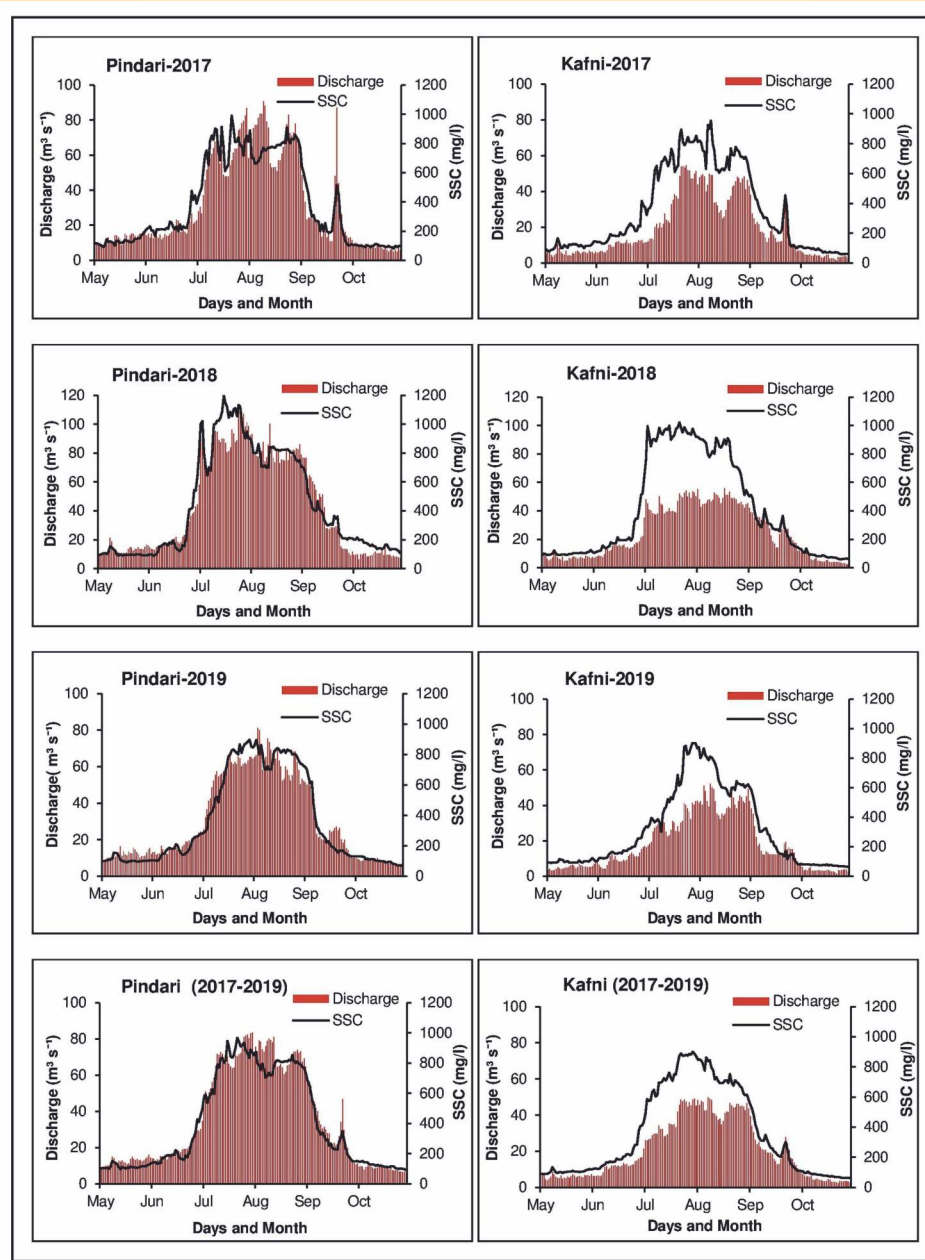


Fig. 59: Daily pattern of SSC and discharge in Pindari and Kafni glacial streams during 2017-19.

The SSC has increased with an increase in the rainfall and resultant discharge amount in both PGS and KGS.

The mean monthly SSC has ranged from 113.49 mg/l (May) to 791.26 mg/l (August) in PGS and from 80.94 mg/l (October) to 737.85 mg/l (August) in KGS during 2017-19. The maximum monthly SSC (974.11 mg/l and 933.89 mg/l) in both PGS and KGS have been found in July 2018 due to the occurrence of high rainfall and discharge amount (Fig. 59). Nearly two-third amount of SSC has been recorded in peak monsoon months (July and August).

The average SSC during 2017-19 has been found about 396.07 mg/l in PGS and about 359.67 mg/l in KGS. When this amount of SSC is compared with discharge in both basins, it has been found that the amount of SSC is comparatively higher in KGS than in PGS. The SSC amount difference within two adjacent valleys may be attributed to the basin area and roughness of the streams. The maximum SSC in PGS has been observed in 2018 (441.66 mg/l), followed by 2017 (387.99 mg/l) and the minimum (358.56) in 2019. A similar pattern has been observed in KGS in the occurrence of SSC (409.04, 353.67, 316.30 mg/l) in the

same years. Thus, SSC is directly related to the occurrence of rainfall and the resultant discharge amount in PGS and KGS (Fig. 59).

The annual variability in SSC during 2017-19 in both basins has been found very high and almost identical i.e., 0.77 (PGS) and 0.81 (KGS). Although, a continuous increase has been witnessed in annual variability in SSC in PGS since 2017 i.e., 0.76 (2017), 0.79 (2018), and 0.83 (2019); but in KGS, it has been found highest (0.85) in 2018, followed by (0.83) 2019

and lowest (0.79) in 2017. Considering the months, the lowest variability has been reported in August, whereas the highest was in September month in both the glaciated valleys (exceptionally in June 2017 in KGS).

The variations in daily, monthly and annual SSL in PGS and KGS have been presented in figure 60. The average daily SSL in PGS has varied from 49.49 tonnes to 6761.55 tonnes, and in KGS, it fluctuates between 13.55 tonnes to 3789.54 tonnes. The PGS recorded the highest SSL of about 10657.28 tonnes on July 25, 2018,

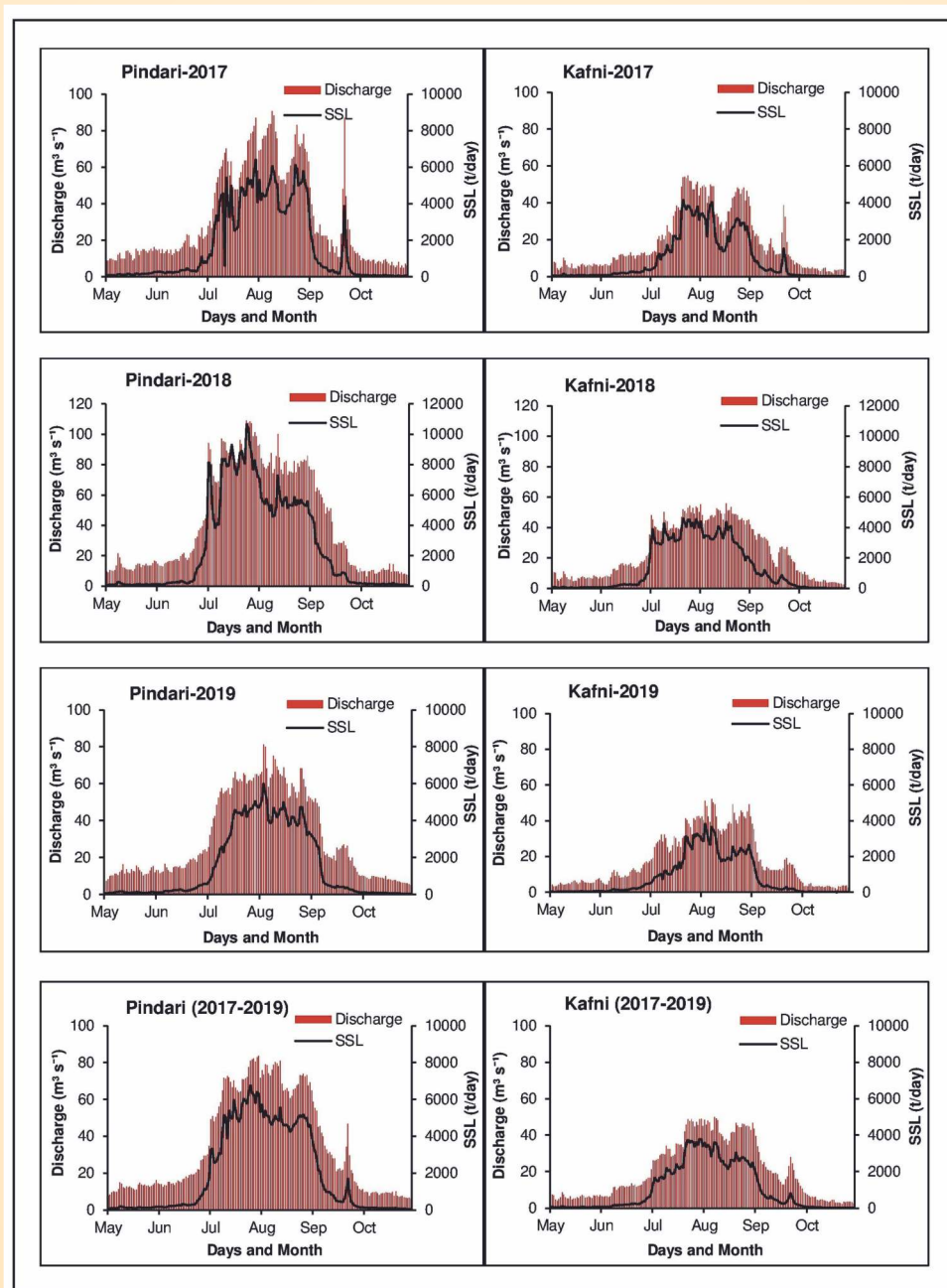


Fig. 60: Daily pattern of SSL and discharge in Pindari and Kafni glacial streams during 2017-2019.

and KGS (4593.11 tonnes) on July 22, 2018. The mean monthly SSL has ranged from 93.09 tonnes/day (October) to 4889.20 tonnes/day (August) in PGS and from 33.51 tonnes/day (October) to 2822.36 tonnes/day (August) in KGS during the study period. About 85 percent of the total annual SSL has been recorded in July and August months. The maximum monthly SSL in both basins, PGS (7569.48) and KGS (3604.24) was recorded in July 2018. The average annual SSL in PGS and KGS has been found about 1928.34 tonnes and 1040.26 tonnes during 2017-19, respectively. It indicates that the SSL is approximately 1.9 times higher in PGS than in KGS. The mean annual SSL has been recorded maximum in 2018 followed by 2017 and 2019 in both basins. SSL has also shown a correspondence with discharge in both adjacent valleys, i.e., increase and decrease consistently with increase and decrease in discharge amount.

Characterization of meteorological parameters over Dokriani Glacier catchment, Central Himalaya: implications for regional perspectives

The Himalayan meteorology is important for understanding the cryospheric-hydrological processes and climate change forecasts. The meteorological observations in the Indian Himalayan region (IHR), notably in glacierized catchments, are scarce.

Therefore, the present study aims to demonstrate a comprehensive investigation of meteorological parameters (e.g., temperature, relative humidity, precipitation, wind speed and direction, radiation fluxes, albedo, and pressures) over the Dokriani Glacier catchment (DGC) using time-series data (2011–2016) obtained from a network of three automatic weather stations (AWSs). The study also provides new insights into characteristics of meteorological variables at inter- and intra-seasonal scales (winter: December–February, Pre-monsoon: March–May, Monsoon: June–September, and Post-monsoon: October–November) (Fig. 61). The results show that the albedo and outflux radiation decreases rapidly with the onset of monsoon season, while there is an increase of relative humidity (RH) and positive degree-days (PDDs). The positive temperature ($>2^{\circ}\text{C}$) at higher elevations ($>5500\text{ m}$) raises serious concerns about the summer accumulation characteristics of the Dokriani glacier. The DGC has an average near-surface temperature lapse rate (NSTLR) of $6.0^{\circ}\text{C km}^{-1}$, higher in the pre-monsoon and lower during the monsoon (Fig. 61). The wind speed and albedo are more sensitive during winter and pre-monsoon seasons. The air temperature, rainfall, and relative humidity exhibit significant seasonal fluctuation, whereas other meteorological variables have a nearly comparable seasonal pattern. The Indian

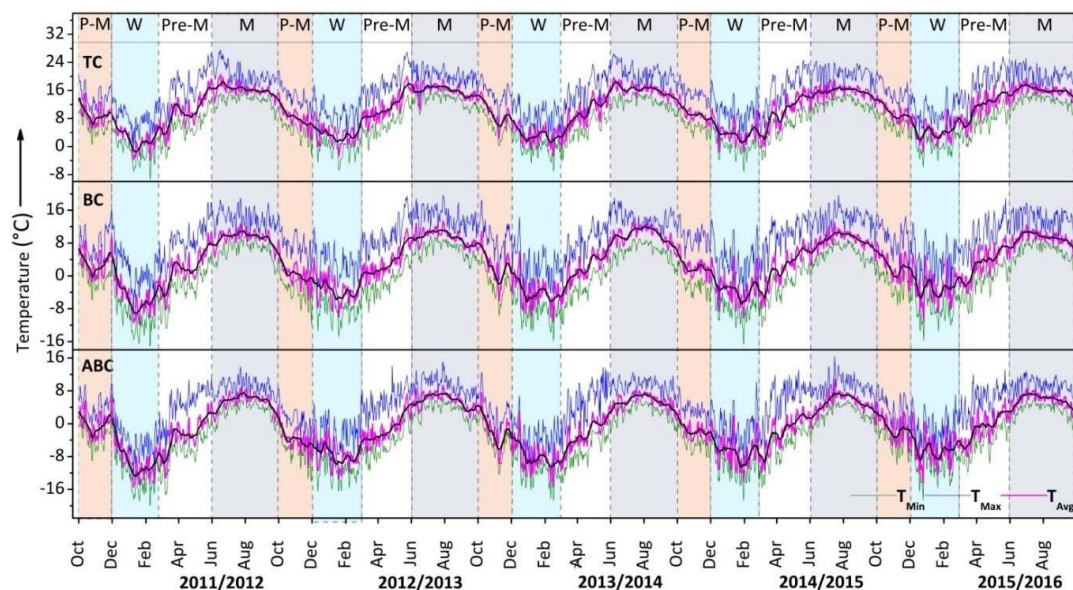


Fig. 61: Variation of minimum, maximum and average temperature at different time scales (daily, monthly, and seasonal) at Tela Camp (TC), Base Camp (BC), and Advance Base Camp (ABC) of Dokriani glacier catchment for five balance years (October 2012 – November 2016). P-M, W, Pre-M, and M indicate the post-monsoon, winter, pre-monsoon, and monsoon, respectively. The thick black line is the mean value of the average temperature.

Summer Monsoon (ISM) significantly influences all climatic factors. This may be utilized to examine the Dokriani glacier's mass budget and melt rate with other dependent factors, such as glacier hypsometry, orientation, surface velocity, and the extent of debris-cover. Furthermore, the dataset of this study may be correlated with hydro-meteorological observations in various regions of the Himalaya and deciphered using a regional climate dataset; for example, the Kedarnath tragedy-2013, and the most recent flash flood that occurred in Raunthi valley, Tapovan on February 07, 2021.

Hydrological importance of Himalayan glaciers: A perspective from Garhwal Himalaya

The meltwater runoff characteristics of the glacierized basins are different from those of purely rain-fed basins. Understanding the hydrological response of the

Himalayan glaciers, where significant rainfall occurs in addition to snow and glaciers, becomes very complex. Large variability has been observed in the meteorological conditions over glacierized regions, with rainfall being the most variable. Meltwater runoff from snow and glaciers is the most important source of runoff for mountain streams during the early ablation season (May and June). The discharge from the glacierized basins is highly regulated by the drainage and meltwater storage characteristics of the glacier. The inter-annual variability in the discharge for the glaciers is low as compared to the diurnal variability. The availability of dependable flows and suitable heads provides excellent conditions for hydropower generation and has resulted in the extensive development of hydropower projects in the Himalaya. However, still, a large potential is yet to be harnessed in Uttarakhand (~70%) and other Himalayan states. To

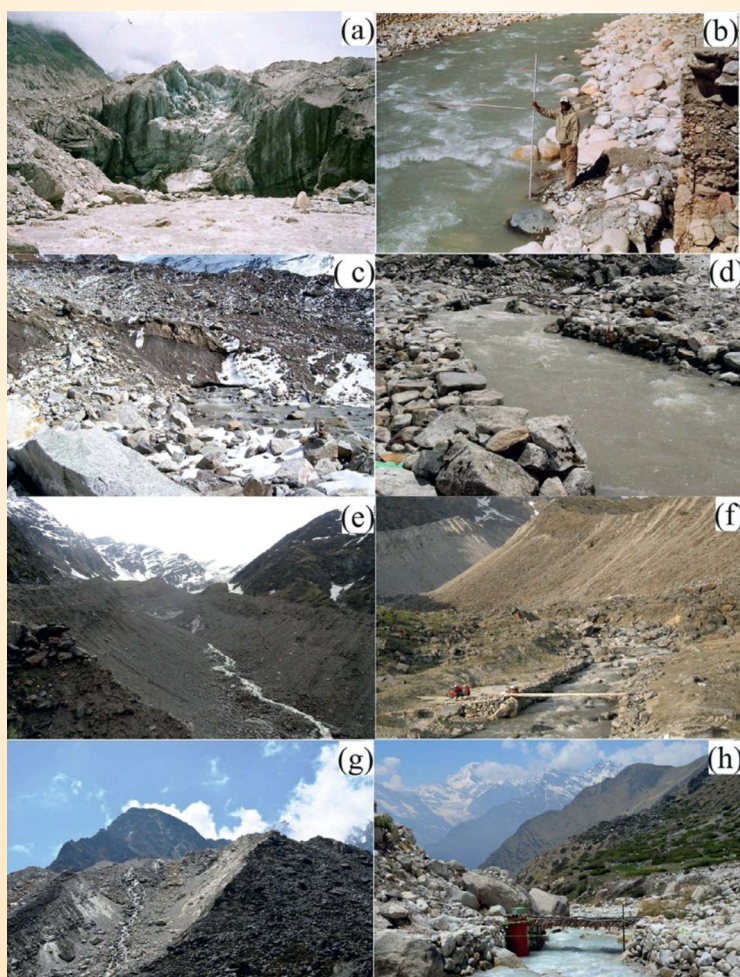


Fig. 62: Location of the snout and proglacial meltwater stream draining from Gangotri Glacier (A), Chorabari Glacier (B), Dokriani Glacier (C), and Dunagiri Glacier (D) along with their discharge measuring site (E, F, G, H) respectively.

develop this potential under the threat of frequent disasters in the state and the absence of hydrometeorological data in glacierized basins, integrated continuous long-term monitoring of glaciers is essential.

Integrated monitoring of glaciers and associated hazards in the Himalaya-Karakoram region

The hydropower generation potential for the Himalayan region is manifested owing to the reservoir of snow and glaciers, high relief, and large rivers which are extensively used for the production of electricity. The planning, designing, and operating of hydropower schemes in the Himalayan region require robust estimation of the discharge, suspended sediment concentration (SSC), suspended sediment load (SSL), sediment yield, erosion rate, etc. Therefore, WIHG is having temporary gauging sites near the snout of the Dunagiri-Bangni, Dokriani, and Gangotri glaciers in Uttarakhand and Siachen Glacier in Ladakh. The recent

disasters in the Himalaya-Karakoram region reflect the lack of long-term continuous time-series of observations. Therefore, to strengthen the network of observatories for continuous long-term observations Automatic Water Level Recorder (AWLR) have been installed over Nubra River, at Panamik, Karakoram, and Din Gad stream (Dokriani Glacier), Uttarakhand.

Recently seismic signals have been used for understanding the processes and chain of events for disasters and have shown the potential for precursory signals to ice-rock avalanches, debris flows, and flash floods indicating a perfect example of earth surface processes. Therefore, three (03) broadband seismometers (BBS) have been installed at Mana Village (Badrinath, Alaknanda Basin), Ruwing Village (Dunagiri, Dhauliganga Basin), and the University of Ladakh (Leh, Indus Basin) for the assessment of glacier-related hazards in the Himalaya-Karakoram.



Fig. 63: Location of the metal bridge at Nubra basin near Panamik (a), selection of the suitable site in the middle of the bridge (b) for the installation of AWLR (c) along with observation (manual) of water level (d), physical parameters using multiparameter water quality kit near Panamik (e) and location of installed BBS at University of Ladakh (f).

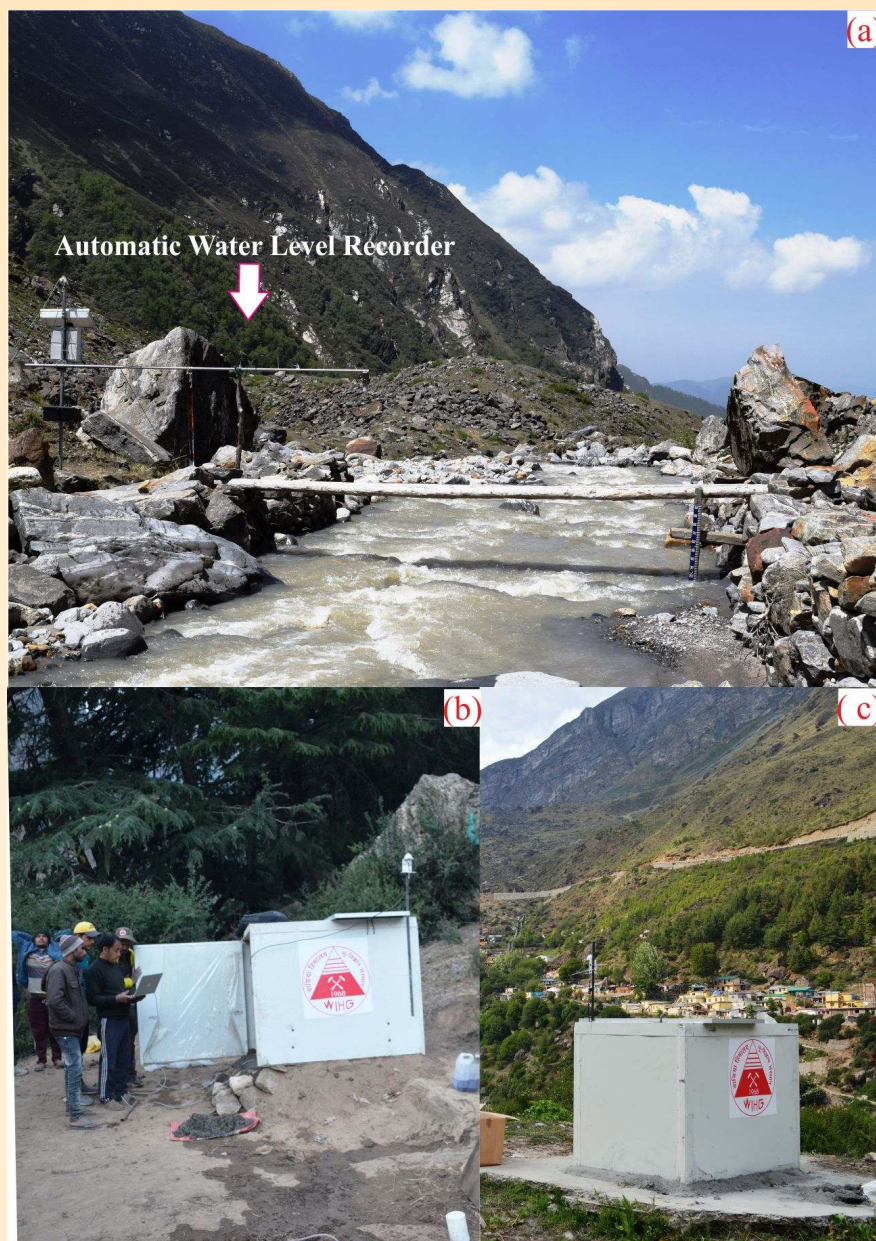


Fig. 64: Installation of Automatic Water Level Recorder (AWLR) near the snout of Dokriani Glacier (a), installation of broadband seismometers at Mana Village (Badrinath) and Ruwing Village (Dunagiri Glacier).

Activity: 6B

Hydrogeology: Himalayan Fluvial System & Groundwaters

(Santosh Kumar Rai and Rouf Ahmad Shah)

Cooperative management of Himalayan Rivers among the riparian states

The Himalaya, being a major geomorphic feature on the Earth, hosts rapidly eroding landforms. These landforms contribute about 6% to 12% of global sediment flux to the oceans. The Indus, Ganga, and

Brahmaputra (or IGB System) (Fig. 65) represent different physical, cultural, and developmental aspects of human societies. Together this fluvial system contributes $\sim 1 \times 10^{12} \text{ m}^3$ of water flux annually to the Bay of Bengal, containing ~ 100 million tons of dissolved solids, and $\sim 1000 - 2300$ million tons of particulate matter.

A strong variation in the distribution of physical erosion in the Himalaya is observed in this study (Fig. 66). Among these, the region containing the two syntaxes (Eastern and Western) and the headwaters of

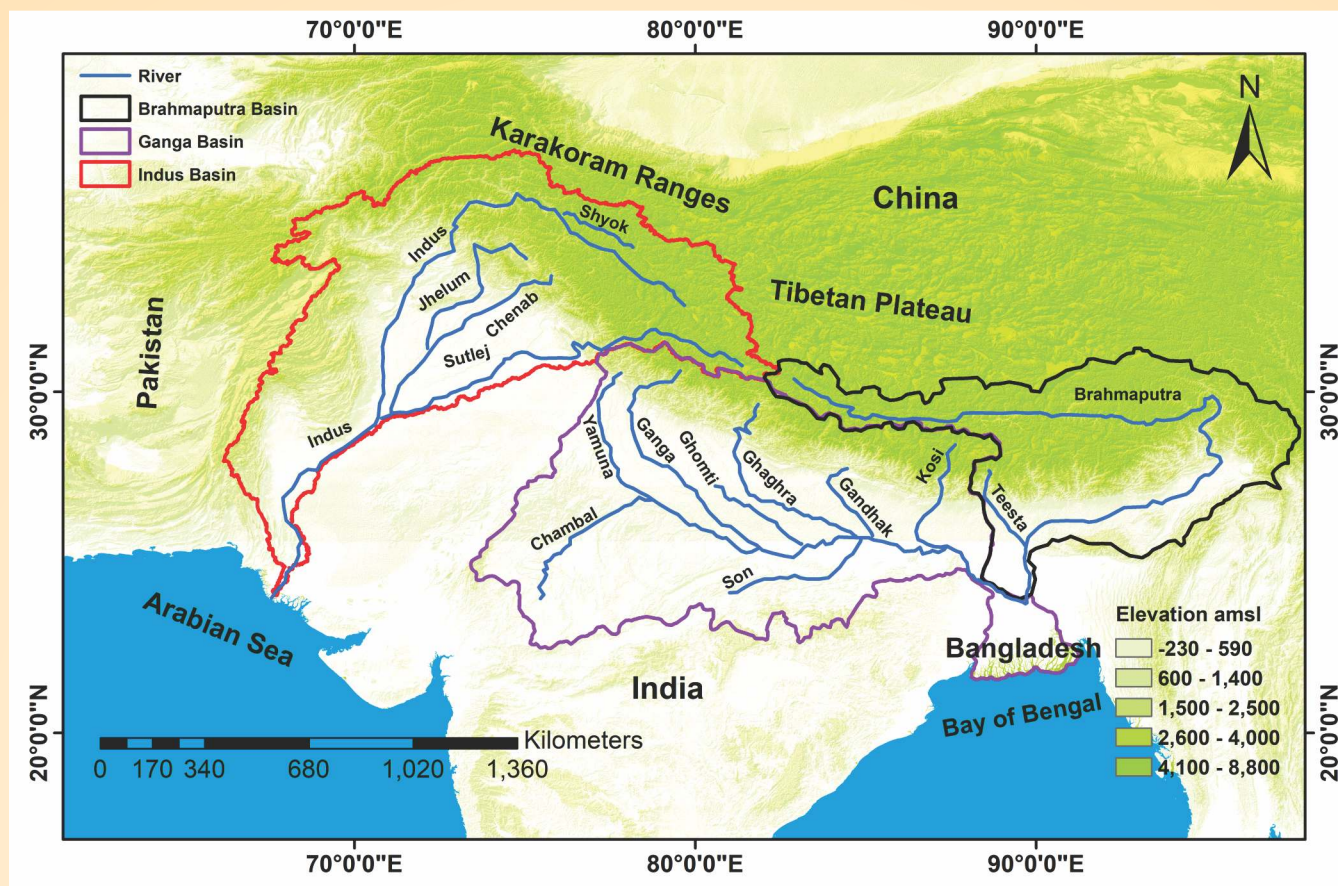


Fig. 65: The Riparian states along with the drainage boundaries of the Indus-Ganga Brahmaputra system.

the Gandak Basin serve as the hotspots of erosion as they yield an enormous amount of sediment (Fig. 66). These hotspots determine the sediment fluxes in the IGB river basins and, by extension, the sediment budget in the Bay of Bengal and the Arabian Sea (Fig. 66). Despite occupying only 0.07% of the total exoreic continental area, these three hotspots in the Himalaya contribute ~8% of sediment to the global riverine sedimentary flux. These sediments finally get partially deposited in the plains and distal fans during their transport to deeper oceans, hence, a critical equilibrium between erosion and sedimentation is maintained. It is suggested that the interlinking of river projects in India will hinder sediment supply in the future. The equilibrium of erosion-sedimentation could shift toward the erosion of Bangladesh's land mass. Therefore, a suitable management plan is needed to address this issue by applying scientific methods and sharing hydrological information. Regular discharge monitoring of the rivers entering the boundaries and interlinking of the Himalayan rivers appear to be key components for the mutual cooperation and development of the riparian states.

Insights into geo-meteorological processes and hydraulic linkages between the water sources in the Doon Valley

The valley of Doon located within the lower reaches of the Himalaya, is richly endowed with surface and groundwater resources due to frequent precipitation events. However, inadequate observational coverage and a paucity of isotopic data on water sources in the region restrict addressing the problems related to local hydrological systems. Towards this, detailed insights into geo-meteorological controls on precipitation and the hydraulic relationship between water sources were provided using stable water isotopes.

Results suggest that inherent variance in isotopic characteristics of precipitation is closely associated with the evolution of different sources of moisture and topographic features. The differences in slopes and intercepts of $\delta^{18}\text{O}$ - $\delta^2\text{H}$ regressions with space and season reveal that evaporation and local recycling regulate the variation of $\delta^{18}\text{O}$ (and $\delta^2\text{H}$) in precipitation (Fig. 67a,b). The back trajectories and d-excess suggest that the Bay of Bengal and Arabian Seas remain the principal

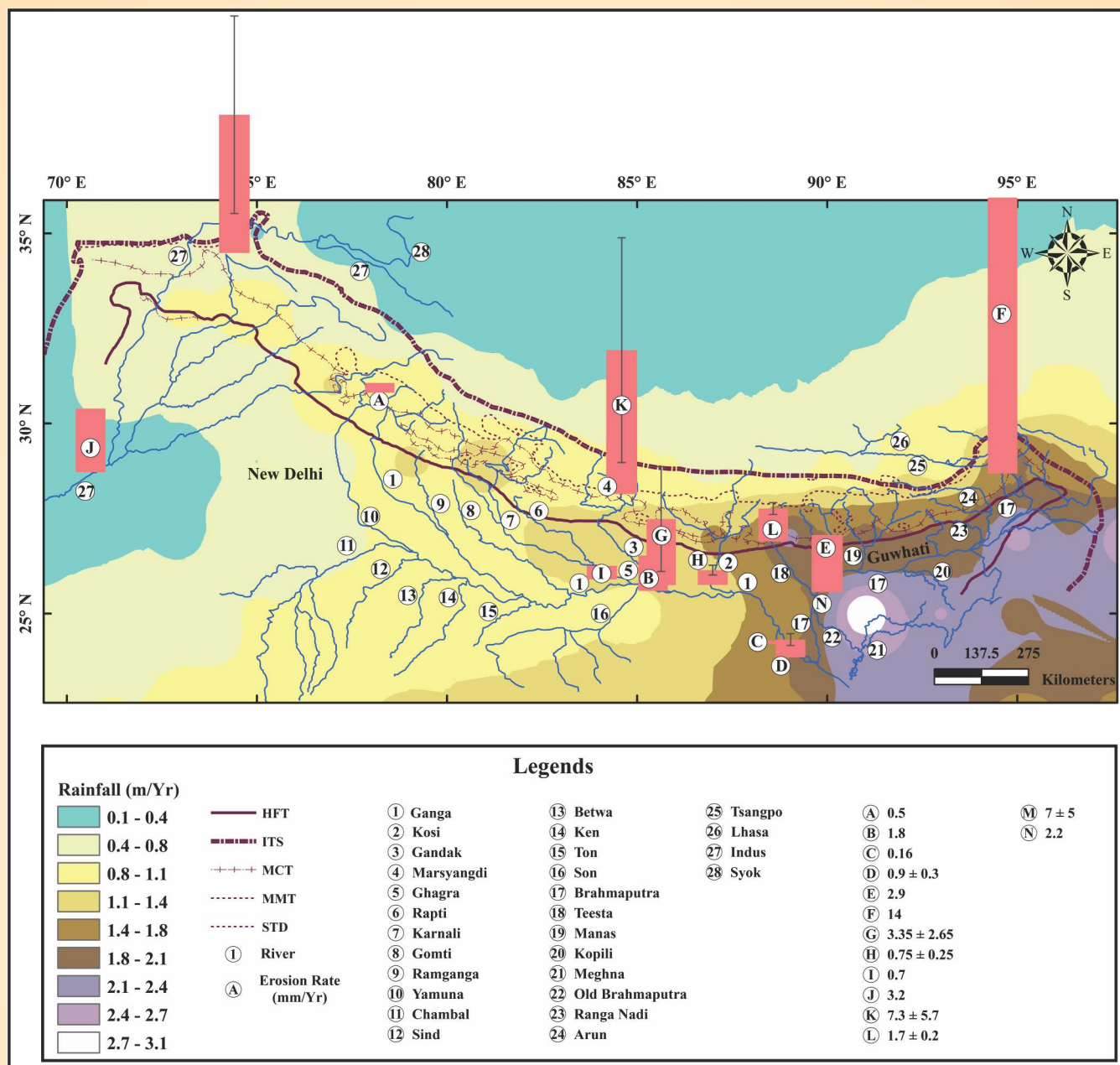


Fig. 66: Rainfall pattern and locations of hotspots of physical erosion (Eastern and Western syntaxes and the Gandak gorge) controlling the sedimentary fluxes from the Himalaya and hence the sedimentary budget of the Bay of Bengal and the Arabian Sea.

moisture sources for precipitation between June and September. While the rain events during December, March, and April represent the moisture signatures sourced from the Mediterranean/Caspian seas; however, a few rain events during November, January, and February are sourced from the Arabian Sea. It was found that 42% of rain events in June were sourced from the Bay of Bengal, while 28% were sourced from the Arabian Sea. These source regions contributed equally (50% each) during July and September; however, their

contribution decreased to 40% in August. The trajectory analysis showed that the westerly contributed 92% of rain events between December and April, and this contribution decreased to 25% during May. In addition, the study proposed a strong hydraulic connection between surface water and groundwater and recharge through high permeable flow paths, where the Indian summer monsoon acts as the dominant replenishment input (Fig. 67b,c,d).

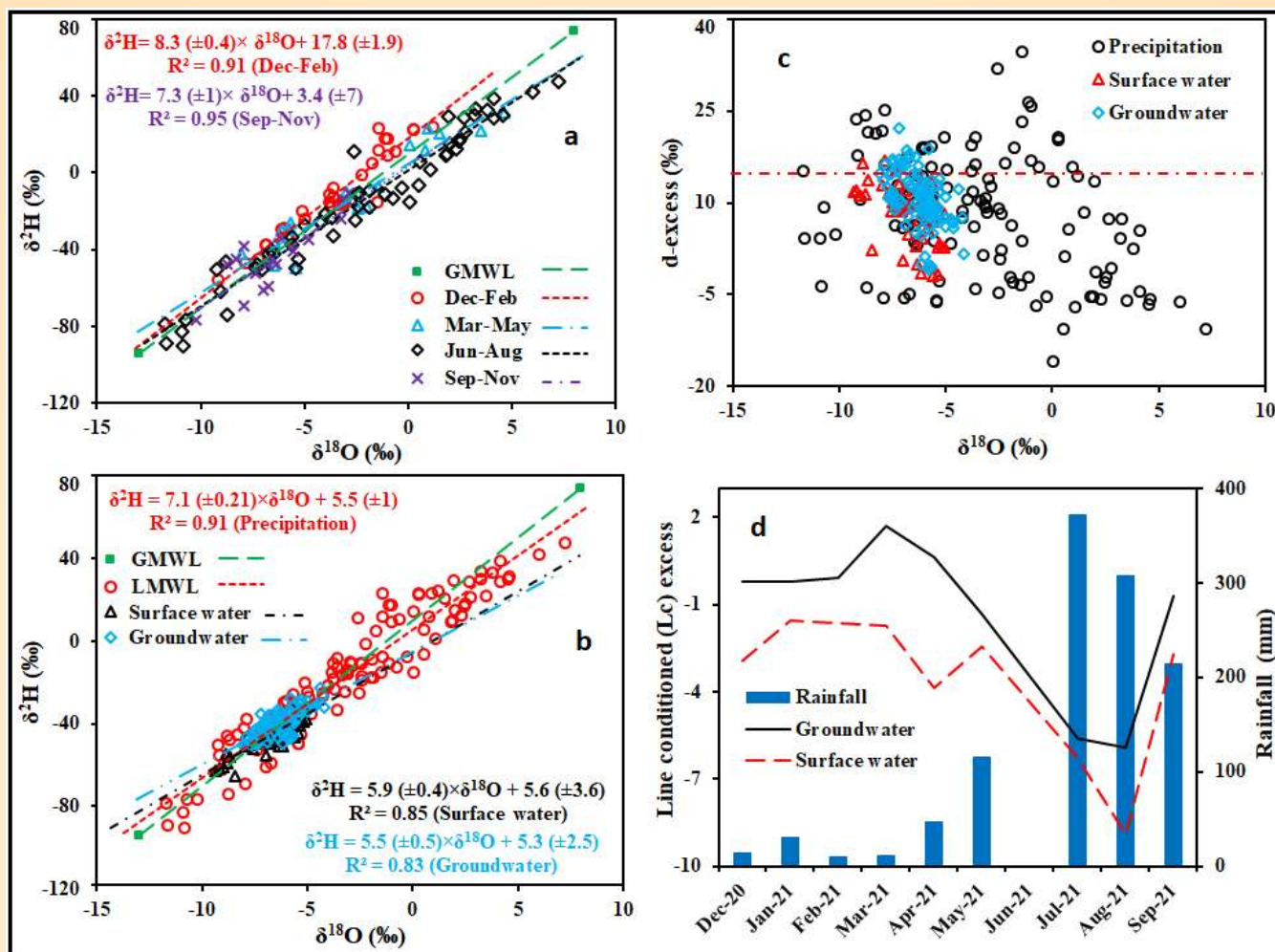


Fig. 67: Scatter plot showing the (a) event and (b) season-based local meteoric water line, (c) relation between $\delta^{18}\text{O}$ and d-excess of precipitation, surface water, and groundwater, and (d) temporal variance in line conditioned excess (lc-excess) in surface and groundwaters in the Doon Valley.

Recharge processes and solute sources of groundwater in the karst settings of the Kashmir Valley, India

In the Kashmir Valley, Triassic limestone displays significant karst geomorphic imprints, which reveal its importance as a productive groundwater reservoir. The groundwater (emerging either as a single large spring or as a closely spaced spring cluster) is the main source of clean and fresh water for >40% of the local population for drinking, especially during summer when demand is high for agro-horticulture and during winter when stream flow is lean. Ionic and stable isotopic composition of karst springs in the three major catchments (Liddar, Bringi, and Kuthar) of the Kashmir Valley, India were used to determine geogenic and anthropogenic solute sources and karst aquifer recharge. The results suggested that although the concentration of most ions in spring water is dominantly controlled by the natural mineralization of carbonate and silicate lithologies (Fig. 68a), the anthropogenic

contribution of NO_3^- , F^- , and Cl^- ions is evident from their higher $\text{NO}_3^-/\text{Na}^{2+}$ and $\text{Cl}^-/\text{Na}^{2+}$ ratios (Fig. 68b). The pollution index estimated and observed at about 1–38% in the Bringi, 9–24% in the Kuthar, and 2–31% in the Liddar. This contributes 50–88% of NO_3^- , F^- , and Cl^- ions to spring flow. Since there has been an increasing trend in both horticultural and built-up practices over a few decades (Fig. 68c) in these catchments, the overuse of pesticides and fertilizers in agro-horticultural plantations on karst ridges affects water quality through sensitive features on the surface.

Further, the karst springs are under-saturated with respect to calcite and dolomite, have higher pCO_2 , and electrical conductivity is inversely related to discharge (Fig. 69a), suggesting an active recharge process, and continued dissolution of the host rocks in most seasons. The study revealed that distinct seasonal patterns in the $\delta^{18}\text{O}$ and $\delta^2\text{H}$ of karst springs can be viewed in the

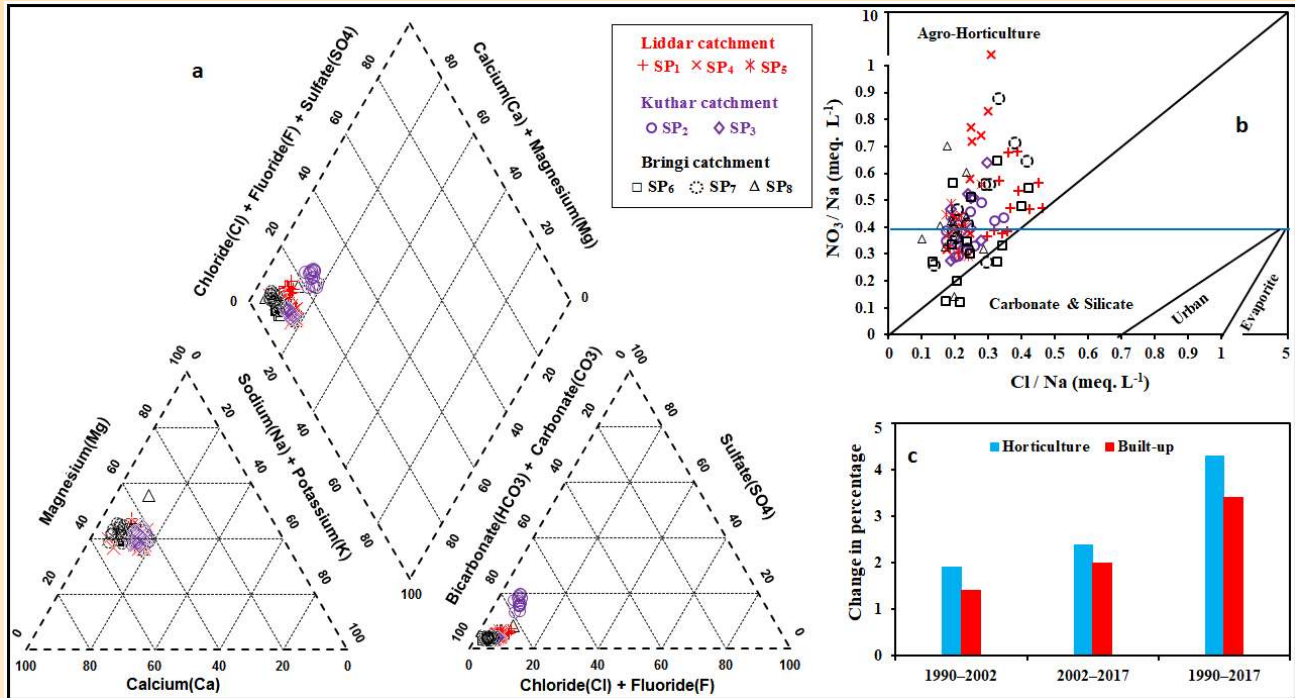


Fig. 68: (a) Piper trilinear plot showing the water types of karst springs in the study region and (b) contribution from anthropogenic forcing, and (c) trend analysis of horticulture and built-up from 1990-2017.

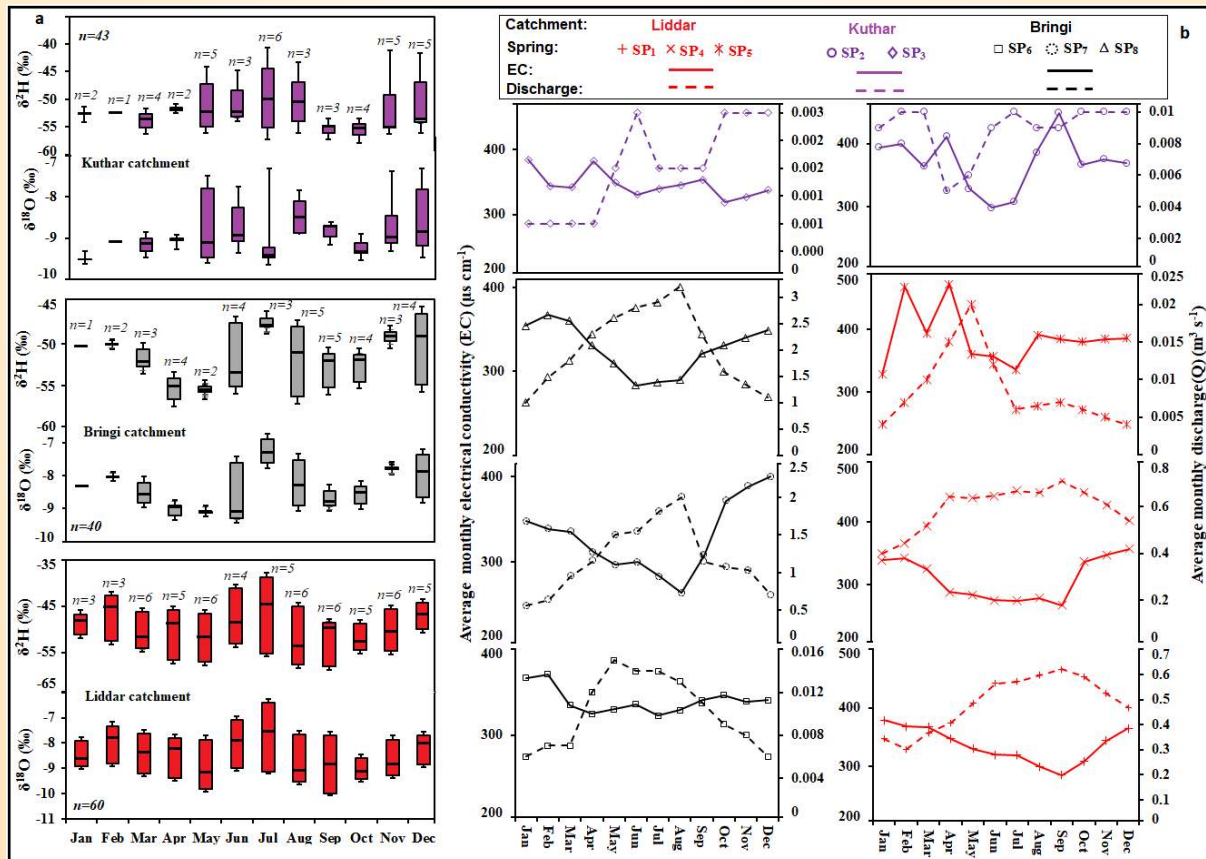


Fig. 69: (a) Spatio-temporal patterns of stable water isotopes, and (b) relationship of electrical conductivity (EC) and discharge (Q) of karst springs in the studied catchments.

context of recharge through differential flow routes and changing seasonal hydro-meteorological conditions at their respective recharge area. A small difference is observed in slopes and intercepts of the karst springs between the studied catchments (Liddar: 5.8 ± 0.11 and 11 ± 0.4 ; Kuthar: 5.1 ± 0.21 and 7.8 ± 1.2 ; Bringi: 6.3 ± 0.17 and 9.8 ± 1). This provides strong evidence of a common recharge water source to karst springs. The results inferred that the lagged effects of δ -depleted winter precipitation signal, reflected in spring flow from March to May, and the rapid response of δ -enriched spring and summer rainfall events (Fig. 69b) can serve as indicators of hydrologic processes associated with karst aquifers in the region. Based on the karst index (ki), the karst springs receive recharge through large conduits in the Liddar and Bringi catchments. While the karst springs in the Kuthar catchment show slow response, providing valuable insights into the hypogene karstification.

Activity: 7

Quantification of strain accumulation/release rate along the Main Himalayan Thrust (MHT) at different time scales

(R.J. Perumal, S. Rajesh, P K R Gautam, Vikas Adlakha, Rajeeb Lochan Mishra, Subham Bose)

The pattern of Strain Release along the MHT at Jammu Sub-Himalaya

The Surin Mastgarh anticline (SMA) marks the active deformation front in the northwest sub-Himalaya near Jammu. The southern limb of the SMA is not truncated by an emergent thrust, unlike other frontal folds along the Himalayan front (Fig. 70). The structural data, deformation pattern, and seismic potential of the SMA have been investigated using field surveys and re-interpretation of seismic profile (Fig. 71). Strath profiles along the Chenab and the Munavar Tawi river valleys indicate active growth of the SMA by layer parallel shortening, and limb rotation accompanied by flexural slip, suggesting an early phase of its development. Lateral migration of the southern limb suggesting limb lengthening and bending at the hinge are the dominant mechanisms of fold amplification with strain localization at the fold core above the floor thrust tip. Bending moment faulting at the hinge led to the formation of crestal grabens or lakes in the south-eastern section of the SMA (Fig. 72). The results of the present study suggest the existence of a weak, less viscous layer beneath a brittle sedimentary detachment. The SMA was initiated as a detachment fold and sequentially deformed by passive roof thrusting.

Therefore, the seismotectonic model of the Jammu Sub-Himalaya is different from that of the central and eastern Himalaya.

Geodetic study

Being the youngest and the southernmost member of the Himalayan plate boundary fault system, the HFT passively accommodates significant north-south crustal shortening across the active Himalayan mobile belt. It has been anticipated that the accumulated crustal strain is getting adjusted aseismically in the frontal Himalaya through the neo-tectonic upliftment of frontal active fault systems. The deformation of the frontal fault in conjunction with the uplift of the Siwalik Hills and the reason for the drastic change in the course of the river Ganga towards SE by abutting the frontal HFT is yet to be known.

By considering the present-day NE movement of the Indian plate; the same style of kinematic movement was expected along the strike of the frontal fault systems and the role played by structures like ridges, and isolated or connected mounts in the shallow crust were ignored. Thus the style of kinematic displacement of the frontal plate boundary fault and the allied active fault systems may be different in accordance with whether such fault systems exist juxtapose to a mountain front or not.

These issues have been studied by analyzing GPS data from Haridwar-Dehradun and Ramnagar networks in the Garhwal and the Kumaun Himalayas respectively and the locations are shown in figure 73. Both the networks are having a combination of permanent and campaign stations. In the Ramnagar network, the inter-seismic deformation of the Himalayan Frontal Thrust (HFT) and the adjoining active fault systems; namely, Pawalgarh and the Dhikala Thrust have been investigated. The crustal velocities were estimated in ITRF2008 and the Indian reference frame using the GAMIT/GLOBK software. Figure 74 shows that in the Ramnagar network, where all the stations are moving toward the northeast direction at a mean rate of 49.63 ± 1.05 mm/yr in the International Terrestrial Reference Frame (ITRF2008).

Using the Ader pole, the ITRF velocities were converted with reference to India and the frontal stations show a southwest movement of ~ 2.70 mm/yr. In this part of the HFT and the allied active faults, the mountain front is absent. The preliminary result of this study shows an uplift rate of ~ 2.84 mm/yr at the HFT in this region; whereas, geological investigations show 3.0 ± 0.6 mm/yr. The East-West trending Pawalgarh

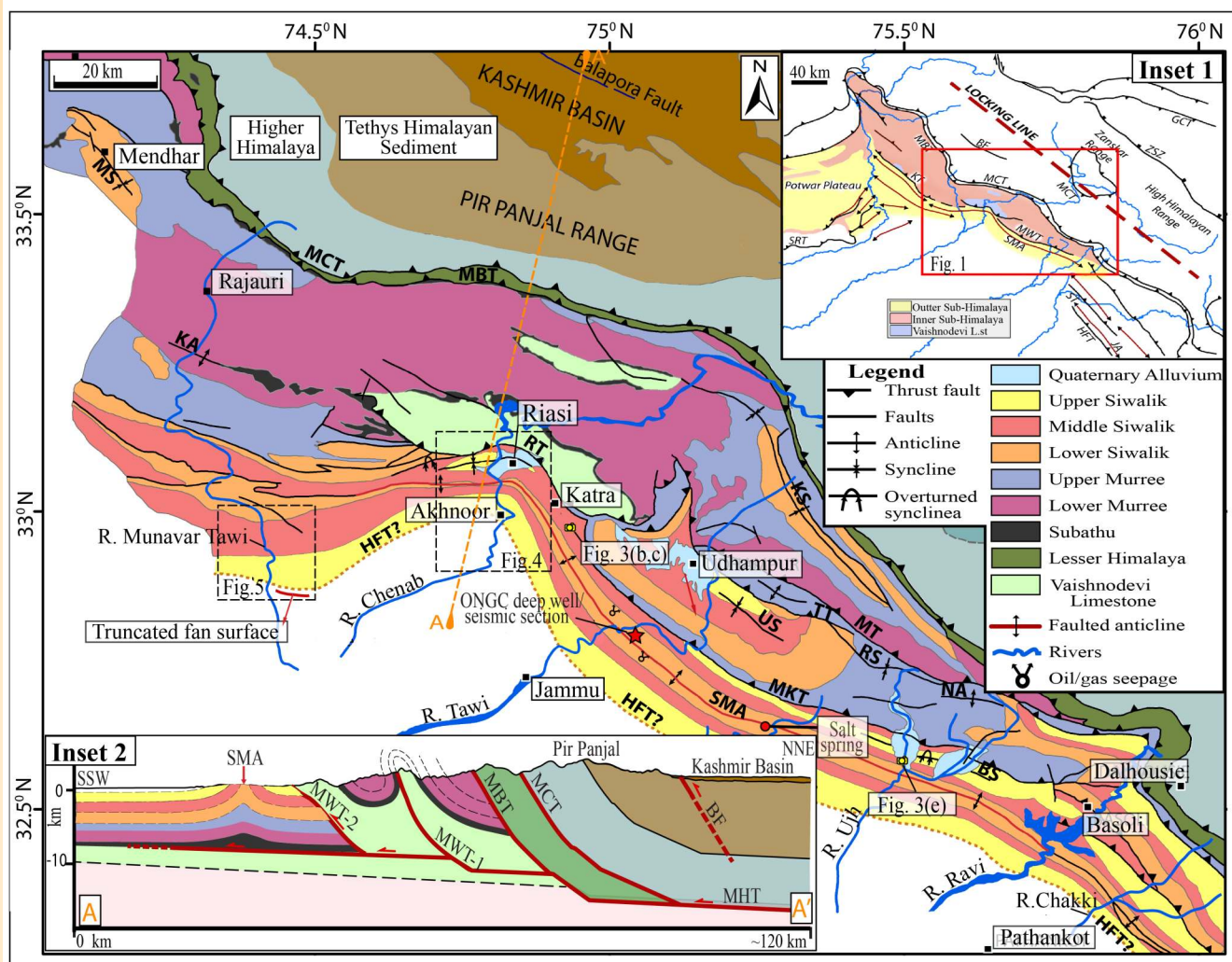


Fig. 70: Geological map of the western part of the northwest Himalaya (after Aravind et al., 2022) showing the present study area.

thrust, which passes through the northern margin of the Pawalgarh Dun shows the geodetic and geological uplift rates of ~ 3.43 mm/yr and 2.0 ± 0.8 mm/yr respectively. The Dhikala thrust, which passes through the proximal part of the Kota Dun shows a geodetic uplift rate almost double (~ 6.87 mm/yr) as that of the geological uplift rate (~ 3.6 mm/yr). Results elucidate that the kinematic behavior of these active fault systems in the frontal extensional deformation zone is strain dissipative. This is observed as inter-seismic upliftment along with oblique convergence of the HFT and the adjoining Pawalgarh and the Dhikala thrust.

The estimated interseismic velocity fields and the strain rates from GPS data with the topography across the Dehradun re-entrant, where a mountain front in the form of Shiwalik Hills is present, were correlated. The

strain rate values were calculated from the GPS-estimated crustal velocities based on the modified least square approach. Stations having velocity uncertainties of more than 2σ are excluded from the surface strain estimation. The strain-rate results show that, in general, the interseismic strain-rate in the Dehradun re-entrant is composite; but spatially distinct and restricted within the tectonic blocks. The frontal part that lies between the HFT and the southern Piedmont fault adjacent to the SE limb of the Siwaliks exhibits both compressional and extensional principal axis of strain. The direction of the predominant compressional strain is sub-parallel to the overall strike of the HFT. The estimated frontal velocities from GPS data show that the crustal blocks at the NW and SE regions across the course of the river Ganges close to Haridwar are in opposite directions. The opposite movements of these crustal blocks

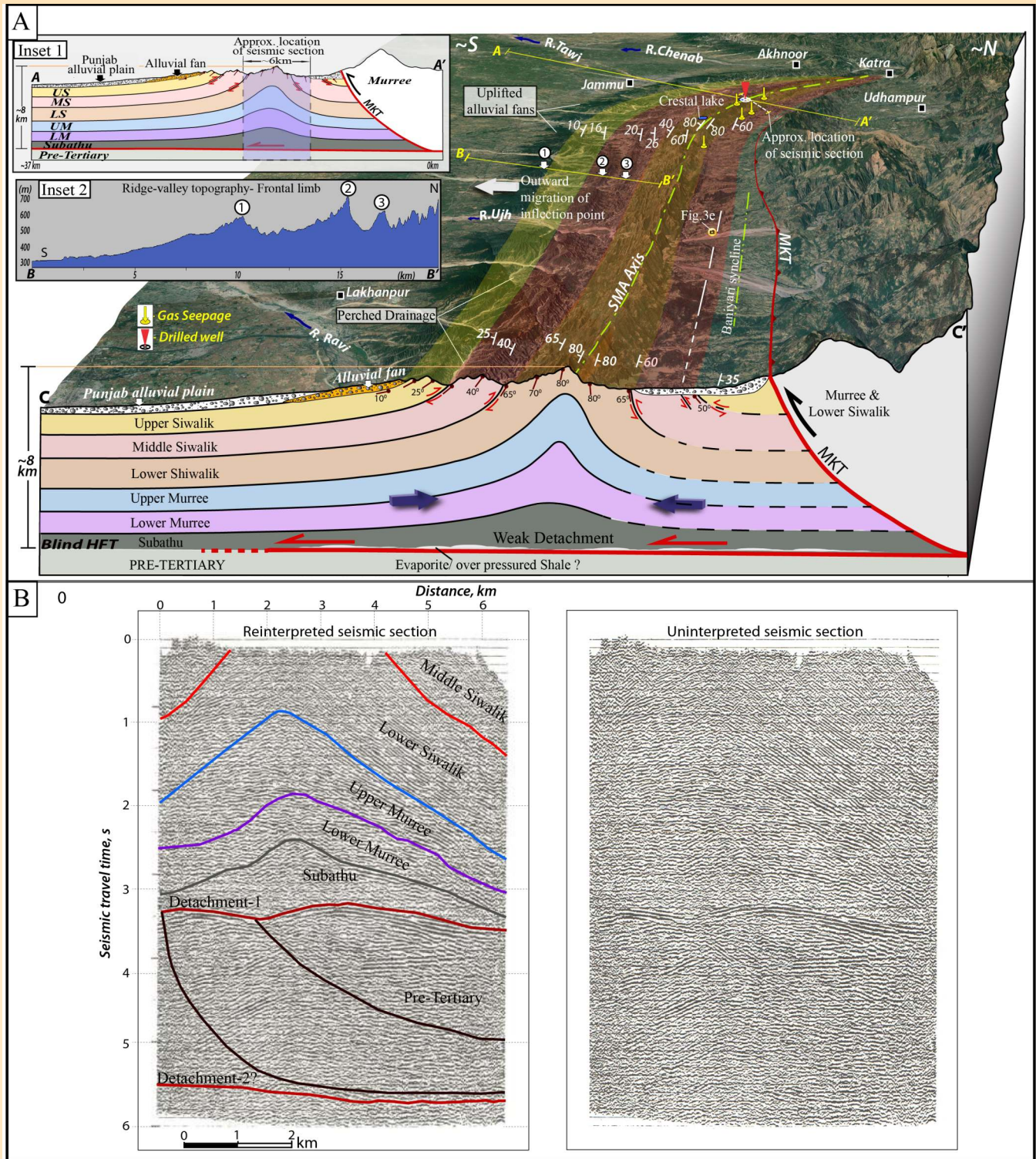


Fig. 71: (A) Three-dimensional depiction of the geometry of SMA along with a simplified ~ NS cross-sectional view (C-C') along the Ravi river valley. (B) Seismic section (right panel) and interpreted section in this study (left panel) published by ONGC. The seismic data clearly shows the near-symmetrical structure of the SMA. The profile shows the detachment structure at a depth of ~8 km. Note: Thick sediment cover is noticed in the Jammu Sub Himalaya.

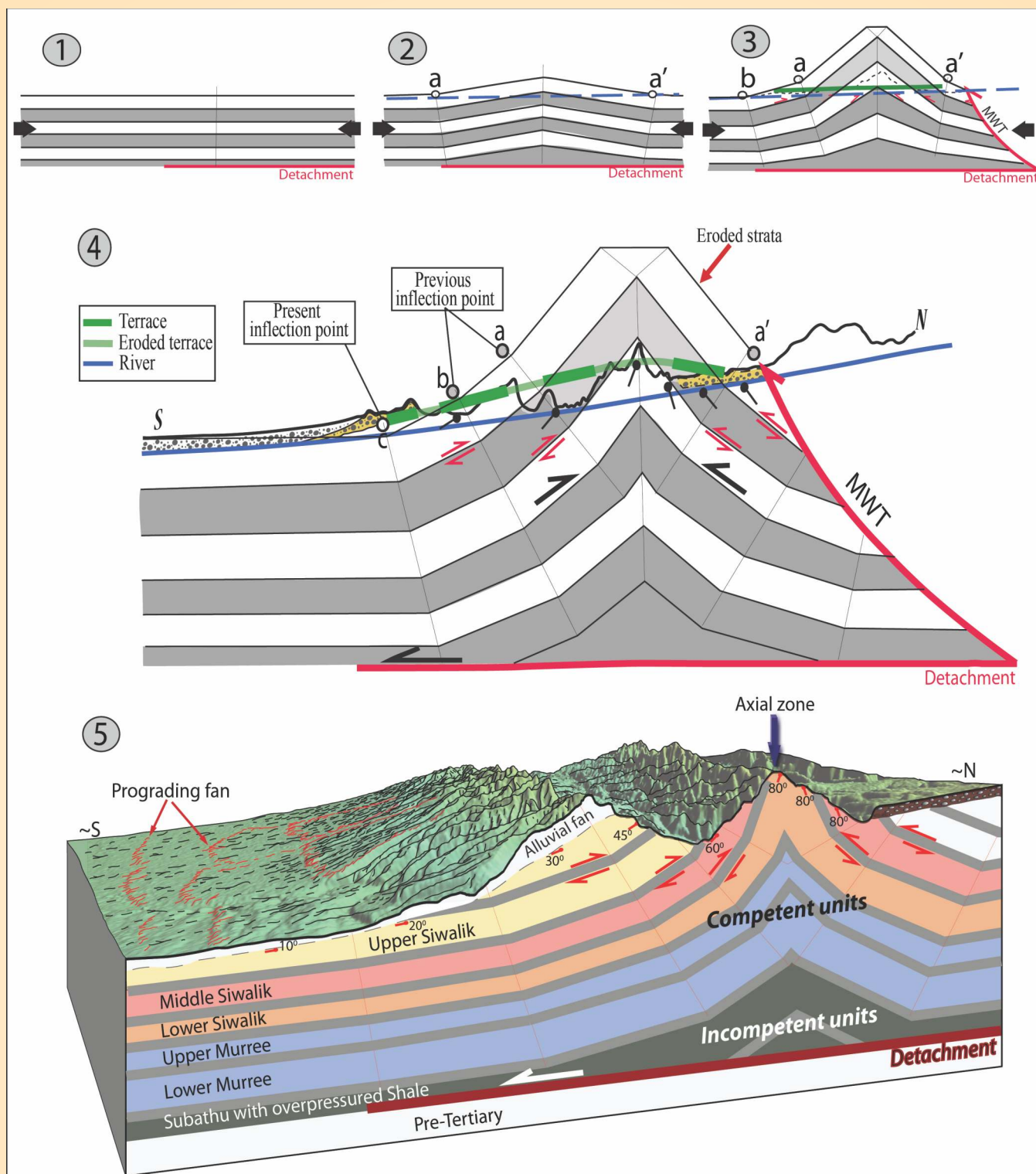


Fig. 72: Illustration showing the stages of formation of the Surin Mastgarh Anticline (SMA).

plausibly cause the eastward frontal migration in the course of the river Ganges. Here the southeastern segment of the Frontal HFT close to the Ganga Tear Fault (GTF) is undergoing significant horizontal shear

strain compared to its northwestern segment. Besides high shear strain is also observed between the GTF and the Delhi Haridwar Ridge (DHR). Thus the comparison of GPS-based interseismic crustal velocity fields of the

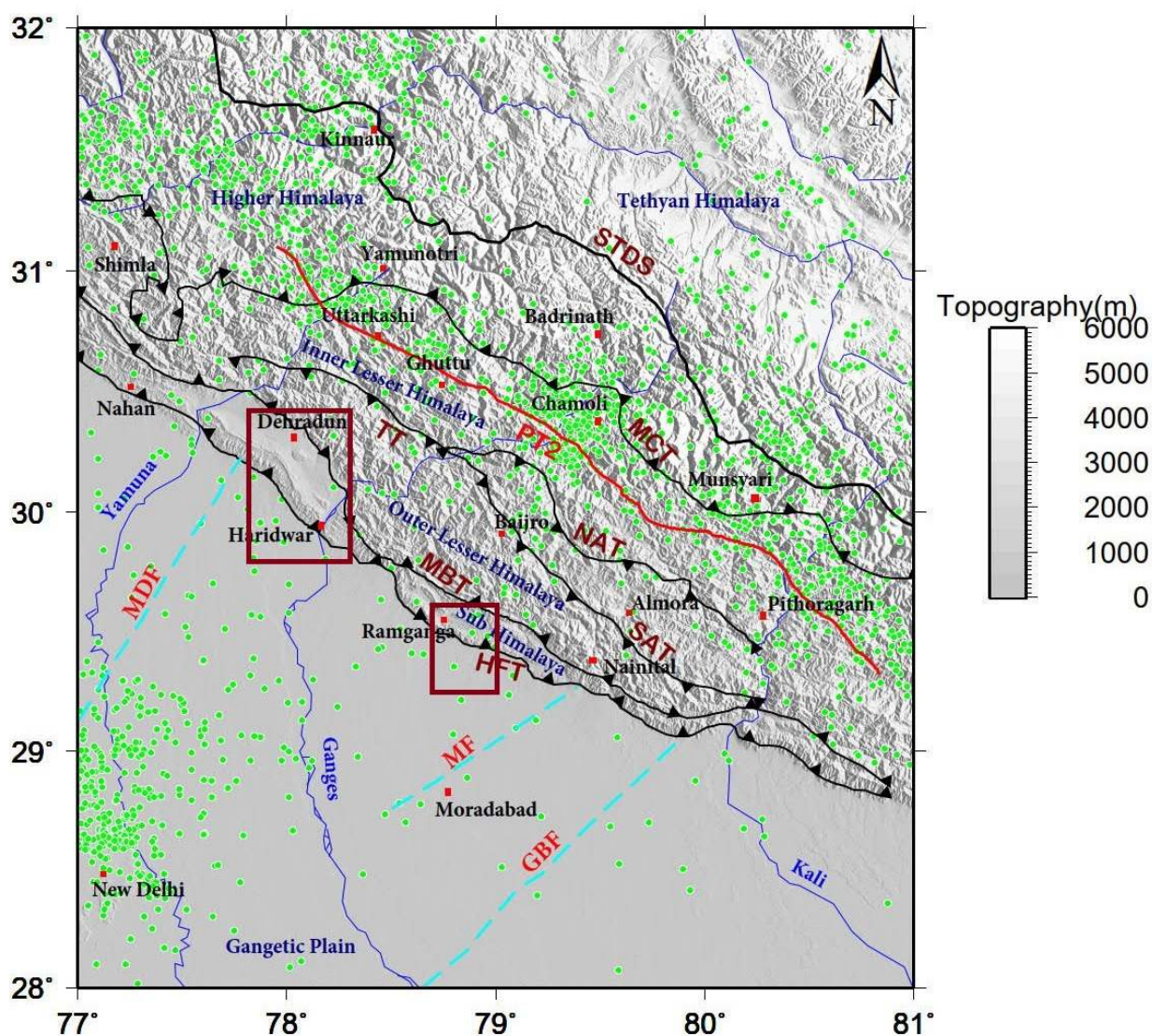


Fig. 73: Study area in the Haridwar-Dehradun and Ramnagar network with background seismicity. Himalayan Frontal Thrust (HFT), Main Boundary Thrust (MBT), Main Central Thrust (MCT), South Tibetan Detachment System (STDS) are marked along with the Mahendragarh-Dehradun Fault (MDF), Moradabad fault (MF), Great Boundary Fault (GBF) and the physiographic transition (PT2). The major morphotectonic zones namely Sub-Himalaya (SH), Outer Lesser Himalaya (OLH), Inner Lesser Himalaya (ILH), Higher Himalaya (HH) and the Tethyan Himalaya (TH) are marked.

HFT at the mountain front in the Dehradun re-entrant and at the non-mountain front in the Kumaun region show distinct styles of kinematic deformation.

Analyzed various topography and terrain models to process the acquired land gravity data. Apart from that; the quality factor, noise, and spectral levels on the acquired gravity data are also done. Estimated the aperiodic temporal gravity signals generated by micro-tremors after modeling out the periodic and static trends in the data to identify the non-tidal temporal causatives.

Thermochronology, structural geology and tectonics

In addition, the evolution of the Karakoram granite batholith was characterized by its crystallization through sub-magmatic flow and solid-state deformation to low-grade metamorphism and exhumation. Demonstrated the progressive decline in deformation (aseismic creep) rates of the Karakoram batholith through the period following collision along the Shyok suture zone (SSZ), Trans-Himalaya, India.

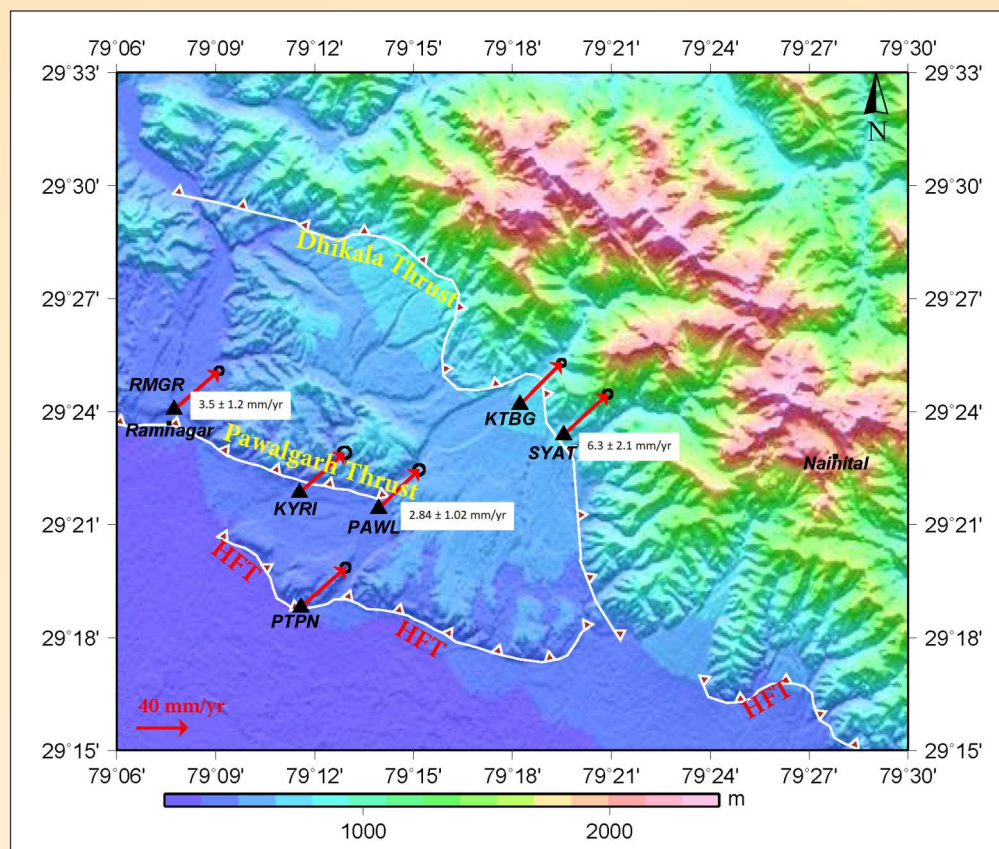


Fig. 74: Station velocities of Ramnagar network in ITRF2008.

Reconstructed the structure and kinematics of deformation of the rocks of the Tethyan Himalayan Sequence (THS) across the South Tibetan Detachment (STD) zone, has also been done for the Bhagirathi valley, India.

New doors of the research have been opened through the detailed fieldwork and litho-tectonic mapping across the Munsiyari Thrust and the Main Central thrust (MCT) zones, Alakananda-Dhauliganga valley, India, across the Main Boundary thrust (MBT) zone, NW Himalaya, along the Mohand Anticline in the sub-Himalayan zone of the Uttarakhand Himalaya, India and along the Saltoro Range and Tethyan Sequence of Zaskar, NW Himalaya, India.

A total of 07 Apatite Fission Track (AFT) ages and 09 Zircon Fission Track (ZFT) ages have been generated along the strike of the Karakoram Fault Zone (KFZ) from the Sasoma-Shyok section of the Ladakh region. The AFT ages range from 3.8 ± 0.5 to 6.9 ± 1.1 Ma and ZFT ages range from $\sim 8.7 \pm 0.7$ to 11.3 ± 0.6 Ma. Transient exhumation history has been obtained using these cooling ages which suggest that the lithounits of the KFZ have exhumed at the rate of $\sim 0.53 \pm 0.05$ mm

yr⁻¹. From ~ 9.9 Ma to 4.8 Ma while the exhumation rate was $\sim 0.62 \pm 0.03$ since 4.8 Ma. Thus, the KFZ in the Ladakh region has exhumed at nearly constant rate since ~ 10 Ma.

New thermochronological data has been obtained from Gianbul Dome, which is a Higher Himalayan gneissic dome present in the rain shadow domain of Zaskar region NW India. The dome is bounded by Zaskar Shear Zone/STDS to the north which is a low angle normal fault showing top to NE shear sense indicator and Chenab Normal Fault to the south which is also a normal fault zone showing top to SW sense of shear. The AFT ages range from 5.7 ± 1.1 to 13.4 ± 0.6 Ma. The mean AFT mean age is 9.4 Ma. The ZFT ages range from 14.6 ± 0.9 to 22.8 ± 2.2 Ma. The mean ZFT age is 17.23 Ma. The older ages lie in the core of the dome and as one moves away from the core of the dome AFT and ZFT ages get young. That indicates the fault movement. 3D thermokinematic modeling has been done using Pecube Fortran-90 program. The 3D modeling suggests the gravitational collapse during the Late Miocene.

SPONSORED PROJECTS

MoES Sponsored Project**Geochemistry and Geochronology of the Tethyan Ophiolites of the Indo-Myanmar Orogenic Belt, Northeast India: Geodynamic and petrogenetic implications and mineralization***(A. Krishnakanta Singh)*

The Neo-Tethyan ophiolite suite of rocks of the W-E trending Indus-Tsangpo Suture Zone (ITSZ) represents the remnants of the Neo-Tethys Ocean, which were obducted on the surface during the collision of the Indian and Eurasian plates. The ITSZ turning sharply southeastward at the eastern Himalayan syntaxis is offset northward by the Sagaing Fault and continues southward along the Indo-Myanmar Orogenic Belt (IMOB). The ophiolite sequences occurring all along the Tuting-Tidding Suture Zone (TTSZ) in the eastern Himalaya, which runs east of the Siang Antiform, have been considered as the south-eastern extension of the ITSZ. The suture zone extends south to the IMOB and the Andaman-Nicobar Island Arc (ANIA).

The ophiolites of the TTSZ viz. Tidding Ophiolite Complex (TOC) and Mayodia Ophiolite Complex (MYOC) and IMOB i.e. Nagaland Ophiolite Complex (NOC) and Manipur Ophiolite Complex (MOC) have been collectively investigated through the mantle-derived peridotite sequence. All the investigated peridotites (lherzolite, Cpx-harzburgite, harzburgite, and dunite) have been serpentinized to varying extents and display a remarkably variable degree of fertility with MgO of 35.22–45.79 wt.%. Their MgO contents increase systematically from lherzolite to harzburgite to dunite. Lherzolite and Cpx-harzburgite samples from MOC have LOI ranging from 4.43 to 10.37 wt.%. LOI in MOC dunite has LOI ranging from 4.83 to 8.98 wt.%. These peridotites are characterized by variable silica content (40.31–43.29 wt.%) and are variable with MgO ranging between 36.37–42.64 wt.%. The samples generally have meager amounts of Al_2O_3 (0.19–1.21 wt.%) and CaO (0.01–0.82 wt.%). The chondrite-normalized REE patterns of lherzolite and Cpx-harzburgite display spoon-shaped REE patterns with LREE-depleted patterns ($\text{La}_N/\text{Sm}_N = 0.51\text{--}2.14$; $\text{La}_N/\text{Yb}_N = 0.06\text{--}0.80$ and a flat to slightly fractionated HREE patterns ($\text{Sm}_N/\text{Yb}_N = 0.25\text{--}0.62$) (Fig. 75). These features suggest that these peridotites are not genetically related to the subduction process. The REE patterns of the lherzolite and Cpx-harzburgite of MOC

are comparable of with the Abyssal peridotites (Niu, 2004) and Mid-oceanic ridge (MOR)-type lherzolite and Cpx-harzburgite from Neo-Tethyan ophiolites, SW Turkey (Aldanmaz et al., 2009).

Bulk-rock SiO_2 concentration in the Harzburgite collected from NOC, TOC, and MYOC ranges between 39.23 and 45.04 wt.% with MgO ranging from 37.31 to – 40.31 wt.%). The samples are high in Cr (1945–4701 ppm) and Ni (1399–2408 ppm). They have ΣREE of 1.15 to 2.55 ppm and show slightly concave patterns with fractionated HREE segments and have had similar U-shaped patterns with relative enrichment in both LREE and HREE and depletion in middle REEs (MREEs) (Fig. 75b, c). The patterns suggest weak LREE enrichment of previously depleted peridotites and are consistent with patterns for forearc peridotites with low REE contents. Similar supra-subduction geochemical signatures for Cr-spinel-bearing peridotites have also been reported from the Neo-Tethyan ophiolites in SW Turkey and Albania peridotites (Aldanmaz et al., 2009). A similar interpretation of fertilized MOR-type peridotites was also proposed for the Luobusa ophiolite, located in the eastern part of the Yarlung Zangbo Suture Zone (Xiong et al., 2015). REE distributions in harzburgites from NOC, TOC and MYOC are compared with harzburgite from Zhongba (Dai et al., 2011) and Luobusa ophiolites, Southern Tibet (Zhou et al., 2005) (Fig. 75b,c). REE distributions in dunites from MOC, NOC, and MYOC are compared with dunites from Xigaze ophiolites, Tibet (Xiong et al., 2017) and dunite pods from the Luobusa ophiolite, southern Tibet (Zhou et al., 2005) (Fig. 75c).

Since the REE content of peridotites is another indicator of mantle melting degree, a non-modal dynamic melting model with a critical mass porosity of 0.1% was used for the studied peridotites. The partial melt model of HREE suggests that the investigated peridotites formed from 19–23% partial melting of the mantle, indicating their refractory nature. This finding is consistent with the degree of partial melting results of Cr# in Cr-spinel. The estimated data shows that the TOC and MYOC peridotites may be a residue of the hydrous melting of the mantle source because, under anhydrous conditions, mantle melting will cease when clinopyroxene is completely consumed, which corresponds to a melting degree of ~20%.

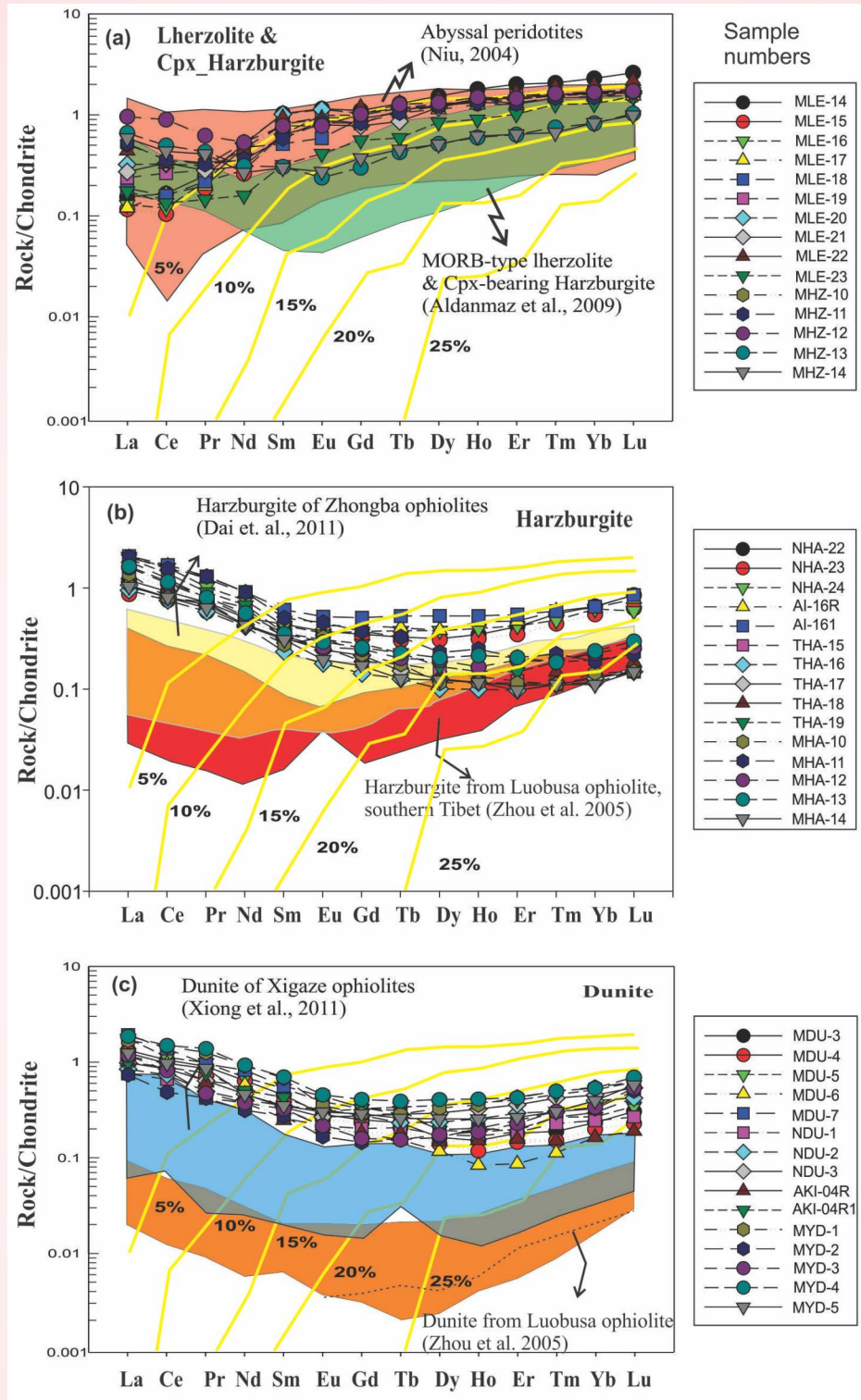


Fig. 75: Comparison of (a) REE distributions in lherzolite and Cpx-harzburgite of MOC with Abyssal peridotites (after Niu, 2004) and mid-oceanic ridge (MOR)-type lherzolite and Cpx-harzburgite from Neo-Tethyan ophiolites, SW Turkey (after Aldanmaz et al., 2009). (b) REE distributions in harzburgites from NOC, TOC and MYOC with harzburgite from Zhongba ophiolites (after Dai et al., 2011) and harzburgite from Luobusa ophiolites, southern Tibet (after Zhou et al., 2005). (c) REE distributions in dunites from MOC, NOC, MYOC with dunites from Xigaze ophiolites, Tibet (after Xiong et al., 2017) and dunite pods from the Luobusa ophiolite, southern Tibet (after Zhou et al., 2005).

High Cr# in spinels may reflect relatively large melt fractions of a fertile peridotite (Dick & Bullen, 1984), and high Fo contents of olivine in the olivine–melt equilibria are not substantially changed by variations in H₂O. This relationship is illustrated by plots of Spinel Cr# vs coexisting olivine Fo content and proposed as 'Olivine–Spinel Mantle Array' or 'OSMA' plot (Fig. 76a). Fo of olivine and Cr# of Cr-spinel are extensively employed to characterize mantle-derived, spinel-bearing peridotites. The Fo–Cr# fractionation trend reflects the differentiation of magma, including various processes, such as crystallization differentiation, magma mixing, and assimilation. All the study rocks plot within or on the edge of the OSMA, consistent with formation by extensive melt extraction. The spinel-olivine pairs in the lherzolite and Cpx-harzburgite plot in the lower end of the abyssal peridotite field, but also in the middle of passive margin peridotites further indicating the fertile nature of the peridotites. This observation further suggests the primary nature of the spinel and olivine compositions and reveals the low to moderate degrees of partial melting suffered by the rock. From this diagram, it is also evident that the abyssal peridotite relict underwent a low degree (< 12%) of partial melting. Their low melting value corresponds to the slow-spreading rate end, which differs from ~ 22% melting of the fast-spreading rate end of the entire spreading rate variation range. The slow-spreading environment for the formation of lherzolite and Cpx-harzburgite is also supported by the absence of sheeted dikes coupled with the paucity of lavas and the presence of thick abyssal sediments (such as limestone and radiolarite). Conversely, harzburgite and dunites of the study area are plotted in the field of SSZ peridotites, suggesting their derivation during the subduction zone tectonic setting. Consequently, it is suggested that the lherzolite, Cpx-harzburgite, Harzburgite, and dunites are all related by increasing degree of depletion due to both partial melting and melt-rock reaction. Peridotites from the Kalaymyo ophiolite and Myitkyina ophiolite of Myanmar crop out at the eastern margin of the IMOB and are also clustered in both the abyssal peridotite field and SSZ peridotites. Thus, both the Kalaymyo and Myitkyina ophiolites have refractory peridotites with compositions similar to the forearc peridotites, and the fertile peridotites are compositionally similar to the abyssal peridotites that are similar to those of peridotites of MOC and NOC of the IMOB.

Similar differentiation of abyssal and forearc signatures of peridotites are observed in the Cr# versus TiO₂ (wt%) in the Cr-spinel plot (Fig. 76b). This plot

shows the degree of melting of mantle rocks and reaction trends with boninite melts, island arc, and mid-ocean ridge basalt melts. The lherzolite and Cpx-harzburgite of MOC have a Cr# value of <40 plot along the abyssal peridotite field, while chromium has Cr # value of >50 of the harzburgite and dunites from NOC, TOC and MYOC follow the trend of forearc peridotites. Mantle-derived peridotites from the adjoining Kalaymyo Ophiolite and Myitkyina Ophiolite are also clustered in both the abyssal peridotite field and SSZ peridotites, suggesting their formation in two distinct tectonic affinities of MOR spreading and SSZ environments. Conversely, peridotites of the ITSZ ophiolites are also generated in the MOR spreading and SSZ setting environments (Yang et al., 2012). Thus, this study confirmed that the mantle peridotites in the ophiolites of northeast India evolved from lherzolite through clinopyroxene-harzburgite and harzburgite then to highly refractory dunite, supporting multistage melting and melt-rock reaction processes during their generation.

Further, comprehensive data of whole-rock and stable isotopic geochemistry along with microfossil assemblages of the carbonate rocks of MOC are discussed to determine the influence of terrigenous contamination during the formation of these carbonates rocks and also to understand their depositional environment and ages. Carbonate rocks have variable SiO₂ concentrations, ranging from 5.79 to 25.31 (wt.%), in a few samples, SiO₂ % is very high, which is due to the presence of silicate minerals in the form of chert and detrital quartz. SiO₂ is the second major oxide present in the carbonate rocks of the study area. CaO values range from 27.89 to 51.57 wt.% whereas MgO concentration ranges from 0.79 to 3.46 (wt.%). The P₂O₅ content in carbonate rocks is an indicator of a reducing environment with organic matter or the presence of phosphate minerals. Genetically, P₂O₅ content is related to the organic matter, viz., fossils. P₂O₅ content ranges from 0.02 to 0.77 (wt. %). A relatively higher percentage of P₂O₅ in a few samples may be due to protected climatic conditions and/or higher salinity in the study areas. The majority of the trace elements known in carbonate rocks are bound to the detrital silica oxide fraction of the limestone. Mg, Sr, and Mn are linked in specific ways with the carbonate phase depending on the similarity of the crystal chemistry of the main components of more abundant carbonate minerals (Sr²⁺ and Ca²⁺ having a similar size and of the same ionic charge, while Mn²⁺ and Ca²⁺ have the same charge but slightly different size) and on the relatively high concentration in the ocean. Sr concentration of the

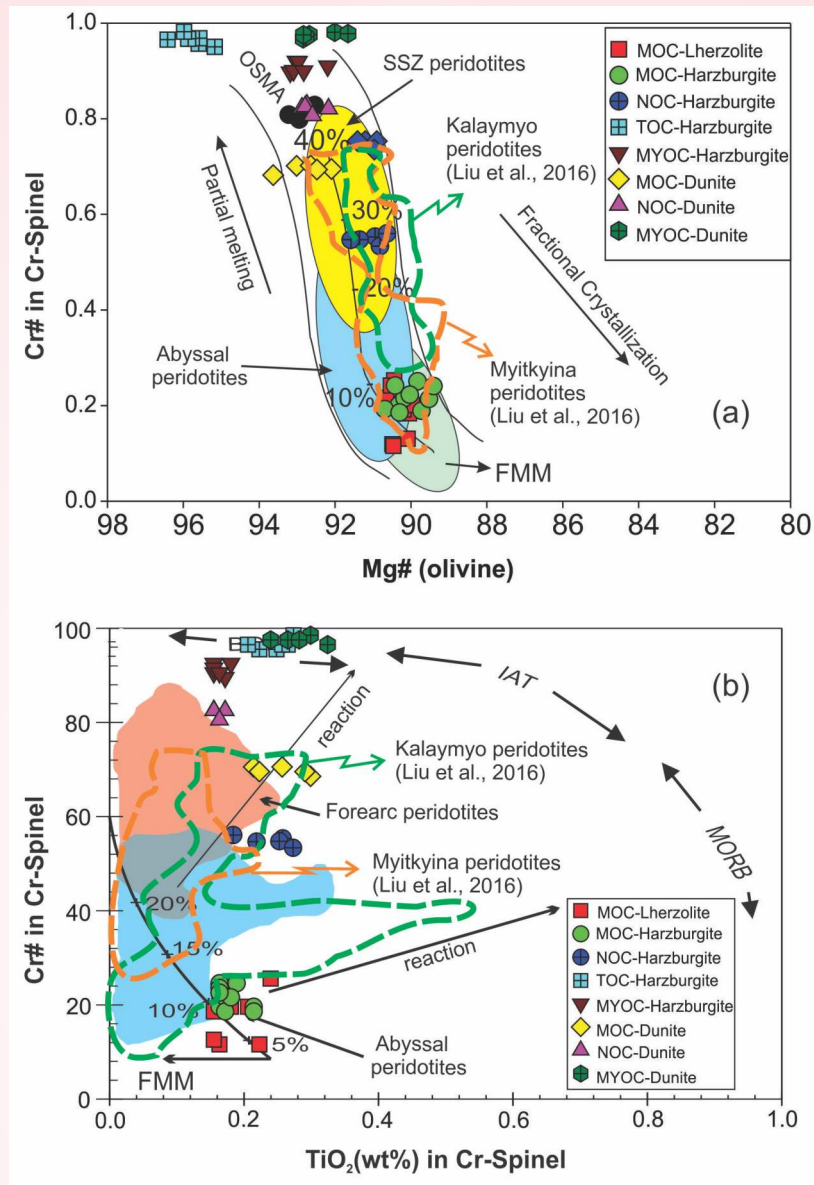


Fig. 76: Binary plots of (a) Olivine Spinel Mantle Array (OSMA) diagram (after Arai, 1994) for harzburgite and dunites from NMO. FMM represents the fertile mantle. (b) The Cr# versus TiO₂ plot for chromite shows the degree of melting of mantle rocks and reaction trends with boninite melts, island arc, and mid-ocean ridge basalt melts. Peridotites from the Kalaymyo ophiolite and Myitkyina ophiolite of Myanmar crop out at the eastern margin of the Indo-Myanmar Orogenic Belt are also shown for comparison. Abbreviations: IAT, island arc tholeiite; SSZ, supra-subduction zone.

carbonate ranges from 332-816 ppm with an average of 574.7 ppm, whereas the concentration of strontium ranges from 324-811 ppm. Sr content for the shallow marine environment (100-400 ppm) and the deep marine environment ranges from 500-3000 ppm. The variations of average Sr concentration in carbonates suggest a relatively deeper environment of deposition. Precipitation under a high saline environment results in a high concentration of strontium. Hence, the high percentage of strontium in the study carbonates might

also indicate the formation of the carbonate under a relatively higher saline environment. The stable calcite becomes progressively enriched in magnesium, and the stable dolomite becomes progressively enriched in calcium with increasing temperature.

Significant variations in REE content are noticed in the different types of carbonates. Yttrium is inserted between Ho and Dy in the REE pattern according to its identical charge and similar radius. The low REE in a

few carbonate samples is probably due to marine carbonate phases, which generally contain significantly lower REE content than detrital clays and heavy minerals. Post-Archean Australian Shale (PAAS)-normalized REE+Y patterns of these carbonates are shown in (Fig. 77). These carbonates exhibit a seawater-like REE pattern with LREE depletion [average $(\text{Nd}/\text{Yb})_{\text{SN(shale normalized)}} = 0.98 \pm 1.5$] and consistent negative Ce_{SN} and positive La_{SN} anomalies. The carbonate minerals precipitated in equilibrium with seawater show distinct negative Ce anomalies, and this may also be reflected in the bulk REE pattern. The $(\text{Dy}/\text{Yb})_{\text{SN}}$ ratio in the carbonates varies from 0.86 to 1.58 (average 1.3 ± 1.5), which is similar to the modern seawater ($\sim 0.8\text{--}1.1$). The high $(\text{Dy}/\text{Yb})_{\text{SN}}$ ratios in MOC carbonates show enrichment in HREE rather than LREE, similar to modern seawater. Positive Eu anomalies are uncommon in seawater, which generally result from input from hydrothermal anomalies, which is unusual in seawater, probably resulting from the diagenetic alteration in the carbonate; a slight increase in the primary or detrital feldspar component and an increased oceanic input of hydrothermally originated fluids at mid-oceanic ridges.

The carbonates show variable oxygen and carbon isotope data ranging for $\delta^{18}\text{O}$ from -6.37 to -9.00‰ (PDB) whereas $\delta^{13}\text{C}\text{‰}$ (PDB) ranges from 1.02 to 1.57‰ (PDB). The marine and freshwater carbonates were discriminated following the equation $Z = a(\delta^{13}\text{C} + 50) + b(\delta^{18}\text{O} + 50)$ in which 'a' and 'b' are 2.048 and 0.498. The carbonates with Z values above 120 are considered marine, whereas those with Z values below 120 would be classified freshwater type. Furthermore, the Z values are less than 120 for all the cement samples and come under the freshwater type. In the present study, all the samples show Z values above 120 ranging from 123.29 to 128.67, indicating their marine origin. The $\delta^{13}\text{C}\text{‰}$ (PDB) and $\delta^{18}\text{O}\text{‰}$ (SMOW) ratios of these carbonates are closely similar to marine limestone (Fig. 78). The $\delta^{18}\text{O}$ versus $\delta^{13}\text{C}$ bivariate diagram with generalized isotopic fields for carbonate components, sediments, limestones, cement, dolomites, and concretions. The PAAS-normalized REE+Y patterns of these carbonates exhibit seawater-like REE patterns with LREE depletion and relative HREE enrichment with negative Ce anomalies and positive Y and Eu anomalies, suggesting that they were deposited under an oxygenated environment with contamination by the hydrothermal activity. Trace elements (Zr, Th) and REE

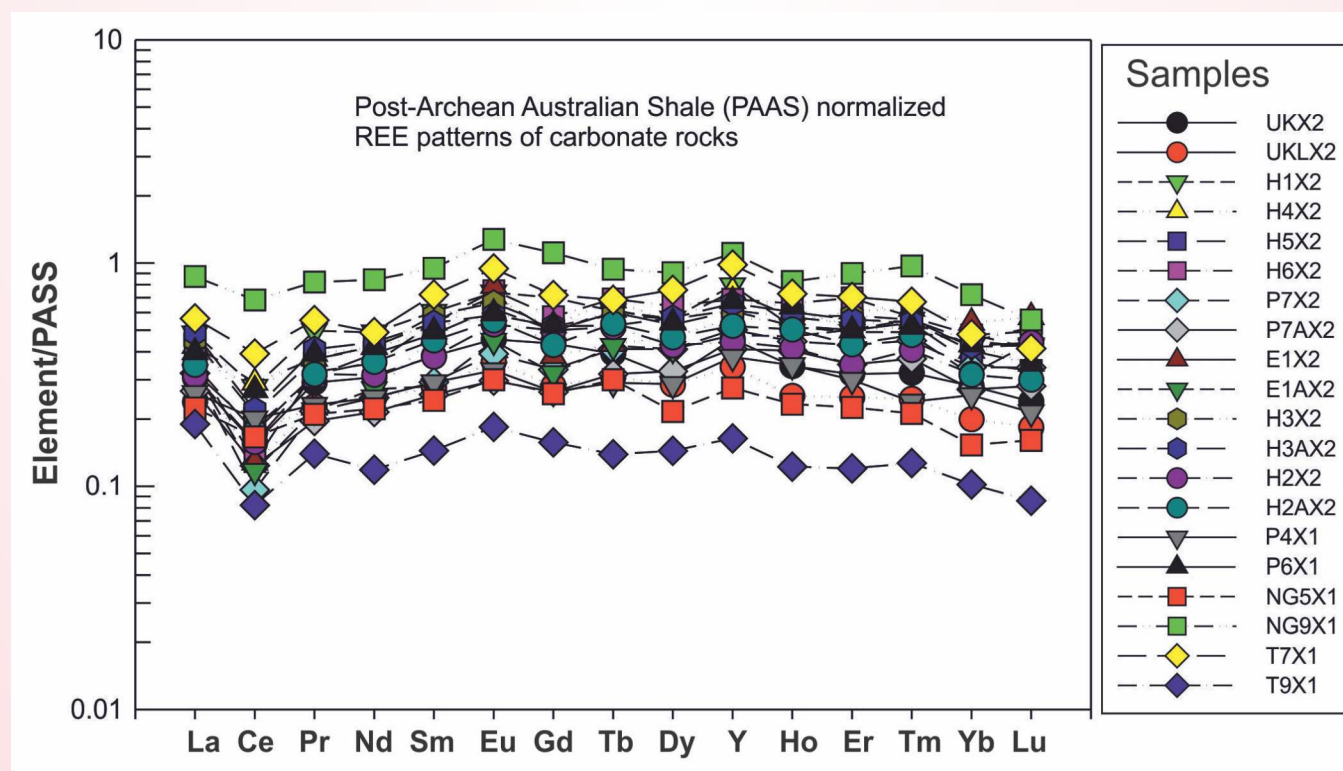


Fig. 77: Post-Archean Australian Shale (PAAS)-normalized REE+Y patterns of carbonate rocks from the ophiolitic mélange zone, Indo-Myanmar Orogenic Belt (IMOB), NE India.

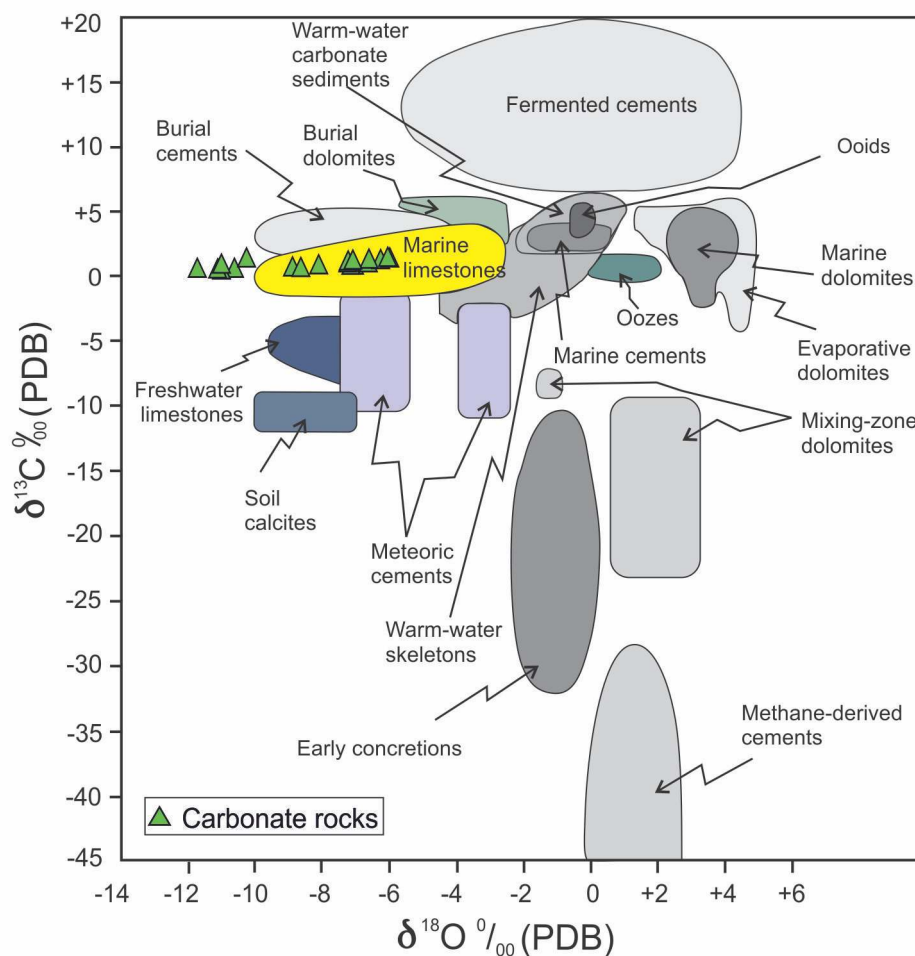


Fig. 78: $\delta^{18}\text{O}$ (PDB) and $\delta^{13}\text{C}$ (PDB) plot for carbonate rocks of the ophiolitic mélange zone, Indo-Myanmar Orogenic Belt (IMOB), NE India.

characteristics further suggest that REE in carbonates have not been affected by detrital materials. Thus it has been concluded that the investigated carbonates are also depleted in $\delta^{13}\text{C}\text{‰}$ (PDB) (1.02 to 1.57‰) and $\delta^{18}\text{O}\text{‰}$ (PDB) (-6.37 to -9.00‰) values which characterize marine precipitates. Further, their Eu anomalies and spread in negative $\delta^{18}\text{O}\text{‰}$ (PDB) values to a lesser extent of $\delta^{13}\text{C}\text{‰}$ (PDB) values also suggest their formation was altered by diagenesis in the shallow marine environment.

USDMA Sponsored Project

One Year Monitoring of Vasudhara Tal, Purvi Kamet (Raykana) Glacier, Dhauliganga Valley, Uttarakhand India

(Kalachand Sain, Manish Mehta, and Vinit Kumar)

The Vasudhara Tal is a proglacial lake that has increased

in area and volume since 1968. In 1968, there was no supraglacial lake on Raykana Glacier, and only two small lakes were present, with a total lake area was $\sim 0.14 \text{ km}^2$. Whereas, in 1990, some new lakes developed in the area, with an increase in the lake area of $\sim 0.22 \text{ km}^2$. Similarly, in 2001 and 2011, the number of lakes and lake areas increased to ~ 0.33 and 0.43 km^2 . The total lake area estimated in 2021 is $\sim 0.59 \text{ km}^2$ (Fig. 79). Further, the retreat of the Raykana Glacier is uneven, with a minimum retreat of 15 m a^{-1} from 1990 to 2001. In contrast, it increased by 38 m a^{-1} between 2017 and 2021. However, the lake area and depth may increase if the glacier shrinks at a similar rate. Therefore, the presence of supraglacial and proglacial lakes on the Raykana and Purvi Kamet glaciers make the area vulnerable to the GLOF threat in the future.

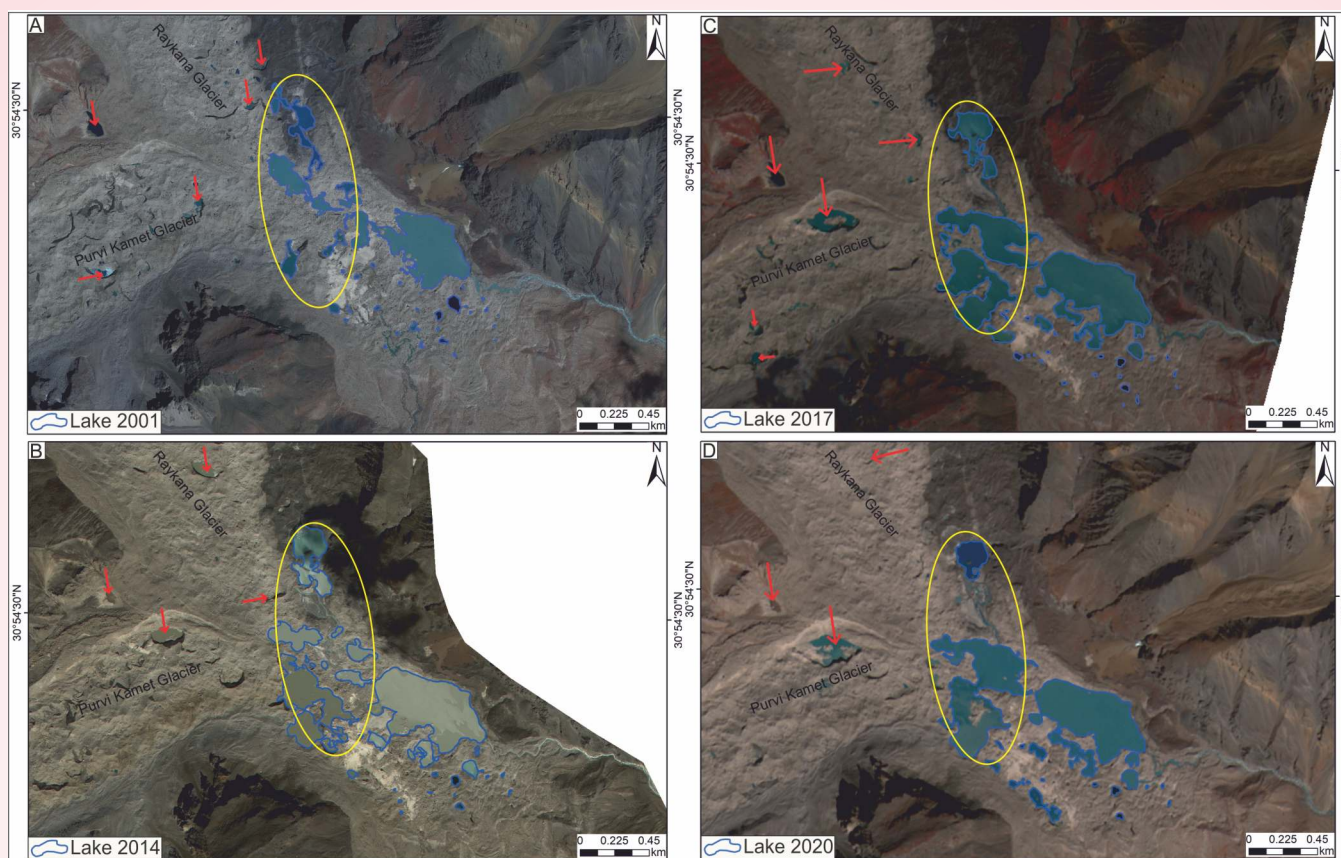


Fig. 79: A) Satellite image of IKONOS-2 (2001), (B) WorldView-2 (2014), (C), and (D) LISS-IV images showing lake changes with marked red and yellow circles.

USDMA Sponsored Project **Long-term monitoring of Gangotri Glacier,** **Garhwal Himalaya**

(Kalachand Sain, Amit Kumar)

The Himalayan Mountain Range contains thousands of glaciers of varying properties, which are spread over 37000 km² and a stretch of 2400 km from East to West. The glacier inventory by the Geological Survey of India indicates there are 9575 glaciers in the Indian Himalayan Region (IHR). It is a well-established fact that changes in the glaciers are a key indicator of climate change; recent observation shows that snow accumulation is reducing while the ablation is increasing in the Himalaya. However, there are only a handful of ground-based studies on the Himalayan glaciers. Therefore, the Department of Science and Technology (DST) has given the Wadia Institute of Himalayan Geology (WIHG), Dehradun the mandate to monitor Himalayan Glaciers. Presently, Uttarakhand State Disaster Management Authority (USDMA) has sponsored a project entitled “Long-term Monitoring of Gangotri Glacier, Garhwal Himalaya” to WIHG in March 2022.

Based on the physical observations during field visits and satellite-based information during the period January to March 2023, it has been observed that the meltwater stream from Gangotri Glacier is originating near the left lateral moraine, flowing across the snout of the glacier (Gaumukh) before moving downward (Fig. 80A). During the end of January and February, surface water in the Bhagirathi River near the snout was found in a frozen state while some water was flowing below the frozen layer (Fig. 80B & C). The base camp was fully covered under snow during winter (Fig. 80 B & C). Based on the high temporal satellite images from January to March 2023, there are no major changes in the snout of the Gangotri Glacier. The Bhagirathi River is found flowing uninterrupted during the observation period (Fig. 81). Remote sensing analysis also indicates that the Raktavarn stream joins Bhagirathi River below the Gangotri Glacier snout. Further, the ground-based information and satellite images indicate that Gangotri glacier witnessed snowfall between January and February 2023, while images of March 2023 indicate melting of snow, exposing the glacier surface and ice (Fig. 81). Based on field observations and satellite data, there is no emanating threat observed in the region.

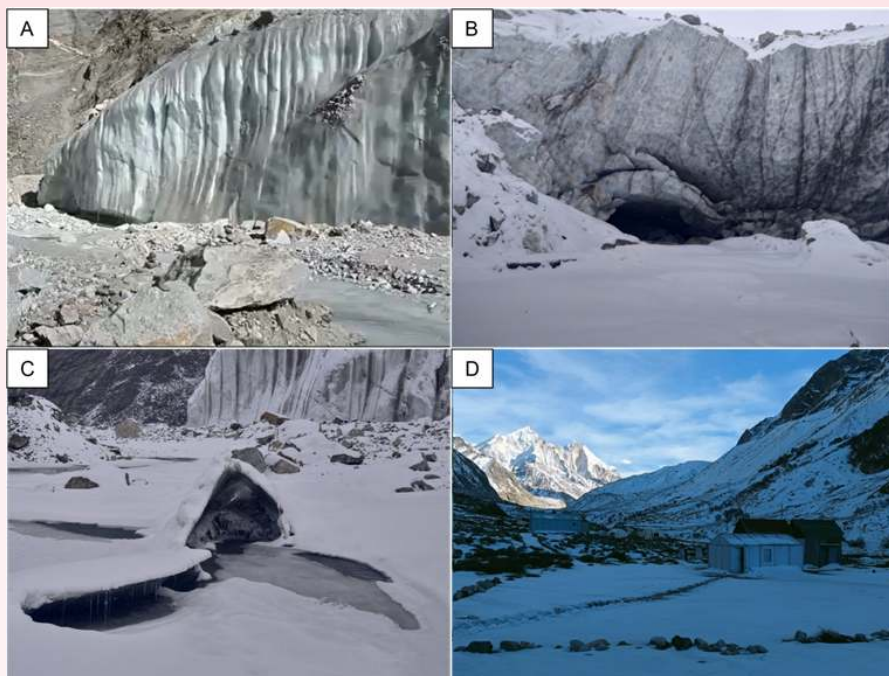


Fig. 80: Field photographs showing the status of the snout of Gangotri Glacier, stream emerging from it, and base camp at Bhojwasa during winters (January-March 2023).

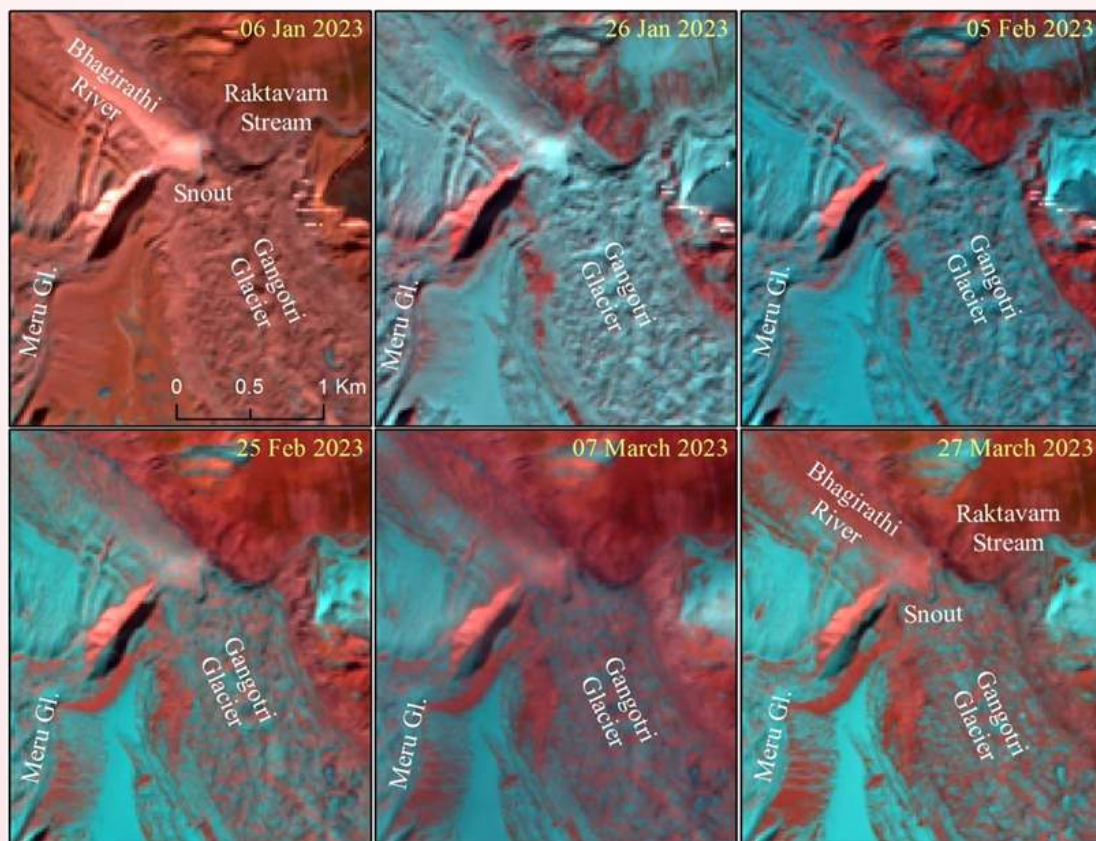


Fig. 81: Satellite images indicating the presence of debris, no damming or lake, and uninterrupted natural flow of Bhagirathi River in the frontal region of Gangotri Glacier from January to March 2023. Moreover, images show the snowfall events around the Gangotri Glacier.

MoES Sponsored Project**Comparative study of weathered/soil profiles developed on Granitic and Basaltic rocks of Higher and Lesser Himalaya in Garhwal region: Implication on climate-tectonic interaction***(Anil Kumar, Pradeep Srivastava, R. Islam)*

In the Indian context, weathering studies are meagre, though a few studies are documented in Peninsular India, almost no work has been done in the Himalayan sector because of the lower preservation potential of weathering profiles owing to their dynamic nature. However, there are several slopes that are relatively stable, and climatic conditions are favourable in developing the in-situ weathering profiles over bedrock. One such slope is identified from the Lesser Himalayan terrains encompassing porphyritic granite rocks and a 6.9 m thick profile were identified at the road cut-face near Lawari village along Tilwara-Ghansali road. The intensity of weathering is evidenced by the high Chemical Index of Alteration (CIA) value (~ 72) in the upper zones of the profile. A-CN-K characterizes the global weathering trend parallel to the A-CN tie line which goes up to the illite zone. With the intensification of weathering, most leachable elements, Ca, Na, and K deplete consistently. U-series isotope analysis-based computed weathering rate is 20 mm/kyr, with the oldest regolith zone having ~ 280 ka weathering age. A nonlinearity is observed in the timescales of development of the weathering profile with zones of intensified weathering during ~ 110 kyr to ~ 100 kyr and ~ 40 kyr to ~ 50 kyr. This increase in weathering rate during particular times can be related to a warm and moist climate favourable to weathering. These are chemically active and leach out of the porous sites of the weathering zones. Also, the weathering products were dated by using U-series isotopes to decipher the in-situ weathering rate. The weathering rate in these terrains ranged between 15 and 50 mm/kyr.

MoES Sponsored Project**Seismic monitoring and seismological parameters evaluation in Garhwal-Kumaun region of Himalaya***(Ajay Paul)*

A seismic network comprised of 7 Broad Band Seismograph (BBS) in Garhwal Himalaya and adjoining Himachal Pradesh region have been used in this project for seismicity monitoring and seismological parameter evaluation. The seismological stations are located at (i) Adibadri, (ii) Tapovan, (iii) Gaurikund (iv)

Chakrata, (v) Dehradun in Garhwal region and (vi) Nahan and (vii) Kotkhai in Himachal Pradesh. Each station is equipped with Trillium-240 broadband seismometer and Centaur digitizers. This seismological network has recorded more than thirty thousand earthquakes during July 2007 – August 2022, out of which 4500 are local events, 9000 are regional events and 17000 are teleseismic events. The epicentral location map indicates that the local earthquakes are occurring in a narrow zone south of the MCT. The magnitude ranges between 1.8 to 5.8, and the majority of events lie within 25 km depth.

Continuous seismic monitoring unveils the dynamicity of the region and helps to reconstruct the scenario of present seismicity and accumulated strain energy. The analysis of more than 4500 well-located local earthquakes are justified within the acceptable error bars (ERZ, $ERH < 5.0$) with hypocentral distances ranging from 0 to 50 km. This region lies in the Central Seismic Gap (CSG), where the accumulated strain energy is sufficient for a future significant rupture. In the recent work, the pattern of earthquake distribution, b-value, fractal analysis (D_c), and stress drop have been described to understand the dynamics and stress condition of the region on a regional and local scale. The influence of stress build-up and subsurface complexity on seismicity in an active continental-continental collisional orogenic belt has been systematically studied. A large set of continuous seismic data were generated and processed. The present findings provide significant insight into the anomalous behaviour of seismic parameters in the CSG regime. The spatial distribution of b-value, magnitude of completeness (M_c), and seismic clusters are mapped separately (Fig. 82). The three different zones show the distribution of Moho depth below the observed seismicity clusters and high elevation difference. The zone B infers a large extent of Moho depth variability with low b-value distribution, which might be accumulating large stresses to generate significant ruptures due to continuous northward convergence of the Indian plate. The behaviour of mid-crustal detachment beneath the Himalayan Seismic Belt (HSB) and the dependence of topographic elevation due to changes in the seismicity pattern have also been illustrated. A significant behaviour and dependence of the b-value, D_c value and stress drop value along the depth, plane and time have been achieved, which depicts the Chamoli region is accumulating considerable stress for the future great earthquake.

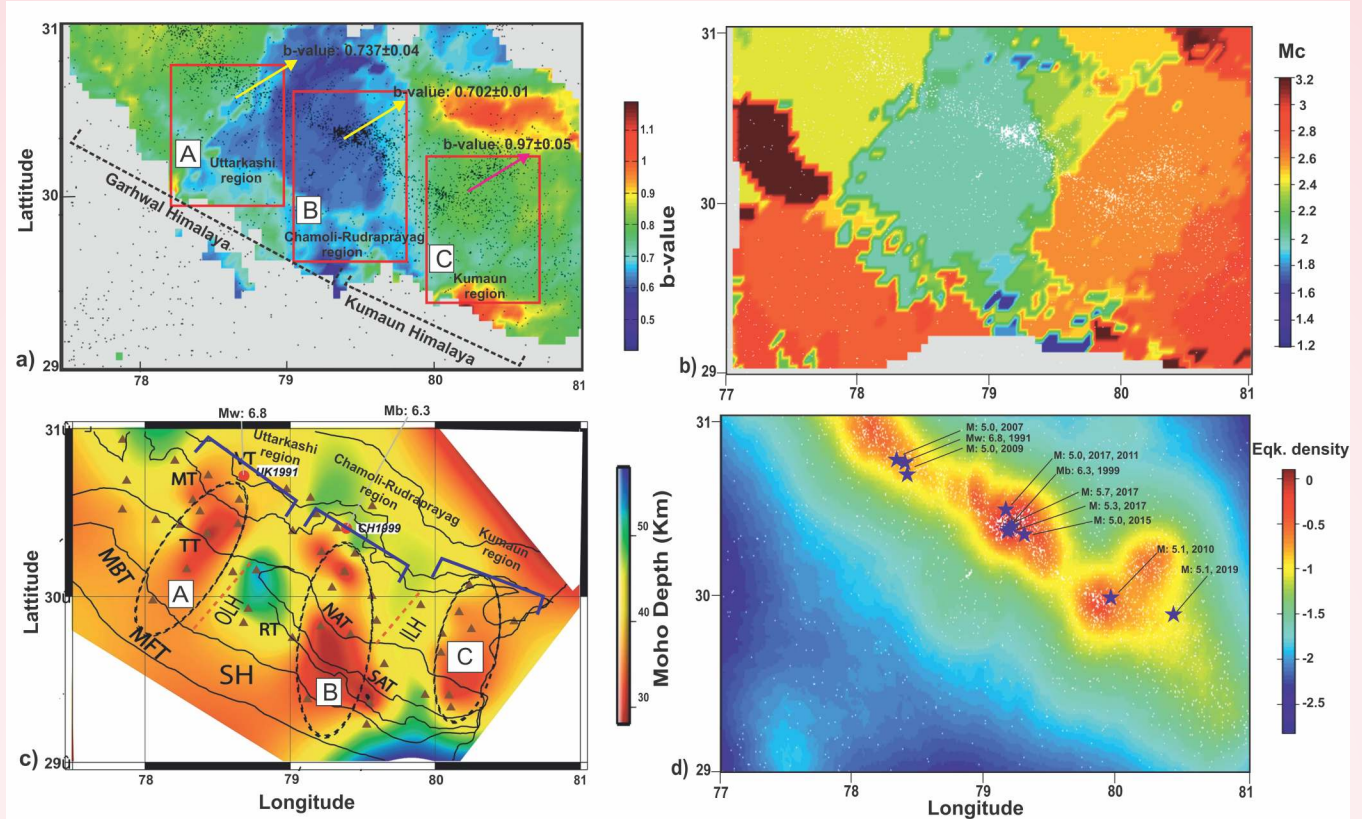


Fig. 82: The estimated results are plotted for (a) mapping of b-value (b) magnitude of completeness (M_c) color plot in the adjoining region of Chamoli. (c) Figure shows the Moho depth distribution (modified after Mandal et al., 2021) and (d) earthquake density with moderate to strong size earthquake locations in the region.

MoES Sponsored Project

Tectono-thermal evolution of the Karakoram migmatites along Shyok and Tangtse Valleys, India: Implications on the tectonics of Karakoram region (Aditya Kharya and H. K. Sachan)

The Karakoram range represents the South Tibetan Crust, or the southern margin of the Asian continent, is located to the north of the Ladakh magmatic arc (LMA). This fault zone extends from Pakistan to the northwest part of India. The southern boundary of the Karakoram range is an active structure. The 800 km long Karakoram Fault Zone (KFZ) is part of a set of faults that accommodate the northward movement of India. In the eastern Karakoram, the KFZ is associated with the migmatites, the large volumes of leucogranite, and amphibolite.

Based on textural relationships, the equilibrium assemblage is interpreted as plagioclase – amphibole(pargasite) – biotite – quartz – titanite – diopside – melt, and plagioclase – amphibole (pargasite) – biotite – quartz – rutile – melt. Amphibole-bearing leucosomes typically have the assemblage Kfs

+ Pl + Qtz + Amp + Ttn + Cpx + Ap ± Bt ± Ms ± Zrn ± Mnz, with hypidiomorphic magmatic textures preserved. The leucosomes are comprised of euhedral to subhedral poikilitic amphibole grains (0.1 to 0.5 mm in length) and biotite, which are aligned along with the regional tectonic fabric. Amphibole grains have biotite, plagioclase, K-feldspar, and quartz inclusions. The amphibole grains display irregular zoning or retain green-brown cores and green rims that have plagioclase inclusions. Small, commonly anhedral, clinopyroxene grains occur with euhedral plagioclase and quartz.

Biotite is dominantly annite (Fig. 83a) with $Mg/(Mg+Fe)$ values ranging between 0.42 and 0.61 apfu. Amphiboles are calcic with CaO values ranging from 10.5 to 12.4 wt% and are consistent with pargasite compositions (see Fig. 83b) according to the IMA 2012 classification (Hawthorne et al., 2012), and cation for amphiboles are calculated following Locock (2014). Plagioclase varies between oligoclase and andesine in composition from Or1.0Ab82.5An16.5 to Or3.6Ab67.8An28.6, and alkali feldspar ranges in composition from Or98.0Ab1.9An0.1 to Or87.7Ab12.3An0.0 (Fig. 83c).

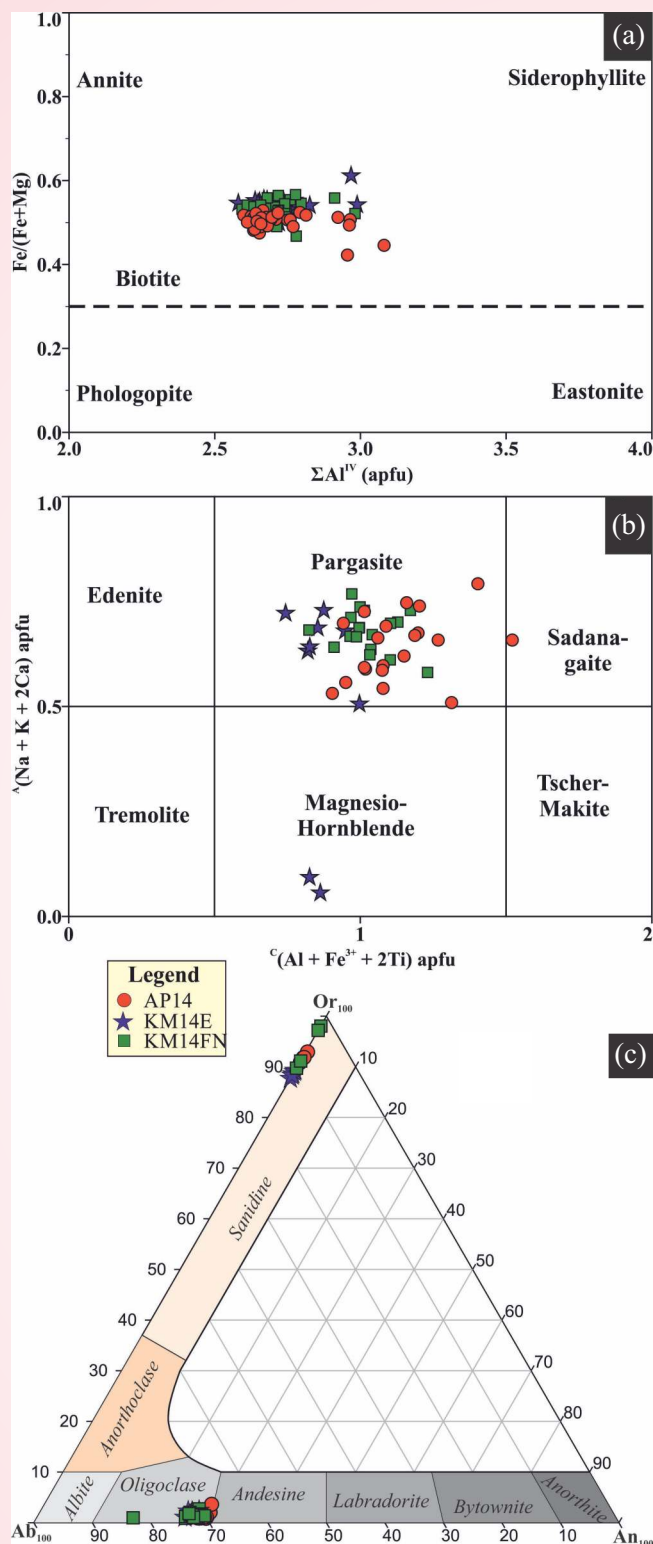
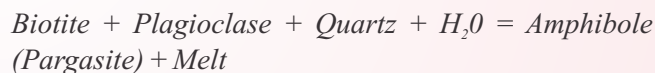


Fig. 83: Chemical classification of minerals (a) Biotite classification diagram after. (b) Amphiboles classification diagram after Hawthorne et al. (2012) (c) The ternary composition diagram for the feldspars group after Wittke (1990) and Deer et al. (2013).

Three samples cover the whole of the migmatite exposed in the Tangse Valley. The bulk compositions for these studied samples were analyzed using XRF (whole rock geochemistry). Further, The XRF and EPMA data were used for the thermodynamic calculation. The pressure and temperature ranges for all pseudo sections are 0.5 to 2.0 GPa and 450°C to 1000°C. Phase equilibria calculations were performed within the 10-component system $\text{K}_2\text{O}-\text{Na}_2\text{O}-\text{CaO}-\text{FeO}-\text{MgO}-\text{Al}_2\text{O}_3-\text{SiO}_2-\text{H}_2\text{O}-\text{TiO}_2-\text{O}_2$. As reasonable approximations for modelling Fe^{3+} in the context of the observed mineral assemblages, O_2 is assumed to be 0.1 weight % (13% Fe_{total}) for sample numbers AP14, KM14E, and 0.01 weight % (22% Fe_{total}) O_2 is assumed for sample number KM14FN because Fe_{total} is nearly an order of magnitude lower than for the other two samples. Compositional isopleths of $^{\text{IV}}\text{Al}$ were calculated for amphibole.

H_2O -fluxed (water-fluxed) melting of rocks is a vital mechanism in the formation of orogenic belts where the growth of crustal-scale shear zones or the underplating of arc-related magmas triggers the permeation of fluid into hot crust. Evidence for the presence of excess water and H_2O -fluxed melting in the migmatites of the study area is the occurrence of poikilitic amphibole megacrysts with quartz inclusions with plagioclase and biotite. The presence of plagioclase, quartz, and biotite inclusions in coarse-grained, poikilitic amphibole is consistent with the following reaction:



Such a hydration reaction has also been suggested for the partial melting of other biotite-plagioclase-quartz-amphibole (peritectic) assemblages Slagstad et al. 2005 Cherneva and Georgieva 2007 Reichardt et al. 2010 Reichardt and Weinberg 2012 Wang et al. 2013.

The pressure-temperature fields represent assemblages that have variances ranging from three to seven (Fig. 84a-c). The modelled compositional isopleths of amphibole ($^{\text{IV}}\text{Al} = 1.5$ to 1.7 apfu) cross the observed equilibrium assemblages at ~ 0.8 to ~ 1.0 GPa and $\sim 640^\circ\text{C}$ to 670°C (Fig. 84). Temperature- H_2O pseudo-sections were calculated in Perple_X at 1.0 GPa for all three samples (Fig. 85) to investigate the amount of water involved in the partial melting process. In constructing such diagrams, calculations were performed within the same chemical systems as for pressure-temperature models; although temperature- H_2O calculations were carried out between 450 and

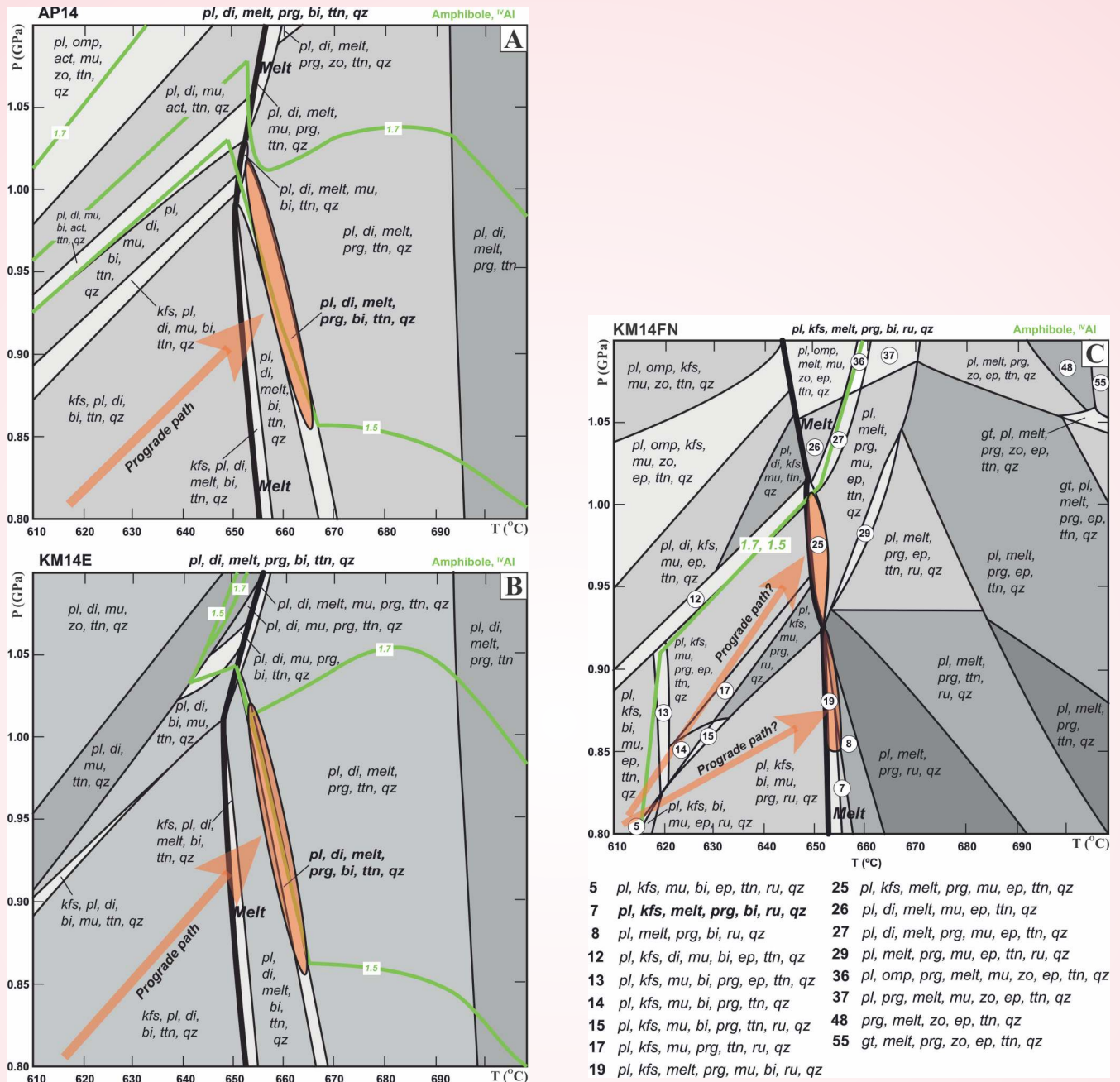


Fig.84: Pressure (GPa)-temperature ($^{\circ}\text{C}$) pseudosections of migmatites for the studied samples. The phase equilibrium fields are shaded with respect to variance, with darker grey corresponding to higher variance. The light green lines are isopleths of ^{10}Al in amphibole, and orange ovals encompass the estimated peak pressure and temperature conditions of migmatization. Melt is present in the equilibrium assemblages on the high-temperature side of the bold lines. The orange arrows trace potential prograde metamorphic paths. (a) pseudosections diagram for sample no AP14, (b) pseudosections diagram for sample no KM14E, and (c) pseudosections diagram for sample KM14FN, having two potential prograde pathways. The various assemblage field is numbered in Fig. C and illustrated as 5 = *pl, kfs, mu, bi, ep, ttn, ru, qz*; 7 = *pl, kfs, melt, prg, bi, ru, qz*; 8 = *pl, melt, prg, bi, ru, qz*; 12 = *pl, kfs, di, mu, bi, ep, ttn, qz*; 13 = *pl, kfs, mu, bi, prg, ep, ttn, qz*; 14 = *pl, kfs, mu, bi, prg, ttn, qz*; 15 = *pl, kfs, mu, bi, prg, ttn, ru, qz*; 17 = *pl, kfs, mu, prg, ttn, ru, qz*; 19 = *pl, kfs, melt, prg, mu, bi, ru, qz*; 25 = *pl, kfs, melt, prg, mu, ep, ttn, qz*; 26 = *pl, di, melt, mu, ep, ttn, qz*; 27 = *pl, di, melt, prg, mu, ep, ttn, qz*; 29 = *pl, melt, prg, mu, ep, ttn, ru, qz*; 36 = *pl, omp, prg, melt, mu, zo, ep, ttn, qz*; 37 = *pl, prg, melt, mu, zo, ep, ttn, qz*; 48 = *prg, melt, zo, ep, ttn, qz*; 55 = *gt, melt, prg, zo, ep, ttn, qz*. The areas outlined by the black boxes are enlarged to the right of each pseudosection in the second column for each sample.

1000°C and 0 to 1.0 wt% H₂O (pure H₂O fluid). Such modelling results indicate that greater than 0.7 wt% H₂O was involved in the migmatization reaction that formed *amphibole (pargasite) + melt* (Fig. 85). This is signified in terms of an increase in the melt volume and lowered the temperature of solidus or melting, which is consistent with the temperature estimates by thermodynamic modelling for the Karakorum migmatites. The results of the present study agree with the earlier studies on the South Tibetan Crust (Karakoram metamorphic terrane) (e.g. Streule et al. 2009; Sachan et al., 2016; Singh et al., 2020), which

suggested an early phase of crustal thickening that was followed by near-isothermal decompression cooling. Isothermal decompression cooling requires that the exhumation of deep-seated rocks should be fast compared to the thermal relaxation rate.

Further, the fluid inclusion study provides several clues related to fluid entrapment (textural evidence concerning pressure-temperature estimates), the composition of syn- or post- migmatization fluids, and activities of fluids during the exhumation processes. This is the first-ever report of a systematic fluid

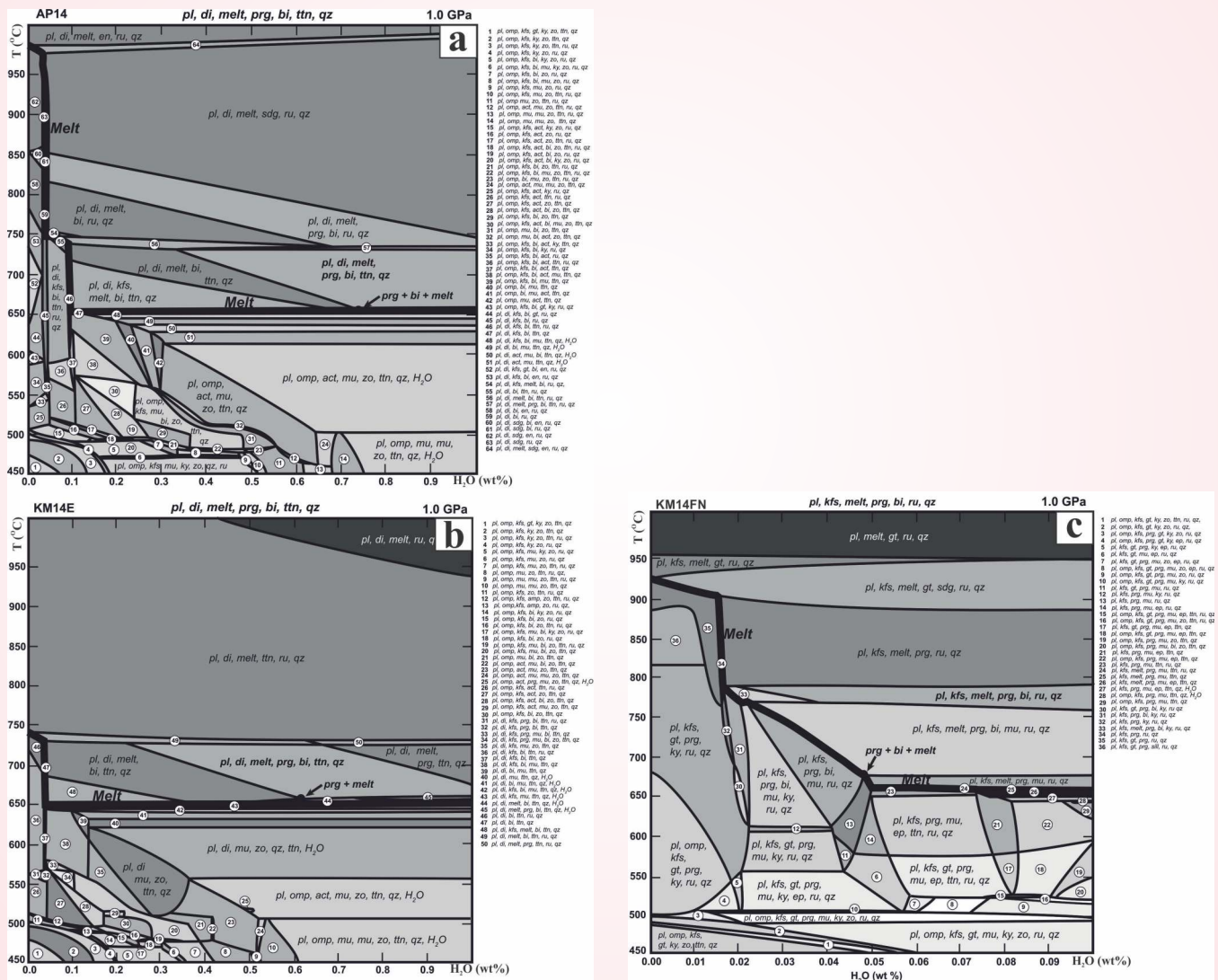


Fig. 85: Temperature(°C)-H₂O pseudosection of the studied samples of migmatites calculated at 1.0 GPa. The phase equilibrium fields are shaded with respect to variance, with darker grey corresponding to higher variance. Melt is part of the equilibrium assemblages to the high-temperature sides of the bold lines. The black circle marks the first appearance of pargasite + biotite + melt with increasing temperature and H₂O concentration. (a) Temperature(°C)-H₂O pseudosection for sample no AP14, (b) Temperature(°C)-H₂O pseudosection for sample no KM14E, and (c) Temperature(°C)-H₂O pseudosection for sample no KM14FN.

inclusion study of migmatites from the Karakorum terrane that integrates data from mineralogical thermodynamic modelling. Special consideration has been given to inclusions that show consonance (textural) within or close to peak- and post-migmatization assemblages. The micro thermometric data of the present study reveal the prevalence of pure CO_2 fluids. The primary carbonic fluid inclusions homogenized in the liquid phase between -17 and -31°C , which translates into a density range of 1.01 to 1.08 g/cm^3 . The secondary carbonic inclusions

homogenized between -1 and -11°C have relatively low-density (0.93 to 0.99 g/cm^3) carbonic fluids trapped at a later stage. The calculated isochores for primary inclusions plot at a higher pressure and temperature than the isochores of secondary inclusions in quartz (Fig. 86). The primary fluid inclusions advocate that fluid was trapped during the host mineral growth. Therefore, they should be formed at High pressure-temperature conditions; however, the calculated isochores for primary mono-phase carbonic (CO_2) inclusions intersect at lower pressure (i.e., 0.59 -

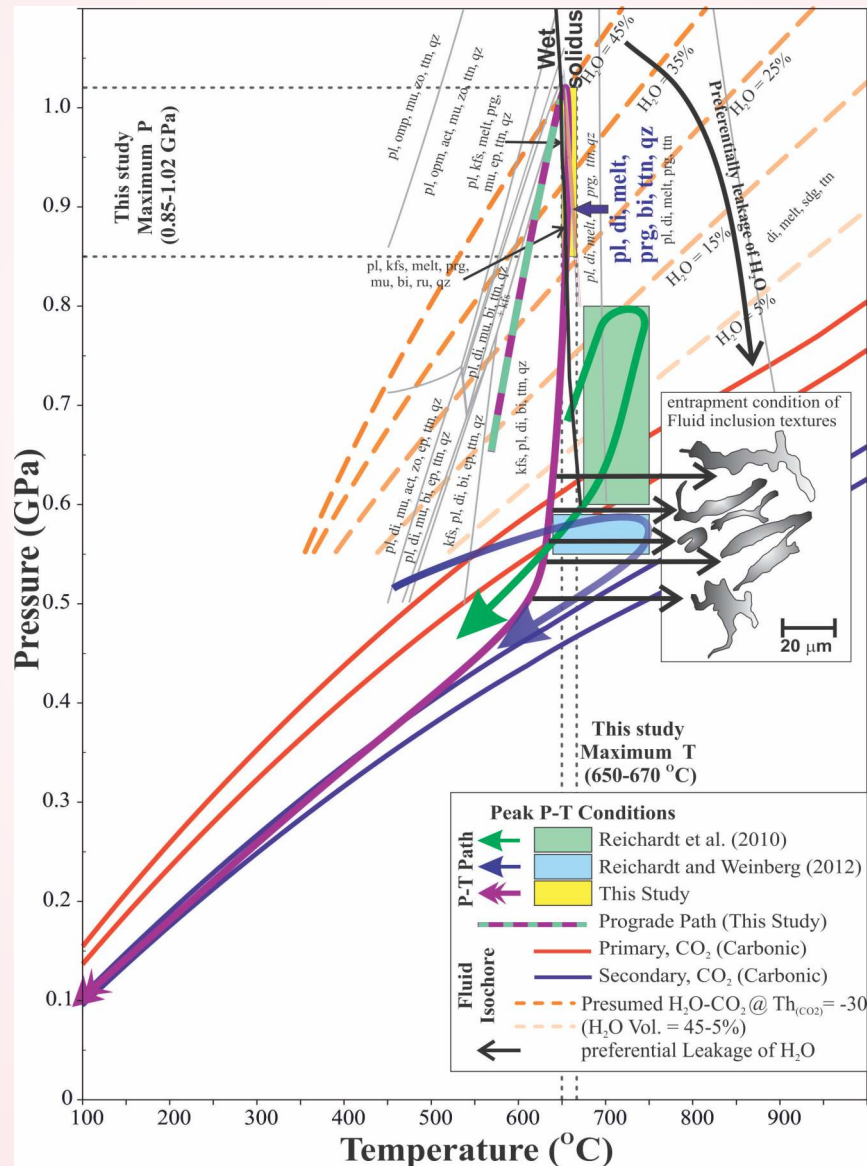


Fig. 86: Fluid-P-T path of Karakorum migmatite constrained from thermodynamic modelling and fluid inclusions study. P-T conditions inferred from phase equilibria modeling (highest P-T, and melt crystallization stages) are shown by the yellow box (for the Present study), whereas the blue box represents the results of Reichardt and Weinberg (2012). Representative isochores of CO_2 inclusions (primary and secondary) are obtained from fluid inclusions micro-thermometry data.

0.55 GPa; 550-670°C) than the peak migmatization conditions. It was presumed that bi-phase primary aqueous-carbonic ($\text{H}_2\text{O}-\text{CO}_2$) inclusions were present in the system initially. However, the H_2O (aqueous) phase was diffused out from the $\text{H}_2\text{O}-\text{CO}_2$ inclusion and mixed with the melts for the migmatization during anatexis. The $\text{H}_2\text{O}-\text{CO}_2$ inclusions isochores drawn (orange dash line, Fig. 86), which goes up to the highest P-T condition (Yellow box, Fig. 86) obtained from thermodynamic modeling. The $\text{H}_2\text{O}-\text{CO}_2$ inclusions isochores (orange dash lines in Fig. 86) show the stepwise diffusion of H_2O (from 45% H_2O to 5% H_2O) from the system and lead to the formation of pure CO_2 inclusions (Fig. 86). The conditions estimated from CO_2 isochore calculations are consistent with pressure-temperature estimates of Reichardt and Weinberg (2012) and may reveal that the fluid was entrapped during the migmatization event. However, the estimated pressure-temperature (i.e., 0.59-0.55 GPa and 550-670 °C) suggested that the primary fluid was re-equilibrated after entrapment (at post-migmatization event) and during the exhumation, as the mechanism suggested by Vityk and Bodnar (1995).

The H_2O from an $\text{H}_2\text{O}-\text{CO}_2$ fluid may be involved in hydration reactions (such as sericitization of plagioclase) during cooling, leaving a residual CO_2 fluid inclusion (Hollister, 1988). However, this was not the case for the studied migmatites because the plagioclase has not been serialized. Henceforth, the H_2O phase from aqueous-carbonic ($\text{H}_2\text{O}-\text{CO}_2$) inclusions most likely went directly into the anatectic melt (orange dash line in Fig. 86).

Exhumation of South Tibtain Crust

The maximum pressure and temperature for migmatization in the Tangtse area range from 0.85 to 1.02 GPa, and 640 to 670°C, with subsequent decompression melting involving fluid-fluxed melting reactions. The decompression melting phenomena is evidenced by the re-equilibrated fluid inclusion microtextures. The H_2O -fluxed melting took place between 15 to 18 Ma, as suggested by the age of leucogranite present in Tangtse Valley (Reichardt et al., 2010). These workers suggested that the Karakorum Shear Zone was developed when a sudden influx of free fluid stimulated H_2O -fluxed melting and the formation of amphibole-bearing migmatite. It can be further interpreted that during the exhumation process, H_2O present in carbonic inclusions escaped into the melt at the last stages of crystallization to form hydrous

minerals, whereas CO_2 remained in the residue. The South Tibetan Crust has exhumed along the Karakorum Fault Zone between 10 and 9 Ma at pressure-temperature conditions of 0.22 GPa and 350°C (Mukherjee et al., 2012).

SERB Sponsored Project

Fluid-P-T evolution of ultramafic-mafic rocks from Spong tang ophiolite, Ladakh, India: Implications for geodynamics of Himalayan mountain chain (Aditya Kharya and H.K. Sachan)

The calcite microstructure of exotic blocks shows thin to tabular thick to an oval twinning pattern due to dynamic recrystallization as a function of temperature from 170 to 300 °C (Burkhard, 1993; Ferrill et al., 2004; Passchier and Trouw 2005). The average values of stable (carbon and oxygen) isotopes of the exotic blocks are $3.2 \pm 1.1\text{‰}$ VPDB and $21.7 \pm 2.8\text{‰}$ VSMOW, respectively (Fig. 87). The carbon and oxygen isotopic ratio is plotted with the previous study carried out by Sen et al. (2013) isotopic data and finds a similar isotopic ratio with the same trend (Fig. 87). The stable carbon and oxygen isotope values lie between the marine and the mantle field (Fig. 87). This indicates that the exotic blocks are of marine origin and may be contaminated by the magmatic fluid either in the source region or fractionated during the metamorphism of the exotic blocks. The obtained isotopic values of the exotic block were compared with the following end members 1) veins of the zildat area (Kharya et al., 2021); 2) ophiocarbonates isotopic values of Nidar Ophiolites given by (Das et al., 2020); 3) Mantle carbonates; 4) Marine carbonates. The stable isotopic values of exotic blocks were more enriched than the ophiocarbonates, Zildat veins as well as mantle carbonates, and slightly depleted from the marine carbonates. This suggests the marine origin of the exotic blocks and ruled out the mantle. The isotopic ratio of exotic blocks was depleted from the marine carbonates (Fig. 87) possibly due to the magmatic fluid derived from the associated magmatic rocks in the mélange zone during the metamorphism. Previous workers (Reuber et al., 1987; Corfield et al., 1999; Sen et al., 2013) advocate that the exotic blocks of ZOM are of limestone and Permian in the age of marine origin. The presence of marble grain reported by Sen et al. (2013) and evidence of low greenschist metamorphism of the exotic block can not be ruled out. The oxygen isotope values of these exotic blocks were slightly fractionated due to changes in temperature during the metamorphism, whereas no significant fractionation was observed in the carbon isotope values. This observation ruled out the contamination or mixing

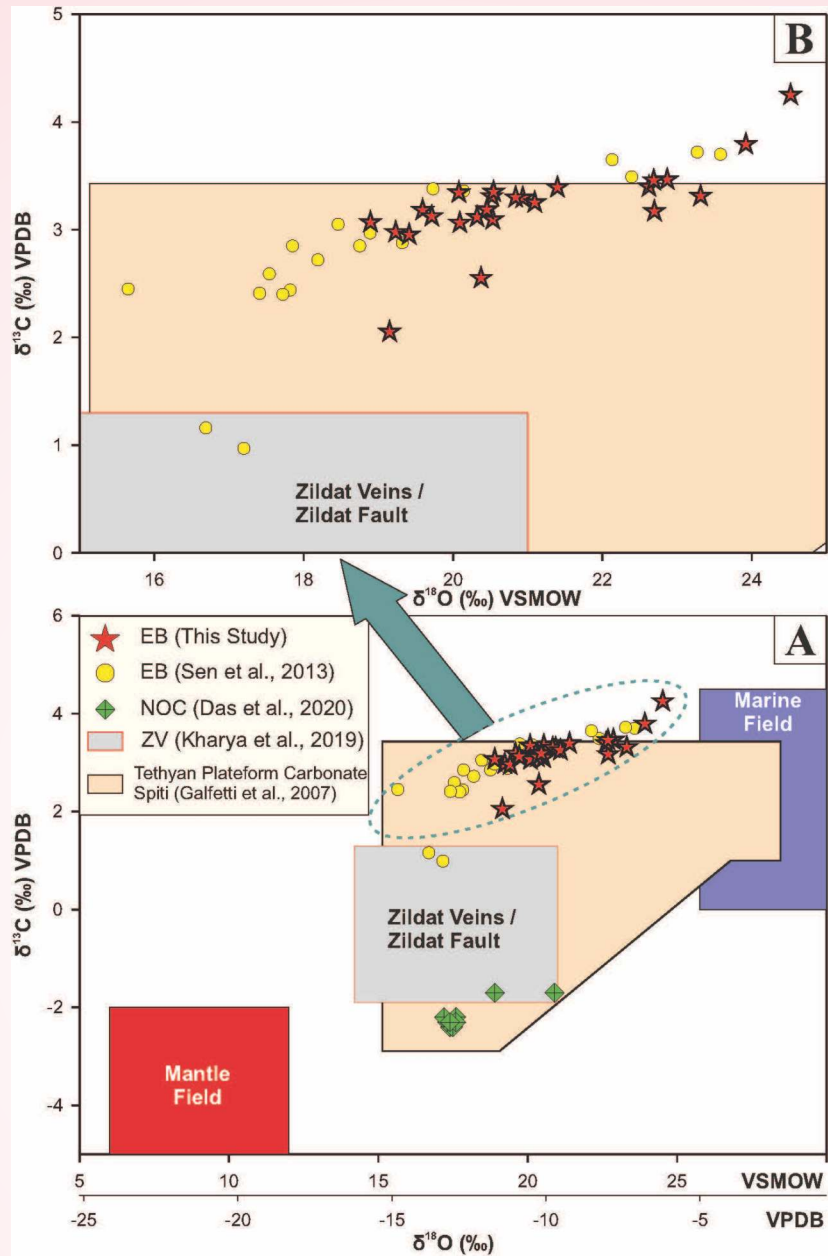


Fig. 87: Bi-variant plot of $\delta^{13}\text{C}$ vs. $\delta^{18}\text{O}$ values of the exotic block. (A) Bi-variant plot showing the data set along with various end members. (B) Distribution of stable ($\delta^{13}\text{C}$ vs. $\delta^{18}\text{O}$) isotope values for the study area. The end members are denoted as: EB = Exotic Block; NOC = Nidar Ophiolitic Complex; ZV = Zildat Veins; VPDB = Vienna Pee Dee Belemnite; VSMOW = Vienna Standard Mean Oceanic Water.

of external fluid in the exotic blocks. The carbon isotope indicates the marine/Platform origin of the exotic block, and fractionation in oxygen isotope values advocates the low grade of metamorphism in the exotic block. The source of exotic blocks was re-examined by the stable isotopic values of Tethys carbonate (Galfetti et al., 2007), along with our data set from this study. Our dataset ($\delta^{13}\text{C}$: 2.1 to 4.3 VPDB; $\delta^{18}\text{O}$: 18.9 to 24.5 VSMOW) lies within the limit of the Tethys carbonates field defined by Galfetti et al. (2007). This further points

out that the exotic block of ZOM is marine or derived from platform Tethys carbonate. The carbon and oxygen isotope results of the present study are plotted along with the Sen et al. (2013) stable isotope data between NOC and TMC in figure 88, which is contradictory to the Sen et al. (2013) observation. The stable isotope ratio from NOC to TMC is not showing any depleted trend. Therefore, it can not be concluded that stable isotopic ratios were depleted by increasing the deformation and shearing, as suggested by Sen et al.

(2013). The carbon and oxygen isotopic ratio was slightly modified, possibly due to the lower greenschist facies metamorphism near the NOC. The fluid isotopic ratio was also calculated using the empirical equations given by O'Neil et al. (1969), Ohmoto (1979), and Bottinga (1968) to re-validate the source of fluid from the fluid inclusion results. The carbon and oxygen isotope values of CO_2 fluid lie in the field of platform/marine carbonate (see Fig. 88). Furthermore, the oxygen isotope ratio of fluid water also lies in the Platform/ marine carbonate field, which suggests that the exotic block originated from the platform carbonate from the Tethys Ocean.

The above-discussed observations ruled out the contribution of magmatic fluid in the exotic block. The last but not least possibility is of the platform carbonate origin. The isotopic values of the exotic blocks compared with the platform carbonates data of the Tethyan Himalaya from Spiti Valley, Zaskar region, point out that the exotic blocks originated from the

Tethyan Himalaya pinched at the eastern margin of the Lamayuru formation or Shergol conglomerate.

Three types of fluid inclusions were identified during the petrographic observation of the study area: the first type (Group-I) of mono-phase vapor/gas inclusions (V) (Fig. 89), the second type (Group-II) of bi-phase inclusions, which are liquid rich with gas/vapor (LV) (Fig. 89), and the third type (Group-III) of multiphase or three-phase solid inclusions. All these features are observed during the petrography and defined by the presence of salt + liquid + gas/vapor (SLV) in an inclusion (Fig. 89).

The Group-I, and II inclusion isochores have given in figure 90 drawn on the basis of the maximum and minimum density of the fluid. The intersection points or overlap area of the Group-I and Group-II inclusions isochore define a P-T region for entrapment of fluids (Fig. 90). The isochore of carbonic (Group-Ia) and aqueous-carbonic (Group-IIa) fluid were intersected

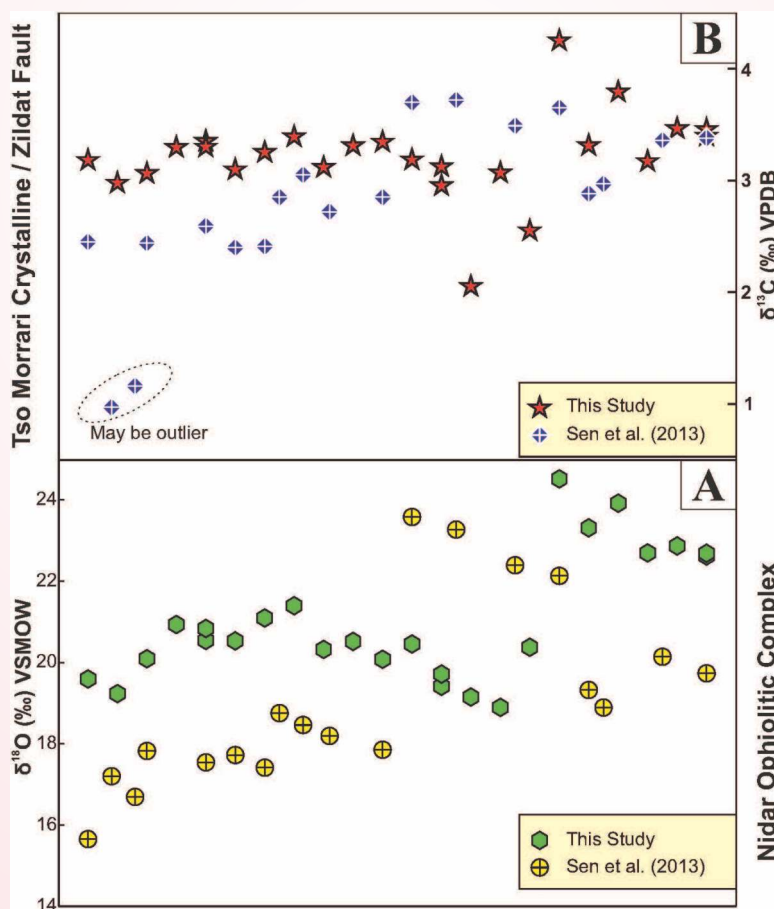


Fig. 88: The Distribution of stable isotope values between Tso Moriri crystalline and Nidar Ophiolitic Complex for this study along with Sen et al., (2013) dataset. (A) Distribution of oxygen ($\delta^{18}\text{O}$) isotope values (B) Distribution of carbon ($\delta^{13}\text{C}$) isotope values.

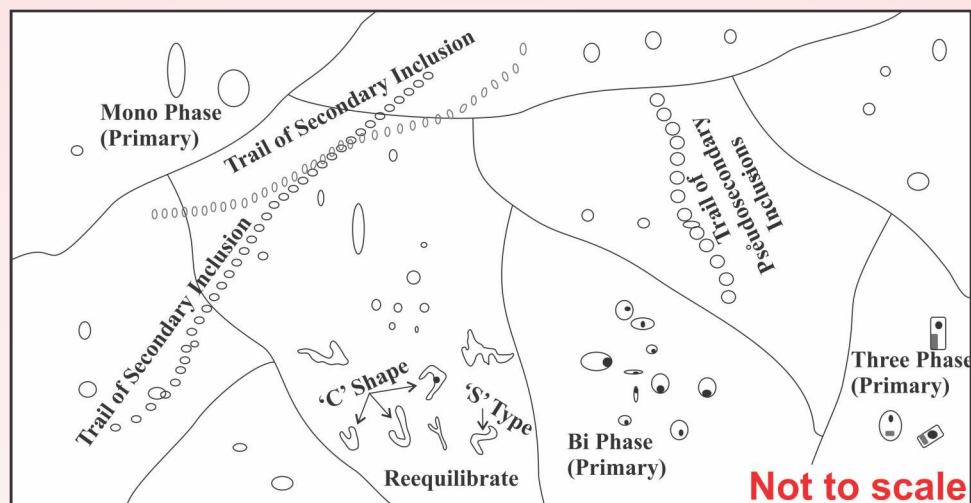


Fig. 89: Schematic diagram of various types of fluid observed.

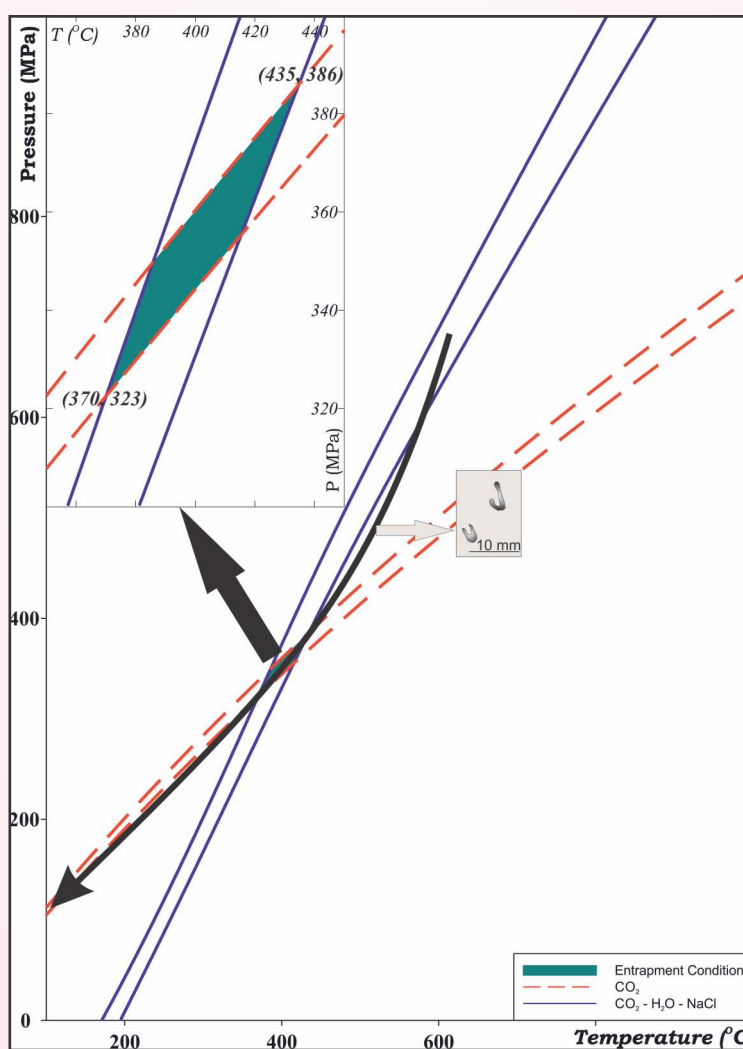


Fig. 90: P-T diagram showing isochores of primary carbonic (CO_2) Monophase (Group-Ia) and aqueous-carbonic ($\text{H}_2\text{O}-\text{CO}_2-\text{NaCl}$) Biphasic (Group-IIa) inclusions. The intersection of carbonic and aqueous-carbonic isochore defines the entrapment conditions for the primary fluids. The number above the isochore shows the density of various isochores.

between 435 °C, 386 MPa, and 370 °C, 323 MPa, and define the entrapment condition for the limestone block. The P–T path for the entrapment defines the isochoric cooling (ICC) (Fig. 90). The data of the present study reveal gradual upliftment of the limestone block from the ocean floor at about 13 km below the surface during Permian time.

The salinity of the aqueous phase ranges between 20.37 and 11.22 wt % NaCl, which suggests the high saline water involved in the formation of the exotic block of carbonate, which is the typical salinity of marine water during the Permian Time (Lowenstein et al., 2005). Therefore, it indicates that the exotic blocks developed in the marine condition possible in the Tethys Ocean and solubility trapping CO₂ through dissolution in the formation water/Tethys Ocean water. The occurrence of three-phase (Group-III) inclusions also advocates the high saline (>28.9 wt % NaCl) marine fluid source of the exotic block. However, CO₂ plays an important role in the formation of carbonates. The CO₂ gas in limestones/ carbonates is trapped due to the dissolution and eventual reprecipitation of calcium carbonate minerals (Vialle et al., 2014). Alternatively, the untreated liquid CO₂ was trapped in the crystal lattices of the carbonate block along with water. The aqueous-carbonic (CO₂ with marine water: H₂O–CO₂–NaCl) fluid might be trapped in the exotic blocks (Golomb, 2003). Pure CO₂ in inclusions might be formed due to partial leakage during the metamorphism or dissolution and eventual reprecipitation of calcium carbonate minerals. The entrapment condition reveals that the CO₂ was trapped in the exotic block at about 13 Km depth.

The stable isotope results of the exotic block carbonates from this study and Sen et al. (2013) data advocate the platform, type origin of the exotic blocks. The isotopic data of the Zildat exotic block is akin to the Tethyan platform carbonate field, as shown by Galfetti et al. (2007), and advocates the Tethys oceanic water source of the exotic block. Furthermore, the $\delta^{13}\text{C}_{\text{CO}_2}$ and $\delta^{18}\text{O}_{\text{CO}_2}$ values of CO₂ in fluid inclusions as well as $\delta^{18}\text{O}_{\text{water}}$ value of the aqueous phase in fluid inclusions advocate the platform origin of the exotic blocks.

These exotics are tectonic units bounded by shear surfaces. Schardt (1898) and Masson (1976) proposed that these tectonic units came from “a distant land” and were “transported en bloc by thrusting.” (Masson 1976). The exotic blocks are observed in mélange by various workers (Hsü, 1968; Raymond, 1975; Cloos & Shreve 1988) globally and were defined as “tectonic

inclusions detached from some stratigraphic units foreign to the main body of the mélange. The exotic Permian limestone blocks, like Permian limestone successions in the Himalayan region, were initially deposited in the near-Gondwana environment on the northern Greater India margin (Li & Shen, 2005).

The $\delta^{13}\text{C}$ values of the exotics in ISZ ranged between 2.1 and 4.3 ‰ VPDB (with an average of 3.2 ± 1.1 ‰ VPDB). This carbon isotopic composition was adjacent to that of the global seawater of the Permian Time (Veizer et al. 1999). The fluid inclusion preserved in the exotic blocks indicates that they were formed at a depth of 13 Km. It suggests that the exotic carbonates are of deep marine water in origin. The enriched stable $\delta^{13}\text{C}$ ratio of exotic blocks indicates a good population of marine invertebrates with calcareous shells and their fast and continuous organic carbon during this period. These carbonates originate from deeper marine conditions and further deposited as a platform in the Zaskar shelf. The exotic block of limestone in the Zildat ophiolitic mélange may be emplaced by extensional faulting and break-up of the platform edge of the Zaskar platform. Such a phenomenon was also observed for the exotic blocks present in western Ladakh (Robertson and Degnan 1993).

UCOST sponsored project

Black carbon personal exposure levels in different polluted micro-environments: A case study from Himalayan foothills

(Chhavi Pandey)

Light-absorbing carbonaceous aerosols (LACs), Black carbon (BC), and Brown carbon (BrC) are majorly produced by incomplete combustion and are predominantly found in the lower troposphere. This work mainly focuses on measuring the eBCs concentration in Dehradun city and its environmental impacts by using portable MicroAeth 350 (MA-350), which is a specialized device designed to measure eBC concentration in the atmosphere and works on 5 different wavelengths, i.e. 880 nm, 625 nm, 528 nm, 470 nm, 375 nm. Mainly, the measurement at 880 nm is interpreted as a concentration of BC because it has a low interference from other types of aerosols. This study is done in five routes, but only two routes are followed majorly figure 91(a,b). In all these five routes approximately 35 hours of sampling have been done, and the overall mean eBC concentration is found to be $18.34 \pm 2.80 \mu\text{g}/\text{m}^3$. The highest and the lowest mean eBC concentrations observed are $30.75 \pm 24.06 \mu\text{g}/\text{m}^3$ and $8.18 \pm 3.39 \mu\text{g}/\text{m}^3$, respectively (Fig. 91c). This level

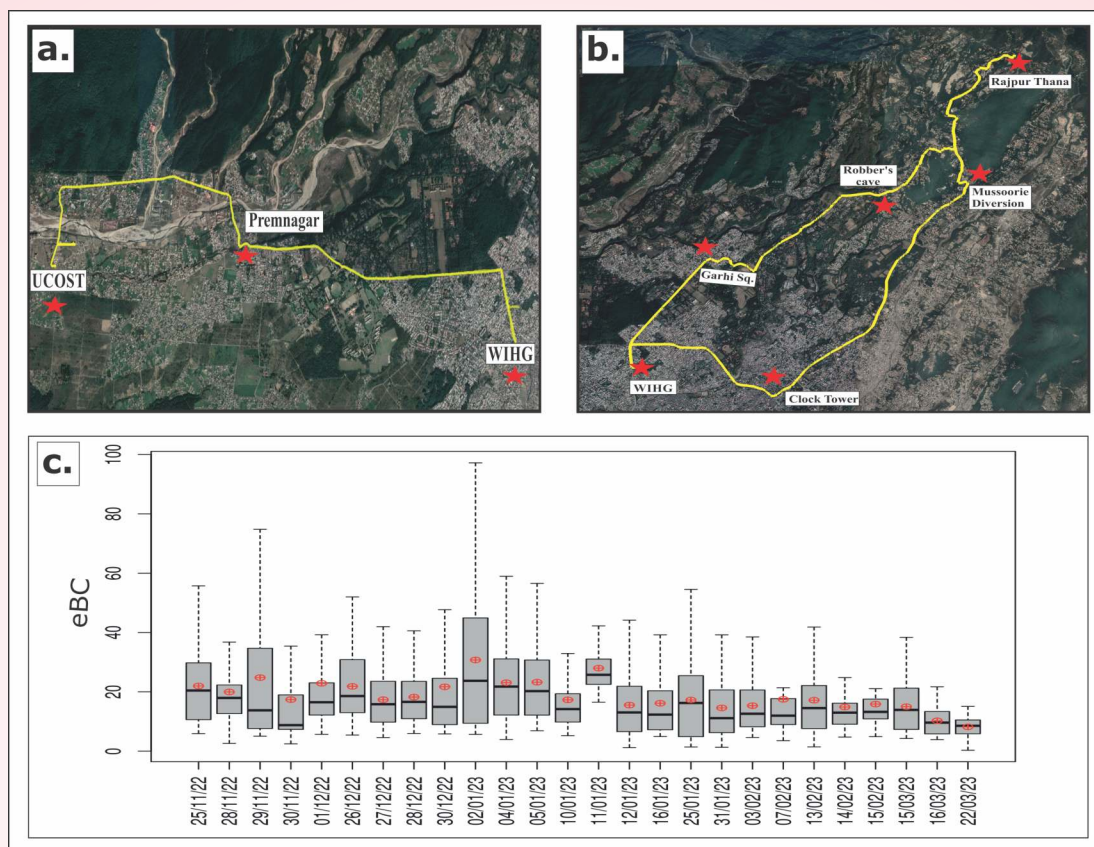


Fig. 91: (a), (b) Mobile monitoring route in Dun Valley; (c) eBC concentration measured at different routes.

of eBC can cause adverse impacts on health as well as the environment such as the melting of glaciers, absorbing and emitting radiations, reduction in albedo (ability to reflect sunlight), etc.

SERB sponsored project **Post-LGM precipitation and temperature variability in western Himalaya** (Som Dutt and Anil Kumar)

Precipitation in Himalayan regions through Indian monsoon and mid-latitude westerlies affect the socio-economic growth of billions of population in South Asia. A slight deviation in intensity and timing of precipitation can cause huge losses of human and animal lives, ecology, agriculture, and economy in and around the region through widespread droughts and floods. It is necessary to prepare high-resolution palaeoclimatic records with absolute records of climate variables from the Himalayan regions to understand the effects of natural forcing and foresee climate change probability in the future. The project is aimed at understanding climate variability in the western Himalayas using multiple-proxies analysis of lake sediments from Himachal Pradesh. The project has been started on 02 March 2023.

MoES Sponsored Project **Tectono-thermal evolution of the Lohit Batholith along Dibang and Lohit Valleys, India using Fission Track and (U-Th)/He Thermochronology** (Vikas Adlakha and Koushik Sen)

The AFT (21 samples) and ZFT (15 samples) analyses have been carried out for the exposed litho-units along the Lohit Valley regions of Arunachal Pradesh using thermal neutron irradiation. Similar investigations have also been carried out in Dibang Valley where a total of 20 samples for AFT analysis and 18 samples for ZFT have been irradiated. A few samples of AHe (9 samples) and Zhe (5 samples) have been sent to an overseas laboratory (Melbourne Thermochronology Lab) for (U-Th)/He analysis to constrain the shallow crustal exhumation history of the litho-units of the Dibang Valley region. In addition, AMS analysis of 20 oriented samples from Lohit Valley have been carried out.

New thermochronological data from Lohit Valley suggest a rapid phase of exhumation as a result of the latest phase of out-of-sequence thrusting along the Walong Thrust zone in this region. This latest phase of rapid exhumation is in good correlation with the morphometry of the Lohit Valley region that suggests

higher values of slope, relief, and normalized index of the eastern LPC than the frontal Lesser Himalayan Sequence. This linkage of exhumation and morphometry results suggest that the present-day topography of the Lohit Valley was established at the latest by Pliocene-Quaternary. It is important to note here that, the rapid exhumation in the eastern Lohit Plutonic Complex lies in a low-precipitation zone that suggests tectonics is a prime driver of exhumation in this region.

MoES sponsored project

Evaluating the condition of deformation during subduction and exhumation of the North Indian continental margin: A study based on structural and crystallographic features of the Tso Morari dome of trans-Himalaya, Ladakh, India

(Koushik Sen and A.K. Singh)

Tso Morari Crystalline Complex (TMCC), located in trans-Himalaya (eastern Ladakh, India), comprises

ultrahigh-pressure eclogites. These rocks experienced deep burial (>80 km) and rapid exhumation during continental subduction, collision, and accretion of the Indian and Eurasian plates. The Electron Probe Micro analyzer (EPMA), Raman spectroscopy, P-T-X Pseudosection modelling, and Electron Backscatter Diffraction (EBSD) is used to study the metamorphic history, the deformation mechanisms and strain regimes corresponding to the peak (HP) metamorphism and post-peak rapid exhumation of the TMCC. A strong linear fabric (L tectonite) is noted in the least retrogressed eclogite. The omphacite [001] axes are parallel to lineation, whereas the (110) poles are perpendicular. These characteristics indicate constrictional strain during peak (HP) metamorphism. Other eclogites exhibit a transitional plano-linear fabric (LS tectonite). The results of the present study suggest that constrictional strain dominated during peak (HP) metamorphism in the TMCC, driven by the buoyant rise of the rocks due to slab break-off and reverse slab pull during and after deep continental subduction (Fig. 92).

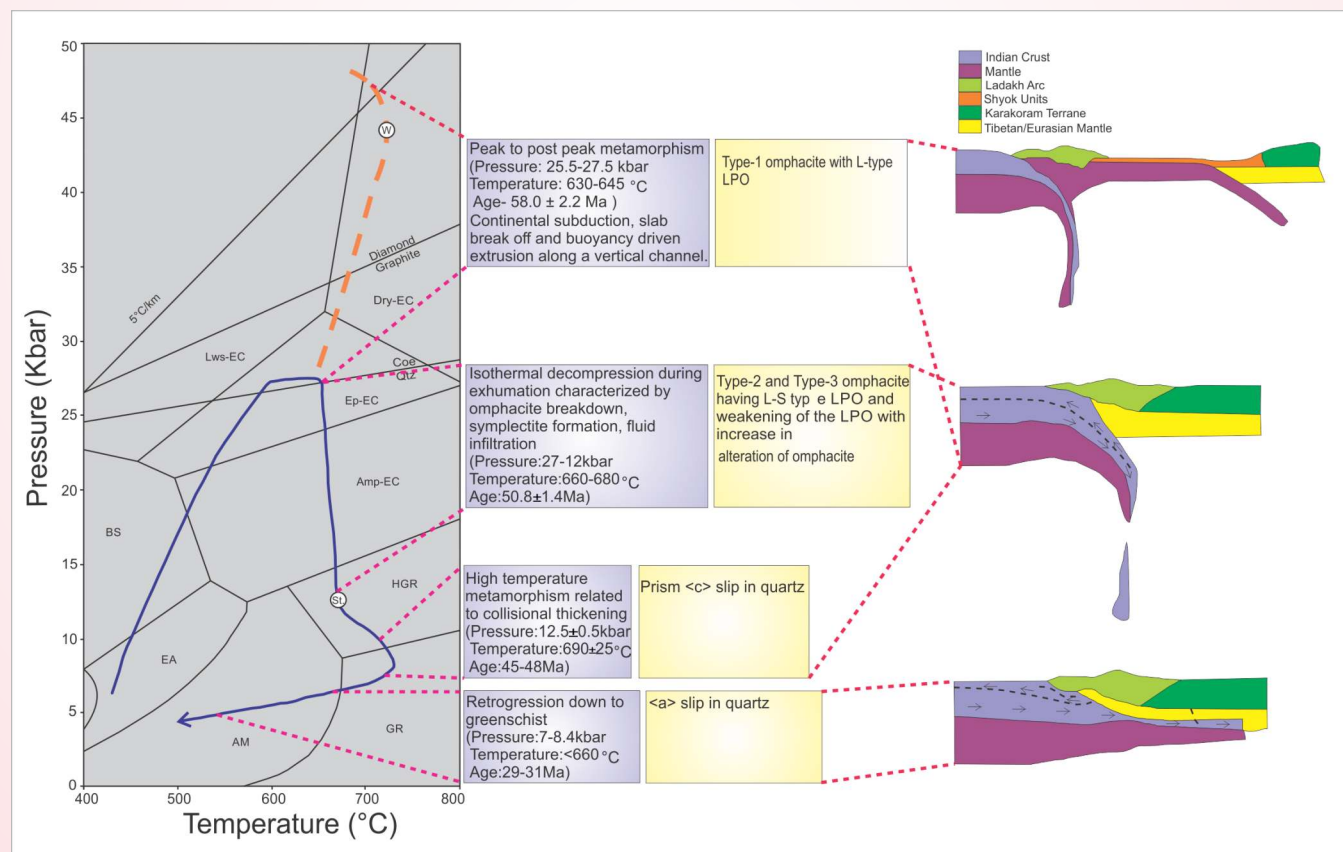


Fig. 92: Diagram showing integrated P-T-t path of the TMCC eclogite (after St. Onge et al., 2013, and Wilke et al., 2015) and development of different types of LPOs in omphacite and quartz. Cartoon showing tectonic evolution of the Indo-Eurasian collision zone in terms of continental subduction, slab break-off, exhumation and collisional thickening also shown. Ages of different metamorphic stages are taken from St. Onge et al., 2013; Guillot et al., 1997, 2008, and de Sigoyer et al., 2004.

This present study suggests peak metamorphism at $\sim 2.75 \pm 0.1$ GPa and $\sim 550 \pm 50^\circ\text{C}$, followed by a decompression stage at $\sim 1.50 \pm 0.1$ GPa and $\sim 580 \pm 50^\circ\text{C}$ and subsequent high-temperature overprint at $\sim 0.85 \pm 0.1$ GPa and $\sim 680 \pm 50^\circ\text{C}$. Diopside+plagioclase symplectite represents post-peak decompression and fluid infiltration. The presence of carbonates as veins, within fractures, and in the matrix suggests late-stage fluid infiltration and metasomatism. The mineral chemistry data of this study and metamorphic modelling resemble a continental eclogite and not an oceanic eclogite.

MoES Sponsored

Multi-Parametric Geophysical Observatory, Ghuttu Garhwal Himalaya for Earthquake Precursory research

(Naresh Kumar, Gautam Rawat, Devajit Hazarika and P.K.R. Gautam)

The Multi-Parametric Geophysical Observatory (MPGO) located at a remote site, Ghuttu of Garhwal Himalaya is situated within the Himalayan seismicity belt (Fig. 93). The observatory has been acquiring continuous geophysical/geochemical/meteorological data useful for earthquake precursory research since the last 15 years. Continuous records of different time series representing temporal changes are useful to denote very

small surface and sub-surface variations in the India-Eurasia collision zone. These changes are compared and assessed with the nearby earthquake activity of low and higher magnitudes. In this observatory, the measurements involve changes in seismic wave velocity, surface deformation through GPS, gravity, resistivity, magnetic field intensity, electromagnetic, and radon gas emission, along with fluctuations in hydrological parameters. In addition, meteorological parameters, i.e. rainfall, atmospheric pressure, atmospheric temperature, in situ temperatures at different depths in a borehole, and water table fluctuations, are recorded continuously. All parameters are sampled at high-resolution intervals of 15 minutes or less. A 68-m deep borehole of diameter 20 cm was drilled penetrating the water table in rock composed of gneisses and schistose to record the near-surface data at some depths. The observatory is also equipped with a Broadband seismograph and a digital accelerograph to evaluate the size of the seismic event and the distance from the observatory.

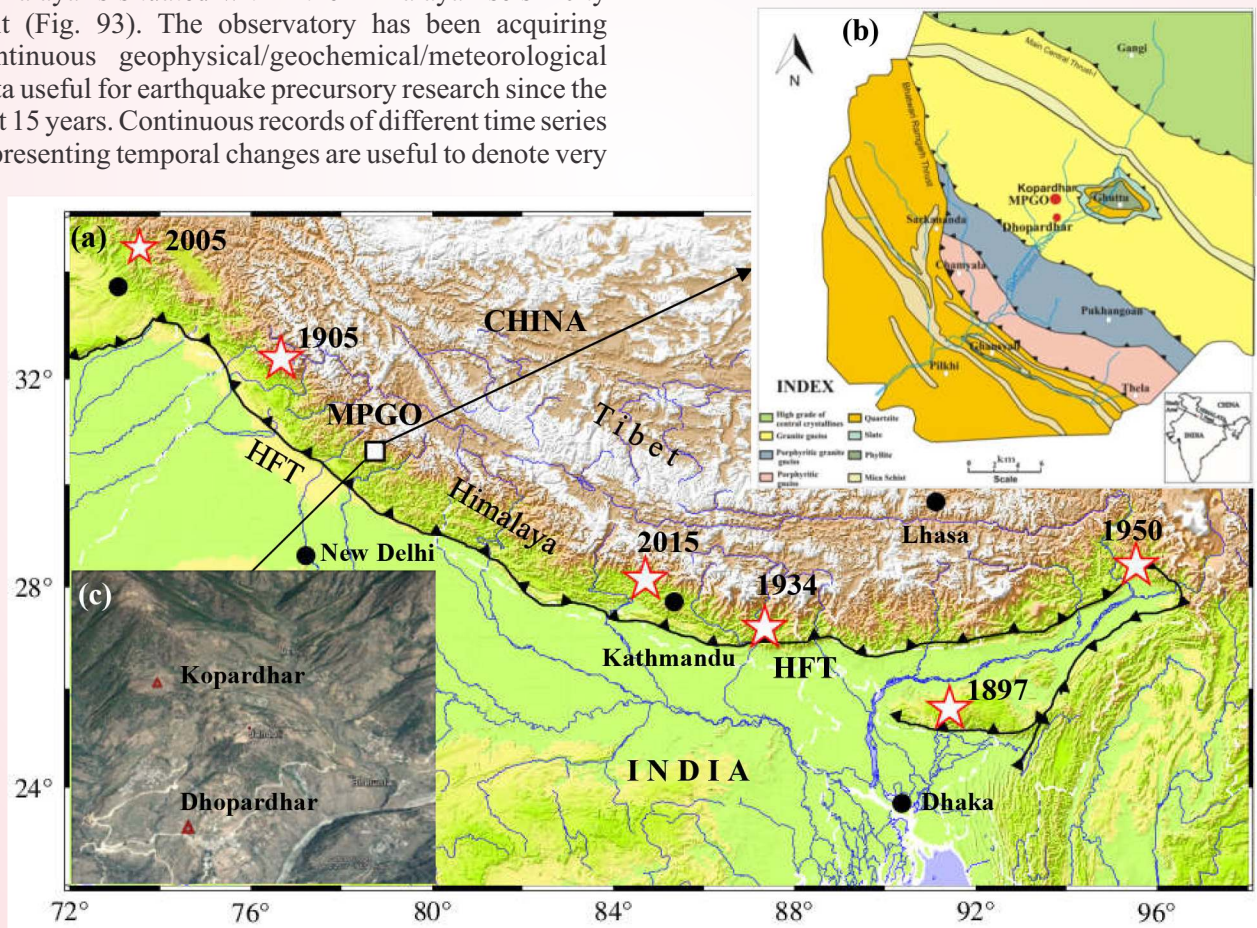


Fig. 93: a) The MPGO, Ghuttu (white rectangle), is situated in the Garhwal Himalaya. The locations of large magnitude earthquakes ($M \geq 7.6$) recorded over the last 150 years is marked using stars. b) Geotectonic setup of the study region, c) Kopardhar and Dharpardhar sites of MPGO are shown on Google Earth map.

Seismic activity in the vicinity of MPGO Ghuttu

Himalaya is seismically a highly active zone with more concentration of earthquake epicenters in the Himalayan Seismic Belt (HSB) located around the surface trace of the MCT covering Lesser and Higher Himalaya regions. The crustal-scale seismicity is concentrated at a depth range of ~10-25 km depth. During 2022-2023, till June 2023, nearly 30 earthquakes of magnitude more than 2.5 occurred within 300 km distance around the MPGO, Ghuttu (Fig. 94). Earthquakes are focused in the upper crust, mostly close to the Main Himalayan Thrust. The data of different parameters are processed and analyzed during these moderate and higher magnitude earthquakes surrounding ~300 km distance from the observatory. The magnitude and epicentre distance are the two important parameters to assess the earthquake precursory signatures in different time series. The seismic index parameter has been used, which is an effective factor of earthquake size and its distance from the recording location to evaluate the earthquake precursors.

Imprint of Diurnal and Semidiurnal Cyclicality in Radon Time Series

Radon-222 is considered an important earthquake precursor because it is a noble gas and for its radioactive decay characteristics. Its half-life is 3.92 days to be propagated at some distances, and more concentrated are observed near the tectonic faults. However, radon anomalies are controlled not only by seismic activity but also by environmental and other related natural phenomena such as atmospheric pressure, atmospheric temperature, and Earth tides. These effects must be assessed and eliminated from the radon signal to enhance its capability as an earthquake precursor. To identify these effects and their modes of variability in radon progeny time series, the singular spectrum analysis (SSA) has been applied to process a 6-month period of data acquired from a 10 m deep borehole. The site also has a superconducting gravimeter for acquiring continuous gravity suitable to detect tidal waves with high accuracy. The results show clear evidence of diurnal and semidiurnal daily periodicities, along with slight signatures of the M2-O1 waves in the radon time

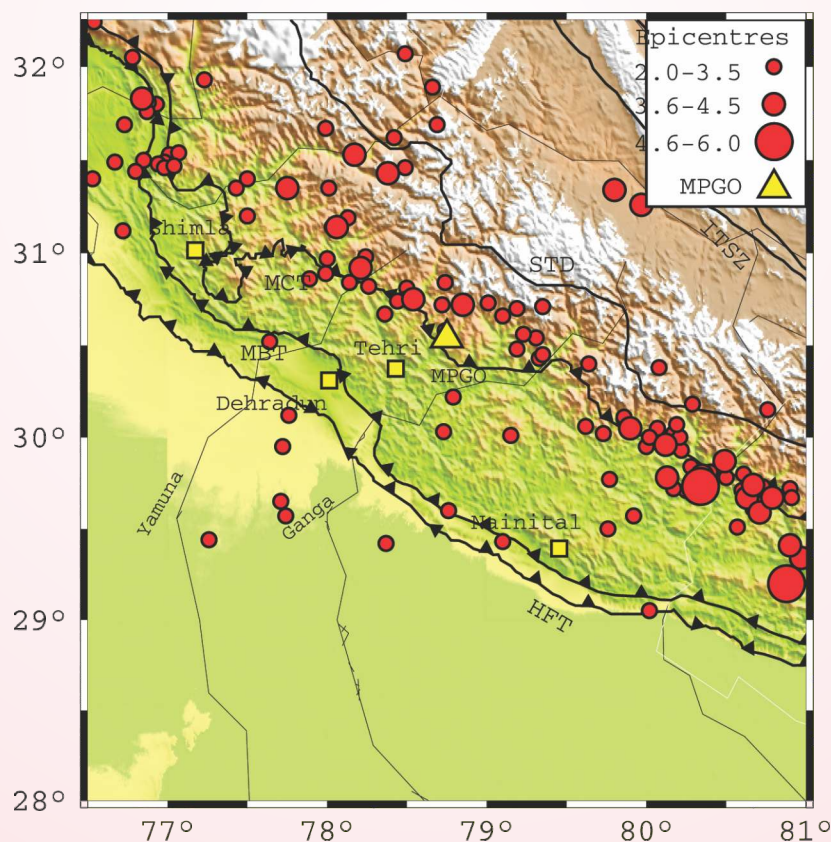


Fig. 94: Recent seismicity (2022-2023) around the MPGO Ghuttu observatory based on the WIHG and National Centre for Seismology (NCS), data. Abbreviations: HFT – Himalayan Frontal Thrust; MBT – main Boundary Thrust; MCT – Main Central Thrust; STD – South Tibetan Detachment

signal. Results show that even at 10 m depth, these effects play a part in controlling radon release from the soil (Fig. 95).

The main motive of the present study is to find the imprint of Earth tides in radon data. The radon data have a set pattern mainly dominated by diurnal (O1 and S1)

and semidiurnal (M2 and S2) variations during the non-monsoon season. Therefore, the time series for a single time period has been studied, considering that the time series for other time periods will reveal similar information related to Earth tides. Radon and all the meteorological data were acquired every 15 min and stored in a Campbell (10X) data logger. A 2 x 2.548 cm

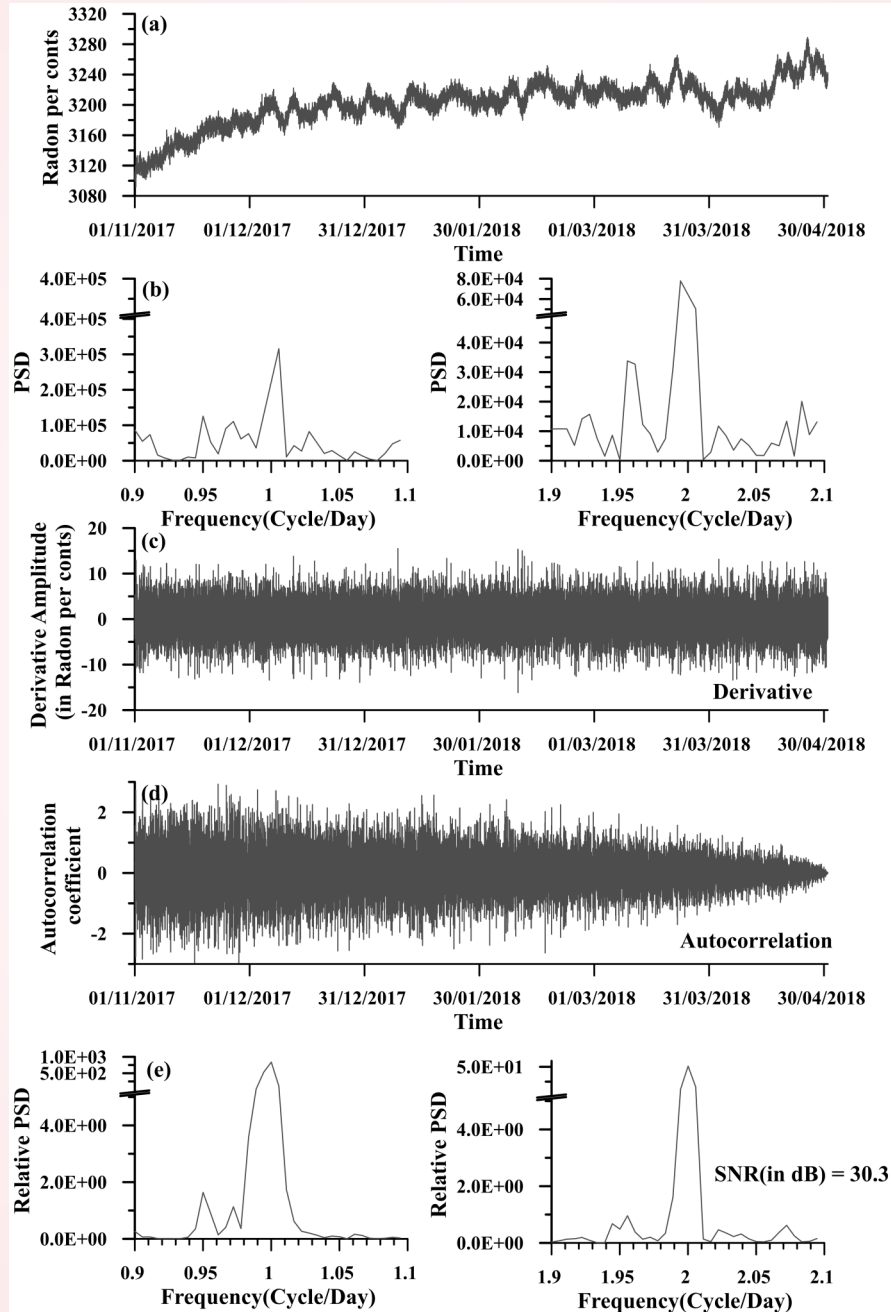


Fig. 95: Denoising method (Richon et al., 2012). a) Radon progeny time series, b) power spectrum by normal FFT on the raw data; insets are part of the spectrum showing 0.9–1.1 cycles/day and 1.9–2.1 cycles/day frequencies. c) Removal of the long-term variations and large anomalies from the radon data, d) application of the autocorrelation function, and e) Fast Fourier transform applied on the autocorrelation function and obtained FFT spectrum; insets are the part of the spectrum showing 0.9–1.1 cycles/day and 1.9–2.1 cycles/day frequencies.

diameter and 2 x 2.548 cm thick NaI scintillation detector (PM-11, Rotem Industries, Israel) with a gamma-ray radon monitoring probe (PM-11) was used to monitor the variation in radon concentration. The PM-11 probe detects radon concentrations between 0.3 and 106 Bq/m³. The accuracy of the measurement is 1 count/h, which is 0.003 Bq/m³. The primary objective is to find Earth tide signals O1 and M2, which show periodicity of 25.819 h and 12.421 h (Richon et al., 2012) respectively. This data set also includes seasonal and annual variations, and therefore it is required to remove long-term periodicities. A Butterworth filter was applied to clean the data for any variations that were longer than 30 days.

The superconducting gravimeter (SG) is a highly accurate gravity measurement instrument used to calculate solid Earth tides. A dual-sphere gravimeter records temporal variation of gravity at an interval of one sample per second installed at Kopadhar of MPMGO, Ghuttu. Continuous data over three years are used to establish the solid Earth tides using the ANALYZE program of ETERNA 3.3 software. The data are first resampled to 1-min intervals to remove the high-frequency vibration induced by local moderate-size and large-magnitude global earthquakes. The highly sensitive SG can measure gravity variation to the sub- μGal level ($1 \mu\text{Gal} = 10^{-9} \text{ m/s}^2 = 10 \text{ nm/s}^2$).

The radon progeny time series recorded at MPMGO Ghuttu has been analyzed by means of the singular spectrum analysis (SSA) to investigate the presence of diurnal, semidiurnal and tidal components (Fig. 95). After SSA, these periodicities related to the atmospheric and tidal effects can be seen on reconstructed components of radon progeny time series. The diurnal and semidiurnal components of the series related to atmospheric temperature and atmospheric pressure have comparatively stronger signals. Once these and other periodic components are identified and extracted from the radon signal, the residual may be related to the occurrence of an earthquake. However, a thorough study is needed, as the present study is basic and leaves the scope to a further detailed investigation.

Assessment of Thoron exhalation from the soil samples of Ghuttu region

This study is conducted to assess the level of Thoron exhalation in the tectonically active Ghuttu window of Garhwal Himalaya from the Radiation health hazard perspective. Thoron, an isotope of radon, emits highly energetic alpha particles, and the high-level exposure of its daughter products is responsible for lung cancer. The study focuses on Thoron transportation via its

emanation and exhalation process. It is useful to analyze the emanation and exhalation rates of the soil for the specific characteristics of radon isotopes and their health hazard. The analysis is based on soil samples collected from different locations of the Ghuttu Window and its vicinity from Tehri Garhwal, Uttarakhand. The results clearly show that the Thoron surface exhalation rate varies from 1040.4 ± 112 to $4077.2 \pm 222 \text{ mBq/m}^2/\text{s}$ with an average of $2701.53 \pm 862.15 \text{ mBq/m}^2/\text{s}$. The Thoron emanation rate ranges from 90.05 to 476.93 mBq/kg/s with a 2 average value of 277.21 mBq/kg/s (Sajwan *et al.*, 2023). A strong positive correlation between the emanation and exhalation rate of Thoron exists. However, some values are quite high in the active tectonic zones, but dose exposure due to Thoron is found below health risk.

Thoron Emanation and Exhalation rate

The Smart Rn-Duo instrument used for Thoron estimation is based on detecting alpha particles emitted from Radon and Thoron. It utilizes a ZnS:Ag based on Lucas scintillation cell for continuous measurement. The measurement cycle for the instrument is 15/30/60 min based on grab or continuous monitoring. The sampling locations were identified based on geological and tectonic inputs and samples were collected from different soil profiles with variations in lithology.

Thoron variability in the study region

The high Thoron surface exhalation and emanation rate in the Ghuttu region is attributed to the rich Thorium content in the soil samples. However, its variation depends on the different geological formations and tectonic features. Data from 28 sites indicate variation in the exhalation rate, which may be attributed to geotectonic features, seismotectonic and crustal deformations (Fig. 96). There is a high average value of exhalation and emanation outside the window (Pokhar Unit), in which some locations are close to the active tectonic units. Higher surface exhalation locations T19 and T23 are close to the thrust tectonics, while the high exhalation rate in T22 is due to low soil density. The constituent minerals of the Pokhar unit are quartz, feldspar, biotite, muscovite, and chlorite. The value of dose exposure due to Thoron obtained from the study area is within the safe range recommended by ICRP 2011 (3 - 10 mSv/y). Also, the dose rate is under the recommended level by WHO 2009 (10 mSv/y). So far, the present radiation dose due to Thoron has no significant health risk in the study area. However, if there is any additional amount due to some manmade

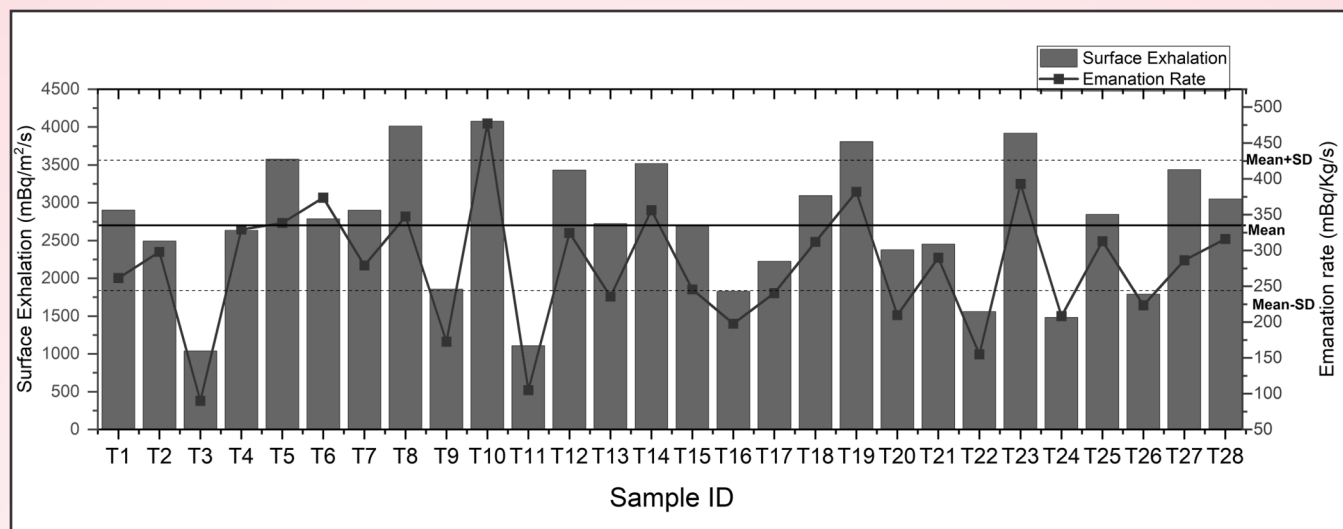


Fig. 96: Variation of Thoron surface exhalation and emanation rate of each location of Ghuttu region.

activities, it may cross the limit, and therefore there should be proper planning.

Earth normal mode studies and gravity noise analysis using Superconducting Gravimeter

A study on gravity variation is conducted using the Superconducting Gravimeter (SG) located at Ghuttu. The ambient noise is estimated and compared with other worldwide SGs. The instrumental noise in the form of parasitic mode has been observed at frequencies ranging from ~ 0.0239 to ~ 0.03207 Hz for the lower and upper sensors of the dual-mode SG station. The quality factor has been estimated in different modes of oscillations. The detection of seismic normal modes in periods shorter than one hour is based on the spectra associated with the six great earthquakes, including the Honshu Japan M9.1 (2011). OSG-051 and trillium 240 Broad Band Seismometer data are analyzed and compared in the seismic normal mode frequency band. Several observations have been made regarding noise sources that affect the gravity data in the seismic normal mode's frequency band. The gravity data corrected for local and regional atmospheric, tidal, and seismic effects have a very good response of long period seismometer than any conventional seismometer. This characteristic and low noise level of the MPOG site makes it a suitable station for long-period seismometer studies.

The working principle of the SG instrument is like an inverted spring-mass system. A small superconducting spherical mass (Niobium metal) of diameter 2.54 cm and ~ 5 grams weight levitates in the magnetic field of a loop current in a superconducting coil. A small change in the gravity field, even to the sub-

microGal level causes a shift in the position of the spherical mass of SG. This shift is denoted in the form of a temporal change in gravity (Arora *et al.*, 2008).

The seismic noise level study at Ghuttu stations is shown in figure 97. The results from our analysis of the seismic noise at Ghuttu station are compared to figure 93 of Rosat *et al.* (2003b). This SG site has a low noise level from ~ -155 to ~ -181 dB in the frequency range 0.0001 to 0.008 Hz, relative to $1 \text{ (m/s}^2\text{)}^2\text{/Hz}$. The low noise level in the gravest mode frequency range (from 3×10^{-4} to 10^{-3} Hz) lies between ~ -162 to ~ -170 dB. While the frequency range between 0.00005 to 0.0003 Hz, the noise level is higher than other SGs and lies between -150 to -162 dB. Compared to other SGs the noise level in the frequency range 0.001 to 0.008 Hz lies in the lower to intermediate range from ~ -176 to ~ -182 dB (relative to $1 \text{ (m/s}^2\text{)}^2\text{/Hz}$). The signal noise magnitude (SNM) values are calculated in the period range 200 to 600 s and 340 to 600 s for the OSG-051 as defined by Banka (1997). The SNM values have been computed for both ranges and compared the results with the worldwide SGs, and it is found in the intermediate range (Fig. 97). The noise level at Ghuttu indicates relatively low compared with other SGs at different worldwide locations. Its noise level is close to SG Strasbourg and ET Metsahovi, which is better than SG Esashi Japan and very well compared to SG Wuhan China. The comparison of noise level with OSGs has been shown in figure 97(b), which lies in the intermediate range for the frequency range 0.001 to 0.003 Hz, compared to another worldwide study (Rosat and Hinderer 2011).

An earthquake of magnitude greater than 6.5 Ms

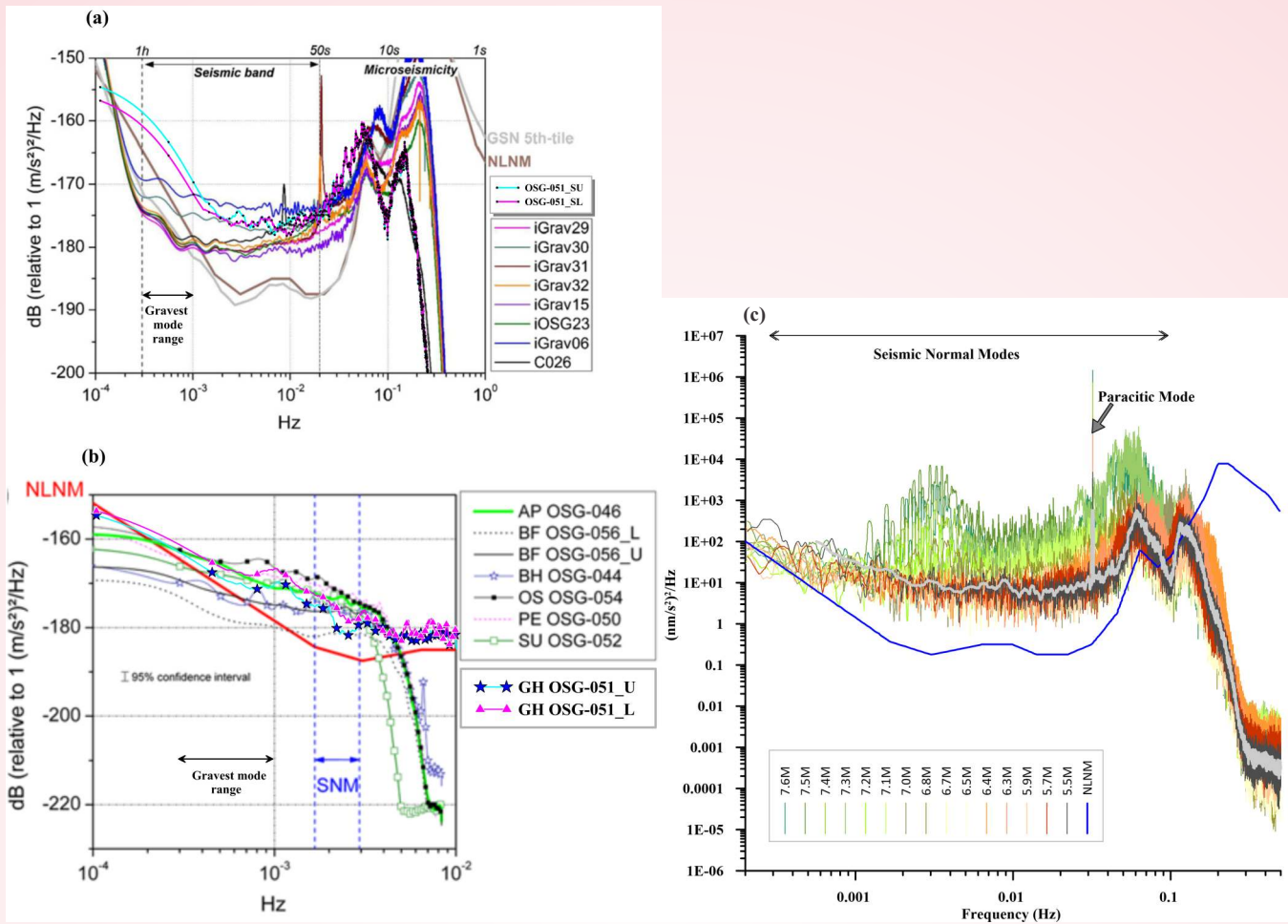


Fig. 97: (a) Fifth percentile of PSD noise levels computed on 1-s sampling data of the eight GWR Superconducting Gravimeters were recorded at the J9 Gravimetric Observatory of Strasbourg (France). The cyan and magenta color noise spectra are projected from the OSG-051 SG, MPGO, Ghuttu (India). The thick brown line represents the new low noise model (NLNM) of Peterson (1993). (b) Noise levels in the seismic band of the OSG-051 (with upper and lower sensor) along with other Observatory SGs. The thick line represents NLNM. (c) The PSD of selected earthquakes of a one-day window after the two hours of the occurrence. The black line shows the weighted average line of the quietest day noise. The blue color line shows *Peterson's new low-noise model (NLNM)*.

can generate the free earth oscillations and, therefore adds additional vibrations in the seismic free oscillations (SFO) frequency band. A data set of the fifteen earthquakes recorded on the SG of Ghuttu is used to compute and compare the amplitude of seismic modes from magnitudes 5.5 to 7.6 Mw worldwide. It has been reported that a large magnitude ($M_s > 6.5$) adds additional vibration in the frequency range of SFO in the SG data (Fig. 97c). Total ten earthquakes of magnitude range 6.8 to 8.1 and the power spectrum of 1 to 20 mHz have been selected.

Noise analysis of gravity records collected with SGs are useful for studying seismic free oscillations (SFO) and other applications. Continuous gravity observations of the five quietest days of the tectonically

active site of MPGO Ghuttu are used to measure noise at different frequency ranges. The amplitude of the low-noise level is ~ 153 to ~ 175 dB (relative to 1 (m/s²)²/Hz) in the seismic band range for both sensors. It is found that the noise level at this site (Ghuttu) is above by an intermediate level as compared to other worldwide SG sites (Fig. 97a). Compared to the iGrav SGs sites for the gravest mode frequency range, this SG site has a relatively high noise level. Compared to worldwide OSGs, the noise level is relatively high. The main point is that no frequency of parasitic mode lies in the normal mode range, while in other SGs, it is reported close to or within the normal mode frequency band of SFOs. It can be mentioned here that superconducting gravimeters can serve as excellent long-period seismographs in the

SFO frequency band. The frequencies of the fundamental spheroidal mode is estimated to range from ${}_0S_6$ to ${}_0S_{32}$.

SERB sponsored project

Development of an enhanced landslide detection model from remote sensing imagery through deep learning.

(Naveen Chandra)

The project aims toward the development of a deep

learning-based landslide detection model from remote sensing images. Initially, the data is collected from the open source platforms. Further, the performance of single-staged deep learning models is evaluated for landslide information extraction through qualitative and quantitative approaches. The status of the project is ongoing since January 2023.

RESEARCH PUBLICATIONS

Papers Published

1. Ahmad, T., Bhat, I.M., Tanaka, T., Bickle, M., Asahara, Y., Chapman, H. & Sachan, H.K. 2022: Tso Moriri Eclogites, Eastern Ladakh: Isotopic and Elemental Constraints on Their Protolith, Genesis, and Tectonic Setting. *Journal of Geology*, 130, 3, 231-252.
2. Ali, S.N., Singh, P., Arora, P., Bisht, P. & Morthekai, P. 2022: Luminescence dating of late pleistocene glacial and glacio-fluvial sediments in the Central Himalaya, India. *Quaternary Science Reviews*, 284, 107464.
3. Baiswar, A., Yadav, J.S., Sain, K., Bhambri, R., Pandey, A. & Tiwari, S.K. 2023: Emission of greenhouse gases due to anthropogenic activities: an environmental assessment from paddy rice fields. *Environmental Science and Pollution Research*, 30(13), 37039-37054. <https://doi.org/10.1007/s11356-022-24838-0>.
4. Bandyopadhyay, S., Sinha, S., Kumar, A., Srivastava, P. & Jana, N.C. 2023: Late Holocene river dynamics and sedimentation in the Lower Ganga plains, India. *Geological Journal*, 58, 1564-1586.
5. Bhambri, R., Kenneth, H., Umesh, K., Haritashya, P.C., Kumar, A., Verma, A., Tiwari, S.K. & Rai, S.K. 2022: Characteristics of surge-type tributary glaciers, Karakoram. *Geomorphology*, 403, 108161.
6. Bhambri, R., Sain, K., Chand, P., Srivastava, D., Tiwari, S.K. & Yadav, J.S. 2023: Frontal Changes of Gangotri Glacier, Garhwal Himalaya, between 1935 and 2022. *Journal of the Geological Society of India*, 99(2), 169-172. <https://doi.org/10.1007/s12594-023-2283-3>.
7. Bhan, U., Boruah, A., Maurya, D.S., Rai, S.K., Goswami, L. & Singh, V.K. 2022: Mineralogy, Organic Richness and Macerated Microbial Studies of the Rohtasgarh Shales in the Vindhyan Basin, India: Implications for Gas Generation Potential. *Journal of the Geological Society of India*, 98, 4, 567-575.
8. Bisht, M.P.S., Bisht, H., Luirei, K., Mehta, M. & Kumar, V. 2022: Kuwari Lake: Potentially Dangerous for Landslide Lake Outburst Flood (LLOF), *Journal Geological Society of India*, 98, 1728-1730.
9. Biswal, S., Lokho, K., Needham, A., Bhandari, A., Shukla, U.K., Whiso, K. & Prakash, K. 2022: Record of additional middle Eocene vertebrate remains from the Mikir Hills, NE India: implications on paleoenvironment and palaeobiogeography. *International Journal of Geosciences*, 13, 609-626.
10. Biswas, M. & Sain K. 2022: Mechanism of Fault Terminations: Theory and Field Examples. *Journal of the Geological Society of India*, 98, 11, 1519-1530.
11. Bose, S., Adlakha, V. & Pundir, S. 2022: Submagmatic flow to solid-state ductile deformation of the Karakoram Batholith, India: insights into syn-tectonic cooling and exhumation. *International Journal of Earth Sciences* 111, 2337-2352. DOI: <https://doi.org/10.1007/s00531-022-02236-8>.
12. Černánský, A., Singh, N.P., Patnaik, R., Sharma, K.M., Tiwari, R.P., Sehgal, R.K., Singh, N.A. & Choudhary, D. 2022: The Miocene fossil lizards from Kutch (Gujarat), India: a rare window to the past diversity of this subcontinent. *Journal of Paleontology*, 96(1), 213-223, <https://doi.org/10.1017/jpa.2021.85>
13. Chakraborty, P.P., Sharma, R., Das, K., Sharma, A. & Saha, S. 2023: U-Pb zircon geochronology of volcanoclastics and encasing sandstones from the Chhoti Khatu section: Bearing on the Neoproterozoic Marwar Supergroup stratigraphy and its global implications. *Geosystems and Geoenvironment*, 2(1), 100111.
14. Chandra, N. & Vaidya, H. 2022: Building detection methods from remotely sensed images. *Current Science*, 122, 11, 1252-1267.
15. Chandra, N., Sawant, S. & Vaidya, H. 2023: An Efficient U-Net Model for Improved Landslide Detection from Satellite Images. *PFG-Journal of Photogrammetry, Remote Sensing and Geoinformation Science*, 91, 13-28.
16. Chanu, N., Kumar, N., Kumar, A., Mukhopadhyay, S., & V. G. Babu 2022: Along-strike variation in the shear wave crustal structure

- of the NE Himalayan and Indo-Burmese arc: Evidence based on surface wave dispersion analysis. *Geological Journal*, 57(12), 5161-5175, <https://doi.org/10.1002/gj.4465>.
17. Chauhan, P., Akmer, M.E., Sain, K. & Kumar, A. 2022. Forecasting of suspended sediment concentration in the Pindari-Kafni glacier valley in Central Himalayan region considering the impact of precipitation: using soft computing approach. *Arabian Journal of Geosciences*, 15(8), 683. <https://doi.org/10.1007/s12517-022-09773-1>
 18. Chauhan, P., Malviya, D., Sain, K., Ray, R.L., Singh, S.K. & Singh, D. 2022. Assessing the vulnerability of watersheds to environmental degradation in the Lesser Himalayan region using satellite data and a series of models. *Geocarto International*, 37 (27), 18372-18399. <https://doi.org/10.1080/10106049.2022.2142958>.
 19. Chauhan, P., Sain, K., Mehta, M. & Singh, S.K. 2022: An Investigation of Cloudburst-triggered Landslides and Flash Floods in Arakot Region of Uttarkashi District, Uttarakhand. *Journal Geological Society of India*, 98, 1685-1690.
 20. Chauhan, R., Kothiyari, G.C., Bhakuni, S.S., Pant, P.D. & Taloor, A.K. 2022: Magnetic fabric and geomorphic characteristic of Neotectonic activity along strike direction of North Almora Thrust, Kumaun Lesser Himalaya, India. *Geodesy and Geodynamics*, 13, 3, 261-274.
 21. Chen, L., Merey, S., Pecher, I., Okajima, J., Komiya, A., Diaz-Naveas, J., Li, S., Maruyama, S., Kalachand, S., Kvamme, B. & Coffin, R. 2022: A review analysis of gas hydrate tests: Engineering progress and policy trend. *Environmental Geotechnics*, 9, 4, 242-258.
 22. Choudhary, S., Sen, K., Rana, S. & Kumar, S. 2022: Petrogenetic history and melt inclusion characteristics of mantle plume-derived ijolites from NE India: implications for multistage crystallization and occurrence of “nanocalciocarbonatites”. *Progress in Earth and Planetary Science* 9, 71, <https://doi.org/10.1186/s40645-022-00531-1>
 23. Choudhary, S., Sen, K., Rana, S. & Kumar, S. 2023: Ultra-hydrous conditions and local readjustment of magnetite in evolving carbonatitic magma at Sung Valley, Shillong Plateau: Evidence from fluid inclusions in calcite and presence of manasseite, ferrogobomite and amesite within magnetite. *Himalayan Geology*, 44 (1), 35-46.
 24. Choudhury, S., Phukan, S., Duarah, B.P., Goswami, D.C. & Mehta, M. 2022: Glacier inventory of the Subansiri River Basin in the Brahmaputra catchment using Landsat satellite data: A case study of the Daisaphu Glacier changes. *Geological Journal*, 57(12), 4939-4954. DOI: 10.1002/gj.4403.
 25. Devrani, R., Kumar, R., Dutt, S. & Jamir, R. 2023: Geoheritage Assessment of a Hermit Cave System at Lakhamandal Valley, Upper Yamuna River Basin, NW Himalaya. *Geoheritage*, 15(1), 30, <https://doi.org/10.1007/s12371-023-00799-9>
 26. Dey, C., Baruah, S., Abdelwahed, M.F., Saikia, S., Molia, N., Borthakur, P., Chetia, T., Bharali, B., Dutta, N., Phukan, M.K., Paul, A., Saitlunga, Hazarika, D. & Kayal, J.R. 2022: The 28 April 2021 Kopili Fault Earthquake (Mw 6.1) in Assam Valley of North East India: Seismotectonic Appraisal. *Pure and Applied Geophysics*, 179, 2167-2182.
 27. Dong, X., Kathayat, G., Rasmussen, S.O. *et al.* 2022. Coupled atmosphere-ice-ocean dynamics during Heinrich Stadial 2. *Nat Commun* 13, 5867, <https://doi.org/10.1038/s41467-022-33583-4>
 28. Gogoi, T., Alam, J. & Chatterjee, R. 2022: Mineralogy and pore structure characterization of Lower Oligocene to Early Miocene formations in parts of Assam-Arakan basin, North East India. *Current Science*, 123, 2, 202-213.
 29. Gupta, A.K., Mandal P. & Sain K. 2023: Modelling of earthquake source parameters and scaling relations in the Uttarakhand Himalayan region, India. *J. Earth Syst. Sci.* 132(73), 1-11.
 30. Gupta, S., Mahesh, P., Kanna, N., Sivaram, K. & Paul A. 2022: 3-D seismic velocity structure of the Kumaun-Garhwal (Central) Himalaya: insight into the Main Himalayan Thrust and earthquake occurrence. *Geophysical Journal International*, 229, 1, 138-149.
 31. Gupta, V., Ram, B.K., Kumar, S. & Sain, K. 2022: A case study of the 12 July 2021 Bhagsunath (McLeod Ganj) flash flood in Dharmashala, Himachal Pradesh: A warning against constricting natural drainage. *Jour Geological Society of India*. 98(5), 607-610.
 32. Gupta, V., Ram, P., Tandon, R.S. & Vishwakarma, N. 2023: Efficacy of Landslide susceptibility

- maps prepared using different bivariate methods: Case study from Mussoorie township, Garhwal Himalaya, *Journal Geological Society of India*, 99, 370-376, <https://doi.org/10.1007/s12594-023-2319-8>
33. Hajra, S., Hazarika, D., Shukla, V., Kundu, A. & Pant, C.C. 2022: Stress dissipation and seismic potential in the central seismic gap of the north-west Himalaya. *Journal of Asian Earth Sciences*, 239, 105432.
 34. Halder, C. & Sain, K. 2023: P-receiver function technique. *Himalayan Geology*, 44(1), 106-116.
 35. Halder, C., Kumar, P., Pandey, O.P., Sain, K. & Kumar, S. 2022: Lower crustal intraplate seismicity in Kachchh region (Gujarat, India) triggered by crustal magmatic infusion: Evidence from shear wave velocity contrast across the Moho. *Geosystems and Geoenvironment*, 1, 100073.
 36. Jagtap, S., Pandey, A., Jayangondaperumal, R., Sharma, A.K., Aravind, A., Singh, I. & Kumar, A. 2022: Active uplift along uncommon bending moment fault in the northern limb of Surin Mastgarh Anticline, Jammu Sub Himalaya. *Himalayan Geology*, 43(2), 442-456.
 37. Jha, V. & Sharma, R. 2022: Formation of polymetallic ores in the metasedimentary rocks of Rangpo area, Sikkim Lesser Himalaya, India: Mineralogical and geochemical attributes. *Geological Journal*, 57, 12, 5061-5082.
 38. Kayal, J.R., Baruah, S., Hazarika, D. & Das, A. 2022: Recent large and strong earthquakes in the eastern Himalayas: An appraisal on seismotectonic model. *Geological Journal*, 57(12), 1-10, DOI: 10.1002/gj.4576
 39. Khan, F., Meena, N.K., Sundriyal, Y. & Sharma, R. 2022: Indian summer monsoon variability during the last 20 kyr: Evidence from peat record from the Baspa Valley, northwest Himalaya, India. *Journal of Earth System Science*, 131(3), 164, <https://doi.org/10.1007/s12040-022-01906-0>
 40. Kharya, A., Rai, S.R., Sachan, H.K., Manish, K. & Kumar, V. 2023: Origin of exotic blocks in Himalaya: a case study from Zildat ophiolitic mélange, Indus suture zone, Ladakh, India. *Carbonates and Evaporites*, 38(1), 11.
 41. Kothiyari, G.C., Malik, K., Dumka, R.K., Nayak, S.P., Biswas, R., Taloor, A.K., Luirei, K., Joshi, N. & Kandregula, R.S. 2022: Identification of Active deformation zone associated with the 28th April 2021 Assam earthquake (Mw 6.4) using the PSInSAR time series. *Journal of Applied Geophysics*, 206, 104811.
 42. Kumar, N., Kumar, N. & Singh, A.K. 2023: Neoproterozoic Felsic Volcano-plutonic Rocks, Tusham Ring Complex, Malani Igneous Suite, NW Indian Shield: Petrogenetic Modeling, Magmatic Source and Geodynamic Evolution. *Geochemistry International*, 61(4), 410-435.
 43. Kumar, N., Singh, S.K., Singh, P.K., Gautam, D.K., Patle, P., Pandey, H.K. & Chauhan, P. 2023: Water accounting of a trans-boundary river basin using satellite observations and WA+ framework. *Physics and Chemistry of the Earth, Parts A/B/C*, 103343. <https://doi.org/10.1016/j.pce.2022.103343>
 44. Kumar, P., Prajapati, K.B., Mahajan, A.K., Pant, D., Meena, N.K., Kumar, A. & Kumar, P. 2022: Evaluating feasibility of biosorption technique for heavy metals removal: limitations and future perspective. *International Journal of Environmental Analytical Chemistry*, 1-25.
 45. Kumar, P.C. & Sain, K. 2022: Seismic Texture of Tertiary successions: insights from Tipam and Barail Formations in the Upper Assam Basin, NE India. *Journal of Geological Society of India*, 98, 1671-1679.
 46. Kumar, P.C., Niyazi, Y., Ovie, O.E., Moscariello, A., Warne, M., Ierodiaconou, D. & Sain, K. 2022: Anatomy of intrusion related forced fold in the offshore Otway Basin, SE Australia. *Journal of Marine and Petroleum Geology*, 141, 105719.
 47. Kumar, Rohtas, Kumar, A., Gupta, S.C., Singh, S.P., Ahluwalia, R.S. & Singh, R. 2022: Moment tensor solutions of some regional events using 3-component single station waveform data. *Journal of Earth System Science*, 131, 4, 239.
 48. Kumar, S., Islam, R. & Srivastava, P. 2023: A review synthesis on the proxies to quantify the in-situ weathering in different climate-tectonic settings with special reference to Himalaya. *Himalayan Geology*, 44, 21-34.
 49. Kumar, S., Sengupta, A., Hermanns, R., Dehls, J., hasin, R.K., Penna, I. & Gupta V. 2022: Probabilistic Seismic Hazard Analysis (PSHA) to Estimate the Input Ground Motions for Co-Seismic Landslide Hazard Assessment: A Case Study on Himalayan Highways, Sikkim India.

- Physics & Chemistry of the Earth Journal, Parts A/B/C, 127, 103157.
50. Kumar, V., Honsberger, I.W., Kharya, A., Sachan, H.K., Rai, S.R. & Kumar, M. 2022: Mineralogical and fluid inclusion constraints on the formation of the Karakorum Migmatite: implications for H₂O-fluxed melting and exhumation of the South Tibetan Crust. *Contributions to Mineralogy and Petrology* 177(6), 60.
 51. Kundu, A., Hazarika, D., Yadav, D.K. & Ghosh, P. 2022: Crustal thickness and Poisson's ratio variations in the Siang Window and adjoining areas of the Eastern Himalayan Syntaxis. *Journal of Asian Earth Sciences*, 231, 105225.
 52. Lamont, E.A., Sousa, F.J., Meigs, A.J., Jayangondaperumal, R., Flowers, R.M., Anilkumar, A., Woodring, D. & Sobel, E.R. 2022: Accretion of the NW Himalayan foreland pre-dates Late Cenozoic climate change. *Terra Nova*, 1-8, DOI: 10.1111/ter.12627
 53. Luirei, K., Kothiyari, G.C. & Mehta, M. 2023: Active tectonics in the Main Boundary Thrust zone, Garhwal Himalaya, as evident from palaeoseismic signatures, morphotectonic features and PSI base ground deformation. *Geological Journal*, 58(1), 195-208. DOI: 10.1002/gj.4586
 54. Luirei, K., Longkumer, L., Kothiyari, G.C., Rawat, S. & Nain, M.Z., 2022. Tectonic implication in the evolution of lake and Quaternary landforms in the Lohawati River basin, Kumaun outer Lesser Himalaya. *Journal of Asian Earth Sciences*, X, 7, 100102.
 55. Majeed, Z., Mehta, M., Ahmad, M. & Mishra, M. 2022: Active rock glaciers of Jhelum basin, Kashmir Himalaya, India. *Indian Journal of Geosciences*, 76(1), 107-124.
 56. Matta, G., Kumar, A., Nayak, A., Kumar, P., Kumar, Amit, Naik, P.K. & Singh, S.K. 2022: Assessing heavy metal index referencing health risk in Ganga River System. *International Journal of River Basin Management*. 2. DOI: 10.1080/15715124.2022.2098756
 57. Maurya, S., Ghosh, R., Sehgal, R.K., Srivastava, P., Shukla, U.K. and Singh, A.P. 2022: Stable isotopic studies of the herbivorous mammals from the marginal Ganga Plain, India: implication for the palaeo-environmental reconstruction. *Geological Journal*, 57(9), 1-14.
 58. Maurya, S., Rai, S.K., Sharma, C.P., Rawat, Suman, Chandana, K.R., Dhahi, A.J., Bhushan, R. & Sarangi, S. 2022: Paleo-vegetation and climate variability during the last three millennia in the Ladakh, Himalaya. *Catena*, 217, 106500.
 59. Meetei, P.N., Ahluwalia, R.S., Rai, S.P., Khobragade, S., Sarangi, S., Goel, M. & Kumar, S. 2022: Spatio-temporal analysis of snow cover and effect of terrain attributes in the Upper Ganga River Basin, central Himalaya. *Geocarto International*, 37, 4, 1139-1159.
 60. Mehta, M., Devrani, R., Luirei, K., Kumar, V. 2022: A report on tectonically sculptured unique glacier landform: a case study from the Tethys Kumaun Himalaya, India. *Geosciences Journal*, 26, 2, 215-224.
 61. Mehta, M., Kumar, V., Kumar, P. & Sain, K. 2023: Response of the Thick and Thin Debris-Covered Glaciers between 1971 and 2019 in Ladakh Himalaya, India—A Case Study from Pensilungpa and Durung-Drung Glaciers. *Sustainability*, 15, 2-21, 4267. <https://doi.org/10.3390/su15054267>
 62. Mennecart, B., Wazir, W.A., Sehgal, R.K., Patnaik, R., Singh, N.P., Kumar, N. & Nanda, A.C. 2022: New remains of *Nalamaeryx* (Tragulidae, Mammalia) from the Ladakh Himalaya and their phylogenetical and palaeoenvironmental implications. *Historical Biology*, 34(12), 2295-2303, <https://doi.org/10.1080/08912963.2021.2014479>
 63. Mohan, K., Thena, T., Nirmal, B., Prakasam, M., Saravanan, K., Sathiyabama, T., Baby, S.R., Shitha, K., Shinde, K. & Pandi, D. 2022: A review on integrated proxy techniques indicating the presence of sub-surface gas hydrates. *International Journal of Oil, Gas and Coal Technology*, 30(2), 175-208.
 64. Mukherjee, B., Sain, K. & Kalyani, K. 2023: A Comparative Study on Appraisal of Lithological Boundaries and Litho-Models Using Well Log Data at Bhogpara Oil Field in Assam of NE India. *Petroleum & Petrochemical Engineering Journal*, 7(1), 000335, <https://doi.org/10.23880/ppej-16000335>
 65. Nagale, D.S., Kannaujiya, S., Gautam, P.K., Taloor, A.K. & Sarkar, T. 2022: Impact assessment of the seasonal hydrological loading on geodetic movement and seismicity in Nepal Himalaya using GRACE and GNSS

- measurements. *Geodesy and Geodynamics*, 13, 5, 445-455.
66. Nanda, A.C., Sehgal, R.K., Singh, A.P., & Singh, N.P. 2022: Mammalian fauna of the Siwalik Group of Indian Subcontinent: Biostratigraphic analysis. *Himalayan Geology*, 43(1A), 17-39.
 67. Nara, D. & Sain, K. 2022: Acoustic full-waveform tomography of realistic 2D synthetic seismic elastic data. *Current Science*, 122, 12, 1407-1414.
 68. Neelavannan, K., Hussain, S.M., Sangode, S.J., Prakasam, M., Sen, I.S., Veerasingam, S., Tyagi, A., Kumar, P. & Singh, P. 2022: A 51 ka sedimentary sequence in a seamount basin, Eastern Arabian Sea: Records for paleoceanographic and paleoclimate conditions. *Journal of Asian Earth Sciences*, 226, 105086.
 69. Negi, M., Saha, S., Ghosh, S.K. & Rai, S.K. 2023: Provenance and sedimentation age of the Proterozoic clastic succession of the Garhwal-Kumaon Lesser Himalaya, NW-India: Clues from U-Pb zircon and Sr-Nd isotopes. *Geological Journal*, 58(2), 605-619.
 70. Niyogi, A., Ansari, T.A., Sathapathy, S.K. et al. 2023: Machine learning algorithm for the shear strength prediction of basalt-driven lateritic soil. *Earth Science Informatics*, 16, 899-917. <https://doi.org/10.1007/s12145-023-00950-8>
 71. Oinam, G., Singh, A.K., Dutt, A., Khogenkumar, S., Joshi, M., Singhal, S. & Bikramaditya, R.K. 2022: Magmatic records of Gondwana assembly and break-up in the eastern Himalayan syntaxis, northeast India. *Gondwana Research*, 112, 126-146.
 72. Ojha, A.K., Srivastava, D.C. & Sharma R. 2022: Fluctuation in the fluid and tectonic pressures in the South Almora Thrust Zone (SATZ), Kumaun Lesser Himalaya; paleoseismic implications. *Journal of Structural Geology*, 160, 104631.
 73. Panda, S., Kumar, A., Srivastava, P., Das, S., Jayangondaperumal, R., Prakash, K. 2022: Deciphering the role of late Quaternary sea level fluctuations in controlling the sedimentation in the Brahmaputra Plains. *Sedimentary Geology*, 442, 106289. <https://doi.org/10.1016/j.sedgeo.2022.106289>
 74. Pandey, A. 2022: Geochemical evidence for a widespread Paleoproterozoic continental arc-back-arc magmatism in the Lesser Himalaya during the Columbia supercontinent assembly. *Precambrian Research*, 375, 106658.
 75. Pandey, A., Kumar, D. & Sachan, H.K. 2022: Mineralogical constraints on petrogenesis and tectonic affiliation of Karnaprayag-Rudraprayag metamafics, Garhwal Lesser Himalaya. *Periodico di Mineralogia*, 91, 1, 21-46.
 76. Pandey, C.P., Ahuja, V., Joshi, L.K. & Nandan, H. 2023: Extreme value analysis of precipitation and temperature over western Indian Himalayan State, Uttarakhand. *Journal of Earth System Science*, 132(2), 1-20.
 77. Pandey, L. & Sain, K. 2022: Joint inversion of resistivity and sonic logs using gradient descent method for gas hydrate saturation in the Krishna Godavari offshore basin, India. *Marine Geophysical Research*, 43, 3, 29.
 78. Pandey, S., Jalal, P., Parcha, S.K. & Sehgal, R.K. 2023: Geochemical characterization of the Middle Cambrian sandstones from Spiti Basin, India: implications for paleoenvironment, provenance, and tectonic setting. *Arabian Journal of Geosciences*, 16, 47. <https://doi.org/10.1007/s12517-022-11058-6>
 79. Pandey, V. & Sain, K. 2022: AVA Analysis of BSR in Fractured filled Gas-hydrates Reservoir in Krishna-Godavari Basin, India. *Journal of the Geological Society of India*, 98, 9, 1253-1260.
 80. Patnaik, R., Singh, N.P., Sharma, K.M., Singh, N.A., Choudhary, D., Singh, Y.P., Kumar, R., Wazir, W.A., Sahni, A. 2022: New rodents shed light on the age and ecology of Late Miocene ape locality of Tapar (Gujarat, India). *Journal of Systematic Paleontology*, 20(1), 2084701. <https://doi.org/10.1080/14772019.2022.2084701>
 81. Paul, A. & Hazarika D. 2022: Occurrences of low-stress drop earthquakes in the eastern Ladakh-Karakoram zone of the Trans Himalaya and their tectonic implications. *Journal of Asian Earth Sciences*, X, 7, 100080
 82. Perumalsamy, C. 2022: The petrogenesis of mafic enclaves and Ladakh granitoids in the southern margin of Ladakh batholith: Evidence of magma mixing and chemical equilibrium. *Journal of Emerging Technologies and Innovative Research*, 9(11), 897-913.
 83. Premi, K., Sen, A.K., Singh, A.K., Singh, W.I. & Chaubey, M. 2023: Genesis of peridotite-hosted

- podiform chromite ore and associated PGE, southern Manipur Ophiolite Complex, northeast India. *Periodico di Mineralogia*, 92, 1021.
84. Pundir, S., Adlakha, V., Kumar, S., Singhal, S. & Das, S. 2022: A newly identified cryogenian (ca. 806 ma) basement tonalite gneiss from the Eastern Karakoram, NW India: Constraints from geochemistry and zircon U-Pb geochronology. *Frontiers in Earth Science*, 10, 1027801. doi: 10.3389/feart.2022.1027801
 85. Rai, S.R., Sachan, H.K., Kharya, A., Groppo, C. & Rolfo, F. 2022: P-T-fluid evolution of migmatites from the Leo Pargil gneissic dome, India: Insights into partial melting and exhumation processes in North Himalayan Domes. *Journal of Asian Earth Sciences* 239: 105389.
 86. Rai, S.R., Sachan, H.K., Spencer, C.J., Kharya, A., Singhal, S., Ojha, A.K., Chattopadhyaya, P. & Pati P. 2022: Zircon geochronology and Hf isotopic study from the Leo Pargil Dome, India: implications for the palaeogeographic reconstruction and tectonic evolution of a Himalayan gneiss dome. *Geological Magazine*, 159(10), 1681-1698.
 87. Ravichandran, M., Gupta, A.K., Mohan, K., Tiwari, S.K., Lakshumanan, C. & Panigrahi, M.K. 2022: Indian monsoon variability during the past 8.5 cal kyr as recorded in the sediments of the northeastern Arabian Sea. *Quaternary International*, 642, 116-132.
 88. Rawat, G. & Luirei, K. 2022. Deep Crustal Resistivity Structure of the Lohit Valley in the Eastern Himalayan Syntaxial Region. *Geological Journal*, 57, 4920-4928. DOI: 10.1002/gj.4422.
 89. Ray, Y., Sinha, S. & Ghosh, S.K. 2022: Provenance of the Proterozoic Lesser Himalayan siliciclastics, northwest Himalaya, India: Implications to terrain accretion and crustal evolution. *Geosystems and Geoenvironment*, 1, 2, 100016.
 90. Sain, K. & Mehta, M. 2022: Atalakodi Route of Hemkund Sahib: A Potential Area of Snow Avalanche. *Journal Geological Society of India*, 98, 863-864.
 91. Sain, K. 2022: Need for Development of AI-based Integrated Warning System (IWS) for Mitigation of Glaciers/Glacial-lakes Related Hazards with Special Reference to Uttarakhand Himalaya. *Journal of the Geological Society of India*, 98, 7, 1012-1014.
 92. Sain, K., Mehta, M. & Kumar, V. 2022: Heavy Rainfall-triggered Flash Floods around the Amarnath Holy Cave. *Journal Geological Society of India*, 98, 1323-1324.
 93. Sain, K., Mehta, M., Kumar, V., Gupta, V. & Chauhan, P. 2023: A Climatic Surprise – Slope Instability Triggered by Heavy Rain in Maldevta Region, Dehradun, Uttarakhand, on 20 August, 2022. *Journal of the Geological Society of India*, 99, 317-320.
 94. Sain, K., Mehta, M., Kumar, V. 2023: Avalanche Hazards Around Kedarnath Temple, Mandakini River Valley, Uttarakhand-A Case Study. *Journal Geological Society of India*, 99, 173-176.
 95. Sajwan, R.S., Joshi, V. & Kumar, N., 2023: Assessment of Thoron exhalation from the soil samples of tectonically active Ghuttu window region: Radiation health hazard perspective. *Himalayan Geology*, 44(1), 1-11.
 96. Sandhu, M., Yadav, R.B.S., Kumar, R., Baruah, S., Singh, A.P., Mishra, M. & Yadav, J.S. 2022: Spatial variability of earthquake hazard parameters, return periods and probabilities of earthquake occurrences in the eastern Himalayan seismic belt. *Physics and Chemistry of the Earth, Parts A/B/C*, 127, 103194.
 97. Sehgal, R.K., Singh, A.P., Gilbert, C.C., Patel, B.A., Campisano, C.J., Selig, K.R., Patnaik, R. & Singh, N.P. 2022: A new genus of treeshrew and other micromammals from the middle Miocene hominoid locality of Ramnagar, Udhampur District, Jammu & Kashmir State, India. *Journal of Palaeontology*, 96 (6), 1318-1335. <https://doi.org/10.1017/jpa.2022.41>
 98. Sen, A., Dey, A. & Sen, K. 2023: Age, petrogenesis, and metamorphic modelling of high-pressure garnet-amphibolite from the Tethyan Himalayan Sequence of Bhagirathi Valley, Western Garhwal Himalaya. *Geological Journal* 58, 981-997.
 99. Sengupta, D., Dutt, S. & Saha, S. 2022: Coherent nature of speleothems petrographic and isotopic proxies for climate change: A case study from northwestern Himalaya. *Geological Journal*, 57(7), DOI:10.1002/gj.4452

100. Sengupta, D., Dutt, S., Saha, S. & Devrani, R. 2023: Geotourism Potential of the Bhiar Dhar Cave, Uttarakhand Himalaya. *Geoheritage*, 15(1), 1-23.
101. Shah, R.A., Jeelani, G., Yadav, J.S. & Rai, S.K. 2022: Hydrogeochemical and stable isotopic evidence to different water origins of karst springs in the western Himalayas, India. *Environmental Earth Sciences*, 81(10), 297.
102. Shah, R.A., Rai, S.K. & Yadav, J.S. 2023: Understanding recharge processes and solute sources of groundwater in karst settings of the Lesser Himalaya, India. *Arabian Journal of Geosciences*, 16(3), 186, 1-18.
103. Shah, R.A., Rai, S.K., Yadav, J.S. & Tiwari, S.K. 2022: Stable isotope hydrology of surface and groundwater from the Doon Valley: geo-meteorological processes and hydraulic linkages. *Hydrological Sciences Journal*, 68(1), 76-90.
104. Sharma, C.P., Kumar, A., Chahal, P., Shukla, U.K. & Srivastava, P. 2023: Debris Flow Susceptibility Assessment of Leh Valley, Ladakh Based on Concepts of Connectivity, Propagation and Evidence Based Probability. *Natural Hazard*, 115, 1833-1859.
105. Shukla, N., Hazarika, D., Kundu, A., S. Mukhopadhyay 2022: Spatial variations of crustal thickness and Poisson's ratio in the northeastern region of India based on receiver function analysis. *Geological Journal*, 57(12) <https://doi.org/10.1002/gj.4469>.
106. Shukla, P.K., Singha, D.K. & Sain K. 2022: Modeling of in-situ horizontal stresses and orientation of maximum horizontal stress in the gas hydrate-bearing sediments of the Mahanadi offshore basin, India. *Geomechanics and Geophysics for Geo-Energy and Geo-Resources*, 8, 3, 90.
107. Shukla, P.K., Singha, D.K., Yadav, P.K. & Sain K. 2022: Petro-physics Analysis and Rock Physics Modeling for Estimation of Gas Hydrate Saturation: A Case Study in the Mahanadi Offshore Basin. *Journal of the Geological Society of India*. 98, 7, 883-892.
108. Shukla, R. & Tiwari, M. 2022: Proterozoic microfossil assemblage from the cherts of Birmania Formation, Western Rajasthan, India. *Journal of Earth System Science*, 131, 3, 141.
109. Sindhuja, C.S., Manikyamba, C., Saha, S., Narayanan, S. & Sridhar B. 2022: Geochemical and carbon isotopic studies of carbonaceous phyllites from Dharwar craton, India-Reconstruction of Precambrian depositional environment. *Precambrian Research*, 372, 106575.
110. Singh D.S., Singh A.K., Dubey C.A., Dharendra Kumar, Sangode S.J., Trivedi A., Agnihotri R. & Singh J. 2022: Multi-Proxy analysis in the Gangotri Glacier region, Garhwal Himalaya: Glacial Stratigraphy and the overview of snout retreat, geomorphic evolution, and palaeoclimate signatures. *Journal of the Palaeontological Society of India*, 67(1), 158-182.
111. Singh, A., Deep, A., Pandey, C. & Nandan, H. 2023: Comparative study of gaseous pollutants for major cities in foothills of Garhwal Himalaya of Uttarakhand. *MAUSAM*, 74(1), 57-72.
112. Singh, A.K., Chung, S.L. & Somerville, I.D. 2022: Introduction, Part 2-Geodynamic evolution of Eastern Himalaya and Indo-Myanmar orogenic belts: Advances through interdisciplinary studies. *Geological Journal*, 57, 12, 4857-4871.
113. Singh, A.K., Chung, S.-L. & Somerville, I.D. 2022: Petrogenesis of mantle peridotites in Neo-Tethyan ophiolites from the Eastern Himalaya and Indo-Myanmar Orogenic Belt in the geo-tectonic framework of Southeast Asia. *Geological Journal*, 57(2), 4886-4919.
114. Singh, A.K., Guruaribam, V., Singh, Y.R., Singh, N.I., Singh, L.R., Chaubey, M., Tewari, V.C., Singh, W. I., Lakhan, N., Devi, L.D. & Chanu, R.S. 2022: Stable isotope geochemistry and microfossil assemblages of carbonate rocks in the ophiolite mélange zone of the Indo-Myanmar orogenic Belt, NE India: Implications on age and depositional environment. *Geological Journal*, 57(2), 5308-5325.
115. Singh, A.K., Guruaribam, V., Singh, Y.R., Singh, N.I., Singh, L.R., Chaubey, M., Tewari, V.C., Singh, W.I., Lakhan, N., Devi, L.D. & Chanu, R.S. 2022: Stable isotope geochemistry and microfossil assemblages of carbonate rocks in the ophiolite melange zone of the Indo-Myanmar orogenic Belt, NE India: Implications on age and depositional environment. *Geological Journal*, 57, 12, 5308-5325.

116. Singh, A.K., Kumar, N., Chung, S.L., Lee, H.Y., Santosh, M., Sharma, R., Kumar, N., Bikramaditya, R.K., Oinam, G. & Lakhan, N. 2023: Tectonic evolution of the neoproterozoic tusham ring complex, Northwestern India: Constraints from geochemistry and zircon U–Pb geochronology, and implications for Rodinia supercontinent history. *Lithos*, 440-441, 107022.
117. Singh, N.P., Patnaik, R., Čerňanský, A., Sharma, K.M., Singh, N.A., Choudhary, D., & Sehgal, R.K. 2022: A new window to the fossil herpetofauna of India: amphibians and snakes from the Miocene localities of Kutch (Gujarat). *Palaeobiodiversity and Palaeoenvironment*, 102, 419-435, <https://doi.org/10.1007/s12549-021-00515-x>
118. Singh, A.P., Sehgal R.K., Singh, N.P. & Kharya, A. 2023: Diet and habitat of late Miocene herbivore mammals from Nurpur, District Kangra, Himachal Pradesh, India. *Geological Journal* 58(2), 740-754.
119. Singh, A.P., Sehgal, R.K., Singh, N.P. 2022: First report of microfauna from Siwalik sediments of Nurpur, District Kangra, Himachal Pradesh, India. *Journal of Earth System Science*, 131, 147. <https://doi.org/10.1007/s12040-022-01880-7>
120. Singh, D., Vardhan, M., Sahu, R., Chatterjee, D., Chauhan, P. & Liu, S. 2023: Machine learning based streamflow prediction in a hilly catchment for future scenarios using CMIP6 data. *Hydrology and Earth System Sciences*, 1-41. <https://doi.org/10.5194/hess-27-1047-2023>
121. Singh, M.R. & Manikyamba, C., R.H., 2022. Subduction-related metabasalts from the western Singhbhum Craton, eastern India - A review. *Journal of the Applied Geochemistry*, 24, 174-184.
122. Singh, M.R. 2022: Geochemistry of metabasites from the western Singhbhum Craton, eastern India: implications for subduction-zone tectonics and mantle-wedge metasomatism. *Geologica Acta*, 20, 1-15.
123. Singh, N. & Chauhan, P. et al. 2022: Tree-Ring isotopic records suggest seasonal importance of moisture dynamics over glacial valleys of the Central Himalaya. *Frontiers in Earth Science*, 10, <https://doi.org/10.3389/feart.2022.868357>
124. Singh, N.A., Choudhary, D., Singh, Y.P., Singh, N.P., Patnaik, R., Tiwari, R.P., Sharma, K.M. 2022: Chondrichthyan and osteichthyan fauna from the middle Miocene deposits of Palasava, Kutch, India: implication for paleoenvironment and paleobiogeography. *Comptes Rendus Palevol*, 21(43), 939-968. <https://doi.org/10.5852/cr-palevol2022v21a43>
125. Singh, N.A., Singh, N.P., Sharma, K.M., Patnaik, R., Tiwari, R.P., Sehgal, R.K., Kumar, V., Wazir, W.A., Singh, Y.P. & Choudhary, D. 2022. First report on late Miocene (Tortonian:~11–10 Ma) charophyte gyrogonites from Tapar, Kachchh District, Gujarat State, western India. *Proceedings of the Indian National Science Academy*, 88, 439-455. <https://doi.org/10.1007/s43538-022-00102-4>
126. Singh, N.P., Deep, S., Čerňanský, A., Sehgal, R.K., Singh, A.P., Kumar, N., Uniyal, P., Kumar, S., Krishan, K. & Patnaik, R. 2022: Fossil lizards and snakes (Diapsida, Squamata) from the late Miocene hominid locality of Haritalyangar, India. *Geobios*, 75, 41-51. <https://doi.org/10.1016/j.geobios.2022.10.003>
127. Singh, N.P., Patnaik, R., cernansky, A., Sharma, K.M., Singh, N.A., Choudhary, D. & Sehgal, R.K. 2022: A new window to the fossil herpetofauna of India: amphibians and snakes from the Miocene localities of Kutch (Gujarat). *Palaeobiodiversity and Palaeoenvironments*, 102, 2, 419-435.
128. Singh, P., Sethy, P.C., Singh, A.K., Singhal, S., Maurya, A.K. & Giri, S.R. 2023: Geochemistry and U–Pb zircon geochronology of the Jutogh Thrust sheet, Himachal Pradesh, NW-Himalaya: Implications to the petrogenesis and regional tectonic setting. *Geological Journal*, 58(1), 131-149.
129. Singh, S., Gautam, P.K., Sarkar, T. & Taloor, A.K. 2022: Characterization of the groundwater quality in Udham Singh Nagar of Kumaun Himalaya, Uttarakhand. *Environmental Earth Sciences*, 81, 19,468.
130. Singh, S., Gupta, A.K., Rawat, Suman, Bhaumik, A.K., Kumar, P. & Rai, S.K., 2021: Paleomonsoonal shifts during ? 13700 to 3100 yr BP in the central Ganga Basin, India with a severe arid phase at ? 4.2 ka. *Quaternary International*, 629, 65-73.
131. Singh, V., Misra, K.G., Yadav, R.R., Yadava, A.K., Vishwakarma, S. & Maurya, R.S. 2022: High-elevation tree-ring record of 263-year summer temperature for a cold-arid region in the western Himalaya, India. *Dendrochronologia*, 73, 125956.

132. Singh, V., Misra, K.G., Yadava, A.K. & Yadav R.R. 2022: Sub-alpine Himalayan birch in cold arid Lahaul-Spiti, Himachal Pradesh, India: a proxy of winter/early spring minimum temperature. *Current Science*, 123, 1, 22-25.
133. Singh, Y.P., Kingson, O., Sharma, K.M., Ghosh, P., Patnaik, R., Tiwari, R.P., Pattnaik, J.K., Kumar, P., Thomas, H., Singh, N.P. & Singh, N.A. 2023: Evolution of the Permo-Triassic Satpura Gondwana Basin, Madhya Pradesh, India: Insights from geochemical provenance and paleoclimate of the siliciclastic sediments. *Geological Journal*, 58(2), 700-721. <https://doi.org/10.1002/gj.4619>
134. Singla, A., Patnaik, R., Singh, N.P., Sharma, K.M. & Sahni, A. 2022: Incisor enamel microstructure of some Neogene muroid rodents of India: taxonomic, evolutionary and biomechanical implications. *Journal of the Palaeontological Society of India*, 67(1), 93-112.
135. Solanki, A. & Gupta, V. 2022: Implications of geomorphometric parameters on the landslide distribution in Kali Valley, Kumaun Himalaya, India - Catena, 215, 106313. <https://doi.org/10.1016/j.catena.2022.106313>
136. Srivastava, P., Dutt, S., Singh, S. & Panda, S. 2022: Holocene variability in Indian summer monsoon in the Himalaya and its foreland, and linkages to the society. *Journal of the Indian Geophysical Union*, 26(4), 258-273.
137. Tandon, R.S., Gupta, V., Venkateshwarlu, B. & Joshi, P., 2022: An assessment of Dungale landslide using unmanned aerial vehicle, ground penetration radar and Slide & RS 2 softwares, *Natural Hazards*, 113, 1017-1042. <https://doi.org/10.1007/s11069-022-05334-7>
138. Thakur, D., Bartarya, S.K., Nainwal, H.C. & Dutt, S. 2022: Impact of environment and LULC changes on groundwater resources in the Soan Basin, western Himalaya. *Environmental Monitoring and Assessment*, 194(9), 612.
139. Thakur, S.S. 2022: P-T-X (Fe-Mg) relations of cummingtonite-sillimanite-cordierite-quartz-H₂O equilibrium: implications on evolution of metamorphic rocks. *Journal of Geological Society of India*, 98, 976-980.
140. Thakur, S.S., Patel, S.C., Chaurasia, C. & Gour, N. 2022: The fate of pyroxenes in mafic xenoliths from the Kinnaur Kailash Granite, Sutlej Valley, NW Himalaya: Effect of retrograde hydration and insights on the rare occurrence of high-grade metamorphic rocks in the Himalayan orogen. *Journal of Petrology*, 63, 1-17.
141. Tiwari, S.K., Sain, K. & Yadav, J.S. 2022: Assessment of Geothermal Renewable Energy with Reference to Tapoban Geothermal Fields, Garhwal Northwest Himalaya, India. *Journal of the Geological Society of India*, 98, 6, 765-770.
142. van der Made, J., Choudhary, D., Singh, N.P., Sharma, K.M., Singh, N.A. & Patnaik, R. 2022: *Listriodon dukkar* sp. nov. (Suidae, Artiodactyla, Mammalia) from the late Miocene of Pasuda (Gujarat, India): the decline and extinction of the Listriodontinae. *PalZ*, 96, 355-383, <https://doi.org/10.1007/s12542-022-00606-w>
143. Venkateshwarlu, M., Babu, N. R., Kapawar, M. R., Kotlia, B. S., Singh, A. K., & Satyakumar, A. V. (2023). Magnetostratigraphy of palaeolake sequence from Kumaun Lesser Himalaya, India: Implications on young geomagnetic excursions. *Geological Journal* 58(4), 1644-1655. <https://doi.org/10.1002/gj.4682>
144. Wadhawan, M., Hazarika, D., Paul, A., Kumar, N., Gupta, V. & Agarwal, M. 2022: Seismic anisotropy and crustal deformation in the Satluj valley and adjoining region of northwest Himalaya revealed by the splitting analysis of Moho converted *P*s phases. *Journal of Asian Earth Sciences*, 238, 105377, <https://doi.org/10.1016/j.jseaes.2022.105377>.
145. Wazir, W.A., Mennecart, B., Sehgal, R.K., Kumar, N., Uniyal, P., Patnaik, R. & Kumar, R. 2022: 3D models related to the publication: New remains of *Nalamaeryx* (Tragulidae, Mammalia) from the Ladakh Himalaya and their phylogenetical and palaeo-environmental implications. *MorphoMuseum M3 Journal*, 8:e142, <https://doi.org/10.18563/journal.m3.142>.
146. Wazir, W.A., Cailleux, F., Sehgal, R.K., Patnaik, R., Kumar, N. & van den Hoek Ostende, L.W. 2022: First record of insectivore from the late Oligocene, Kargil Formation (Ladakh Molasse Group), Ladakh Himalayas. *Journal of Asian Earth Sciences*, X, 8, 100105. <https://doi.org/10.1016/j.jaesx.2022.100105>
147. Wazir, W.A., Sehgal, R.K., Čerňanský, A., Patnaik, R., Kumar, N., Singh, A.P., Uniyal, P. & Singh, N.P. 2022: A find from the Ladakh

Himalaya reveals a survival of madtsoiid snakes (Serpentes, Madtsoiidae) in India till the late Oligocene. *Journal of Vertebrate Paleontology*, 41(6), e2058401. <https://doi.org/10.1080/02724634.2021.2058401>

148. Yadav, A., Kumar, N., Shukla, V., Verma, S.K. & V. Chuahan 2023: Imprints of Diurnal and semidiurnal cyclicity in Radon time series of MPGO, Ghuttu Garhwal Himalaya: Evidence based on singular spectrum analysis. *Pure and Applied Geophysics*, 180, 1081-1097, <https://doi.org/10.1007/s00024-023-0321-z>.

149. Yadav, J.S., Tiwari, S.K., Rai, S.K., Shah, R.A., Yadav, R.B.S. & Kumar, R. 2022: Characterization of meteorological parameters over Dokriani Glacier catchment, Central Himalaya: implications for regional perspectives. *Meteorology and Atmospheric Physics*, 134(5), 88.

Book/Book chapter

150. Adlakha, V & Sain, K. 2022: Crustal evolution of the Himalaya since Paleoproterozoic. Edited Chapter, *In: Cengiz, M. & Karabulut, S. (Eds.), Earth's crust and its evolution -From Pangea to the present continents*. DOI: 10.5772/intechopen.104259

151. Nallusamy, Babu, Mohapatra, Euniksha, Perumalsamy, C., Vijay Anand S, Shri Niveditha R, Sharath Raj B, Syed Hamim Jeelani, Lingadevaru. M, Krishnakumar A, Kocherla Muralidhar, Sundararajan. M & M.A. Mohammed Aslam, 2022: Magnetic susceptibility, mineralogical and geochemical studies of Neoproterozoic sandstone of Badami group, Kaladgi basin, Dharwar craton, SE India. *Geological Developments in Anthropocene*, Excel India Publishers, 294-311.

152. Bhambri, R., Chand, P., Nüsser, M., Kawishwar, P., Kumar, A., Gupta, A.K., Verma, A. & Tiwari, S.K. 2022: Reassessing the Karakoram Through Historical Archives. Edited Chapter, 139-169. *In: Saikia, A. & Thapa, P. (eds.), Environmental Change in South Asia: Essays in Honor of Mohammed Taher*. Springer International Publishing, Cham, https://doi.org/10.1007/978-3-030-47660-1_8

153. Gupta, V, Sain, K. & Tandon, R.S. 2022: Landslides and slope instability in Mussoorie and Nainital townships (Uttarakhand) in present

climate - change scenario. Edited Chapter, 391-411, *In: Unnikrishnan, A.S., Tangang, F. & Durrheim, R.J. (eds.), Extreme Natural Events: Sustainable Solutions for Developing Countries*, Publisher Springer Singapore, <https://doi.org/10.1007/978-981-19-2511-5>

154. Kumar, A., Devrani, R. & Srivastava, P. 2022: Landscapes and Paleoclimate of the Ladakh Himalaya. Edited Chapter, 308-320. *In: Pandey, M., Pandey, P.C., Ray, Y., Arora, A., Jawak, S.D. & Shukla, U.K. (eds.), Advances in Remote Sensing Technology and the Three Poles*.

155. Kumar, R., Devrani, R., Dangwal, A., Deshmukh, B. & Dutt, S. 2022: Extreme Hydrological Event-Induced Temporal Variation in Soil Erosion of the Assiganga River Basin, NW Himalaya. Edited Chapter, 308-320. *In: Pandey, M., Pandey, P.C., Ray, Y., Arora, A., Jawak, S.D. & Shukla, U.K. (eds.), Advances in Remote Sensing Technology and the Three Poles*.

156. Lokho, K. 2023: Darashaw Noshervan Wadia: A Lonely Khaki-Clad Figure Silently Hitting Every Stone in the Neighbourhood. Edited Chapter, 15-48. *In: Tripathi, P.M., Sharma, N.K., Paramanik, V. & Singh, V.P. (eds.), Descendants of Kanād. Life sketches of some Indian Scientists*, Scientific Publishers.

157. Lokho, K. 2023: Leading Ladies in the Earth Sciences in India. Edited by Vikram Rai, *Book Rivers*, Lucknow, 84-87.

158. Rai, S.K., Shah, R.A. & Das, S. 2022: Cooperative management of Himalayan rivers among the riparian states. *In: Water Scarcity, Contamination and Management*. Tiwari AK, Kumar A, Singh, AK, Singh TN, Suozzi E, Matta, G, Russo SL (eds), Elsevier, Radarweg, AE Amsterdam, Netherlands, 5, 59-71.

159. Sain, K. & Kumar P.C. 2022: Meta-attributes and Artificial Networking: A New Tool in Seismic Interpretation. AGU-John Wiley & Sons.

160. Sain, K. & Nara, D. 2023: Active Seismic Tomography: Theory & Applications. Willey publications, 144p. (ISBN: 978-1-119-59489-5)

161. Kumar, A., Sain, K. & Verma, A. 2022: Hydrological importance of Himalayan glaciers: A perspective from Garhwal Himalaya. *In Current Directions in Water Scarcity Research*, 5, 559-571.

162. Wadhawan, M., Hazarika, D., Saikia, S. 2023: Application of teleseismic receiver function in investigation of crustal thickness and Poisson's ratio. Edited Chapter, 32. *In: Recent Developments in Using Seismic Waves as a Probe for Subsurface Investigations: Theory and Practices*, published by Taylor & Francis Group, <https://doi.org/10.1201/9781003177692>,
163. Paul, A. & Hazarika, D., 2022: Seismic anisotropy for understanding the dynamics of crust and upper mantle: A case study in the northwest Himalaya and eastern Ladakh-Karakoram zone. Edited Chapter, 42. *In: Recent Developments in Using Seismic Waves as a Probe for Subsurface Investigations: Theory and Practices*, published by Taylor & Francis Group, <https://doi.org/10.1201/9781003177692>,
166. Coggon, R.M., Sylvan, J.B., Teagle, D.A.H., Reece, J., Christeson, G.L., Estes, E.R., Williams, T.J. & the Expedition 390 Scientists 2022: Expedition 390 Preliminary Report: South Atlantic Transect 1. International Ocean Discovery Program. <https://doi.org/10.14379/iodp.pr.390.2022>.

Excursion Guide

167. Ahmad, T., Kumar, S., Jayananda, M., Jayangondaperumal, R., Sachan, H.K. & Kumar, A. 2022: Excursion Guide: Two NS transects across Trans-Himalaya, Ladakh. Special Publication 5, Wadia Institute of Himalayan Geology.
168. Jayangondaperumal, R. & Mishra, R.L 2022: Excursion Guide to The Himalayan Frontal Fold-Thrust Belt, FIGA-2022, WIHG, 16-18 November 2022, post-congress field, 141-151.

State-of-the-Art Reports

164. Tiwari, S.K. & Kumar, A. 2022: A report on 6th National Geo-Research Scholars Meet-2022 emphasis on "Geoscience in Ladakh" held at Leh Union Territory of Ladakh. *Himalayan Geology*, 43(2), 2022
165. Kumar, A. & Bisht, P. 2022: 1st Indian Quaternary Congress (IQC)-2022 Organized by the Association of Quaternary Researchers (AoQR). *Journal of Palaeosciences*, 71(1), 113-115.

Field Guide

169. Singh, P., Sethy, P.C., Rastogi, H., Singh, M.R., Singh, A.K., Thakur, S.S. & Singhal, S. 2023: Geological Field Observations along the Pandoh Syncline: The Mandi-Kataula-Bajura Section of Himachal Pradesh, NW-India. In *Structural Geology and Tectonics Field Guidebook-Volume 2*, 79-201, Cham: Springer International Publishing. ISBN 978-3-030-60142-3

SEMINAR/SYMPOSIA/WORKSHOP ORGANIZED

The 6th National Geo-Research Scholars Meet-2022 organized jointly by the University of Ladakh, Leh, and Wadia Institute of Himalayan Geology, Dehradun at the University of Ladakh, Leh during 7-10 June 2022

The University of Ladakh and Wadia Institute of Himalayan Geology, Dehradun jointly organized the 6th National Geo-Research Scholars Meet at the premises of the University of Ladakh, Leh, during June 07-10, 2022.

India has a unique geological history covering geological-geodynamic processes representing Precambrian to Quaternary geological time scale. The Trans-Himalayan Ladakh is a product of collisional tectonics and provides an ideal opportunity to investigate and understand various geological, geodynamics processes, tectonic control, climate change, natural resources, etc. The region has a suitable geological setup for the formation of economically feasible mineral deposits. As of now, many places in various parts of Ladakh have shown sporadic occurrences of lithium, uranium, gold, copper, precious stones, etc. Since these occurrences have not been paid due attention, it is high time to re-look into it with the help of advanced technology. Ladakh is one of the unique tectonic domains to study the trend of climate change during the last 100 years. The region attracts lots of tourists by its unique landscape, and it is the ideal place for geo-tourism. Updated knowledge is primarily based on data from the field, state-of-the-art instrumentation, and evolving models. Young researchers are consistently contributing to the growth of geoscience research. The major aim of the NGRSM is to supplement the efforts, inspire and encourage young researchers to improve their quality of research work, refine their ideas, and promote novel geoscience research in the country. Keeping in view of such objectives, the theme of "Geosciences in Ladakh Himalaya" was chosen for the conference.

A total of 93 geo-research scholars, including from 48 national Institutions/ IITs/ Central and State Universities/ IISc/IISER located all over India with eminent resource persons attended this event of national importance. Under the main theme of 'Geoscience in Ladakh', the sub-theme covered areas such as fold belts and cratons of India, climatic change and geological

processes, natural hazard and mitigation, and geo-resources. A total of 93 posters were presented in two sessions based on the above-described sub-themes. The 6th NGRSM also focused on field training for young researchers. Field training was conducted along two transacts: Transact-A (Mahe-Sundo) and Transact-B (Leh- Taru-Chiling) to the young researchers. The training was helpful to the young researchers in understanding several geodynamic processes combined with the lecture series by eminent scientists.

The Chief Guest of the inaugural ceremony, Shri Umang Narula, IAS, Advisor to Lt. Governor of Ladakh UT and Pro-Chancellor, UoL, emphasized the geoscientific investigation in the Ladakh Himalaya. Sh. Narula added that the Himalaya is the largest source of fresh water and precious minerals. In the welcome address, Prof. S.K. Mehta, Vice-Chancellor, UoL, Prof. Talat Ahmad, Chairman of Governing Body of WIHG, and Prof. Kalachand Sain, Director, WIHG, enlighten the importance and recent advances in geosciences. Dr Riyaz M K Khan (UoL), convenor, gave the vote of thanks. The abstract volume and the excursion guides were released during the meeting.

During session-1, there were six lectures by the experts. Dr. R.J. Perumal (National convener of the meet, WIHG), in his keynote lecture, talked about an appraisal of the evolution and paleoseismicity of the Himalaya. Prof. Santosh from Kumaun University gave a lecture on the tectono-magmatic evolution of the Ladakh Himalaya. Prof. M. Jayananda (University of Hyderabad) in his keynote lecture stressed the lateral flow of the hot orogenic crust and the formation of orogenic plateaus: Insights from Neoproterozoic Eastern Dharwar craton and Tibetan plateau. Dr. Kalachand Sain (Director, WIHG) emphasized the development of an Integrated Warning System (IWS) for the mitigation of Glacial Geo-hazards. Dr. Sain, in his talk, focused on state of the, art seismic techniques for subsurface imaging with special reference to the exploration of hydrocarbon and understanding of geo-tectonic implications of Indian provinces. Dr. Rakesh Bhambri discussed the monitoring of Himalayan glaciers and associated hazards using ground and space observations. Dr. Bhambri highlighted the importance of monitoring Himalayan glaciers for water resource management and hazard mitigation. He reported that glaciers in the Karakoram revealed irregular behaviour as compared to the central and eastern Himalayas. Dr.

Anil Kumar stressed on Late Quaternary landscape evolution of the Indus River, Ladakh Himalaya: Climate- Tectonic interaction.

On Days 2 and 3, the fieldwork, along the two transects, was organized by exchanging the research scholars in two batches (each batch consists of ~45 participants). In transect-A, the expert showcased the

ophiolitic melange sequence and ultrahigh-pressure rocks in the Indian continental crust. This is the classic example where high-pressured rocks with low-temperature orogeny is evidenced. Along the transect-B, outcrop scale exposures of Ladakh Batholith with mafic and felsic crystallization processes, thrust-fold in the molasses, neo-tectonic activity along the Upshi-



(a) Inauguration of 6th NGRSM 2022 and (b) Releasing of abstract volume



Photograph of fieldwork where eminent scientists exposed the young research scholars to the geology, geodynamics, and earth surface processes of the Ladakh Himalaya



(a) Photograph of fieldwork where eminent scientists exposed the young research scholars to the geology, geodynamics, and earth surface processes of the Ladakh Himalaya (b) Dignitaries relaxing after a hectic day



Prof. Kalachand Sain, Prof. S.K. Mehta, and Prof. Talat Ahmad felicitating the Chief Guest Ven. Bhikshu Sanghasena

Basgo Thrust, paleo foods in the Indus and Zaskar counter thrust was the center for discussion.

On Day 4, the first session (Session – 3) had keynote lectures and sessions chaired by Prof. M. Jayananda. The keynote lectures were delivered by Dr. Vikram Gupta, Dr. R.K. Sehgal, and Dr. Sameer K. Tiwari. Dr. Gupta presented an overview of landslide hazards and their mitigation in the northwestern Himalaya and related the hazard to the fluctuating climatic conditions. Dr. R.K. Sehgal discussed the abundance of biomarkers in the Siwalik foreland basin and provided a broader aspect of bio-stratigraphic development in the Indian continent. He also displayed the recent discovery of snake fossils from the Kargil Molasse. Dr. Sameer K. Tiwari provided an overview of geothermal energy in the Himalaya. He explained the trends and potential role of green energy for a sustainable future to young researchers.

Session-4, was an 'Oral poster presentation', where 33 posters were presented by various geo-research scholars, and the session was moderated by Dr. Rakesh Bhambri and Dr. Akhtar R Mir. Subsequently, a 'Walk through poster' session where a detailed discussion on each poster was made by various researchers.

In session-5, Prof. Talat Ahmad and Prof. Santosh Kumar provided an overview of the two days of fieldwork along Transect A (Mahe-Sundo) and Transect B (Ganglas- Phyang-Taru). Prof. Talat explained the India-Eurasia collision mechanism and the evolution of litho-tectonic units using field-based data. Prof. Santosh Kumar explained the emplacement of Ladakh Batholith, magma mixing, formation of magmatic enclaves, and hybridization processes. Both the peers spellbound the listeners with the subject proficiency and bundle of knowledge. This session was chaired by Prof. S K Mehta, Vice-Chancellor, UoL. Student feedback was sought out where students praised the efforts made

by the resource persons during the lectures and in the field.

At last, the closing ceremony session was conducted. Closing remarks were given by Prof. Kalachand Sain, Director, Wadia Institute of Himalayan Geology, Dehradun; Prof. S. K. Mehta, Vice-Chancellor, UoL; Guest of Honour Mrs. Rinchen Lhamo, a Member of the National Minority Commission, Government of India and Chief Guest Ven. Bhikshu Sanghasena, Founder President Mahabodhi International Meditation Centre, Leh. All Resource Persons and winners of the best poster presentation were felicitated. A Vote of Thanks was given by Mr. Imteeaz Kacho, Registrar, UoL.

The 3rd Triennial Congress of the Federation of Indian Geosciences Association (November 16-18, 2022)

The Wadia Institute of Himalayan Geology (WIHG), Dehradun has successfully organized the 3rd Triennial Congress of the Federation of Indian Geosciences Association (FIGA) during November 16-18, 2022. The congress provided a common platform to eight Geosciences Associations and seven Geosciences institutions/ministries to discuss the role of geosciences on the societal challenges for sustainable socio-economic development and recommend policies for implementation at national and international levels. Professional organizations like IGU, GSI, SPG, OSI, AEG, AHI, PSI, and ISES and institutions like MoES, NCESS, AMD, CSIR-NGRI, IIG, KDMIPE-ONGC, WIHG discussed scientific progress on the theme "Geosciences of Himalaya for Sustainable Development". Under this theme, a wide range of new research outcomes on various topics, e.g. Geodynamics, crustal evolution and mantle structures, Climate variability and landscape evolution, Earthquakes: genesis and mitigation, Landslides and their risk reduction, Floods: past and present, Glacial Dynamics and hazards, Natural water and thermal springs, Precious minerals and hydrocarbons were presented by the participants.

Around 200 presentations were delivered at this event with PAN-India participation from different Universities/Institutes/Organizations of India along with 16 keynote lectures by experts of undertaken themes. The congress started with the welcome address of Chairman & Congress Director, Dr. Kalachand Sain and introductory remarks of Professor V. P. Dimri, President of FIGA shared their views on the association as a united body to represent various geoscientific associations in India for the progress of geosciences in India and roles of geosciences in nation building. The



A group photograph of the participants during the 3rd Triennial Congress of the Federation of Indian Geosciences Association



Release of the book “Meta Attributes and Artificial networking” by Shri Pushkar Singh Dhami CM Uttarakhand during FIGA Conference



Dignitaries participating in the FIGA conference

participants were motivated by the messages of the dignitaries like Dr. Jitendra Singh, Minister of State (Independent charge) of the Ministry of Science and Technology & Ministry of Earth Sciences; Dr. (Mrs.) N. Kalaiselvi, Secretary, Department of Scientific and Industrial Research and Director General; Dr. S. Chandrasekhar, Secretary, Ministry of Science and Technology, Department of Science and Technology, Government of India; Dr. M. Ravichandran, Secretary, Ministry of Earth Sciences, Government of India and through the gracious presence of Sh. Pushkar Singh Dhami, Honorable Chief Minister of Uttarakhand.

The congress was preceded by a short course on Artificial Intelligence and Machine Learning (AI/ML) in which a session on the role of AI/ML in Earth sciences was conducted by Dr. Kalachand Sain and Dr. Priyadarshi Chinmoy Kumar. The participants of the congress also benefitted through a post-congress field visit along the Himalayan mountain front in the Mohand-Dehradun-Mussoorie section organized by the Convenor, Prof. R Jayagondaperumal.

A national conference and exhibition on "Akash for Life" (November 4–7, 2022)

A national conference and exhibition on "Akash for Life" was organized by the Department of Space, Government of India, in cooperation with WIHG, ISRO, IIRS, USAC, Uttaranchal University, Vibha, and associated Ministries of the Government of India, to help shape solutions to the challenge of climate change and related environmental concerns based on the synergy of Indian philosophical tradition and modern science. This event was organized at Uttaranchal University, Dehradun, Uttarakhand, during November 4–7, 2022, and Eminent scientists, academics, traditional knowledge experts, practitioners, industry leaders, policymakers, social workers, and students have actively participated in this mega event. In exhibitions, public outreach initiatives, and various science displays, WIHG actively contributed and participated part.

AWARDS AND HONOURS

- Dr. Ningthoujam Premjit Singh received the prestigious Prof. R. C. Misra Award in Geosciences - 2022 for outstanding contribution in the field of geoscientific research on June 29, 2022, on the Foundation Day of Wadia Institute of Himalayan Geology.
- Drs. Kalachand Sain and his team received the “Best Paper Award” by WIHG, Dehradun for the research paper entitled “A Perspective on Rishiganga-Dhauliganga flash flood in the Nanda Devi biosphere reserve, Garhwal Himalaya, India” published in the Journal of the Geological Society of India.
- Dr. Manish Mehta and Dr. Vinit Kumar received appreciation letter from the National Disaster Management Authority (NDMA) of India for their contribution as an Expert Member of the joint study team constituted by NDMA to “Understand the causes of the Flash Flood in River Rishiganaga & Dhauliganaga & Suggest Mitigation Preparedness measures to prevent future events” and detailed report.

PH.D. THESES

| Sl. No. | Name of Student | Supervisor | Title of the Theses | University | Awarded/ Submitted With date |
|---------|-------------------------------|---|--|--|------------------------------|
| 1. | K. Premi | Dr. A.K. Singh Prof. A.K. Sen | Petrogenesis of mantle rocks and chromitite in southern Manipur ophiolite complex, NE India | Indian Institute of Technology (IIT), Roorkee | Awarded May 2022 |
| 2. | Abhishek Kundu | Dr. Devajit Hazarika, Dr. Parthapratim Ghosh | Lithospheric structure and deformation in the north-eastern part of the Indian plate in the Eastern Himalayan Syntaxis | Baranas Hindu University (B.H.U.), Varanasi | Awarded May, 2022 |
| 3. | Laxmi Pandey | Dr. Kalachand Sain | Rock Physics for Anisotropy of Gas hydrates reservoir in Krishna Godavari Basin | AcSIR-NGRI, Hyderabad | Awarded July 2022 |
| 4. | Vivekanand Pandey | Dr. Kalachand Sain | Quantitative Assessment of gas-hydrates in KG basin | Osmania University, Hyderabad | Awarded July 2022 |
| 5. | Richa Kumari | Dr. Naresh Kumar, Dr. Parveen Kumar Dr. Sandeep | Investigation of various crustal parameters of Kinnaur Himalaya using Seismological Data | B.H.U., Varanasi | Awarded August 2022 |
| 6. | Meenakshi Devi | Dr. Vikram Gupta Dr. K. Sarkar | Landslide hazard zonation in the Bhagiratji valley, Garhwal Himalaya | I.I.T. (I.S.M.) Dhanbad. | Awarded August 2022 |
| 7. | Sakshi Maurya | Prof. S. Sarangi, Prof. S.K. Rai, | Reconstruction of Palaeoclimate record from Ladakh, Northwestern, Himalaya, India" | I.I.T. (I.S.M.) Dhanbad. | Awarded August 2022 |
| 8. | Choudhurima-yum Pankaj Sharma | Prof Pradeep Srivastava Prof U.K. Shukla | Paleoclimatic Reconstruction from the Late Pleistocene-Holocene Sedimentary Archives of Ladakh Himalaya | B.H.U., Varanasi | Awarded September 2021 |
| 9. | Anjali Sharma | Dr. Ajay Paul Dr. Dinesh Kumar | Modeling of empirical accelerograms, evaluation of seismic hazards in the central seismic gap region of Himalaya based on site effects and simulated accelerograms | Kurukshetra University, Kurukshetra | Awarded November 2022 |
| 10. | Shantahjara Biswal | Dr. Kapesa Lokho Prof. Kuldeep Prakash | Biostratigraphy, depositional history and paleogeography of the Sylhet Limestone Formation, southeastern Mikir Hills, Northeast India | B.H.U., Varanasi | Awarded November 2022 |
| 11. | Sandeep Kumar | Dr. Vikram Gupta Prof. Y.P. Sundriyal | Role of lithology in landslide distribution and dynamic slope stability analysis of active landslides in Goriganga river valley, Uttarakhand, India | H.N.B. Garhwal University, Srinagar | Awarded November 2022 |
| 12. | Pratap Ram | Dr. Vikram Gupta Dr. Neeraj Vishwakarma | Landslide hazard, Risk & Vulnerability Ass of the Mussoorie and Nainital township, NW Himalaya | National Institute of Technology (NIT), Raipur | Awarded December 2022 |

| Sl. No. | Name of Student | Supervisor | Title of the Theses | University | Awarded/ Submitted With date |
|---------|--------------------|---|--|-------------------------------------|------------------------------|
| 13. | Rohit Singh Sajwan | Dr. Naresh Kumar, Dr. Parveen Kumar | Radon Concentration in Ghuttu Window, Garhwal Himalaya: Implication for Progeny metrological and Seismic Variability | H.N.B. Garhwal University, Srinagar | Awarded December 2022 |
| 14. | Vaishali Shukla | Dr. Naresh Kumar, Prof. Charu C. Pant | Seismogenesis of the Garhwal Himalaya and its correlation with Earthquake precursory signatures: Constraints from recent seismicity and earthquake source characterization | Kumaun University, Nainital | Submitted July 2022 |
| 15. | Monika | Dr. Parveen Kumar Dr. Sandeep | Attenuation studies of Uttarakhand Himalaya and its implication in strong motion simulation | B.H.U., Varanasi | Submitted July 2022 |
| 16. | Anil Tiwari | Dr. Ajay Paul Dr. Rajeev Upadhyay | Source mechanisms of earthquakes in Kumaun-Garhwal region, NW Himalaya, India and its seismotectonic implications | Kumaun University, Nainital | Submitted August 2022 |
| 17. | Sandeep Panda, | Dr. Pradeep Srivastava Prof. Kuldeep Prakash | Understanding fluvial architecture of Brahmaputra foreland and extreme events vis-à-vis climate and tectonics | B.H.U., Varanasi | Submitted December 2022 |
| 18. | Venus G. | Dr. A.K. Singh Prof. Y. Raghmani Singh | Micropalaeontology study and Isotope Geochemistry of pelagic sediments of Ophiolite melange zone of Manipur, Northeast India | Manipur University, Imphal | Submitted December 2022 |
| 19. | Govind Oinam | Dr. A.K. Singh Prof. M. Joshi | Petrological and U-Pb Geochronological studies of magmatic rocks from the Siang window, Arunachal Himalayas, Northeast India | B.H.U., Varanasi | Submitted December 2022 |
| 20. | Manas M | Dr. Barun K. Mukherjee Prof. R. Dubey | Genetic facets of Ophiolite-Melange of Indus-Tsangpo Suture Zone, Western Ladakh Himalaya, India | I.I.T. (I.S.M.) Dhanbad. | Submitted December 2022 |
| 21. | Ambar Solanki | Dr. Vikram Gupta Prof. M. Joshi | Geomorphic control of landslides in the Kali valley. Kumaun Himalaya | B.H.U, Varanasi | Submitted February 2023 |

PARTICIPATIONS IN SEMINARS / SYMPOSIA / MEETINGS

- The national workshop on “Chronological Systematics and their applications in Earth sciences” organized by Geochronology Group, Inter-University Accelerator Centre (IUAC), during April 19-21, 2022.

Participant: M.R. Singh

- A virtual consultation meeting on “India's Adaptation Communication on the Himalayan Ecosystem Sectoral Working Group”, organized by the Ministry of Environment Forest and Climate Change (MoEFCC) on May 24, 2022.

Participant: Amit Kumar

- A meeting for discussion on the issues related to “Hydrological Studies in Badrinath Dham”, held under the chairmanship of the Secretary, Department of Water Resources, River Development & Ganga Rejuvenation, Ministry of Jal Shakti on May 31, 2022.

Participant: Amit Kumar

- A webinar on the possibility of “Indo-Norwegian Collaboration on Geo-hazards and Geo-resources in the Himalaya” organized by Wadia Institute of Himalayan Geology, Dehradun, on June 01, 2022.

Participant: Amit Kumar

- 6th National Geo-Research Scholars Meet-2022 organized jointly by the University of Ladakh, Leh, and Wadia Institute of Himalayan Geology, Dehradun at the University of Ladakh, Leh, during 7-10 June 2022

Participants: Kalachand Sain, Naresh Kumar, Chinmay Halder, Vinit Kumar, Manish Mehta, Amit Kumar, Akshaya Verma, Rakesh Bhamri, Sameer Tiwari, Som Dutt

- National Conference on "Glacial Lake Outburst Floods (GLOFs) and Landslide Lake Outburst Floods (LLOFs) Disasters in Himalayan Regions" organized by at the Indian Institute of Technology, Roorkee, in collaboration with Bureau of Indian Standards, India on June 15, 2022.

Participant: Swapnamita Choudhuri

- 15th Uttarakhand State Science and Technology Congress, organized by Uttarakhand State Council for Science and Technology (UCOST) held at

Graphic Era (Deemed to be University), Dehradun during June 22-24, 2022.

Participant: Chhavi Pandey

- SERB-DST sponsored workshop on "A Field and lab-based workshop on biomonitoring of rivers using diatoms" organized by Agharkar Research Institute (ARI), Pune during July 18-29, 2022.

Participant: Sudipta Sarkar

- International conference on “Climate and Weather-Related Extremes (ICCWE-2022), New Dimensions, Challenges, and Solutions”, held at Indian Institute of Technology, Roorkee, during September 19-20, 2022.

Participant: Chhavi Pandey

- International Symposium on Sustainable Urban Environment (ISSUE-2022) held at University of Petroleum and Energy Studies (UPES), Dehradun during October 13-14, 2022

Participant: Subhajit Saha

- An online workshop on “Geotourism potential of India and its development” organized by Geological Survey of India at Kolkatta, during October 13-14, 2022.

Participant: Kapesa Lokho

- Reducing Risk & Building Resilience: Capacity Building in the Mountain States, organized by Academy of Administration (ATI) Nainital, and National Institute of Disaster Management (NIDM), New Delhi, October 20-21, 2022.

Participant: Naveen Chandra

- A meeting on the “Development and Deployment of an Integrated Operational Warning System (IOWS) in Dhauliganga River basin, Chamoli, Uttarakhand” at Disaster Mitigation and Management Centre of Secretariat, Uttarakhand, on November 02, 2022

Participant: Amit Kumar

- 2nd International Conference on “Aerosol, Air Quality & Climate Change over the Himalayan Region of Uttarakhand” (AAC-2022) held at the Department of Physics, HNB Garhwal University, Srinagar Garhwal, Uttarakhand, during November 04-06, 2022.

Participant: Chhavi Pandey

- XIII Biennial National Conference of Physics Academy of North East (PANE-2022) organized by the Department of Physics, Manipur University, Imphal, Manipur, held during November 8-10, 2022 (online).

Participant: Chhavi Pandey

- 3rd Triennial Congress of Federation of Indian Geosciences Associations (FIGA) on Geosciences of “Himalaya for Sustainable Development”, organized by Wadia Institute of Himalayan Geology, Dehradun, during November 16-18, 2022,.

Participants: Scientists and Research Scholars of the Institute

- 65th Annual General Body Meeting of Palaeontological Society of India on November 16, 2022, during the 3rd Triennial Congress of the Federation of Indian Geosciences Associations (FIGA) at Wadia Institute of Himalayan Geology, Dehradun.

Participant: Kapasa Lokho

- International Conference on “Environment and Human Health: Global Issues” organized by Department of Botany and Microbiology, Gurukula Kangri (Deemed to be University) Haridwar, Uttarakhand, during December 07-08, 2022;

Participant: Chhavi Pandey

- American Geophysical Union (AGU) Fall meeting held during December 12-16, 2022 (online)

Participants: Supriya Deogharia and Parveen Kumar

- International meeting on “Use of Advanced Technologies in Disaster Management” by Uttarakhand State Disaster Management Authority (USDMA), Government of Uttarakhand held during March 21-22, 2023.

Participant: Amit Kumar

- International conference on “Radiation Awareness and Detection in Natural Environment- RADNET-2023” organized by National Radon Network Society held at Dolphin (PG) Institute of Biomedical and Natural Sciences, Dehradun, during March 2-4, 2023.

Participant: Chhavi Pandey

- An online training course on “Isotopes in soil Science” organized by University Tubingen, during March 06-10, 2023.

Participant: Prakasam M.

DISTINGUISHED LECTURES DELIVERED IN THE INSTITUTE

| Sl. No. | Date | Speaker | Event & Topic |
|---------|--------------------|--|--|
| 1 | April 06, 2022 | Dr. Kalachand Sain Director, WIHG | विश्व भूवैज्ञानिक दिवस “भीषण हिमालयी आपदाओं के संभावित भूकंपीय पूर्वसूचक एवं सतही गतिकी: एक पूर्व चेतावनी विधि” |
| 2 | May 11, 2022 | Dr. Kalachand Sain Director, WIHG | National Technology Day |
| 3 | June 29, 2022 | Dr. Rajendra Dobhal Director General, Uttarakhand State Council for Science and Technology, Uttarakhand | Foundation Day "Analysing R & D systems in India: Future ahead" |
| 4 | September 09, 2022 | Dr. Kalachand Sain Director, WIHG | Himalaya Diwas "Importance of Himalaya Diwas" |
| 5 | January 05, 2023 | Shri Ashok Kumar (IPS) DGP- Uttarakhand | New Year Talk "Cyber Security" |
| 6 | February 02, 2023 | Shri Rajesh Kumar Srivastava Former CMD, ONGC | IGU's Electrotek and Geometrics Endowment Lecture "Opportunities in the Indian E&P Sector: Advances in Seismic API" |
| 7 | February 28, 2023 | Dr. Kalachand Sain Director, WIHG | National Science Day "Geo-hazards in the Himalaya and Plausible Mitigation" |

DISTINGUISHED LECTURE SERIES RELATED TO CELEBRATIONS OF “AZADI KA AMRIT MAHOTSAV”

Azadi ka Amrut Mahotsav is an initiative of the Government of India to celebrate and commemorate 75 years of progressive India and the glorious history of its people, culture, and achievement. In connection with the "*Azadi ka Amrut Mahotsav*", WIHG, Dehradun organized Distinguished Lecture Series by Eminent Scientists and Renowned Professors. During the reporting period, 10 distinguished lectures were organized (Coordinated by Dr. Devajit Hazarika).

| S.No | Name of Speaker | Topic of the lecture | Date |
|------|---|---|-------------------|
| 1 | Matthew J. Kohn, Boise State University, USA | Long-lived (>20 Myr) partial melts in the Greater Himalaya-evidence and geodynamic implications | April 28, 2022 |
| 2 | Gasper Monsalve , Universidad Nacional de Colombia, Medellín Campus. | Continental Margins: Strength of the lithosphere, crustal thickening and the nature of the crust-mantle transition - Examples from the Central Himalayas and Northern Andes | May 18, 2022 |
| 3 | Prof. Patrick O'Brien, University of Potsdam, Germany | Himalayan Mountains: the metamorphic memory of a multistage evolution | June 27, 2022 |
| 4 | Prof. M. Jayananda University of Hyderabad | Evolving Archean Earth and origin of habitable continents: Insights from the Dharwar craton | July 08, 2022 |
| 5 | Prof. Anupam Chattopadhyay, University of Delhi | Fault reactivation, intraplate seismicity, and the central Indian Shield | August 12, 2022 |
| 6 | Prof. S.C. Patel, Indian Institute of Technology, Bombay | Magmatism vis-à-vis Deformation and Metamorphism in the Himalayas | August 26, 2022 |
| 7 | Prof. Dapeng Zhao, Tohoku University Sendai, Japan | The big mantle wedge from Japan Trench to East China | August 29, 2022 |
| 8 | Prof. Marcus Nüsser, Heidelberg University, Germany | Cryosphere changes and local adaptation strategies: socio-hydrological case studies from the Upper Indus Basin | October 11, 2022 |
| 9 | Dr. S. K. Varshney, International Division DST, New Delhi | Approaches to International S&T cooperation | February 24, 2023 |
| 10 | Dr. Kalachand Sain WIHG, Dehradun | Geo-hazards in the Himalaya and Plausible Mitigation through AI/ML approaches | March 02, 2023 |

LECTURES DELIVERED/ INVITED TALK BY INSTITUTE SCIENTISTS

| Name of Institute Scientist | Venue/Organizer/Venue/Institute | Date | Topic |
|-----------------------------|---|--------------------|---|
| Anil Kumar | International workshop on 'Luminescence dating: developments in protocols, age models and applications' organized by The Academy of Scientific Research & Technology (ASRT), Egypt & Centre for Science and Technology of the Non-aligned and Other Developing Countries (NAM S&T Centre) | April 06 -07, 2022 | Luminescence dating: developments in protocols, age models and applications |
| Manish Mehta | National Institute of Disaster Management, New Delhi (Online) | April 26, 2022 | Glacial Lake Outburst Flood |
| Kapesa Lokho | The XXVIII Indian Colloquium on Micropaleontology and Stratigraphy held during May 3-7, 2022 at the Department of Environmental Sciences Savitribai Phule Pune University, Pune. | May 03-07, 2022 | The magnificent power of microfossils: case studies in refining stratigraphic age, depositional environment and collisional tectonics in the Indo-Myanmar range |
| Vikram Gupta | Webinar on the possibility of "Indo-Norwegian Collaboration on Geo-Hazards and geo-resources in the Himalaya" | June 01, 2022 | Landslide Hazard in the Himalaya: Characterization and Assessment |
| Anil Kumar | 6th National Geo Research Scholars Meet (NGRSM) at the University of Ladakh, Leh organized by WIHG, Dehradun, and University of Ladakh. | June 07-10, 2022 | Late Quaternary landscape evolution of the Indus River, Ladakh Himalaya: Climate-Tectonic interaction |
| Rakesh Bhamri | 6th National Geo Research Scholars Meet (NGRSM) at the University of Ladakh, Leh organized by WIHG, Dehradun, and University of Ladakh. | June 07-10, 2022 | Karakoram glaciers |
| Sameer Tiwari | 6th National Geo Research Scholars Meet (NGRSM) at the University of Ladakh, Leh organized by WIHG, Dehradun, and University of Ladakh. | June 07-10, 2022 | Geothermal Springs of Himalaya: Source of green energy for a sustainable future |
| Vikram Gupta | 6th National Geo Research Scholars Meet (NGRSM) at the University of Ladakh, Leh organized by WIHG, Dehradun, and University of Ladakh. | June 07-10, 2022 | An overview of Landslide Hazard in the present climate change scenario |

| | | | |
|----------------------|---|--------------------|---|
| Swapnamita choudhuri | NIH and Uttarakhand State Council for Science and Technology (UCOST), Govt. of Uttarakhand, at Graphic Era University, Dehradun | June 22, 2022 | Inventory of Glaciers and Glacier Lakes in NE Himalaya |
| Vinit Kumar | Forest Research Institute (FRI) Dehradun | June 23, 2022 | Himalayan Geo-Environment and hazards (Landslides, cloud burst, Flash Floods, Avalanches, Glacial lake outburst floods) |
| Ajay Paul | Forest Research Institute (FRI) Dehradun | June 24, 2022 | A natural disaster-education and preparedness |
| Vinit Kumar | WIHG, Dehradun | June 30, 2022 | Study of Himalayan Glaciers |
| Rakesh Bhambri | Ministry of Jal Shakti Shram Shakti Bhavan Rafi Marg, New Delhi | July 12, 2022 | Monitoring of Himalayan Glaciers and associated hazards by Wadia Institute of Himalayan Geology |
| Amit Kumar | WIHG, Dehradun | July 15, 2022 | Importance of hydrological and meteorological observations in monitoring Himalayan glaciers and related hazards |
| Vikram Gupta | Online refresher course in Geography - Jawaharlal Nehru University, New Delhi | July 19, 2022 | Landslide Hazard Assessment and Modelling |
| Rakesh Bhambri | WIHG, Dehradun | July 29, 2022 | Monitoring of Himalayan Glaciers and associated hazards |
| A.K. Singh | Refresher Course organized by Dept. Geology, KU, Kurukshetra and UGC-Human Resource Development Centre, KU, Kurukshetra | August 08, 2022 | Remnants of the ancient oceanic lithosphere at suture zone: How was it possible and what does it tell us |
| Parveen Kumar | Ram Charitra Manas School, Karnal, Haryana | August 14, 2022 | Earthquake education and mitigation |
| Vinit Kumar | National Institute of Disaster Management (NIDM), MoHA, GOI, (Online) | August 17, 2022 | Glacial Lake Outburst Flood Risk Assessment |
| Pinkey Bisht | U- SERC, Dehradun | August 23, 2022 | Pleistocene glaciation and deglaciation: implications in the present context of climate change |
| Barun K. Mukharjee | 18th CGPB Sub-Committee X Meeting, Geological Survey of India (Online) | September 01, 2022 | Study of Chromite vein in Ladakh ophiolite |
| Pankaj Chauhan | Himalaya Diwas at WIHG, Dehradun | September 09, 2022 | The Himalaya: Development and Destruction |
| Som Dutt | Hindi Pakhwara, WIHG, Dehradun | 26 September, 2022 | |

| | | | |
|-----------------|--|----------------------|--|
| Kapesa Lokho | WIHG, Dehradun | September 19, 2022 | Geology, people and culture of Northeast India (In Hindi) |
| Bappa Mukherjee | In pre-conference, continue education course of GEO India-2022 conference at JECC Jaipur, organised by ONGC, KDMIPE, Dehradun. | October 12, 2022 | Non seismic techniques in Hydrocarbon exploration |
| Vikram Gupta | Jamia Milia Islamia University, New Delhi | November 02, 2022 | Landslide Hazards, risk and their mitigation measures in the Himalaya National Conference on Landslide Risk Assessment and Mitigation in India |
| Chinmay Halder | Katwa college, West Bengal, India, | November 03, 2022 | Basics of Geophysics and its career opportunities |
| Vikram Gupta | 3rd Triennial Congress of Federation of Indian Geosciences Association on "Geosciences of Himalaya for Sustainable Development", held at WIHG, Dehradun | November 16, 2022 | Landslide and related hazards in the present climate change scenario in the Himalaya: a way forward for sustainable development |
| Pankaj Chauhan | 21 days DST-NGP sponsored training program on Geospatial Technologies scheduled to be held between November 10-30, 2022 at Department of Civil Engineering, Graphic Era Dehradun, Uttarakhand. | November 19, 2022 | Remote Sensing in Geosciences |
| Anil Kumar | National Institute of Disaster Management and Kazi Nazrul University, Asansol (Online) | November 23-29, 2022 | Flood records from the Himalaya: issues and challenges |
| Manish Mehta | National Institute of Disaster Management, New Delhi (Online) | December 07, 2022 | Melting of Glaciers in Himalaya |
| N.K. Meena | Accelerator Users Committee (AUC)-73 organized by Inter-University Accelerator Centre (IUAC), New Delhi | December 15-18, 2022 | Paleoclimate reconstruction from peat records of Chopta Bugyal, Central Garhwal Himalaya |
| M. Prakasam | Accelerator Users Committee (AUC)-73 organized by Inter-University Accelerator Centre (IUAC), New Delhi | December 15-18, 2022 | Paleoclimate and Himalayan weathering changes during the Late Quaternary: a multi proxy records from the Northern Indian Ocean Sediments. |
| Sudipta Sarkar | Accelerator Users Committee (AUC)-73 organized by Inter-University Accelerator Centre (IUAC), New Delhi | December 15-18, 2022 | Holocene paleoclimatic changes from the North-Western Himalaya using lake and peat sediments |
| Mahesh Kapawar | Webinar organized by the Department of Geology, Parul Institute of Applied Sciences, Parul University, Gujrat | December 27, 2022 | Paleomagnetism: a case study from India |
| Kunda Badhe | WIHG Dehradun | December 29, 2022 | Gold Mine |

| | | | |
|----------------------|---|-------------------|--|
| Swapnamita Bhoudhuri | Seminar on "Environment and Sustainable Development", organized by Haflong Government College in collaboration with Government of Assam | January 30, 2023 | Dima Hasao to Joshimath: Mountain hazards, Resilience and the Future |
| Anil Kumar | 4th workshop on Association for Luminescence Dating (ALD), India at Indian Institute of Science and Education Research (IISER), Kolkata from | February 3, 2023 | Luminescence Dating and Applications |
| Pankaj Chauhan | Govt. Inter collage Khati, Kapkot, Bageshwar, Uttarakhand | February 07, 2023 | Man and Environment |
| Vikram Gupta | Doon University, Dehradun | February 09, 2023 | Landslide and related hazards in the present climate change scenario in the Himalaya: a way forward for sustainable development |
| Chhavi P. Pandey | 17th Uttarakhand State Science and Technology Congress-2023, Regional Science Center, Vigyan Dham, Jhajra, Dehradun | February 11, 2023 | International Day for Women and Girls in Science |
| Vikram Gupta | Workshop on "Disaster Resilience in Mountains: Need for Capacity Capacity Building" Administrative Training Institute, Nainital | February 24, 2023 | Promoting eco-friendly tourism models and sustainable structures for mountain tourist destinations rather than emulating multi-storied concrete structures - regulations |
| Som Dutt | 'Monsoon Seminar' series (online), organized by Louisiana State University, USA. | March 01, 2023 | Short term variability in Indian summer monsoon strength since MIS 3 |
| Pankaj Chauhan | Golden jubilee celebration at HNB Garhwal University, Srinagar Garhwal | March 02, 2023 | The Himalaya: Development or Destruction and the role of the early warning system |
| Parveen Kumar | HNB Garhwal University, Srinagar | March 03, 2023 | Steps to be adhered at the time of earthquake |
| Gautam Rawat | Workshop on Data Analytics using Advanced Mathematical Tools, Gurukul Kangri (Deemed to be University) in collaboration with Uttarakhand Science and Education & Research (USERC) | March 13-18, 2023 | Python for Beginners and data visualisation using Python |
| Chhavi P. Pandey | Workshop on Data Analytics using Advanced Mathematical Tools, Gurukul Kangri (Deemed to be university) in collaboration with Uttarakhand Science Education & Research (USERC) | March 13-18, 2023 | Installation of R Packages, extreme value theory & Hands on training on data sets |
| Kapesa Lokho | ONGC, Dehradun | March 17, 2023 | Biostratigraphy, Paleoenvironment, and Paleogeography reconstruction of NE Himalaya, India |
| Rakesh Bhamri | WIHG, Dehradun | March 31, 2023 | हिमालय के हिमनदों और सम्बंधित आपदाओं की निगरानी: संभावनाएं और चुनौतियाँ |

MEMBERSHIP

| | |
|--|--|
| R. J. Perumal Associate Editor : Executive Council member: | Journal of Geological Society of India for three years w.e.f. 2022 The Geological Society of India |
| Rakesh Bhambri Scientific Editor : | Journal of Glaciology, published by Cambridge University Press during 2022-23 |
| Manish Mehta Expert member: Expert member: Expert member: | Joint study team constituted by USAC to "Site inspection of Kedarnath reconstruction works" (Nominated by Director WIHG) NGT for Zonal Master Plan (ZMP) of the Bhagirathi Eco Sensitive Zone (BESZ) Area (Nominated by Director WIHG) Joint study team constituted by USDMA to understand the cause of Avalanche at Kedarnath area (Nominated by Director WIHG) |
| Vinit Kumar Expert member: | Joint study team constituted by USDMA to understand the cause of Avalanche at Kedarnath area (Nominated by Director WIHG) |
| Amit Kumar Member: | Geological Society of America (GSA) |
| Anil Kumar Member: Member: | The Association of Quaternary Researchers (AoQR), India The Association of Luminescence Dating (ALD), India |
| Subhojit Saha Member: | A Life Member of the Indian Association of Sedimentologists (IAS) |
| Pinkey Bisht Member: Member: Member: Member: | The Association of Quaternary Researchers (AoQR), India A Life Member of Himalayan Geology American Geophysical Union (AGU) The panel discussion in the one-day National seminar on "Northwest & Central Himalayan Natural Disasters held at Doon University, Dehradun on 28th March 2023 |
| Chhavi P. Pandey Member: | A Life Member of Himalayan Geology |
| Kapesa Lokho Member: Member: Member: | Elected as a Fellow of the Geological Society of India Organizing committee for the 21st Convention, Indian Geological Congress Elected as Executive Council of the Palaeontological Society of India for the tenure 2022-2024 |

PUBLICATION AND DOCUMENTATION

The Publication & Documentation section brought out the (i) 'Himalayan Geology' volumes 43(2) 2022 and 44(1) 2023; (ii) Annual Report of the Institute for the year 2021-22 (bi-lingual); (iii) Hindi magazine 'Ashmika' volume 28 (2022); (iv) Abstract & Souvenir volume for the 3rd Triennial Congress of the Federation of Indian Geosciences Associations on “Geosciences of Himalaya for Sustainable Development” held during November 16-18, 2022, (v) Field Excursion Guide for 6th National Geo-Research Scholars Meet, held on June 7-10, 2022, and (vi) Publicity brochures, etc.

The section was also involved in the dissemination of the publications to individuals, institutions, lifetime subscribers, book agencies, national libraries, and indexing agencies, under an exchange program, and maintaining the sale & accounts of publications. Apart from this, works pertaining to the printing of publicity brochures, letterheads, certificates, etc., are also taken up.

The website (<http://www.himgeology.com>) of Himalayan Geology (journal) is functioning along with

an online manuscript submission facility under this section. All information regarding the journal, including contents and abstracts is updated from time to time on the website. Online access to the currently published volume to the online subscribers and lifetime members (those who have been given the choice to obtain the volumes in soft copy through online access/email) has also been provided. At present, 171-lifetime subscribers receive the journal through online access/email. The journal is indexed in UGC CARE, Scopus, Web of Science (SCIE), Thomson Reuters/Clarivate Analytics (US), Elsevier (Netherlands), and Indian Citation Index (India) regularly etc. The current impact factor of the journal is 1.311 (Source: Clarivate Analytics).

The section also provides the facility and technical support services of A0 size scanning and printing to the scientists, research scholars, and other staff of the Institute. During this period, more than 223 maps and posters were printed for display in laboratories, workshops/seminars and exhibitions, etc. and 198 maps/sheets were scanned.

LIBRARY

The Library of Wadia Institute of Himalayan Geology has a special status owing to its best collection of books, monographs, journals, e-books, etc., on the mountain building process and geological and geophysical phenomena with special reference to the Himalaya. Also, the collection and services offered make it one of the best libraries in the country in the field of earth sciences. The scientists, researchers, project staff, and students make full utilization of the Library while publishing their research work in reputed peer-reviewed journals. Specialists and professionals across the country also visit our Library to consult thematic and rare collections available at the Library. The Library has more than 6882 selected e-books from different publishers and societies on the thrust areas of the research in the Institute.

Acquisition of Documents: The Library has paid and subscribed to 58 International and 2 Indian Journals, and 11 magazines during this year. A total of 30 reference books were added. In addition to this, a total number of 133 books have been purchased for the Hindi Collections.

National Knowledge Resource Consortium (NKRC): The Library is a member of NKRC and continues to receive the support of Consortia towards online access to Elsevier's "Earth and Planetary Science collection", Wiley's "Earth, Space & Environmental Sciences"; Springer "Earth and Environmental Science and Chemistry" collections. WIHG Library has access to the publications of the American Institute of Physics, American Physical Society, Derwent Innovation Index (with Web of Knowledge), Emerald Group Publishing, IEEE, NPG: Nature -Main Journal, NPG: Nature Geoscience, Royal Society of Chemistry, Science magazine, Springer Journals, Taylor & Francis, Web of Science, Elsevier-Scopus, Wiley & Blackwell, iThenticate (Plagiarism Detection Software). All these publishers contribute online access to more than four hundred journals' titles, apart from WIHG subscriptions.

Grammarly, Knimbus, E-Journals, E-books and Pro-Quest databases (Dissertations and Theses, Science and Technology E-Books) were also purchased during this period.

Reprography facility: The Library serves as a central facility for the reprography. This facility is being extended to the scientific and administrative sections of the Institute. A total of 65000 (approx) pages were copied during the reporting year.

Computer Facility: The Library has a hub of computers for the users to access the e-books and e-journals and other e-resources available, either subscribed by WIHG Library or available through NKRC. This facility was also extended to the students and summer trainees. The hub is also being used for conducting several tests towards the recruitment of the administrative and technical staff of the Institute.

The WIHG library provides the following services to support Scientific, Technical, and Administrative work: (i) Reprographic Services, (ii) Reference and Consultation Services, (iii) Electronic information resource access, (iv) Document Delivery Services, (v) CD-ROM Database, (vi) CAS and SDI, (vii) Printing of Article, (viii) Scanning of Document, (ix) Plagiarism Check, and (x) Circulation Service. The Library organized a training program in collaboration with Knimbus Online P.V.T., New Delhi in virtual mode. The training program dealt with the improvement of Remote Access searching skills using Knimbus software. The WIHG participants got benefits from this online training. The training was coordinated by Dr. Balam, WIHG, Dehradun, and Mr. Akash Arora from Knimbus, New Delhi.



WIHG Library

S.P. NAUTIYAL MUSEUM

S. P. Nautiyal Museum is a major axis of education and continues to connect people with knowledge and information related to geological and allied research in the Himalaya. Museum, as usual, remained the main centre of attraction for the students and general public not only from the far-flung corners of India but also from overseas.

The Museum rethought ways to offer a unique experience to our audience and introduced a Virtual Museum Tour from our official website (www.wihg.res.in), which allowed users to explore the museum remotely. The museum organized various ambitious programs outside its venues, including public programs and touring exhibitions. These exhibition the highlighted the Institute's activities and the achievements and rare collections of the museum.

This year, the museum participated in an outdoor exhibition on various occasions as follows:

- Akash Tattva, Uttaranchal University, Dehradun, 04th – 07th November, 2022
- 3rd Triennial Congress, Federation of Indian

Geosciences Association, WIHG, Dehradun, 16th - 18th November, 2022

- Dehradun International Science & Technology Festival, Vigyan Dham, Dehradun, 25th – 27th November, 2022
- 108th Indian Science Congress, 3rd - 7th January, 2023, Nagpur, Maharashtra, India
- India International Science Festival (IISF), Bhopal, MP, 21st – 24th January, 2023
- “Pride of Uttarakhand Expo” in Rural Science Congress, UCOST, Vigyan Dham, 10th – 12th February, 2023
- Vasant Utsav, Rajbhavan, Dehradun, 3rd - 5th March, 2023

Open days were observed on the National Technology Day (May 11, 2022), Foundation Day (June 29, 2022), Founder's Day (October 23, 2022) and National Science Day (February 28, 2023). Like in previous years, enormous number of students and general public visited the museum on these occasions.



Shri Ashok Kumar (IPS), DGP Uttarakhand, visiting Museum on the occasion of New Year Talk on 5th January 2023

TECHNICAL SERVICES

Analytical Services

The number of samples analyzed by various instruments are listed in the following table:

| Laboratory/Instruments | Number of samples analyzed | | |
|---|----------------------------|---------------|---------------|
| | WIHG Users | Outside Users | Total |
| Inductively Coupled Plasma Mass Spectrometer (ICP-MS) Lab | 452 | 611 | 1063 |
| Laser Ablation Inductively Coupled Plasma Mass Spectrometer (LA- MC-ICP-MS) Lab | | | |
| Liquid mode | 197 | 54 | 251 |
| Solid mode | 19 | 4 | 23 |
| Stable Isotope Lab | 365 | 40 | 405 |
| Luminescence Dating (TL/OSL) Lab | 60 | 28 | 88 |
| Fission Track Lab | 18 | - | 18 |
| Mineral Separation Lab | 65 | 25 | 90 |
| Sample Preparation Lab | | | |
| Slide preparation | 545 | 609 | 1154 |
| Sample powdering | 436 | 623 | 1059 |
| XRD Lab | Newly Installed | | |
| X-Ray Fluorescence Spectrometer (XRF) Lab | 839 | 1029 | 1868 |
| Scanning Electron Microscope (SEM) Lab | 180 | 94 | 274 |
| Laser Micro Raman Spectrometer (LMRS) & Fluid Inclusion Lab | 43 | 20 | 63 |
| Rock magnetic & Paleomagnetism Lab | 150 | - | 150 |
| Dendrochronology Lab | 12 Tree cores | Nil | 12 Tree cores |
| Micropaleontology Lab | 320 | - | 320 |
| Laser Particle Size Analyzer (LPSA) Lab | 178 | 19 | 197 |
| Sedimentology Lab | - | - | - |
| Vibratory Sieve Shaker | - | 51 | 51 |
| Clay Slide Preparation | - | - | - |
| Palynology Lab | 54 | - | 54 |
| Laser Water Isotope Analyzer (LWIA) Lab | 572 | 174 | 746 |
| Water Chemistry Lab (Ion-Chromatograph) | 484 | 117 | 601 |
| Total Organic Carbon Lab | 516 | - | 516 |

Technical Coordination, Planning, Monitoring, and Evaluation (TCPME) section

The TCPME section is responsible for various tasks, including receiving and reviewing project proposals, forwarding them to the Director for consideration, and

transmitting them to funding agencies. It scrutinizes tour programs for scientists and scholars and liaises with stakeholders for funding. TCPME provides scientific inputs to Institute authorities and DST, New Delhi, and prepares responses to parliamentary

questions. It arranges internal and external reviews of scientists' work and monitors the progress of projects. Additionally, TCPME maintains a record of communicated papers and abstracts for publication in journals, books, and conferences.

Photography Section

The WIHG Photography section captures high-quality images of institute functions and activities. These digital images are used for institute web pages and report preparation. During the reporting period (2022-2023), approximately 7000 photographs and video recordings (150GB) were taken using high-resolution DSLR cameras. These covered various events, such as Foundation Day, Founders Day, National Science Day, National Technology Day, New Year's Day, Republic Day, Independence Day, Women's Day, Seminars/Symposia, cultural programs, and superannuation programs, etc. Additionally, around 400 photographs were taken of rocks and fossils in the museum. Scientists used cameras for field and laboratory work, while project members and research scholars have access to cameras from a shared pool as needed.

Drawing Section

The Drawing Section provides the cartographic needs of the Scientists of the Institute for in-house as well as sponsored project works. During this year, the section has provided sixteen geological maps/structural maps/geomorphological maps/seismicity diagrams for the scientists and research scholars of the Institute. Besides, the tracing of three topographic sheets/aerial photo maps was carried out along with the preparation of the three geological columns. The section has also provided name labels and thematic captions during different activities and functions of the Institute.

Sample Preparation Laboratory

The Sample Preparation Lab of WIHG, Dehradun, is a world-class analytical facility that prepares samples for high-end geochemical, structural, sedimentological, and geotechnical investigations. Currently, ordinary and EPMA thin-sections slides are being prepared in this facility. Mineral Separation and slide preparation work for the geochronological and thermochronological

investigation is an integrated component of this facility. The Lab also performs the powdering of rock samples for XRF, ICPMS, and OSL investigations. The Lab is equipped with Buehler, Struers make rock cutting and polishing machines. In addition, the lab also has a Frantz Magnetic Barrier Separation, Fritsch Jaw Crusher, and Disk Mill, Holman Wilfley Table, Automatic Polishing machine. Such a high-end facility is being used by researchers of various R & D institutes and universities all across India.

Computer and Networking Section

WIHG Computer & Networking Section takes care of all the computational requirements of the Institute to facilitate important research work free of any IT-related worries. The role and responsibilities of the Computer Section has increased manifold after the Corona pandemic. The employees of the Computer Section work diligently to provide uninterrupted IT services to the Institute. The pandemic changed the way meeting, seminars, interviews, etc. are conducted, and ever since not only have many of the important meetings been conducted online but important seminars, conferences, workshops, and interviews have also been organized and conducted online or in hybrid mode successfully. As a part of celebrating the 75th year of India's Independence, WIHG has been organizing Distinguished Lectures by Eminent Scientists/Professors around the year. Most of these lectures have been conducted online using MS Teams and WIHG Computer Section has been instrumental in the successful conducting of these lectures by providing all-round support for the same. Even during the offline events, requisite arrangements as per the requirement were made for the success of the events.

After the Joshimath disaster, scientific instruments have been installed at various locations by the Institute. WIHG Computer Section extended its services to the installation and configuration of data servers at the Geophysics division for the live streaming, storage, sharing, and backup of scientific data.

IPv6, the latest version of IP, was developed to overcome the challenge of a limited pool of IPv4 addresses. Conforming to the orders from the Ministry, the IPv6 implementation has been successfully done by the computer section.

As per the instructions from the S & T Ministry, the Cyber Jagrookta Diwas (CJD) is being organized on the first Wednesday of every month to create awareness about the latest cyber threats and cyber hygiene for the prevention of cyber crimes. Lectures and presentations were given not only to the Institute employees and research scholars, but efforts have also been made towards educating the security guards, gardeners, and housekeeping staff so that they can also be made fully aware of these threats and safeguard against any loss arising from it.

The Computer Section manages various servers which have been installed and configured by the Computer Section. All the servers are working on a secure Linux environment and using the latest Open Source Technology. The different types of servers being used are DNS, Mail, Web, Application, etc. The Institute is connected with the National Knowledge Network through a high-speed 1 Gbps link. For uninterrupted internet connectivity, a standby internet bandwidth leased line connectivity link has also been taken. The section has not only maintained a virus and spyware-free environment by adopting centralized anti-virus and anti-spyware solutions but has also been adopting the latest preventive security measures in this regard.

Apart from the above, the WIHG Computer Section also:

- Provides support for hardware trouble-shooting, maintenance requirement, software and other facilities like data backup, data retrieval, etc.
- Uses the latest networking technologies for excellent speed and reliability of all the network-related services, which are the need of the hour.
- Maintains and upgrades the network of offices as well as in the WIHG residential colony, Guest House and Research Scholars cum Transit Hostel so that the researchers can have 24-hour access to the online resources essential for their ongoing scientific research.
- Provides a VPN facility to facilitate the access of Institute resources securely over a public network.
- Maintains the different web portals hosted by the Institute viz., Institute website, Institute publication portal, WAICS (Wadia Analytical Laboratory Instrument Facility and Consultancy Advisory Services) portal.

Apart from this, extensive use of open source software has been done by the section on different computers, workstations, and servers, thereby saving considerable financial resources that may have been spent in purchasing other commercial paid software and solutions.

CELEBRATIONS

National Technology Day

Technology Day was celebrated in the Institute on May 11, 2022, by observing an Open Day. On this occasion, a

seismological observatory was inaugurated followed by a formal address by Dr. Kalachand Sain, Director of the Institute.



Moments of National Technology Day celebration at WIHG.

8th International Yoga Day

International Yoga Day was celebrated on 21st June 2022 in the Institute. Since 2015, International Yoga Day has been celebrated on June 21 every year. The theme of this year's Yoga Day celebrations is 'Yoga for Humanity'. WIHG employees and research students participated in Yoga under the directive and guidance of Ms. Pooja Devi, Assistant Professor Department of Yogic Science, Govt. PG College Dakpathar, Dehradun.





Employees of the Institutes practicing Yoga on the International Yoga Day

Foundation Day

The Foundation Day of the Institute was celebrated on June 29, 2022. On this occasion, Dr. Rajendra Dobhal,

Director General, Uttarakhand State Council for Science and Technology (UCOST), Govt. of Uttarakhand delivered a Foundation Day Lecture on the



Felicitations of the Guest-of-Honour, Dr. Rajendra Dobhal, Director General of UCOST, Uttarakhand during the Foundation Day program

topic “Analysing R & D systems in India: Future ahead” The occasion was also marked by the distribution of awards. Prof. R. C. Misra awards for the year 2022 was awarded jointly to Dr. Ashutosh Pandey, Assistant Professor, Pondicherry University, Puducherry, and Dr. Ningthoujam Premjit Singh, WIHG, Dehradun, in recognition of their outstanding contribution in the field of Geosciences. The best research paper award was given to Dr. Kalachand Sain, Director, WIHG, Dr. Amit Kumar, Dr. Manish Mehta, Dr. Akshaya Verma,

Dr. Sameer K. Tiwari, Dr. Purushottam K. Garg, Dr. Vinit Kumar, Dr. Santosh K. Rai, Dr. Pradeep Srivastava & Dr. Koushik Sen for the research paper entitled “A Perspective on Rishiganga-Dhauliganga Flash Flood in the Nanda Devi Biosphere Reserve, Garhwal Himalaya, India ” published in the journal “Journal of the Geological Society of India ”. The best performance award was given to Shri S.K. Srivastava (Administrative Officer).



Dr. Kalachand Sain receiving the 'Best Paper Award' from Dr. Rajendra Dobhal



Shri S.K. Srivastava receiving the 'Best Performance Award' from Dr. Rajendra Dobhal

Independence Day

The Institute celebrated the Independence Day on August 15, 2022. Flag hoisting was followed by a

formal address by Dr. Kalachand Sain, Director of the Institute. As a mark of Independence Day celebrations, various programs were organized, such as tree



Flag hoisting, formal address by Dr. Kalachand Sain, Director WIHG and various sports activities as a part of Independence Day Celebration

plantation, drawing competitions, and games for the Institute employees and their children. Prizes were distributed to the winners of various events.

Founder's Day

The Birth Anniversary of Prof. D. N. Wadia was celebrated on October 23, 2022, as 'Founder's Day'. In Honour of Prof. D. N. Wadia, a floral tribute was paid by Institute staff on the occasion.

Swachhata Hi Seva campaign

Swachhata Hi Seva campaign under Swachh Bharat

Mission was celebrated at WIHG, Dehradun, on October 02, 2022. This event is celebrated every year. A pledge was taken by all the institute employees. During this event, various activities were carried out, such as mass pledge of all employees of the Institute, sanitization, and cleaning of rooms and labs by the employees, lectures delivered by Dr. Kalachand Sain, Director WIHG and Shri Pankaj Verma, Registrar, WIHG on the importance of Garbage free, clean and green campus of WIHG, and all the employees contributed towards cleaning the campus of WIHG.



Moments during the Swachhata Hi Seva campaign

Vigilance Week

The Vigilance Awareness Week- 2022-2023 was observed this year from October 31 to November 06, 2022. All the scientists and staffs of the institute took the Integrity pledge along with Rashtriya Ekta Diwas pledge on October 31, 2022.



Republic Day

Dr. Kalachand Sain, Director, unfurled the National Flag on Republic Day, January 26, 2023, and addressed the gathering, followed by sweet distribution.



Republic Day Celebration on January 26, 2023

National Science Day

The institute observed 'National Science Day' on February 28, 2023. Dr. Kalachand Sain, Director, WIHG delivered the 'National Science Day Lecture' on "Geo-hazards in the Himalaya and Plausible Mitigation" followed by an interaction session with Ms. Sushma Rawat, Director, Exploration, ONGC, Dehradun. The Institute also observed an 'Open Day' on February 28, 2022, wherein laboratories were kept open to students and the public. A large number of school children, college students, and other public from Dehradun visited the Laboratories.



Ms. Sushma Rawat interacting with researchers of WIHG, Dehradun



Demonstrations of scientific labs and museum to school students during National Science Day

Outreach program

Wadia Institute of Himalayan Geology (WIHG), Dehradun successfully runs an outreach program entitled “भूकंप के लिए तैयारी करने और खतरे की कमी के लिए शिक्षा और जागरूकता कार्यक्रम: (“Education and

awareness program for earthquake preparedness and hazard mitigation”).

Under this program people from the villages, school, universities, organisations and general public are educated for preparation and steps to be adhered at



Interaction with the School children at WIHG seismological observatory



Earthquake awareness lecture at Kendriya Vidayala (OLF) Raipur, Dehradun

the time of the earthquake. Mock drill is also performed. The WIHG earthquake observatory is visited by hundreds of visitors and researchers of the Institute take this opportunity to educate them for earthquake awareness. Further to fulfil the objectives of this outreach program more comprehensively various schools, villages and institutes are visited. WIHG prepared pamphlets containing what to do and what not to do during and after an earthquakes and distributed among the school children, as well as the general public. To educate about earthquake, several lectures through slide shows and videos have been delivered, and mock drills have been performed at various schools/institutions and villages. During 2022-2023, the scientist of the Institute interacted directly with nearly 3300 persons of different regions of the Uttarakhand state under this awareness program. The Institute Scientists visited (i) Rajkiya Prathamik Vidyalaya, Ambiwala, (ii) Eklavya Adarsh Vidyalaya, Kalsi, (iii) JNV, Shankarpur (iv) FRI, Dehradun (v) Ram Charitra Manas School, Karnal, Haryana, (vi) KV OLF, Raipur, and (vii) Garhwal University, Srinagar.

The following organizations/schools visited the WIHG earthquake observatory in 2022-23: (1) Doon Scholar School, Dehradun, (2) RIMC, Dehradun, (3) St. Kabir Academy School, Dehradun, (4) UPES Dehradun, (5) Officer Trainee state Forest, Dehradun, (6) University of Ladakh, Leh, (7) Doon University, (8) Quantum University, Roorkee, (9) Kutch University, (10) Guru Nanak Mission Public School, Vikas Nagar, (11) Doon Business School, Selaqui, (12) Central University, Punjab, (13) Universal Academy, Dehradun, (14) Shikshankur the Global School, Dehradun, (15) Tonsbridge School, Dehradun, (16) Walham Boys school, Dehradun, (17) Montessoriee School, Dehradun.

International Women's Day

International Women's Day is a significant event that is celebrated globally on the 8th of March every year. This year, the theme of International Women's Day was "Embrace Equity". It is a day to celebrate the social, economic, cultural, and political achievements of women and to advocate for gender equality.

The International Women's Day was celebrated on March 13, 2023 at WIHG, Dehradun. Dr. Geeta Khanna, Chairperson, State Commission for Protection of Child Rights, Uttarakhand, was the chief guest of the event. The event was started with a welcome address by



Moments during the celebration of international Women Day-2023

Dr. Kalachand Sain, Director WIHG which was followed by the motivating speech by Prof. Talat Ahmad, Chairman of the Governing Body of the Institute. Finally, the Chief guest delivered her lecture on the importance of women's empowerment and gender equality that was thought provoking and inspiring for all. The event was celebrated by scientists,



Moments during the celebration of international Women Day-2023

research scholars and other staff of the Institute. There was an interactive session, where some of the scientist and research scholars shared their thoughts. At the end,

on behalf of the Institute, a small token of appreciation & gratitude was presented to all the Women colleagues.

DISTINGUISHED VISITORS TO THE INSTITUTE

- Prof. Marcus Nüsser, South Asia Institute, University of Heidelberg, Germany
- Shri Ashok Kumar , IPS , Director General of Police, Uttarakhand
- Miss Gita Khanna, Journalist, film director, and women's rights and human rights activist
- Ms. Sushma Rawat, Director, Exploration, ONGC, Dehradun
- Dr. Lipika Dey, Principal Scientist at TCS Research
- Prof. Arvind Kumar Mishra, Director, CSIR-CIMFR, Dhanbad



Prof. Marcus Nüsser, Germany



Shri Ashok Kumar , DGP, Uttarakhand



Miss Gita Khanna, women's rights and human rights activist



Ms. Sushma Rawat, Director, Exploration, ONGC

STATUS OF IMPLEMENTATION OF HINDI

The Institute follows the policy and guidelines of Rajbhasha Vibhag and regularly submits its quarterly and half-yearly progress reports to Rajbhasha Vibhag, Department of Science and Technology. Institute also presents the half-yearly reports to NARAKAS, Dehradun. Rajbhasha Implementation Committee is monitoring the implementation of Hindi in the Institute under the chairmanship of the director of the Institute. The committee monitors and plans for progressive increment in official language use. The committee takes cognisance of the progress in the Hindi implementation through its regularly organised quarterly meetings.

Rajbhasha Implementation Committee regularly organises quarterly workshops to promote official language use. In these workshops, the committee organised various lectures to popularise and encourage using Hindi in scientific research, lessons on Hindi typing, and information about rules and regulations for Rajbhasha implementation.

Under the banner of the Rajbhasha Implementation Committee, Institute celebrates Hindi Pakhwara from 14 Sep to 28 Sep 2022 in the Institute. This year Hindi Pakhwara is inaugurated with the inauguration program of the Hindi Diwas program in Surat, Gujrat, by Honourable Home Minister Shri Amit Shah.

During Hindi pakhwara, Institute Scientists delivered various lectures about general scientific interests. Among notable talks were from Drs Swapnmita Vaidswaran, Somdutt, Gautam Rawat, Kapesh Lokho and Shri Tajendra Ahuja. Essay competitions and debates for school children were organised and participated in by various Schools from Dehradun city.

The committee arranged lectures for eminent personalities from the region. In this series, Professor Sushil Upadhyay, Principal Chamanlal Degree College, Landhora, Haridwar, delivered a Lecture on new words and the challenges of their uses. Another lecture by notable personality Shri Anup Nautiyal on the Himalayan Charter for Uttarakhand elaborates on the basic needs of Uttarakhand state for its progressive and sustainable future. Talks from reputed Heart Specialist Dr Priti Sharma from Max Hospital and Psychologist Dr Saloni Gupta provide information to Institute employees about the basics for keeping good health. A Photography competition and Akhil Bhartiya Kavi Sammelan were other attractions of the Pakhwara celebrations.

In the closing ceremony of the Pakhwara, Prof (Dr.) Anita Rawat, Director, Uttarakhand Science Education and Research Centre (USERC), Department of Information and Science Technology, Govt. of Uttarakhand, is the chief guest of the closing ceremony of the pakhwara. In her remark, she emphasised the role of the mother tongue in the development of human society. In the end, the chief guest distributed prizes to winners of different events.

This year the 28th issue of the Annual Hindi Magazine “Ashmika” was published. Authors from various organisations and employees of the Institute contributed articles to the magazine. The articles in the magazines are informative and well-appreciated by the readers. The attempt is to get more and more popular science articles in Hindi.



Moments during the closing ceremony of the Hindi Pakhwara with Prof (Dr.) Anita Rawat, Director, Uttarakhand Science Education and Research Centre (USERC), Govt. of Uttarakhand

MISCELLANEOUS ITEMS

1. Reservation/Concessions for SC/ST employees

The government's orders on reservations for SC/ST/ OBCs are followed in recruitment to posts in various categories.

2. Monitoring of personnel matters

Monitoring of personnel matters relating to employees of the Institute is done through various Committees appointed by the Director/Governing Body from time to time.

3. Mechanism for redressal of grievances

The Grievance Redressal Committee (GRC) consisting of five senior scientists/officers, is operational in this institute. During the reporting period, a total of three grievances were received. Two of them were related to recruitment and one regarding interaction with journalists. All the three were received through the Prime Minister's office (PMO). The grievances of the applicants against the posts advertised were related to their disqualified application. Two grievances were replied after looking into the relevant documents and one citing website information.

4. Welfare measures

The Institute has various welfare measures for the benefit of its employees. Various advances like House Building Advance, Conveyance Advance, Festival Advance, etc. are given to the employees. There is a salary Earner's Cooperative Society run by the Institute employees that provides loans to its members as and when required. The Institute also runs a canteen for the welfare of the employees and students. As a welfare measure, the Institute is providing recreational facilities to its employees.

5. Mechanism for redressal of complaints of sexual harassment of women employees at workplaces

To safeguard the women employees and to enquire into the complaints of sexual harassment of women

employees at workplaces in the Institute, a separate Committee has been constituted. The Committee consists of five members: the Chairperson and four other members of the Committee, with a member from the Wild Life Institute of India, Dehradun. For the reporting period, one RTI was received. Another case was forwarded from the competent authority for the committee's evaluation. The committee submitted an appropriate report after deliberations among the members.

6. Status of Vigilance Cases

No vigilance case is pending in the year 2022-2023.

7. Information on the RTI cases

The details of information on the RTI cases during the year 2022-23 are as under:

| Details | Opening balance as on 01.04. 2022 | Received during the year 2022- 2022 | Number of cases transferred to other public authorities | Decisions where requests/ appeals were rejected | Decisions where requests/ appeals were accepted |
|--------------------------|-----------------------------------|-------------------------------------|---|---|---|
| Requests for information | 0 | 64 | 0 | 1 | 63 |
| First appeals | 1 | 5 | 0 | 0 | 6 |

8. Sanctioned Staff strength (category wise)

| Group/ Category | Scientific | Technical | Administ-rative | Ancillary | Total |
|-----------------|------------|-----------|-----------------|-----------|------------|
| A | 63 | 0 | 2 | 0 | 65 |
| B | 0 | 4 | 14 | 0 | 18 |
| C | 0 | 60 | 22 | 35 | 117 |
| Total | 63 | 64 | 38 | 35 | 200 |

9. Sanctioned and released budget grant for the year 2022-2023

| | | |
|-----------|---|-------------------|
| Plan | : | Rs. 4366.00 Lakhs |
| Non- Plan | : | NIL |
| Total | : | Rs. 4366.00 Lakhs |

STAFF OF THE INSTITUTE

Scientific Staff:

| | | | |
|-----------------------------------|--|------------------------------|---------------|
| 1. Dr. Kalachand Sain | Director | 47. Dr. P. Chinmoy Kumar | Scientist 'B' |
| 2. Dr. H.K. Sachan | Scientist 'G' (Retd. on 31.5.2022) | 48. Dr. Chinmay Haldar | Scientist 'B' |
| 3. Dr. Vikram Gupta | Scientist 'F' | 49. Dr. Subhojit Saha | Scientist 'B' |
| 4. Dr. Pradeep Srivastava | Scientist 'F' (Tech. Resig- nation w.e.f. 02.07.2022) | 50. Dr. Jairam Singh Yadav | Scientist 'B' |
| 5. Dr. Ajay Paul | Scientist 'F' | 51. Dr. Subham Bose | Scientist 'B' |
| 6. Dr. R. Jayangonda Perumal | Scientist 'F' | 52. Dr. Naveen Chandra | Scientist 'B' |
| 7. Dr. A.K. Singh | Scientist 'F' | 53. Dr. N. Premjit Singh | Scientist 'B' |
| 8. Dr. K.S. Luirei | Scientist 'E' | 54. Dr. Tariq Anwar Ansari | Scientist 'B' |
| 9. Dr. (Mrs.) Kapesa Lokho | Scientist 'E' | 55. Dr. Bappa Mukherjee | Scientist 'B' |
| 10. Dr. R.K. Sehgal | Scientist 'E' | 56. Dr. Rajeeb Lochan Mishra | Scientist 'B' |
| 11. Dr. Santosh Kumar Rai | Scientist 'E' | 57. Dr. Mahesh Kapawar | Scientist 'B' |
| 12. Dr. Jayendra Singh | Scientist 'E' | 58. Dr. Kunda Badhe | Scientist 'B' |
| 13. Dr. B.K. Mukherjee | Scientist 'E' | | |
| 14. Dr. Naresh Kumar | Scientist 'E' | | |
| 15. Dr. Gautam Rawat | Scientist 'E' | | |
| 16. Dr. Devajit Hazarika | Scientist 'E' | | |
| 17. Dr. Kaushik Sen | Scientist 'E' | | |
| 18. Dr. Satyajeet Singh Thakur | Scientist 'E' | | |
| 19. Dr. Narendra Kumar Meena | Scientist 'E' | | |
| 20. Dr. Param Kirti Rao Gautam | Scientist 'E' | | |
| 21. Dr. Dilip Kumar Yadav | Scientist 'E' | | |
| 22. Dr. Manish Mehta | Scientist 'E' | | |
| 23. Dr. Rajesh S. | Scientist 'D' | | |
| 24. Dr.(Mrs)Swapnamita Choudhuri | Scientist 'D' | | |
| 25. Dr. Vikas | Scientist 'D' | | |
| 26. Dr. Som Dutt | Scientist 'D' | | |
| 27. Dr. Anil Kumar | Scientist 'D' | | |
| 28. Sh. Saurabh Singhal | Scientist 'D' | | |
| 29. Dr. Narendra Kumar | Scientist 'D' | | |
| 30. Dr. Parveen Kumar | Scientist 'D' | | |
| 31. Dr. Vinit Kumar | Scientist 'C' | | |
| 32. Dr. Aditya Kharya | Scientist 'C' | | |
| 33. Dr.(Ms) Suman Lata Srivastava | Scientist 'C' | | |
| 34. Dr.(Mrs) Chhavi Pant Pandey | Scientist 'C' | | |
| 35. Dr. Paramjeet Singh | Scientist 'C' | | |
| 36. Dr. Sameer Kumar Tiwari | Scientist 'C' | | |
| 37. Dr. Sudipta Sarkar | Scientist 'C' | | |
| 38. Dr. Pinkey Bisht | Scientist 'C' | | |
| 39. Dr. Rakesh Bhambari | Scientist 'C' | | |
| 40. Dr. Amit Kumar | Scientist 'C' | | |
| 41. Dr. C. Perumalsamy | Scientist 'C' | | |
| 42. Dr. Pratap Chandra Sethy | Scientist 'C' | | |
| 43. Dr. M. Prakasam | Scientist 'B' | | |
| 44. Dr. Mutum Rajnikanta Singh | Scientist 'B' | | |
| 45. Dr. Rouf Ahmad Sah | Scientist 'B' | | |
| 46. Dr. Pankaj Chauhan | Scientist 'B' | | |

Technical Staff:

| | |
|---------------------------------|--------------------------|
| 1. Shri Sanjeev Kumar Dabral | Sr. Tech. Officer |
| 2. Shri Rakesh Kumar | Sr. Tech. Officer |
| 3. Shri N.K. Juyal | Sr. Tech. Officer |
| 4. Shri C.B. Sharma | Executive Engineer |
| 5. Shri T.K. Ahuja | Technical Officer |
| 6. Shri S.S. Bhandari | Technical Officer |
| 7. Shri Rambir Kaushik | Technical Officer |
| 8. Shri Bharat Singh Rana | Technical Officer |
| 9. Shri Gyan Prakash | Asstt. Pub & Doc Officer |
| 10. Dr. Balram | Librarian |
| 11. Shri R.M. Sharma | Sr. Lab. Technician |
| 12. Smt. Sarita | Sr. Tech. Assistant |
| 13. Shri Rakesh Kumar | Sr. Tech. Assistant |
| 14. Ms. Sakshi Maurya Chaudhary | Sr. Tech. Assistant |
| 15. Ms. Disha Vishnoi | Sr. Tech. Assistant |
| 16. Shri Vipin Chauhan | Technical Assistant |
| 17. Shri Deepak Kumar | Technical Assistant |
| 18. Shri Akash Khati | Technical Assistant |
| 19. Shri Pramod Kumar | Technical Assistant |
| 20. Shri Rahul Lodh | Lab Assistant |
| 21. Shri Nain Das | Lab Assistant |
| 22. Shri Prateek Negi | Artist cum Modeller |
| 23. Shri Nand Ram | Elect.-cum-Pump Optr. |
| 24. Shri Tarun Jain | Draftsman |
| 25. Shri Pankaj Semwal | Draftsman |
| 26. Shri Anil Singh | Draftsman |
| 27. Shri Santu Das | Section Cutter |
| 28. Shri Puneet Kumar | Section Cutter |
| 29. Shri Amit Bhandari | Jr. Photographer |
| 30. Shri Hari Singh Chauhan | F.C.L.A. |
| 31. Shri Ravi Lal | F.C.L.A. |
| 32. Shri Preetam Singh | F.C.L.A. |
| 33. Shri Sanjeev Kumar | F.C.L.A. |
| 34. Shri Deepak Tiwari | F.C.L.A. |
| 35. Shri Ajay Kumar Upadhaya | F.C.L.A. |

| | | | |
|----------------------------|--|------------------------------|-------------------|
| 36. Ms. Sangeeta Bora | F.C.L.A. | 27. Sh. Dinesh Kumar Singh | Lower Divi. Clerk |
| 37. Sh. Deepak Kumar | F.C.L.A. (Tech. Resig- nation w.e.f 04.07.2022) | 28. Ms. Rachna | Lower Divi. Clerk |
| 38. Km. Anjali | F.C.L.A. | 29. Mrs. Pushpa Barthwal | Lower Divi. Clerk |
| 39. Sh. Ajay Kumar | F.C.L.A. | 30. Sh. Amit Kumar | Lower Divi. Clerk |
| 40. Sh. Vipin Kumar Aditya | F.C.L.A. | 31. Sh. Pintu Kumar | Lower Divi. Clerk |
| 41. Sh. Nitesh Kumar | F.C.L.A. | 32. Sh. Naved Khan | Lower Divi. Clerk |
| 42. Sh. Rajat Tomar | F.C.L.A. | 33. Sh. Vishesh Kumar Gautam | Lower Divi. Clerk |
| 43. Sh. Abhishek Kumar | F.C.L.A. | 34. Ms. Saba | Lower Divi. Clerk |
| 44. Sh. Sandeep Singh | F.C.L.A. | 35. Sh. Manjeet Rana | Lower Divi. Clerk |
| 45. Sh. Ajit Kumar | F.C.L.A. | | |
| 46. Shri B.B.Panthri | Field Attendant (Retd. on 31.12.2022) | | |
| 47. Sh. Narender Manral | Field Attendant | | |
| 48. Sh. Aakash Sharma | Field Attendant | | |
| 49. Sh. Ashish Singh | Field Attendant | | |
| 50. Sh. Aakash Saini | Field Attendant | | |

Administrative Staff:

| | |
|-------------------------------|---|
| 1. Shri Pankaj Kumar Verma | Registrar |
| 2. Shri S.K. Srivastava | Admini. Officer |
| 3. Shri Manas Kumar Biswas | Store & Purchase Officer |
| 4. Shri Rahul Sharma | Asstt. Fin. & Acc. Officer |
| 5. Mrs. Prabha Kharbanda | Accountant |
| 6. Sh. Ankit Rawat | Sr. Personal Assit. |
| 7. Smt. Rajvinder Kaur Nagpal | Stenographer, Gr. II |
| 8. Ms. Shalini Rawat | Stenographer, Gr. II |
| 9. Mrs. Kalpana Chandel | Assistant (Retd. on 30.11.2022) |
| 10. Mrs. Anita Chaudhary | Assistant |
| 11. Mrs. Neelam Chabak | Assistant |
| 12. Mrs. Seema Juyal | Assistant |
| 13. Sh. Yashpal Singh Bisht | Jr. Hindi Translator |
| 14. Mrs. Suman Nanda | Assistant |
| 15. Shri Kulwant Singh Manral | Assistant |
| 16. Sh. Vijai Ram Bhatt | Upper Divi. Clerk |
| 17. Shri Girish Chander Singh | Upper Divi. Clerk |
| 18. Sh. Rajeev Yadav | Upper Divi. Clerk |
| 19. Sh. Amardeep Kumar | Upper Divi. Clerk |
| 20. Sh. Ajay Singh | Upper Divi. Clerk (Resignation on 30.6.22) |
| 21. Sh. Dhanveer Singh | Upper Divi. Clerk |
| 22. Mrs. Megha Sharma | Upper Divi. Clerk |
| 23. Mrs. Surbhi | Upper Divi. Clerk |
| 24. Sh. Vishal Kumar | Upper Divi. Clerk (Resignation on 30.6.22) |
| 25. Ms. Richa Kukreja | Stenographer, Gr. III |
| 26. Sh. Deepak Jakhmola | Lower Divi. Clerk |

Ancillary Staff:

| | |
|-------------------------------|---------------------------------|
| 1. Sh. Manmohan | Driver |
| 2. Sh. Vikkee Tomar | Driver |
| 3. Sh. Bhupendra Kumar | Driver |
| 4. Sh. Rajesh Yadav | Driver |
| 5. Sh. Pradeep Shah | Drive |
| 6. Mrs. Deveshawari Rawat | M.T.S. |
| 7. Shri S.K. Gupta | M.T.S. |
| 8. Mrs. Omwati | M.T.S. (Retd. on 30.09.2022) |
| 9. Shri Jeevan Lal | M.T.S. (Retd. on 31.07.2022) |
| 10. Shri Surendra Singh | M.T.S. |
| 11. Shri Satya Narayan | M.T.S. |
| 12. Shri Rohlu Ram | M.T.S. |
| 13. Shri H.S. Manral | M.T.S. |
| 14. Shri G.D. Sharma | M.T.S. |
| 15. Sh. Dinesh Parsad Saklani | M.T.S. |
| 16. Shri Pritam | M.T.S. |
| 17. Shri Ramesh Chand Rana | M.T.S. |
| 18. Shri Ashish Rana | M.T.S. |
| 19. Sh. Sunil Kumar | M.T.S. |
| 20. Shri Harish Kumar Verma | M.T.S. |
| 21. Sh. Kamlesh Singh | M.T.S. |
| 22. Sh. Rajkiran Singh | M.T.S. |
| 23. Sh. Abdul Basit | M.T.S. |
| 24. Sh. Yogender Saklani | M.T.S. |
| 25. Ms. Deepti Pandey | M.T.S. |
| 26. Ms. Sakshi Chauhan | M.T.S. |

Contracutal Staff:

| | |
|------------------------------|--------|
| 1. Sh. Rezaw Uddin Chaudhary | Driver |
| 2. Sh. Vijay Singh | Driver |
| 3. Shri Rudra Chettri | M.T.S. |
| 4. Shri Laxman S. Bhandari | M.T.S. |
| 5. Shri Kalidas | M.T.S. |
| 6. Shri Ummed Singh | M.T.S. |

MEMBERS OF THE GOVERNING BODY/RESEARCH ADVISORY COMMITTEE/FINANCE COMMITTEE/BUILDING COMMITTEE

Governing Body

| Sl. | Name | Address | Status |
|-----|---|--|-----------------------------------|
| 1. | Prof. Talat Ahmad | Vice Chancellor, University of Kashmir Hazratbal, Srinagar, Jammu & Kashmir-190006 | Chairman |
| 2. | Dr. Srivari Chandrasekhar, Secretary to the Government of India | Department of Science and Technology, Technology Bhawan, New Mehrauli Road, New Delhi- 110 016 | Member |
| 3. | Prof. Shakil Ahmad Romshoo | Vice-Chancellor, Islamic University of Science & Technology, 1-University Avenue, Awantipora, Pulwama Jammu and Kashmir-192122 | Member |
| 4. | Shri Vishvajit Sahay | Additional Secretary & Financial Adviser, Department of Science & Technology, Technology Bhawan, New Mehrauli Road, New Delhi-110016 | Member |
| 5. | Dr. O.P. Mishra | Scientist 'G', Ministry of Earth Sciences, Government of India, Prithvi Bhavan, Opp. India Habitat Centre, Lodhi Road, New Delhi- 110003 | Member |
| 6. | Prof. M. Jayananda | Head, Centre for Earth and Space Sciences, University of Hyderabad, P.O. Central University, Gachibowli, Hyderabad-500 046 (Telangana) | Member |
| 7. | Prof. Pulak Sengupta | Professor, Department of Geological Sciences, Jadavpur University, 188, Raja Subodh Chandra Mallick Road, Poddar Nagar, Jadavpur Kolkata-700032, WB | Member |
| 8. | Prof. N.V. Chalapathi Rao | Professor, Department of Geology, Banaras Hindu University (BHU), Ajagara, Varanasi-221005, UP | Member |
| 9. | Prof. Anupam Chatoopadhyay | Department of Geology, 34 Chhatru Marg, University of Delhi, (North Campus) Delhi-110007 | Member |
| 10. | Prof. Saibal Gupta | Professor & Head, Dept. of Geology & Geophysics, Indian Institute of Technology, Kharagpur, Kharagpur -721302, WB | Member |
| 11. | Prof. S.C. Patel | Professor, Department of Earth Sciences, Indian Institute of Technology-Bombay, Powai, Mumbai-400076, Maharashtra | Member |
| 12. | Dr. Kalachand Sain | Director, Wadia Institute of Himalayan Geology, Dehradun- 248001 | Member Secretary |
| 13. | Sh. Pankaj Kumar | Registrar, Wadia Institute of Himalayan Geology, Dehradun- 248001 | Non-Member Asstt. Secretary |

Research Advisory Committee

| Sl. | Name | Address | Status |
|-----|------------------------------|--|------------------|
| 1. | Dr. Shailesh Nayak | Director, National Institute of Advanced Studies, Indian Institute of Science campus, Bengaluru-560012 | Chairman |
| 2. | Prof. T. N. Singh | Director, Indian Institute of Technology, Patna, Bihta, Patna-801 106 (Bihar) | Member |
| 3. | Prof. D.C. Srivastava | Emeritus Professor, Department of Earth Sciences, Indian Institute of Technology-Roorkee, Roorkee-247667, Uttarakhand | Member |
| 4. | Shri Rajesh Kumar Srivastava | Director, Oil and Natural Gas Corporation Limited, 5, Nelson Mandela Road, Vasant Kunj, New Delhi-110070 | Member |
| 5. | Dr. Rasik Ravindra | 608, Lalleshwari Apart Sector 21D, Faridabad-121001 | Member |
| 6. | Prof. Rajesh K. Srivastava | Professor & Former Head, Department of Geology, Banaras Hindu University, Varanasi- 221005, UP. | Member |
| 7. | Dr. Binita Phartiyal | Scientist 'E', Birbal Sahni Institute of Palaeoscience, 53, University Road, Lucknow- 226007, UP | Member |
| 8. | Dr. Prakash Chauhan | Director, Indian Institute of Remote Sensing, 4, Kalidas Road, Dehradun- 248001 | Member |
| 9. | Dr. O.P. Mishra | Scientist 'G' and Head, NCS, Ministry of Earth Sciences, Government of India, Prithvi Bhavan, Opp. India Habitat Centre, Lodhi Road, New Delhi-110003 | Member |
| 10. | Dr. Prasun Jana | Deputy Director General, Geological Survey of India, Dehradun-248001 | Member |
| 11. | Prof. Kusala Rajendran | Centre of Earth Sciences, Indian Institute of Science, Bengaluru-560012 | Member |
| 12. | Prof. L. S. Chamyal | Head, Department of Geology, Faculty of Science, The M.S. University of Baroda Vadodara-390002, Gujarat | Member |
| 13. | Prof. Santanu Banerjee | Department of Earth Sciences, Indian Institute of Technology Bombay Powai, Mumbai-400076, Maharashtra | Member |
| 14. | Dr. V. Balaram | Scientist 'G' (Retd.), SCIR-NGRI, Hyderabad, Consultant IUAC, Delhi | Member |
| 15. | Prof. Devesh K. Sinha | Oceanography and Marine Geology, Department of Geology, Delhi University, Delhi- 110007 | Member |
| 16. | Prof. Saibal Gupta | Professor & Head, Department of Geology & Geophysics, Indian Institute of Technology-Kharagpur Kharagpur-721302, West Bengal | Member |
| 17. | Dr. Kalachand Sain | Director, Wadia Institute of Himalayan Geology, Dehradun-248001 | Member |
| 18. | Dr. Vikram Gupta | Scientist 'F', Wadia Institute of Himalayan Geology, Dehradun-248001 | Member Secretary |

Finance Committee

| Sl. | Name | Address | Status |
|-----|----------------------------|---|----------|
| 1. | Shri Vishvajit Sahay | Additional Secretary & Financial Adviser, Department of Science & Technology, Technology Bhavan, New Mehrauli Road, New Delhi- 110 016 | Chairman |
| 2. | Prof. Anupam Chattopadhyay | Department of Geology, 34 Chhatra Marg, University of Delhi (North Campus) Delhi-110 007 | Member |
| 3. | Dr. Kalachand Sain | Director, Wadia Instt. of Himalayan Geology, Dehradun-248001 | Member |
| 4. | Shri Pankaj Kumar | Registrar, Wadia Institute of Himalayan Geology, Dehradun-248 001 | Member |
| 5. | Shri Rahul Sharma | Assistant Finance & Accounts Officer, Wadia Institute of Himalayan Geology, Dehradun-248 001 | Member |

Building Committee

| Sl. | Name | Address | Status |
|-----|--|--|------------------|
| 1. | Dr. Kalachand Sain | Director, Wadia Institute of Himalayan Geology, Dehradun-248001 | Chairman |
| 2. | Shri Vishvajit Sahay or his/ her nominee | Additional Secretary & Financial Adviser, Department of Science & Technology Technology Bhavan, New Mehrauli Road, New Delhi-110016 | Member |
| 3. | Representative of Survey of India | Hathibarkala, Dehradun | Member |
| 4. | Chief Engineer or his/ her nominee | CPWD, Dehradun- 248001 | Member |
| 5. | Shri Ashish Kumar Singh | SE (Civil), Tel Bhawan, Oil & Natural Gas Corporation, Dehradun-248001 | Member |
| 6. | Dr. R. Jayangondaperumal | Scientist-'F', Wadia Institute of Himalayan Geology, Dehradun-248001 | Member |
| 7. | Shri Rajesh Kumar | Sr. Principal Scientist, Head ASD, CSIR- Indian Institute of Petroleum Haridwar Road, Dehradun-248005 | Member |
| 8. | Shri Pankaj Kumar | Registrar, Wadia Institute of Himalayan Geology, Dehradun-248001 | Member |
| 9. | Shri C.B. Sharma | Executive Engineer, Wadia Institute of Himalayan Geology, Dehradun-248001 | Member Secretary |

***STATEMENT
OF
ACCOUNTS***

P.S.SETHI & CO.
CHARTERED ACCOUNTANTS

Dehradun Off:10, Indraprastha Enclave, Simla By Pass, Po Majra, Dehradun (U.K)
Tel.No. 9837562985, 7579912500 Email: rkguptasre@gmail.com, pssethiddn@gmail.com



Tel.No. 9528173229, 9897226991

Email: rk Gupta091@gmail.com, rk Gupta tarke@yahoo.com

**AUDITOR'S REPORT ON CONSOLIDATED FINANCIAL
STATEMENTS**

The Members of Governing Body,
Wadia Institute of Himalayan Geology,
33, GMS Road, Dehradun
Uttarakhand

We have audited the accompanying Consolidated Financial Statements of **WADIA INSTITUTE OF HIMALAYAN GEOLOGY, 33, GMS Road, Dehradun** for the year ended March 31st, 2023 which comprises Balance Sheet, Income and Expenditure Account, Receipt and Payment Account and summary of significant accounting policies.

Society's management is responsible for the preparation of these Financial Statements in accordance with law. This responsibility includes the design, implementation and maintenance of internal control relevant to the preparation and presentation of the financial statements that give a true and fair view and are free from material misstatement, whether due to fraud or error.

Our responsibility is to express an opinion on these financial statements based on our audit. We conducted our audit in accordance with the Standards on Auditing issued by the Institute of Chartered Accountants of India. Those Standards require that we comply with ethical requirements and plan and perform the audit to obtain reasonable assurance about whether the financial statements are free from material misstatement.

An audit involves performing procedures to obtain audit evidence about the amounts and disclosures in the financial statements. The procedures selected depend on the auditor's judgment, including the assessment of the risks of material misstatement of the financial statements, whether due to fraud or error. In making those risk assessments, the auditor considers internal control relevant to the Society's preparation and fair presentation of the financial statements in order to design audit procedures that are appropriate in the circumstances. An audit also includes evaluating the appropriateness of accounting policies used and the reasonableness of the accounting estimates made by management, as well as evaluating the overall presentation of the financial statements.



We believe that the audit evidence we have obtained is sufficient and appropriate to provide a basis for our audit opinion.

In our opinion and to the best of our information and according to the explanations given to us, the financial statements give the information required by the Act in all material respects and give a true and fair view in conformity with the accounting principles generally accepted in India subject to our comments given in Annexure-"1":

- a) in the case of the Balance Sheet, of the state of affairs of the Society as at March 31st, 2023;
- b) in the case of the Income and Expenditure Account of the deficit for the year ended on that date; and
- c) in the case of the Receipt and Payment Account, of the cash flows for the year ended on that date.


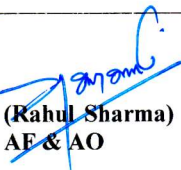


FOR P.S. SETHI & CO
CHARTERED ACCOUNTANTS

CA RAKESH GUPTA
FCA, DISA (ICAI)
FRN: 04545C
M.NO: 402349

Date: 18th September, 2023

Place: Dehradun

Action Taken Report on observations of the Chartered Accountant- Annexure-1 to the Consolidated Financial Statement of Audit Report (F.Y. 2022-23)

| Sl. No. | Comments/Observations by Chartered Accountants | Replies and Action taken by the Institute |
|---------|--|--|
| 1. | The Institute has not booked the current liability for the retirement benefit of the employees as per Accounting Standard-15 "Employee Benefits" as issued by the Institute of Chartered Accountants of India. The actuary valuation is required for ascertaining the current liability for the retirement benefits of the employees. | The points raised by Audit is noted for compliance. |
| 2. | The physical verification of Fixed Assets and Library for the financial year 2022-23 has not been undertaken. The reason for not complying with the rule laid down in GFR regarding physical verification of Assets may be specified. | Physical verification for the year 2021-22 has already been completed. Action with regard to the physical verification for the year 2022-2023 is in progress and report will be submitted to the audit shortly. |
| 3. | To maintain the accounts of institute it is suggested that customization is required for integration of whole store inventories and assets with accounts. It helps to computerization of Assets Registers/Stock Register. | All the accounting reports will be generated through the software. Suggestion for integration of Store and Accounts is noted and action will be taken on the subject shortly. The Institute is in process for obtaining ERP solution. |
| 4. | The Institute is maintaining the payment process through TSA (PFMS) online portal. It has been observed that advance payment for field tours is being given on demand of the employee and after the tour the balance amount of advance is being deposited in the UBI account resulting in actual expenditure not being booked in TSA. It is suggested that the advance amount should be given only to the extent of 80 to 90 percent of the employee's demand value so that the actual expenditure can be recorded in the TSA portal. | Noted for compliance |
| 5. | During the audit it has been noticed that e-Assets register is not properly maintained. | Noted for compliance |
| 6. | GST on Guest House Room Rent are not collected and deposited to Govt. | Noted for compliance |
| | FOR P.S. SETHI & CO CHARTERED ACCOUNTANTS  CA RAKESH GUPTA (FCA, DISA (ICAI), |  (Rahul Sharma) AE & AO  (Pankaj Kumar) Registrar  (Dr. Kalachand Sain) Director |

WADIA INSTITUTE OF HIMALAYAN GEOLOGY
33, GENERAL MAHADEO SINGH ROAD, DEHRADUN

BALANCE SHEET
(AS AT 31st MARCH 2023)

| (Amt in Rs...) | | | |
|--|----------|---------------------|---------------------|
| PARTICULARS | SCHEDULE | CURRENT YEAR | PREVIOUS YEAR |
| <u>LIABILITIES</u> | | | |
| Corpus/ Capital Fund | 1 | 68,39,86,424 | 86,11,82,286 |
| Reserves and Surplus | 2 | - | - |
| Earmarked/ Endowment Fund | 3 | 32,07,880 | 28,20,394 |
| Secured Loans & Borrowings | 4 | - | - |
| Unsecured Loans & Borrowings | 5 | - | - |
| Deferred Credit Liabilities | 6 | - | - |
| Current Liabilities & Provisions | 7 | 13,01,49,469 | 2,11,92,389 |
| TOTAL | | 81,73,43,773 | 88,51,95,069 |
| <u>ASSETS</u> | | | |
| Fixed Assets | 8 | 39,49,12,712 | 36,43,16,605 |
| Investments from Earmarked/ Endowment Funds | 9 | 1,09,706 | 1,04,043 |
| Investment- Others | 10 | - | - |
| Current Assets, Loans & Advances | 11 | 42,23,21,355 | 52,07,74,421 |
| TOTAL | | 81,73,43,773 | 88,51,95,069 |
| Significant Accounting Policies | 37 | | |
| Contingent Liabilities and Notes on Accounts | 38 | | |

AUDITOR'S REPORT

"As per our separate report of even date"

FOR P.S. SETHI & CO.
CHARTERED ACCOUNTANTS



(RAHUL SHARMA)
 A.F. & A.O.

(PANKAJ KUMAR VERMA)
 Registrar

(DR. KALACHAND SAIN)
 Director

Date : 18th September, 2023
 Place : Dehradun

WADIA INSTITUTE OF HIMALAYAN GEOLOGY

33, GENERAL MAHADEO SINGH ROAD, DEHRADUN

**INCOME & EXPENDITURE ACCOUNT
(FOR THE YEAR ENDED 31st MARCH 2023)**

(Amt in Rs...)

| S.NO. | PARTICULARS | SCH. | CURRENT YEAR | PREVIOUS YEAR |
|----------|---|------|-----------------------|---------------------|
| A | <u>INCOME</u> | | | |
| | Income from sales/ services | 12 | - | - |
| | Grants/ Subsidies | 13 | 39,09,62,940 | 48,49,36,400 |
| | Fees/Subscription | 14 | - | - |
| | Income from Investments | 15 | 9,79,376 | 6,83,880 |
| | Income from Royalty, Publication etc. | 16 | 1,16,540 | 1,23,782 |
| | Interest earned | 17 | 1,13,84,114 | 1,14,33,194 |
| | Other Income | 18 | 80,86,162 | 2,69,25,223 |
| | Increase/ Decrease in Stock (Goods & WIP) | 19 | - | - |
| | TOTAL (A) | | 41,15,29,133 | 52,41,02,479 |
| B | <u>EXPENDITURE</u> | | | |
| | Establishment Expenses | 20 | 45,94,51,879 | 33,84,23,026 |
| | Other Research & Administrative Expenses | 21 | 9,58,83,522 | 9,21,93,882 |
| | Expenditure on Grant/ Subsidies etc. | 22 | - | - |
| | Interest/ Bank Charges | 23 | 44,49,113 | 61,82,397 |
| | Depreciation Account | 8 | 6,66,53,157 | 6,08,84,656 |
| | Increase/ Decrease in stock of | | | |
| | Finished goods, WIP& Stock of Publication | A-2 | (40,466) | (1,41,188) |
| | (Profit)/ Loss on sale of Assets | 36 | 14,45,341 | - |
| | TOTAL (B) | | 62,78,42,546 | 49,75,42,774 |
| | Surplus/ (Deficit) being excess of Income over Expenditure (A - B) | | (21,63,13,413) | 2,65,59,706 |
| | Transfer to Special Reserve (Specify each) | | - | - |
| | Transfer to / from General Reserve | | - | - |
| | SURPLUS /(DEFICIT) CARRIED TO CAPITAL FUND | | (21,63,13,413) | 2,65,59,706 |

AUDITOR'S REPORT

"As per our separate report of even date"

**FOR P.S. SETHI & CO.
CHARTERED ACCOUNTANTS****CA RAKESH GUPTA
(F.C.A., DISA (ICAI))****(RAHUL SHARMA)
A.F. & A.O.****(PANKAJ KUMAR VERMA
Registrar****(DR. KALACHAND SAIN)
Director**Date : 18th September, 2023
Place: Dehradun

WADIA INSTITUTE OF HIMALAYAN GEOLOGY
33, GENERAL MAHADEO SINGH ROAD, DEHRADUN

RECEIPTS & PAYMENTS ACCOUNT
(FOR THE YEAR ENDED 31st MARCH 2023)

(Amt in Rs...)

| PARTICULARS | SCH. | CURRENT YEAR | PREVIOUS YEAR |
|--|------|-----------------------|-----------------------|
| RECEIPTS | | | |
| Opening Balance | 24 | 31,55,09,620 | 16,12,86,247 |
| Grants - in - Aids | 26 | 45,09,62,940 | 63,24,36,400 |
| Grants - in - Aids/Other Receipts (Ear Marked) | 27 | 12,00,000 | 4,72,000 |
| Loan & Advances | 28 | 41,63,48,510 | 26,83,65,058 |
| Loan & Advances (Ear Marked) | 31 | - | - |
| Fees/Subscription | 14 | - | - |
| Income from Investments | 15 | 9,79,376 | 6,83,880 |
| Income from Royalty, Publication etc. | 16 | 1,16,540 | 1,23,782 |
| Interest earned | 17 | 1,39,86,021 | 1,43,19,875 |
| Other Income | 18 | 80,86,162 | 2,69,25,223 |
| Investment (L/C Margin Money) | 34 | - | 2,65,55,293 |
| TOTAL | | 1,20,71,89,170 | 1,13,11,67,758 |
| PAYMENTS | | | |
| Establishment Expenses | 20 | 45,94,51,879 | 33,84,23,026 |
| Other Administrative Expenses | 21 | 9,58,83,522 | 9,06,63,722 |
| Expenditure on Grant/Subsidies Etc. | 22 | - | - |
| Interest/ Bank Charges | 23 | 44,49,113 | 61,82,397 |
| Loans & Advances | 29 | 32,82,23,028 | 27,95,39,089 |
| Loans & Advances (Ear Marked) | 32 | - | 5,511 |
| Investment (L/C Margin Money) | 35 | - | 4,77,544 |
| Fixed Assets | 36 | 10,03,80,058 | 10,03,66,848 |
| Ear Marked Fund Expenses | 33 | 8,18,177 | - |
| Grant - in - Aid (Ear Marked) Refunded | 30 | - | - |
| Closing Balance | 25 | 21,79,83,393 | 31,55,09,620 |
| TOTAL | | 1,20,71,89,170 | 1,13,11,67,758 |

AUDITOR'S REPORT

"As per our separate report of even date"

FOR B.S. SETHI & CO.
CHARTERED ACCOUNTANTS

CA RAKESH GUPTA
(FCA, DISA (ICAI))


(BAHUL SHARMA)
A F & A.O


(PANKAJ KUMAR VERMA)
Registrar


(DR. KALACHAND SAIN)
Director

Date : 18th September, 2023
Place: Dehradun

WADIA INSTITUTE OF HIMALAYAN GEOLOGY,
33, GMS ROAD DEHRADUN

SCHEDULE FORMING PART OF ACCOUNTS FOR THE YEAR ENDED 31ST MARCH, 2023

SCHEDULE – 37: SIGNIFICANT ACCOUNTING POLICIES

1. ACCOUNTING CONVENTION

The financial statements are prepared on the basis of historical cost convention, unless otherwise stated and on the cash method of accounting except interest accrued on fixed deposit.

2. INVESTMENTS

Investments classifieds as “long term investments” are carried at cost.

3. FIXED ASSETS

- a) Fixed Assets are stated at net book value as recommended in the “Uniform Accounting Format” of financial statements for the Central Autonomous Bodies as made compulsory by the Ministry of Finance w.e.f. 01.04.2001.
- b) Additions to fixed assets are taken at cost of acquisition, inclusive of freight, duties and taxes, incidental and direct expenses related to acquisition.

4. DEPRECIATION

- a) Depreciation is provided on Written down Value method as per rates specified in the Income Tax Act, 1961.
- b) When an asset is discarded or sold or deleted, the original cost is deducted from the gross block, the W.D.V. is deducted from the W.D.V. block and accumulated depreciation on the asset upto the date of deletion is deducted from accumulated depreciation of the respective block.
- c) In respect of addition to/ deduction from fixed assets during the year, depreciation is considered on full yearly basis.



WADIA INSTITUTE OF HIMALAYAN GEOLOGY,
33, GMS ROAD DEHRADUN

5. MISCELLANEOUS EXPENDITURE

Deferred revenue expenditure, if any, will be written off over a period of 5 years from the year it is incurred.

6. ACCOUNTING FOR SALES & SERVICES

The consultancy services provided by the institute is accounted for on net service basis.

7. GOVERNMENT GRANTS / SUBSIDIES

- a) Government grants of the nature of contribution towards Capital Cost are directly credited to Corpus Fund and Other Revenue cost are transferred to Income & Expenditure account and the surplus or deficit after deducting all the expenses is transferred to Capital / Corpus fund.
- b) Grants towards Earmarked / Endowment Funds are directly transferred to the respective fund account.
- c) Government grants / subsidy are accounted on realization basis.


(Rahul Sharma)
A.E. & A.O


(Pankaj Kumar Verma)
Registrar


(Dr. Kalachand Sain)
Director

Date : 18th September, 2023

Place: Dehradun



WADIA INSTITUTE OF HIMALAYAN GEOLOGY,
33 GMS ROAD, DEHRADUN

SCHEDULE FORMING PART OF ACCOUNTS FOR THE YEAR ENDED 31ST MARCH, 2023

SCHEDULE – 38: CONTINGENT LIABILITIES AND NOTES ON ACCOUNTS

1. CONTINGENT LIABILITIES

(Amount in Rs.)

| | | |
|----|--|---------|
| a) | Claims against the Entity not acknowledged as debts | - Nil - |
| b) | In respect of | |
| | i) Bank Guarantees given by /on behalf of the Entity | - Nil - |
| | ii) Letter of credit opened by Bank on behalf of the entity | - Nil - |
| | iii) Bills discounted with banks | - Nil - |
| c) | Disputed demands in respect of | |
| | i) Income –tax (TDS) | - Nil - |
| | ii) Sales tax | - Nil - |
| | iii) Municipal Taxes | - Nil - |
| d) | In respect of claims from parties for non-execution of orders, but contested by the Entity | - Nil - |

2. CAPITAL COMMITMENTS

| | | |
|---|--------------------------|---------|
| Estimated Value of contracts remaining to be executed on capital account and not provided for (net of advances) | | |
| a) | Construction of Building | - Nil - |
| b) | Other Assets | - Nil - |

3. LEASE OBLIGATIONS

| | |
|---|---------|
| Future obligations for rentals under finance lease arrangements for plant and machinery amount to Rs. Nil | - Nil - |
|---|---------|

4. CURRENTS ASSETS, LOANS AND ADVANCES

In the opinion of the Institute, the current assets, loans and advances have a value on realization in the ordinary course of business, equal at least to the aggregate amount shown in the Balance Sheet.

5. TAXATION

In view of there being no taxable income of the Institute under income tax Act, 1961, no provision for Income Tax has been considered necessary



WADIA INSTITUTE OF HIMALAYAN GEOLOGY,
33 GMS ROAD, DEHRADUN

6. FOREIGN CURRENCY TRANSACTIONS

| | | |
|------|--|---------|
| a) | Value of Imports Calculated on C.I.F basis: | |
| i) | Purchase of finished goods | - Nil - |
| ii) | Raw Materials & Components (including in transit) | - Nil - |
| iii) | Capital goods | - Nil - |
| iv) | Stores, Spares and Consumables | - Nil - |
| b) | Expenditure in foreign currency | |
| i) | Travel (for attending Seminar/Conference abroad) | - Nil - |
| ii) | Remittances and Interest payment to Financial Institutions / Banks in Foreign Currency | - Nil - |
| iii) | Other expenditure | |
| | Commission on Sales | - Nil - |
| | Legal and Professional Expenses | - Nil - |
| | Miscellaneous Expenses | - Nil - |
| c) | Earnings | |
| i) | Value of Exports on FOB basis | - Nil - |
| ii) | Grants for Projects | - Nil - |

7. The payments to auditors during the F.Y. 2022 -23 is as follows:

| | | |
|-----|--------------------------|----------|
| | Remuneration to auditors | |
| i) | As Auditors | 55,000/- |
| | Taxation matters | - Nil - |
| | For Management Services | - Nil - |
| | For Certification | - Nil - |
| ii) | Others | - Nil - |

8. Separate Financial Statements have been prepared for:

- Wadia Institute of Himalayan Geology.
- Contributory/ General Provident Fund.
- Pension Fund.
- Consolidated financial statement of projects sponsored by other Agencies.
- Individual financial statements of Projects sponsored by other agencies.

9. Corresponding figures for the previous year have been regrouped / rearranged, wherever necessary.

10. Annexed Schedules & Annexures are an integral part of the Balance Sheet as on 31st March, 2023, Income and Expenditure Account and Receipt & Payment for the year ended on 31st March, 2023.


(Rahul Sharma)
A.F. & A.O


(Pankaj Kumar Verma)
Registrar


(Dr. Kalachand Sain)
Director

Date : 18th September, 2023
Place: Dehradun



WADIA INSTITUTE OF HIMALAYAN GEOLOGY, DEHRA DUN

PUBLICATIONS AVAILABLE FOR SALE

HIMALAYAN GEOLOGY

(These volumes are the Proceedings of the Annual Seminars on Himalayan Geology organised by the Institute)

| | | (in Rs) | (in US \$) |
|--|--------|---------|------------|
| Volume 1 | (1971) | 130.00 | 26.00 |
| Volume 2* | (1972) | 50.00 | |
| Volume 3* | (1973) | 70.00 | |
| Volume 4* | (1974) | 115.00 | 50.00 |
| Volume 5 | (1975) | 90.00 | 50.00 |
| Volume 6 | (1976) | 110.00 | 50.00 |
| Volume 7 | (1977) | 110.00 | 50.00 |
| Volume 8(1) | (1978) | 180.00 | 50.00 |
| Volume 8(2) | (1978) | 150.00 | 45.00 |
| Volume 9(1) | (1979) | 125.00 | 35.00 |
| Volume 9(2) | (1979) | 140.00 | 45.00 |
| Volume 10 | (1980) | 160.00 | 35.00 |
| Volume 11 | (1981) | 300.00 | 60.00 |
| Volume 12 | (1982) | 235.00 | 47.00 |
| Volume 13* | (1989) | 1000.00 | 100.00 |
| Volume 14* | (1993) | 600.00 | - |
| (in Hindi) | | | |
| Volume 15* | (1994) | 750.00 | |
| (Available from M/s Oxford & IBH Publishing Co. Pvt. Ltd., New Delhi, Bombay, Kolkata) | | | |
| Volume 16* | (1999) | 1000.00 | 100.00 |

Journal of Himalayan Geology

(A bi-annual Journal : published from 1990 to 1995)

| | (in Rs) | (in US \$) |
|---------------------|---------|------------|
| Annual Subscription | | |
| Institutional | 500.00 | 50.00 |
| Individual | 100.00 | 25.00 |

Volume 1 (1990) to Volume 6 (1995)*

HIMALAYAN GEOLOGY

(A bi-annual Journal incorporating Journal of Himalayan Geology)

| | (in Rs) | (in US \$) |
|----------------------|---------|------------|
| Annual Subscription: | | |
| Institutional | 500.00 | 50.00 |
| Individual | 100.00 | 25.00 |

Volume 17 (1996)*

HIMALAYAN GEOLOGY

| | (in Rs) | (in US\$) |
|--|---------|-----------|
| Revised Annual Subscription (w.e.f. 1997): | | |
| Institutional | 750.00 | 50.00 |
| Individual (incl. postage) | 100.00 | 25.00 |

Volume 18 (1997) to Volume 26 (2005)*

Volume 27 (2006) to Volume 32 (2011)*

Volume 33 (2012)

Volume 34 (2013) to Volume 36 (2016)*

Volume 37 (2015) to Volume 38 (2017)

Volume 39 (2018) to Volume 43 (2022)

| | (in Rs) | (in US\$) |
|--|---------|-----------|
| Revised Annual Subscription (w.e.f. 2018): | | |
| Institutional | 2000.00 | 150.00 |
| Individual (incl. postage) | 600.00 | 50.00 |

Volume 44 (2023)

| | (in Rs) | (in US\$) |
|--|---------|-----------|
| Revised Annual Subscription (w.e.f. 2018): | | |
| Institutional | 3000.00 | 225.00 |
| Individual (incl. postage) | 1000.00 | 100.00 |

OTHER PUBLICATIONS

Geology of Kumaun Lesser Himalaya, 1980
(by K.S. Valdiya) Rs. 180.00
US \$ 50.00

Geology of Indus Suture Zone of Ladakh, 1983
(by V.C. Thakur & K.K. Sharma) Rs. 205.00
US \$ 40.00

Bibliography on Himalayan Geology, 1975-85 Rs. 100.00
US \$ 30.00

Geological Map of Western Himalaya, 1992 Rs. 200.00
(by V.C. Thakur & B.S. Rawat) US \$ 15.00

Excursion Guide :The Siwalik Foreland Basin Rs. 45.00
(Dehra Dun-Nahan Sector), (WIHG Spl. Publ. 1,1991) US \$ 8.00
(by Rohtash Kumar and Others)

Excursion Guide : The Himalayan Foreland Basin Rs. 180.00
(Jammu -Kalakot-Udhampur Sector) (WIHG Spl US \$ 15.00
Publ. 2, 1999) (by A.C. Nanda & Kishor Kumar)

Glacier Lake Inventory of Uttarakhand Rs. 500.00
(by Rakesh Bhambri et al. 2015) US \$ 50.00

Siwalik Mammalian Faunas of the Himalayan Foothills Rs. 1200.00
With reference to biochronology, linkages and migration US \$ 100.00
(by Avinash C. Nanda, 2015)

Lithostratigraphy, Biostratigraphy and Palaeogeography Rs. 600.00
of the Eastern Karakoram, India US \$ 50.00
(by K.P. Juyal, 2018)

Note: 'Journal of Himalayan Geology' & 'Himalayan Geology' have been merged and are being published as Himalayan Geology after 1996.

*** Out of Stock**

Life Time Subscription of Himalayan Geology (Individuals only)

Fee for Print copy : India: 7500.00 Abroad: US\$ 750.00
Fee for Soft copy : India: 4000.00 Abroad: US\$ 250.00

Trade Discount (In India only)

1-10 copies: 10%, 11-15 copies: 15% and >15 copies: 20%

Offer (for a limited period): A free set of old print volumes (1971 to 2012, subject to availability) of 'Himalayan Geology' will be provided to the new registered Life Time Subscribers (Postage to be borne by the subscriber).

Publications: may be purchased from Publication & Documentation Section and Draft/Cheque may be drawn in the name of The Director, Wadia Institute of Himalayan Geology, 33- General Mahadeo Singh Road, Dehra Dun – 248 001

Phone: 0135-2525430 Fax: (91)0135-625212 Website: <http://www.himgeology.com> E-mail: himgeol@wihg.res.in



Wadia Institute of Himalayan Geology

(An Autonomous Institute of Dept. of Science & Technology, Govt. of India)

33, General Mahadeo Singh Road, Dehradun-248001 (INDIA)